THSD7A, the second autoantigen in membranous nephropathy : new diagnostic test and identification of the immunodominant epitopes

Kristel Zaghrini

UNIVERSITÉ CÔTE D'AZUR

ÉCOLE DOCTORALE
SCIENCES DE LA VIE ET DE LA SANTÉ

THÈSE DE DOCTORAT

THSD7A, le second auto-antigène de la glomérulonéphrite extra-membraneuse : nouveau test diagnostique et identification des épitopes immunodominants

Kristel ZAGHRINI

Institut de Pharmacologie Moléculaire et Cellulaire, CNRS, UMR 7275

Présentée en vue de l'obtention du grade de docteur en Sciences de l'Université Côte d'Azur
Mention : Interactions moléculaires et cellulaires

Dirigée par Gérard LAMBEAU

Soutenue le 6 Mai 2019, devant le jury composé de :

Andreas SCHEDL	Directeur de recherche, INSERM, iBV, Nice	Président du jury
Sonia BERRIH-AKNIN	Directeur de recherche, INSERM, Centre de myologie, UPMC, Paris	Rapporteur
Marco PRUNOTTO	Directeur de recherche, Hoffmann-La-Roche, Bâle, Suisse	Rapporteur
Hanna DEBIEC	Directeur de recherche, INSERM, Hôpital Tenon, UPMC, Paris	Examinateur
Véronique BRAUD	Directeur de recherche, CNRS, IPMC, Valbonne	Examinateur
Gérard LAMBEAU	Directeur de recherche, CNRS, IPMC, Valbonne	Directeur de thèse

ANR AGENCE NATIONALE DE LA RECHERCHE · FRM FONDATION RECHERCHE MÉDICALE · cnrs · SIGNALIFE · ipmc

"You give but little when you give of your possessions. It is when you give of yourself that you truly give."

Kahlil Gibran, The Prophet

To my parents.

Acknowledgments

The work presented in this thesis would not have been possible without the effort of several wonderful people. I sincerely appreciate the inspiration, support and guidance of all those who made this PhD possible.

First and foremost, I would like to extend my sincere gratitude to Dr. Gérard Lambeau for his dedicated help, advice, inspiration, encouragement and continuous support throughout my PhD. You believed in me like nobody else did, you taught me how good scientific research is done and you allowed me to grow as a research scientist. Your unwavering enthusiasm and your mission for providing high–quality work has finely shaped my career. I doubt that I will ever be able to convey my appreciation fully, but I owe you my eternal gratitude.

I would like to thank the members of the PhD committee: Dr. Andreas Schedl, Dr. Sonia Berrih–Aknin, Dr. Marco Prunotto, Dr. Hanna Debiec and Dr. Véronique Braud for having accepted to participate in this committee and evaluate my work. I thank Dr. Sonia Berrih–Aknin and Dr. Marco Prunotto for their reports and their insightful comments. I also thank my PhD advisors Dr. Andreas Kistler and Dr. Andreas Schedl for their cooperation and for evaluating the work progress during my PhD.

I also gratefully acknowledge the Laboratory of Excellence SIGNALIFE program for the PhD fellowship and Konstanze Beck for her generous administrative assistance.

I thank all our collaborators particularly Dr. Pierre Ronco, Dr. Laurence Beck and Dr. Jack Wetzels for their tremendous help in the inclusion of patients in this study and for their valuable advices and discussions.

I would also like thank all the lab members for all their priceless support and for making my stay at IPMC more pleasurable. Joana, thank you for your scientific input and for all the memorable travel journeys that we had together. Your friendship shall always be remembered. Guillaume, thank you for the numerous scientific discussions, and for your cheerfulness in the difficult times. Christine, thank you for your kindness, your positive attitude and for the moral support you provided me. Barbara, thank you for the help in collecting the patients' clinical data. Agnès, thank you for your gentleness, your humor and your enthusiasm for research. Alice, Franck and Joëlle, thank you for your kindness and for the stimulating discussions in the last stage of my PhD. I acknowledge the previous lab members especially Vesna for her friendliness and for sharing her research expertise, Joel for his helpfulness and for his assistance at the beginning of my PhD, Louise for her kindness and Sarah for her amiability and friendship. I thank also the staff of IPMC and specially the colleagues in IPMC R+2 for their cooperation and insightful discussions.

Last but not least, I owe my deepest gratitude to my family. For mom and dad who raised me, supported me, taught me and loved me. Without your help, I wouldn't have become who I am. To you I dedicate this work. For my brother and sister, who provided me with endless support and encouragement, your infallible love and trust has always been my strength. Finally, a special thanks for Léopold my loving and patient partner, your faithful support got me through the last stages of the PhD.

Table of Contents

List of figures

List of tables

Abbreviations

ACE	Angiotensin–Converting Enzyme
AchR	Acetylcholine Receptor 1
ANCA	Anti–Neutrophilic Cytoplasmic Autoantibody
AR	Aldose Reductase
BSA	Bovine Serum Albumin
C6	Complement Component 6
CD	Cluster of Differentiation
CFH	Complement Factor H
CTLD	C–Type Lectin Domain
COMP	Cartilage Oligomeric Matrix Protein
CysR	Cystein–Rich Domain
Dsg	Desmoglein
DTT	Dithiothreitol
ECM	ExtraCellular Matrix
E. coli	Escherichia coli
EGF	Epidermal Growth Factor
eGFR	estimated Glomerular Filtration Rate
ELISA	Enzyme–Linked Immunosorbent Assay
EM	Electron Microcopy
ESRD	End–Stage Renal Disease
FAK	Focal Adhesion Kinase
FNII	Fibronectin type II domain
GBM	Glomerular Basement Membrane
Gp330	Glycoprotein 330 (megalin)
GWAS	Genome–Wide Association Study
HLA	Human Leukocyte Antigen
LY75	Lymphocyte Antigen 75 (also called DEC–205)
MRC1	Macrophage Mannose Receptor 1

MRC2	C–type Mannose Receptor 2 (also called Endo180)
MuSK	Muscle–Specific Kinase
HEK293	Human Embryonic Kidney 293 cells
HN	Heymann Nephritis
HUVEC	Human Umbilical Vein Endothelial Cells
IgG	Immunoglobulin G
IIFT	Indirect ImmunoFluorescence Test
JAK2	Janus kinase 2
KDIGO	Kidney Disease Improving Global Outcomes
LBD	Ligand Binding Domain
LRP4	Lipoprotein receptor–related protein–4
MAC	Membrane Attack Complex
MBL	Mannose Binding Lectin
MG	Myasthenia Gravis
MHC	Major Histocompatibility Complex
MN	Membranous Nephropathy
MusK	Muscle–Specific Kinase
NEP	Neutral Endopeptidase
PDB–ID	Protein Data Bank– Structure Identifier
PLA2R1	Phospholipase A2 Receptor 1 (also called M–type receptor)
$PM_{2.5}$	Particulate Matter 2.5 μm
PTM	Post–translational Modification
RU	Relative Unit
SNP	Single Nucleotide Polymorphism
SOD2	Superoxide Dismutase 2
sPLA2	secreted PhosphoLipase A2
TGF– β	Transforming Growth Factor–beta
THSD7A	Thrombospondin type 1 Domain–containing 7A
TSP–1	Thrombospondin –1
vWF_C	von Willebrand Factor Type C

1 Introduction – Membranous nephropathy

1.1 Autoimmune diseases

Protecting and defending the host against infectious agents is the chief function of the immune system. There are two cases where the deficiency of the immune system can lead to pathologies (Wang et al., 2015). In the first, the deficient immune system is incapable of protecting host against pathogens. In the second, the immune system fails to distinguish between self and non–self–molecules and the breach of tolerance leads to an autoimmune disease.

Autoimmune diseases affect 3–5% of the general population, with autoimmune thyroid disease and type I diabetes being the most common forms. Noteworthy, there are around 100 different autoimmune diseases that can be either organ–specific as in the case of primary biliary cirrhosis where the autoantibodies react to autoantigens localized in a specific tissue, or can also be organ non–specific as in systemic lupus erythematosus where the autoantibody reactivity targets several tissues (Yu et al., 2014).

It has been shown that the development of an autoimmune reaction can be triggered by environmental factors and depends on genetic predisposition (Wang et al., 2015). The environmental factors include microorganisms, xenobiotics, infectious agents and nutrition and can influence the microbiota whereas the genetic factors include gene mutations, HLA susceptible loci and epigenetic mechanisms. These factors stimulate the autoimmune response which will lead to tissue damage. The epidemiology of the different autoimmune diseases varies with age, sex, ethnicity and geographic localization with an increased frequency of autoimmune responses in women, and typical large female–to–male ratios ranging from 10:1 to 1:1.

Circulating autoantibodies targeting various structures of the cell are a common characteristic of autoimmune diseases and mediate tissue damage through different mechanisms. First, the autoantibodies can lead to destruction of the cell through

complement activation and antibody–dependent cell–mediated cytotoxicity as in the case of autoimmune thyroid disease which is mediated by anti–thyroid autoantibodies (Rodien et al., 1996). A second important pathogenic mechanism is the immune complex–mediated damage as in systemic lupus erythematosus.

The immune complexes produced in response to soluble antigens are usually eliminated by phagocytosis. If the clearance fails mainly because of the large amounts of immune complexes, tissue damage can occur. Furthermore, the circulating immune complexes can deposit and cause glomerulonephritis, vasculitis or even arthritis (Lleo et al., 2010). Autoantibodies may also bind to cell surface receptors and either activate or block different signaling pathways. In Myasthenia Gravis, autoantibodies target different key protein components of the postsynaptic neuromuscular junction (like the acetylcholine receptor AchR, the muscle–specific tyrosine kinase MUSK or the low–density lipoprotein receptor–related protein 4 LRP4) and disrupt the neuromuscular transmission by different mechanisms, dependent or not from activation of the complement pathway (Berrih-Aknin et al., 2014).

1.2 Membranous Nephropathy

1.2.1 Kidney physiology

The kidney is the main filtrating organ in mammals. The basic functional unit in the kidney is the nephron which regulates the excretion of metabolic wastes, re–uptake of salt, water and important components such as nutrients, vitamins or proteins. In addition to its role in fluid homeostasis, the kidney is essential for the control of blood pressure, vitamin D synthesis and bone mineralization (Scott et al., 2015). An adult human kidney contains between 1 to 2.5 million of nephrons. Each nephron comprises a glomerulus where blood filtration occurs and a segmented tubular resorption compartment ending into the collecting duct (Figure 1.1–A). Every day, 150 to 180 liters of blood are filtered through the glomerular capillaries. During the tubular transport, the primary urine is modified, and most of the fluid is reabsorbed before becoming the final urine, approximately 1.5 liters per day (Puelles et al., 2011).

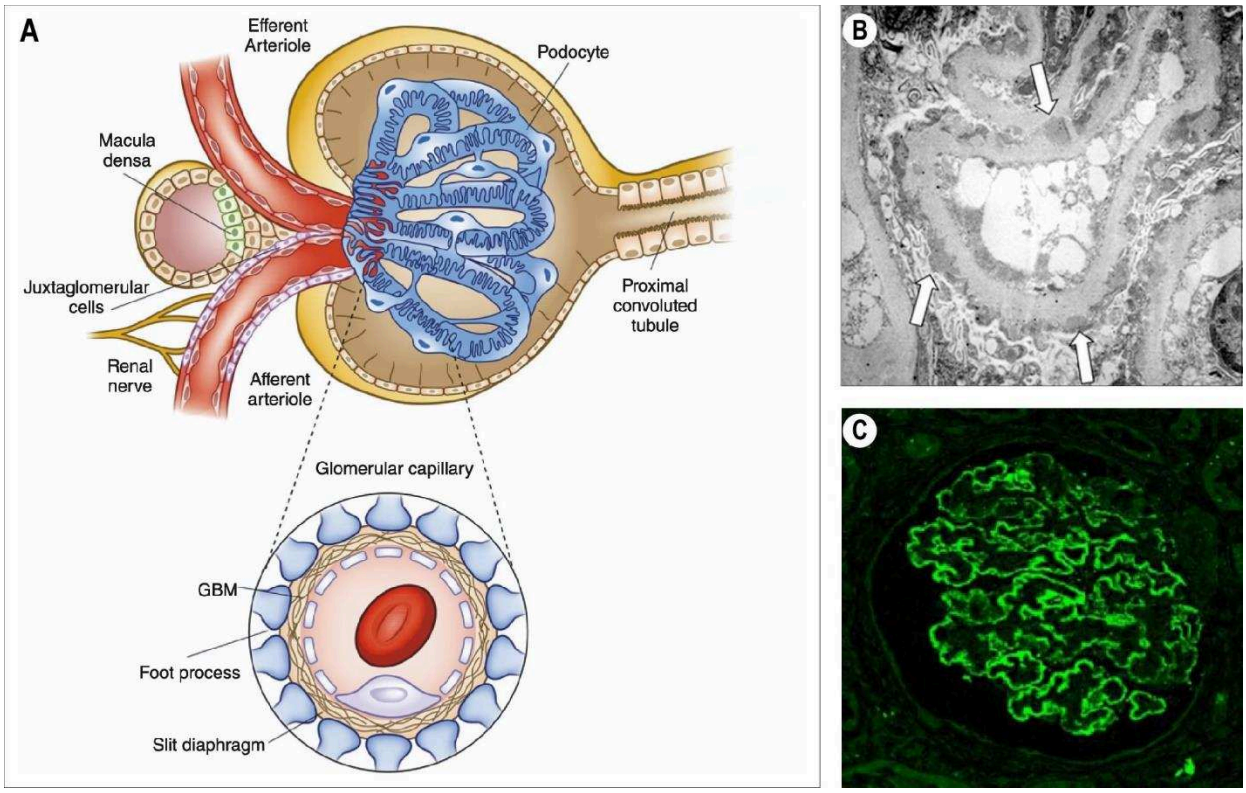

Figure 1.1 – Physiology of the glomerulus in representative modification of the GBM in MN. (A) Structure of the renal glomerulus and the filtration barrier. *Adapted from (Pollak et al., 2014) with copyright permission from "Clinical Journal of American Society of Nephrology: CJASN"*. (B) Electron microscopy showing the immune deposits (arrows) in subepithelial space of the glomerulus in membranous nephropathy. *Adapted from* (Lai et al., 2015) *with copyright permission from "Elsevier"*. (C) Immunofluorescence staining of glomerulus showing granular deposits the glomerular basement membrane. *Adapted from (Debiec et al., 2014) with copyright permission from "SpringerLink"*.

The glomerulus (after the Latin word glomus for a ball of yarn) is the most complex biological membrane system that allows plasma filtration with total restriction to high–molecular–weight proteins and blood cellular components, generating the primary urinary ultrafiltrate (Haraldsson et al., 2008). This membrane, first proposed by Karl Ludwig in the 1800s, (Jarad et al., 2009) is termed as the glomerular filtration membrane. It assembles three different layers organized as follows: the podocytes, intimately wrapped around the glomerular capillaries and sharing with the glomerular endothelial cells an extracellular matrix known as the glomerular basement membrane (GBM) (Figure 1.1–A) (Scott et al., 2015). The foot processes of two adjacent podocytes interdigitating and forming the slit diaphragm consisting of multiple adhesion proteins such as nephrin, podocin, etc. (Jarad et al., 2009). In mammals, the slit diaphragm can be compared to a dialysis membrane with a cut–off value of around 60 kDa, close to the molecular mass of albumin, the most abundant protein in our blood. Any dysfunction of the glomerulus will lead to pathologies collectively called glomerulonephritides.

1.2.2 Glomerulonephritides

Glomerulonephritides comprise a group of rare kidney diseases affecting about 20% of chronic kidney disease cases. The most common types of glomerulonephritides include IgA nephropathy, membranous nephropathy, membranoproliferative glomerulonephritis, minimal change disease and focal segmental glomerulosclerosis. Rare forms of glomerulonephritides include dense deposit disease and C3 glomerulonephritis (Floege et al., 2016). Interestingly, although the Anti–Neutrophilic Cytoplasmic Autoantibody (ANCA) disease is not a glomerulonephritis but a vasculitis that affects kidney function by targeting the small vascular endothelial cells near the podocytes (Jennette et al., 2017). The clinical course of the disease varies from coincidental detection of proteinuria and increased serum creatinine levels in asymptomatic patients to weight gain and edema in nephrotic patients. The definitive diagnosis of glomerulonephritis is done after a kidney biopsy and immunohistological examination (Figure 1.1–BC).

Clinical manifestations in the different age categories can be an indicator of the type of glomerulonephritides: minimal change disease and focal segmental glomerulosclerosis are more common in children and young adults while membranous glomerulonephritis occurs

in older subjects. Regional differences are also important in distribution of glomerulonephritides: while the incidence of IgA nephropathy is higher in Asian subjects, focal segmental glomerulosclerosis is higher in the USA and Canada (Floege et al., 2016; Johnson et al., 2003). Of interest, the annual incidence of glomerulonephritides in a Europe is as follows: 2.5/100,000 case per adult for IgA nephropathy, 1.2/100,000 case per adult for membranous glomerulonephritis, between 0.6 and 0.8/100,000 case/adult for minimal change disease and for focal segmental glomerulosclerosis and 0.2/100,000 case/adult for membranoproliferative glomerulonephritis (McGrogan et al., 2011).

1.2.3 Definition of MN

Membranous nephropathy (MN) is a rare autoimmune kidney disease with a worldwide incidence of 1/100,000 new cases per year (Maisonneuve et al., 2000). The disease affects patients of all ages, ethnic groups but is quite surprisingly for an autoimmune disease, more common in men than women (ratio 2:1) (Ronco et al., 2017). However, MN is more likely to occur in individuals older than 50 years and is less in the pediatric population.

MN is defined by the increased thickness of the glomerular basement membrane (GBM), due to the presence of large amount of immune complexes sitting there (Figure 1.1 – BC) (Farquhar et al., 1957; Glassock, 2010; Mellors et al., 1957; Movat et al., 1959). In the common idiopathic form of the disease, the immune complexes consist predominantly of IgG4 autoantibodies colocalized with a known or unknown target antigen and are associated with the complement factor C3 in a peripheral capillary loop pattern on immunofluorescence and in electron–dense subepithelial deposits on electron microscopy.

Definitive diagnosis of MN relies on subepithelial immune–complex deposits on renal biopsy visible by electron microscopy (Figure 1.1–B) (Churg et al., 1973; Lai et al., 2015). The early stage I, is characterized by small immune deposits scattered in the subepithelial space. The stage II is characterized by spikes of the GBM around the subepithelial deposits. The stage III is characterized by a basement membrane element surrounding the immune deposits and the stage IV is characterized by complete incorporation of the immune deposits into the GBM.

1.2.4 History of MN

In 1957, David Jones described membranous nephropathy as a distinct morphological entity from minimal change lesions (previously called lipoid nephrosis), membranoproliferative glomerulonephritis (previously called lobular glomerulonephritis) and focal segmental glomerulosclerosis (or probably chronic moderate glomerulonephritis) (Jones, 1957). The histopathological patterns of membranous nephropathy showed GBM thickening visualized as spike–like extrusions seen on light microscopy, a fine granular capillary wall deposition of IgG and complement seen by immunofluorescence in addition to electron dense subepithelial immune deposit seen by electron microscopy (Figure 1.1–BC) (Beck, 2017; Bell, 1946; Ma et al., 2013; SP. Makker, 2011).

In 1959, Heymann and colleagues. discovered that an intraperitoneal injection of a crude kidney extract from Sprague Dawley rats (prepared in Freund's adjuvant supplemented with heat–killed Mycobacterium tuberculosis H37Ra in Lewis rats) induced clinical and pathological lesions similar to what is seen in human membranous nephropathy (Heymann et al., 1959). Several weeks after the immunization, rats developed immune deposits in the kidneys in addition to proteinuria, hypoalbuminemia and hyperlipidemia.

Although Heymann suggested that the immune deposits were due to an autoimmune production against the glomerular tissue, these deposits were long thought to result from glomerular trapping of circulating immune complexes in the blood. In 1978, nearly simultaneously, Couser and colleagues and Van Damm and colleagues showed that an intrinsic antigen present on the podocytes can serve as target for the circulating antibodies rather than the hypothesis of circulating antigen captured by the kidney (Couser et al., 1978; Van Damme et al., 1978). Further studies revealed in 1982 that megalin (gp330) (a membrane glycoprotein of the renal proximal tubular brush border) was the main pathogenic antigen in Heymann nephritis (HN) (Kerjaschki et al., 1982). Proteinuria was shown to be dependent on complement activation (C3, C6 and C5b–9) which in turn causes podocyte injury, cytoskeletal reorganization and loss of the slit diaphragm molecular structure (Cybulsky et al., 1986).

This animal model, now called the rat Heymann nephritis model of MN, provided further impetus to identify the autoantigens involved in the different forms of human MN.

However, while megalin was not identified as an autoantigen in human MN and despite intensified efforts, the identification of the human antigens remained elusive for more than 20 years. Indeed, it is only in 2002 that NEP was identified by Debiec and colleagues. as the first human MN antigen in a very rare alloimmune form of MN (Debiec et al., 2002). This was followed in 2009 by the identification of PLA2R1 as the major autoantigen for about 70% of patients with adult MN (Beck et al., 2009) and in 2014 by the identification of THSD7A as a second autoantigen for 2–5% of another group of patients with adult MN (Tomas et al., 2014). The detailed description of these antigens is provided in chapter 1.3.1.2 of this manuscript.

1.2.5 Multiple clinical forms of MN

MN can be defined as primary (or idiopathic) in about 85% of all MN cases because there is no obvious cause of the disease (hence idiopathic). In the remaining 15% of other cases, MN can be defined as secondary to a "primary" disease affecting another organ, including various cancers, infections, other autoimmune diseases, etc. (see below for a full definition).

– Primary (idiopathic) MN and possible causes (etiologies)

The term idiopathic or primary is used when no obvious cause of MN can be determined after careful examination of the patient, analysis of patients' history and after all laboratory tests regularly performed to assess glomerulonephritis and causes have remained negative (search for cancers, other autoimmune diseases, diabetes, etc.) (Table 1.1).

The etiology of primary MN in general or when associated with anti–PLA2R1 or anti–THSD7A autoantibodies remains in fact largely unknown. Genetically, aside from some rare cases in which more than one member of the same family is affected, MN is not a hereditary transmitted disease (Bockenhauer et al., 2008; Scolari et al., 1998). A genetic polymorphism is detected in PLA2R1 and HLA–D class II MHC alleles and confers a high degree of susceptibility to idiopathic MN, up to 80–fold (Coenen et al., 2013; Stanescu et al.,

2011). However, the pathway behind this predisposition and loss of the self–tolerance to the podocytic antigen is not yet elucidated.

As MN is highly prevalent in the elderly, a number of other diseases have been found to be associated with MN, without being able to demonstrate causality. It is thus unclear whether these diseases are simply co–incidental or at the origin of MN (hence providing a primary cause of secondary MN), or may constitute aggravating factors facilitating the progression of MN to severe cases. For example, MN has been associated with many infections by viruses such as HIV, HBV or HCV (Gupta et al., 2015; Xie et al., 2015), cancers (Cambier et al., 2012; Lefaucheur et al., 2006), autoimmune diseases (Thyroïdites, rhumatoïd arthritis, antiphospholipid antibodies, etc.) (Asami et al., 2016), other nephritis (Alport, IgA nephropathy, etc.) (Nishida et al., 2015), sarcoidosis (Stehlé et al., 2015) or syndromes like Sjogren's (Yoshida et al., 1996) or paraneoplastic ones.

Molecular mimicry has been proposed to be a trigger for anti–PLA2R1 autoimmune reactivity but this remains to be demonstrated (Fresquet et al., 2015). Indeed, Fresquet and colleagues has proposed that an immune response against a viral or bacterial agent may turn into an autoimmune response by cross–reactivity with a self–component, here PLA2R1. Using bioinformatic analysis against microbial protein databases, they identified a protein identity between the sequence LTLENCK in the N–terminal CysR domain of PLA2R1 and the corresponding sequence in the D–alanyl–D alanine carboxypeptidase, a bacterial cell wall enzyme common in several bacterial species including *Clostridium* species.

Recently, an increased incidence of MN has been observed in some regions of China which has been attributed to the environmental air pollution with $PM_{2.5}$ particles (Xu et al., 2016). The molecular mechanisms linking pollution and MN have not yet been identified but interactions between the human genetics and the environment have been proposed (Zhang et al., 2018). In this context, it is suggested that expression of PLA2R1 in the lungs can be upregulated in response to environmental pollution and airway damage. This could trigger an interaction with the antigen presenting cells in the inflamed lungs and lead to the autoimmune reaction against PLA2R1 expressed in the podocyte (Salant, 2019).

As for the THSD7A–associated MN, investigating the possible events that trigger the immune system is currently limited by the low prevalence of this disease, thus rendering

data collection and analysis even more problematic than for PLA2R1–associated MN. Nonetheless, a recent still unpublished study identified a small peptide in the N–terminal region of THSD7A that shares homology with the above immunodominant epitope peptide in PLA2R1. The homology modeling revealed two important areas for antibody binding suggesting that a pathogenic epitope structure may be present in both THSD7A and PLA2R1 and act as a common MN entry point (Rhoden et al., 2017). The above studies and different scenarios remain so far quite speculative. Analysis of large cohorts of THSD7A–associated and PLA2R1–associated MN patients with detailed natural history and serum samples available before the onset of MN disease are still needed to identify the real causes of primary MN and the nature of autoantibodies before worsening of the disease, as it was shown for Systemic Lupus Erythematosus or Pemphigus vulgaris (Arbuckle et al., 2003; Li et al., 2003). Furthermore, the above possible scenarios should be demonstrated by using animal models where such "nephritogenic" peptides or full antigens are injected and processed by the immune system to raise an autoimmune response and induces MN disease.

– Secondary MN

MN should be referred to as secondary MN when there is not only an association with another disease but when it is demonstrated that this latter disease is the underlying cause of MN, as evidenced by targeted therapy of the disease leading to both the cure of the disease and remission of MN. Secondary MN have been found to be "linked" to chronic viral diseases (Hepatitis B and C), cancers (Couser et al., 1974), medications (nonsteroidal anti–inflammatory agents) and autoimmune diseases (systemic lupus erythematosus, ANCA etc.) (Table 1.1) (Larsen et al., 2013; Ronco et al., 2015).

As discussed above, the association between MN (with a primary unknown cause) and other diseases and the causal link between the two diseases (hence secondary) is complicated. Diagnosis of primary versus secondary MN is not always straightforward, thus histopathological features are used to define the form of MN (Huang et al., 2013; Larsen et al., 2013). In contrast to what is known for idiopathic MN, subendothelial and mesangial immune deposits are found in secondary MN. In the case of Lupus– or HIV– associated MN, tubulo–reticular inclusions in endothelial cells can also be detected. Furthermore, an

important difference between the two forms of MN resides in the immunoglobulin subclasses found in immune deposits. In primary MN, IgG4 is the main IgG subclass present in immune deposits, especially at late stages, while IgG1 and IgG3 subclasses can be occasionally detected at the early stages. Thus, primary MN is proposed to be an IgG4–mediated disease. In contrast, in secondary forms of MN, IgG1, IgG2 and IgG3 are predominant and a full house IgG deposition (A, M, G) as well as C1q can be detected in the different stages of the disease (Ma et al., 2013). A detailed description of the IgG subclass predominance can be found in chapter 1.3.1.3. of this manuscript.

– MN by maternal alloimmunization

Very rare cases of MN can affect newborn subjects who present with severe renal lesions and nephrotic range proteinuria, in addition to respiratory distress syndrome and hypertension. These cases are related to a rare alloimmune form of MN where the mother has bi–allelic mutations in the gene coding for NEP (neutral endopeptidase) and are natural knock–out for this gene. The fetus, having inherited a functional allele of the gene from the father, is heterozygous and expresses NEP during development. During the pregnancy (or following a previous miscarriage), the mother is immunized against NEP and develops antibodies which are then transferred through the placenta into the blood flow of the fetus and reach the embryonic kidneys. Thirteen days after birth, the antibody titer decreases in the neonate's circulation and the disease enters into remission, confirming the passive transfer of antibodies from the mother to the fetus, similarly to what occurs in the passive Heymann nephritis model (Debiec et al., 2002; Vivarelli et al., 2015).

Interestingly, in these cases of alloimmune MN, two distinct scenarios were documented: in the first scenario where the main IgG subclass is IgG1, a direct effect of anti–NEP antibodies has been shown on NEP enzymatic activity as well as a pathogenic role due to complement activation. In the second scenario, antibodies were mainly of IgG4 subclass with slight amount of IgG1. Here, the complement pathway was not activated and the IgG4 antibodies had weak inhibitory effect on the NEP enzymatic activity.

Table 1.1 – Classification of the different MN forms and their characteristics. (*) percentage of prevalence calculated based on data in Larsen et al. 2013.

Table 1.1 – Classification of the different MN forms and their characteristics

MN Human forms	Antigen (Mass)	Prevalence (%)	Targeted population Sex ratio Male/female	Antibody subclass	Role of complement	Pathogenicity of antibodies (based on active immunization or passive transfer)	References
Primary		85 (of all cases)					(Beck, 2017; Ponticelli et al., 2014)
PLA2R1-associated MN	PLA2R1 (180 kDa)	70 (of primary cases)	Mostly adults, (age ≥50 years) 2:1 M:F	IgG4>IgG1, IgG3	Likely (C3 and C5b-9 in immune deposits)	Yes, passive transfer based on MN relapse of a human kidney transplanted in a PLA2R1-ab positive patient No available experiments in rodents (endogenous PLA2R1 not expressed in mouse and rat podocytes)	(Beck et al., 2009; Hofstra et al., 2012; Segawa et al., 2010; Yang et al., 2016)
THSD7A-associated MN	THSD7A (250 kDa)	3 (of primary cases)	Mostly adults, 1.3:1 M:F	IgG4>IgG1 >IgG3	Likely	Yes, passive transfer based on MN relapse of a human kidney transplanted in a THSD7A-ab positive patient see also mouse model below	(Tomas et al., 2014; Tomas et al., 2016; Wang et al., 2018)
Double negative	unknown	27	Mostly adults, (age ≥50 years) 2:1 M:F	IgG4>IgG1 >IgG3	Likely	Yes, likely	(Hoxha et al., 2015)
Secondary		15 (of all cases)		IgG, IgA, IgM			(Beck, 2010; Glassock, 1992; Jefferson et al., 2003)
Childhood cBSA	cationic BSA (66 kDa)	<1 (of secondary cases)	Children <5 years	IgG1, IgG4	Likely	Yes, immunization of dogs, mice, rats and rabbits with cBSA. IgG deposits and complement activation in immunized rabbits	(Debiec et al., 2011; Ronco et al., 2015)
Hepatitis B (other infections)	?	14*	Children/ adults	IgG1>IgG4	Likely	not tested	(Larsen et al., 2013)
Sarcoidosis	?	5*	Children/ adults	IgG1>IgG4	Likely	not tested	(Larsen et al., 2013)
Neoplasms	?	15*	Children/ adults	IgG1>IgG4	Likely	not tested	(Larsen et al., 2013)
Other autoimmune diseases (SLE, thyroiditis, etc.)	multiple	58*	Children/ adults	IgG1>IgG4	Likely	not tested	(Larsen et al., 2013)
Alloimmune	NEP	<1%	Neonates	IgG1>IgG4	Yes	Yes, passive transfer from mothers' anti-NEP antibodies	(Debiec et al., 2002; Vivarelli et al., 2015)

Table 1.1 – Classification of the different MN forms and their characteristics

MN animal models	Antigen (Mass)	Prevalence (%)	Targeted population Sex ratio Male/female	Antibody subclass	Role of complement	Pathogenicity of antibodies (based on active immunization or passive transfer)	References
Rat Heymann Nephritis	Megalin (LRP2)	NA	Rodents	rat IgG	Yes complement activation	Yes, active model of Fx1A to rats and passive transfer of anti-Fx1A in rabbits	(Feenstra et al., 1975; Heymann et al., 1959; Kerjaschki et al., 1997; Salant et al., 1988)
Heymann's mouse model	mouse kidney extract	NA	Mouse	mouse IgG	Yes	Yes, active model	(Meyer-Schwesinger et al., 2011)
	NC3 collagen	NA	Mouse	mouse IgG	Yes	Yes, passive model	(Zhang et al., 2012)
THSD7A mouse model	THSD7A	NA	Mouse (Balb/C)	Human total IgG Rabbit IgG	Yes	Yes, passive transfer of human or rabbit anti-THSD7A to mice	(Tomas et al., 2016)

1.2.6 Genetics of MN

Long before PLA2R1 was identified as the major autoantigen in MN, the association of MHC class II and HLA–DQA1 with primary MN has been documented (Klouda et al., 1979; Vaughan et al., 1989). These findings are in accordance with the known risk of autoimmune disease linked to HLA–DQ and HLA–DR (Stanescu et al., 2011) (Chapter 1.1).

More recently, a genome–wide association study (GWAS) in 556 patients from three different Caucasian populations of idiopathic MN identified 2 loci associated with high risk of idiopathic MN (Stanescu et al., 2011). On the chromosome 2q24 containing the gene coding for PLA2R1 (Ancian et al., 1995), the SNP (Single Nucleotide Polymorphisms) rs4664308 was shown to be the target of an autoimmune response. Also, on the chromosome 6p21 containing the gene coding for the HLA–DQA1, the SNP rs2187668 was significantly associated with MN. Interestingly, the 4–fold increase in risk with genetic polymorphism in PLA2R1 augments to 80–fold when combined with homozygosity for HLA–DQA1. The explanation for this increase is still unknown. It is noteworthy that the SNP rs2187668 was strongly associated with MN in Caucasian patients but not in Afro–American patients (Saeed et al., 2014). A sequencing analysis of PLA2R1 in a cohort of 95 patients with either circulating anti–PLA2R1 or PLA2R1 antigen staining detected in kidney deposits led to the identification of 18 SNP variants in PLA2R1, of which 2 were not described previously, 7 were rare variants (<1%) and 9 were common variants. They confirmed 6 of the common polymorphisms as significantly associated with MN (Coenen et al., 2013).

In Han Chinese patients, a GWAS in 261 patients with idiopathic MN identified DRB1*15:01 and DRB1*03:01 as two independent risk alleles for MN (Cui et al., 2017). Another study also showed that HLA–DRB1*15:01 and HLA–DRB3*02:02 alleles are independently and strongly associated with MN in general and with PLA2R1–associated MN in the Chinese population (Le et al., 2017).

1.2.7 Natural history of MN

Understanding the natural history of MN is important to determine if treatment of the disease is appropriate or useful (Glassock, 2010). In 1993, Schieppati et al. studied the natural history of 100 patients with biopsy–proven idiopathic MN diagnosed between 1974

and 1992 and followed for a minimum of 6 months (Schieppati et al., 1993). The patients only received symptomatic treatment consisting of diuretic and antihypertensive drugs. The study showed that a significant fraction of MN patients receiving only symptomatic treatment seem to have a benign course.

After a five year follow up period, 65% of the patients reached partial or complete remission of proteinuria while 16% developed ESRD and required dialysis. The probability of maintaining normal renal function was 88% after 5 years and 73% after 8 years. Additionally, they showed that patients younger than 50 and females had a better prognosis (62% of females and 59% of men had complete or partial remission).

In a more well–defined cohort of 328 patients with only nephrotic syndrome from Spain (Glassock, 2010; Polanco et al., 2010), 32% of patients reached spontaneous remission and most of the remissions occurred in the first two years of follow–up. The study also showed that a progressive decrease of proteinuria by at least 50% during the first year was an indicator of spontaneous remission. Female gender, low serum creatinine and treatment with conservative treatments also tended to associate with remission.

These observations showed that initiating treatment upon diagnosis is not essential except in cases of severe nephrotic syndrome and that it is important to identify new biomarkers of disease severity to identify the patients who are going to develop renal failure and who urgently require the use of immunosuppressive therapy. Some of these observations form the basis for the recommendations found in the KDIGO guidelines for membranous nephropathy, as further developed below (KDIGO Clinical Practice Guidelines)

1.2.8 Clinical features of MN

Clinically, 80% of patients with MN suffer from nephrotic syndrome, i.e. with proteinuria >3.5g/day. It is only in 41% of cases that edema is observed, meaning that MN can manifest in patients without any sign of disease. Hypertension is detected in 55% of cases (Schieppati et al., 1993) and venous thromboembolism occurs in 7% of MN patients, more frequently in the first two years after diagnosis (Lionaki et al., 2012). As mentioned earlier, signs of MN include: proteinuria, hypoalbuminemia, hyperlipidemia, and edema

(Ma et al., 2013). The outcome of the disease varies from spontaneous remission to end stage renal disease (ESRD). Spontaneous remission occurs in 40% of cases within the first two years of presentation. This is usually linked to low proteinuria levels, female sex and age below 50 years. The remaining patients can be divided into those with persistent proteinuria fluctuating between nephrotic and sub–nephrotic ranges or those who reach ESRD at a median age of 5–10 years after diagnosis (Ponticelli et al., 2014; Ronco et al., 2017). In patients receiving renal transplantation, MN recurrence occurred in 42% and 35% before and after the identification of PLA2R1 and its value as a biomarker of disease activity respectively (Dabade et al., 2008; Quintana et al., 2015).

1.2.9 Treatment of MN

Before the identification of the autoantigens in MN, a series of treatment strategies have been used with different drugs aimed at non–specifically suppressing the immune system (Ruggenenti et al., 2007). Steroids were the first drugs used in the treatment of MN (syndrome, 1979) but later showed poor efficiency as it is not superior to symptomatic treatment alone (Radhakrishnan et al., 2012). More powerful treatments including alkylating agents and steroids were shown effective (Ponticelli et al., 1998) however the cytotoxic effect of these agents discouraged nephrologists to use these treatments (Ruggenenti et al., 2007). Furthermore, calcineurin inhibitors showed beneficial signs in the induction of remission. However, the necessity for long treatment periods raised concerns for nephrotoxicity (Cattran et al., 2001). Among other immunosuppressive treatments, Rituximab showed encouraging results in the treatment of MN as early as 2001 and is now one of the most commonly used immunosuppressors in MN (Remuzzi et al., 2002; Ruggenenti et al., 2015). MN patients at high risk achieve remission and have improved renal function after treatment with rituximab. Furthermore, treatment with Rituximab in complement with the antiproteinuric treatment did not affect safety in the randomized controlled trial of GEMRITUX (Dahan et al., 2017).

Cattran and colleagues. validated a predictive, semi–quantitative algorithm model of idiopathic MN (Cattran et al., 1997). They showed that proteinuria and creatinemia during the first six months after diagnosis was important to predict the outcome of the disease. This model categorized patients based on proteinuria and kidney function: low risk patients

(normal renal function and proteinuria <4 g/day), medium risk patients (normal renal function and proteinuria >4 g/day and <8g/day) and high–risk patients (with or without renal insufficiency and proteinuria >8 g/day).

Currently, the evaluation and treatment of MN patients follow the Kidney Disease–Improving global outcomes (KDIGO) guidelines established in 2012 (Radhakrishnan et al., 2012). It recommends clinicians to initiate a symptomatic treatment using anti–hypertensive drugs such as angiotensin–converting enzyme (ACE) inhibitors or angiotensin receptor blockers for an initial 6 months period. The initiation of immunosuppressive treatment in patients with nephrotic syndrome is recommended when at least one of the listed conditions is fulfilled:

– Proteinuria superior to 4g/day and remains at over 50% of the baseline value, and does not decrease progressively after the initiation of the conservative treatment of at least 6 months;

– The presence of severe or life–threatening symptoms related to the nephrotic syndrome;

– A 30% or more increase in serum creatinine levels within 6 to 12 months from the time of diagnosis with an estimated glomerular filtration rate (eGFR) not lower than 25–30 ml/min per 1.73m^2 and not explained by any superimposed complication.

1.3 Physiopathology of MN

1.3.1 Immunoregulation and inflammation in MN

The initiation of an autoimmune response can be the result of a loss of tolerance at the central or peripheral level due to the modification in expression or conformation of the autoantigen (including post–translational modifications generating neoepitopes on the self–protein) or to epitope molecular mimicry. In MN, the following evidence support a role of various immune cells in raising the autoimmune response, with a possible role for a loss of peripheral tolerance. The increase in Th2 cytokines stimulates B lymphocytes to produce IgG4 antibodies targeting the specific antigens involved in MN (Hirayama et al., 2002; Kuroki et al., 2005). Detection of circulating autoantibodies secreted by plasma cells arising from B lymphocytes indicates that the B lymphocytes have a major role in the pathogenesis

of the disease (Wang et al., 2011). Cui et al. used predictive algorithms to predict T–cell epitopes within the CTLD1 and CTLD7 domains of PLA2R1, potentially linking the T–cell and B–cell epitopes of PLA2R1 (Cui et al., 2017). Besides the B–T cell education system to produce antibodies, other immune cells like Tregs play a fundamental role in the control of tolerance (Gratz et al., 2014; Sakaguchi et al., 2010). The imbalance between the self–specific effector T cells that attack tissues and the Treg cells that normally controls these latters leads to autoimmune diseases. Recent studies have shown that patients with active MN have low levels of Treg cells (Roccatello et al., 2016; Rosenzwajg et al., 2017). A successful treatment with Rituximab leads to depletion of B cells and a concomitant increase of Treg cells before clinical remission of proteinuria. Inversely, the percentage of Tregs remains low in patients not responding to Rituximab or receiving only a symptomatic treatment.

Very little is known about the inflammatory cell infiltration in the glomeruli of patients with MN. B cells infiltrates have been described in membranous nephropathy mostly in the tubulointerstitium part of the nephron but not in the glomeruli (Segerer et al., 2008). These infiltrated B cells along with T cells and dendritic cells form tertiary lymphoid organs in the inflamed tissue with a complex cell organization similar to that of the secondary lymphoid organs, suggesting a sustained local production of autoantibodies possibly associated with chronic inflammation. On the other hand, cell infiltration in the glomeruli was shown to be two–fold higher in cancer–associated MN as compared to idiopathic MN patients (Lefaucheur et al., 2006). Within the glomeruli, the mesangial cells constitute a particular cell type that strongly respond to the local inflammation and may participate to MN physiopathology. In vitro cultured rat mesangial cells have been shown to express PLA2R1 and release secreted PLA2–IIA in response to TNF–alpha or other inflammatory stimuli (Beck et al., 2003). In vivo, in the rat Thy–1 glomerulonephritis model, an overexpression of PLA2R1 and sPLA2s has been observed in the glomeruli, together with invasion by immune cells (Beck et al., 2006). However, the role of mesangial cells in local inflammation possibly leading to accelerated podocyte injury, as well as the expression and role of PLA2R1 and sPLA2s in these cells, all in the context of the Heymann rat nephritis model and of human MN, is simply unknown. Finally, in line with the role of PLA2R1 in cellular senescence (Augert et al., 2009; Vindrieux et al., 2013), it is interesting to note the increased staining of the senescence marker p16(INK4A) in the kidney biopsy of patients

with glomeulonephritis, suggesting a role for somatic cellular senescence in the progression of the disease (Sis et al., 2007).

1.3.2 Immune complexes

In most cases of MN, i.e. idiopathic MN, immune deposits consist of immune complexes between podocyte proteins and IgG autoantibodies and various factors from the complement pathway. In this section, we will introduce the different hypotheses explaining the formation of these deposits in addition to a thorough review of the different antigens and IgG subclasses involved.

1.3.2.1 Mechanisms of deposition of immune complexes

Back to the initial studies, Heymann proposed that the deposition of immune complexes in the active glomerulonephritis rat model resulted from binding of free circulating autoantibodies to a "fixed antigen" located *in situ* in the glomerulus and not from a soluble antigen already present in serum and pre–forming circulating immune complexes (Okuda et al., 1965; SP. Makker, 2011). The concept of circulating immune complexes as a source of the glomerular deposits proposed by Germuth and Dixon et al. was adapted to explain the granular deposits in active Heymann nephritis model (Dixon et al., 1961; Germuth et al., 1955). Heymann's hypothesis was experimentally proven later by Van Damme, Couser and colleagues. Extending the rat Heymann passive model, they demonstrated by *ex vivo* bloodless kidney perfusion that injection of autoantibodies free of antigen rapidly formed *in situ* immune complexes with a fixed podocyte antigen thus supporting the "fixed antigen" model (Figure 1.2) (Couser et al., 1978; Van Damme et al., 1978). In rats, the antigenic target called "megalin" is highly expressed at the surface of the proximal tubular cells and also at the sole foot processes of the podocytes (Kerjaschki et al., 1983). Upon binding of the IgG to megalin at the surface of the podocyte membrane, the membrane–bound antigen would undergo shedding by proteolysis (Chapter 5.3.2.) and subsequent cross–linking with circulating antibodies and immobilization in the GBM, thus escaping clearance by endocytosis. Repeated cycles of this mechanism would lead to large immune deposits (Kerjaschki et al., 1983).

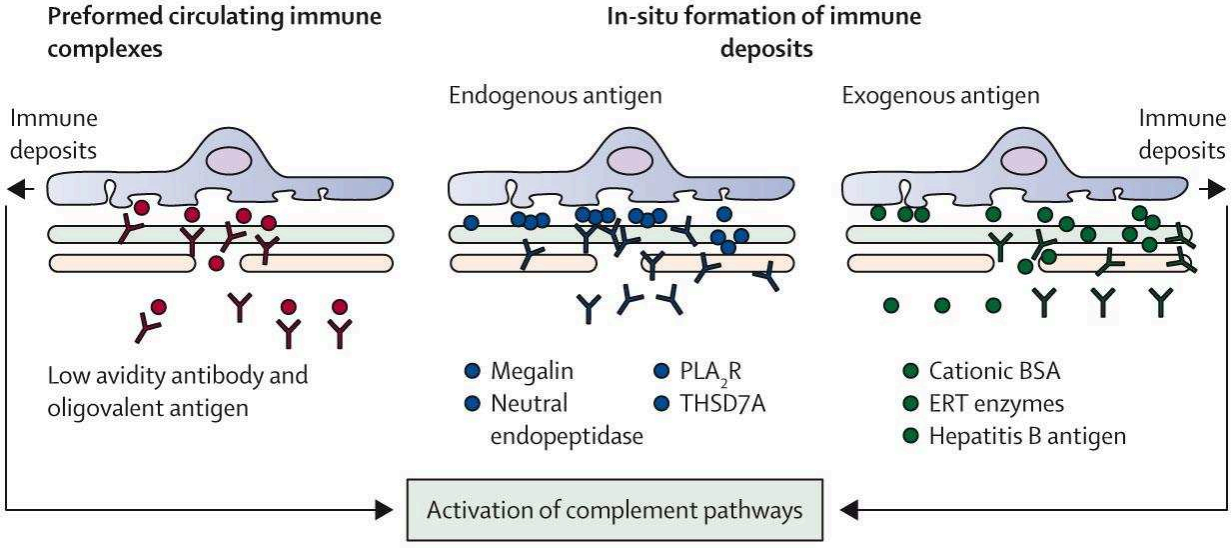

Figure 1.2 – Possible scenarios for immune complex formation and deposition in MN. Three possible scenarios would occur to explain the formation and accumulation of the immune complexes. On the left, pre–formed circulating immune complexes would accumulate and form deposits in the GBM. In the center, endogenous proteins expressed on the podocyte (Megalin, NEP, PLA2R1, THSD7A) can be directly targeted by circulating autoantibodies. On the right, circulating antigens can be first "planted" in the GBM and this is followed by the *in–situ* binding of circulating free antibodies. This is the case for cBSA, enzyme replacement therapy or the hepatitis B antigen. The accumulated antibodies would then activate the complement pathways (classical, alternative or lectin pathway) and induce podocyte injury and proteinuria. *Adapted from (Ronco et al., 2015) with copyright permission from "Elsevier".*

Nowadays, three potential scenarios have been proposed for subepithelial immune complex formation in the various forms of primary and secondary MN (Figure 1.2) (Glassock, 2009; Ronco et al., 2015). In the first scenario that follows the Heymann hypothesis, an “intrinsic antigen” is endogenously expressed at the foot processes of the podocytes and serve as a target for circulating antibodies to form immune complex deposition *in situ*. This scenario applies for the four identified integral membrane glycoproteins of podocytes including megalin in the Heymann nephritis model (Heymann et al., 1959), NEP in neonatal MN (Debiec et al., 2002), as well as PLA2R1 (Beck et al., 2009) and THSD7A (Tomas et al., 2014) in adult MN. The second scenario corresponds to a “planted antigen” extrinsic to the glomerulus (Figure 1.2). The autoantigen, from a variety of sources, leaves the circulation and gets trapped in the subepithelial space. This is the case for cationic bovine serum albumin (cBSA) in secondary MN (Debiec et al., 2011). Deposition of circulating cBSA along the anionic glomerular capillary wall is followed by anti–cBSA IgG binding and leads to immune complex formation *in situ*. The third scenario involves the deposition of pre–formed “circulating immune complexes” (Figure 1.2). This mechanism was only documented in rare cases of MN secondary to infection by the hepatitis B virus (HBV). HBV antigens were detected free or IgG–associated in the serum and the glomerular capillary walls of two MN patients (Takekoshi et al., 1979). However, this scenario was never confirmed in corresponding animal models of MN. It should be pointed out that the above scenarios are not exclusive one to another, and they may "co–operate" to form immune deposits.

1.3.2.2 The antigens in MN

Membranous nephropathy is a remarkable autoimmune disease in which an experimental animal model, the Heymann's model, was established much before we knew the antigens and the underlying molecular mechanisms responsible for the various forms of human MN. Indeed, the molecular pathogenesis of the Heymann's model was established long before the identification of any human antigens, and actually most of what we know today about human MN was in fact established in the Heymann's model and could be predictable from this model.

Walter Heymann and his colleagues established the first experimental model of MN in the late 50s, and it was about 20 years later that megalin (gp330 or Lrp2) was identified as the main nephritogenic antigen in rat podocytes (Figure 1.3) (Heymann et al., 1959; Kerjaschki et al., 1982). Unfortunately, translation of the Heymann nephritis model to the human physiopathology was not possible as it turned out that megalin is not the autoantigen in human MN. Furthermore, megalin is mostly located in the proximal brush border in humans and was recently found to be involved in another rare autoimmune kidney disease called "Anti–Brush Border Antibody" (ABBA) disease (Larsen et al., 2018).

It was in 2002, 20 years after the identification of megalin in the rat model, that the seminal work of Debiec and colleagues. identified NEP as the first human antigen in the rare alloimmune form of MN (Figure 1.3) (Debiec et al., 2002). However, NEP was not the antigen for the more frequent form of "sporadic" idiopathic adult MN and it was only in 2009, exactly 50 years after the Heymann rat model was established, that PLA2R1 was identified as the major autoantigen in adult MN for about 70–80% of MN patients (Figure 1.3) (Beck et al., 2009). THSD7A was then identified as a second autoantigen for another group of patients of about 3% (Figure 1.3) (Tomas et al., 2014). Together, the antigens and autoantigens have now been identified for about 80% of MN patients. However, we still miss the autoantigen(s) for the remaining group of about 20% of patients with adult MN, who are "double negative" for PLA2R1 and THSD7A, and these patients are thus still "orphans" for the antigenic target of their MN disease.

– Megalin in Heymann Nephritis

In the early 80s, megalin was identified as the principal pathogenic antigen in Heymann nephritis (Kerjaschki et al., 1982). Also known as gp600, gp330 or LRP2, megalin is a giant type 1 transmembrane glycoprotein of 600 kDa that belongs to the low–density lipoprotein receptor superfamily (LDLR) (Figure 1.3). In rat kidneys, megalin is located in large amounts in the renal proximal tubule but also in the podocytes (Kerjaschki et al., 1983). In human kidneys, megalin is highly expressed in the proximal tubules, and in fact lower levels in podocytes (Prabakaran et al., 2011).

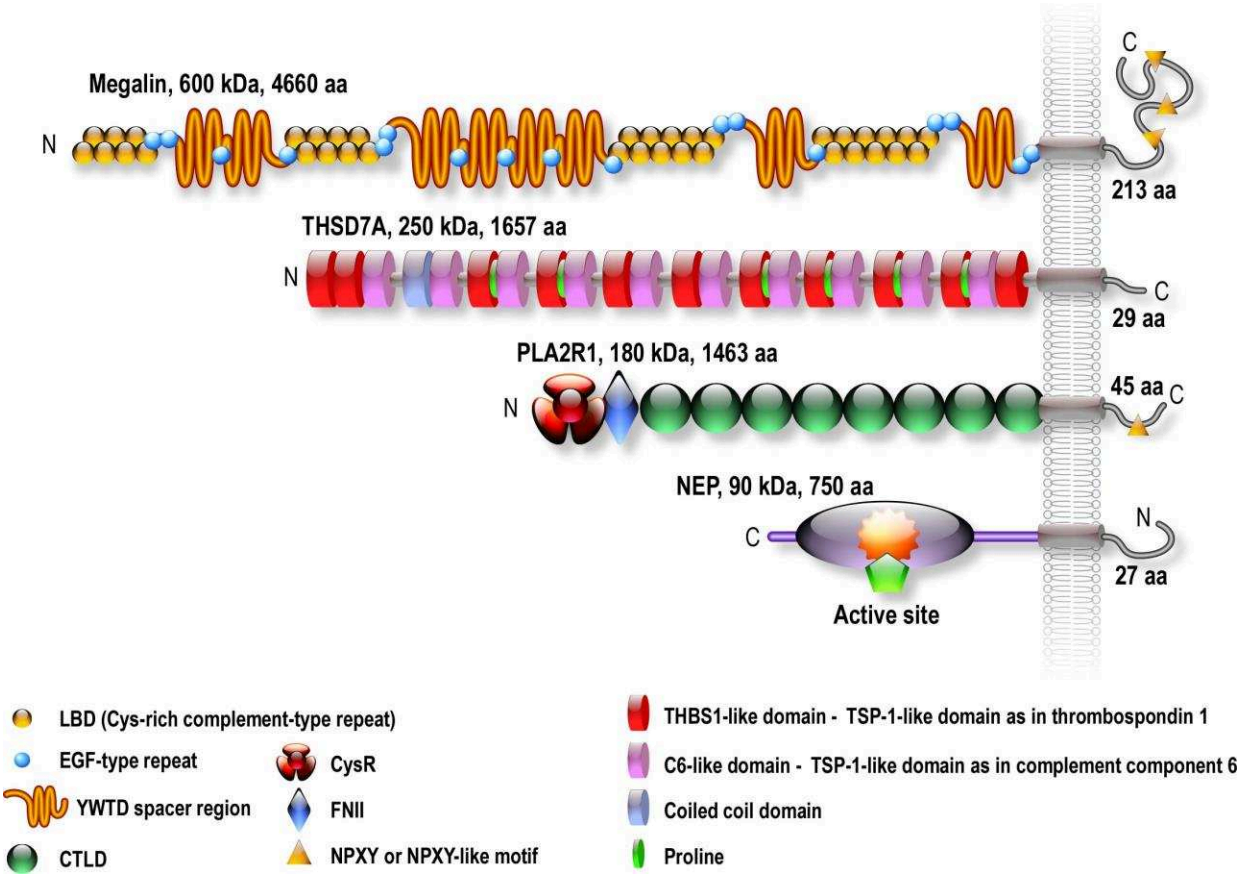

Figure 1.3 – Schematic structures of the four antigens implicated in MN. Megalin is the antigen of the Heymann nephritis model. PLA2R1 and THSD7A are the antigens in 70–80% and 3% of patients with idiopathic MN, respectively. NEP is the antigen responsible for a rare alloimmune form of MN. The antigens are ranked by size, megalin being the largest antigen with a molecular mass of 600 kDa, followed by THSD7A, 250 kDa, PLA2R1 180 kDa and NEP, 90 kDa. Megalin contains four ligand binding domains (LBD) with each domain containing one ligand binding repeat flanked with epidermal growth factor–type repeats. Megalin also contains 3 NPXY internalization motifs. THSD7A is formed by an alternation of TSP–1 repeat and C6–like repeats with a short intracellular tail but no obvious internalization signal. PLA2R1 is composed of a cysteine–rich domain followed by a type–II fibronectin domain and eight C–type lectin domains (CTLDs) and a cytoplasmic tail with an NPXY internalization motif.

Although the investigation of the Heyman nephritis model contributed greatly to our understanding of the pathophysiology of human MN, it was limited by the fact that megalin was not the main autoantigen in patients' immune deposits (Table 1.1).

– The neutral endopeptidase (NEP)

The neutral endopeptidase (NEP) is the first human podocytic antigen identified in a rare form of alloimmune–associated MN in the neonates. NEP (also known as Neprilysin or Enkephalinase or CD10) is a transmembrane zinc–containing metalloproteinase of 90–110 kDa (Figure 1.3). It is expressed in the kidney in podocytes, in the brush borders of the proximal tubules and in the vascular walls of the kidney. It is also expressed in various tissues and cells including brain, smooth muscle cells, cardiomyocytes and neutrophils. In the brain, NEP degrades the β–amyloid peptide involved in the Alzheimer's disease. NEP also degrades many peptides such as substance P, glucagon and oxytocin. In the kidneys, NEP cleaves angiotensin II, bradykinin and natriuretic peptides, thereby participating in the regulation of blood circulation in nephrons (P. Judge, 2015).

In neonate alloimmune MN, the mother has a homozygous null mutation in the MME (Metallomembrane Endopeptidase) gene while the father has a functional gene. During pregnancy or following a previous miscarriage, the mothers' immune system is exposed to the NEP expressed by the fetus and initiates a typical immune reaction against NEP. The maternal IgGs (mainly of IgG1 or IgG4 subclass) cross the placenta, bind to fetal glomerular podocytes expressing NEP and cause antenatal renal disease (Table 1.1). Kidney biopsy staining of the infant shows an unusual form of glomerulonephritis with distended Bowman's spaces and collapsed capillary tufts.

It is important to mention that although the life span of the maternal IgG is short, the antenatal nephron loss may lead to chronic renal failure in the adult life (Debiec et al., 2002; Debiec et al., 2004; Vivarelli et al., 2015). These findings also demonstrate that a podocyte antigen can be at the origin of formation of immune deposits in human MN (following the above scenario for in situ antigen). However, alloimmune cases of MN are very rare, and NEP is not the autoantigen in adult primary MN.

– The phospholipase A2 receptor 1 (PLA2R1)

Secreted phospholipases A2 are abundant in snake and bee venoms and are responsible for many toxicities towards preys (Gutiérrez et al., 2013). This includes neurotoxic, myotoxic, pro–inflammatory and cardiovascular toxic effects. The molecular mechanisms involved in these toxic effects are multiple and were proposed to be due to either the complex enzymatic activity of venom sPLA2s or to direct binding to putative soluble and membrane–bound proteins (Kini et al., 1989).

In the early 90's, two novel receptors for sPLA2s were discovered in the team of Dr. Lambeau. A first type of sPLA2 receptors of around 40–50 kDa was identified in rat brain neurons (hence called N–Type) and binds neurotoxic sPLA2s (Lambeau et al., 1989). This N–type receptor has not been cloned and thus its structure, endogenous ligands and function are still unclear. Several brain proteins have been identified by others since then but their relationship to N–type receptors is unclear (Šribar et al., 2014). A second sPLA2 receptor of 180 kDa was discovered in rabbit skeletal muscle cells in 1990 and called the M –type phospholipase A2 receptor (now called PLA2R1) (Lambeau et al., 1990). The M – type receptor was purified, partially sequenced and finally cloned from rabbit and human species in our laboratory (Ancian et al., 1995; Lambeau et al., 1994) and also from mouse and bovine species by Shionogi Pharmaceuticals in Japan (Higashino et al., 1994; Ishizaki et al., 1994).

Molecular cloning has revealed that PLA2R1 belongs to the C–type lectin superfamily and share a number of structural properties with 3 other proteins from the mannose receptor lectin subgroup: the macrophage mannose receptor (MRC1), Endo180 (MRC2) and DEC205 (LY75) (East et al., 2002). PLA2R1 is a large type I transmembrane glycoprotein of 180 kDa and consists of a large extracellular domain, a single transmembrane segment and a short cytoplasmic tail (Figure 1.3).

The extracellular domain of PLA2R1 consists of an N–terminal Cysteine–rich (CysR) domain, a fibronectin type II domain (FNII) and 8 different C–type Lectin (CTLD) domains in tandem (Ancian et al., 1995; Ancian et al., 1995; Lambeau et al., 1994).

Human PLA2R1 was cloned from kidney tissue (Ancian et al., 1995), but it was not known that the protein is specifically expressed in the podocytes until it was identified as the target autoantigen in MN. However, PLA2R1 is also expressed in proximal tubules and

overall (Vindrieux et al., 2014), its relative and precise cellular distribution along the nephron and in the different sections of the kidney is still incomplete. Depending on the species, PLA2R1 is also expressed by immune tissues and cells such as spleen, macrophages and type II alveolar cells in the lungs, but also liver, pancreas, small intestine and colon including Paneth cells (Cupillard et al., 1999; Schewe et al., 2016), thyroid, testis, ovaries and placenta (Ancian et al., 1995; Granata et al., 2005; Higashino et al., 1994). Of note, large differences in the expression of PLA2R1 exist among species, and PLA2R1 is not expressed in mouse and rat kidney podocytes (Meyer-Schwesinger et al., 2015).

The biological roles of PLA2R1 are not well understood (Girard et al., 2014; Lambeau et al., 1999). PLA2R1 is likely a multifunctional and multiligand receptor. PLA2R1 has been shown to bind and inhibit, as well as quickly internalize and degrade multiple sPLA2s, and acts as an endogenous receptor for several sPLA2s (Ancian et al., 1995; Ancian et al., 1995; Cupillard et al., 1999; Lambeau et al., 1995; Nicolas et al., 1995; Rouault et al., 2007; Zvaritch et al., 1996). In line with these $sPLA_2$ binding properties, it may play a role in controlling sPLA2 enzymatic activity in various inflammatory conditions like sepsis and asthma (Hanasaki et al., 1997; Nolin et al., 2016). PLA2R1 binds collagen, suggesting a role in cell adhesion (Ancian et al., 1995; Skoberne et al., 2014; Takahashi et al., 2015) and different types of sugars, indicating some functions as a lectin (Ancian et al., 1995; Lambeau et al., 1994). Finally, PLA2R1 has been proposed to function as a tumor suppressor gene by initiating replicative or oncogene–induced senescence through the p53 pathway or other signaling pathways (Augert et al., 2013; Vindrieux et al., 2013; Vindrieux et al., 2014).

After half a century of extensive investigations to discover the human autoantigens of idiopathic MN, a collaboration between the team of David Salant and Laurence Beck in Boston and our team has finally led to the identification of PLA2R1 as the major autoantigen in adult MN (Table 1.1) (Beck et al., 2009). It all started when Dr. Laurence Beck was testing the reactivity of serum from MN patients by western blot using crude extracts of human glomerular proteins. It is only under non–reducing that a strong and specific reactivity was found against a protein of about 180 kDa. From 37 patients with idiopathic MN, 27 (70%) recognized the 180 kDa band.

In contrast, serum from control donors or secondary MN failed to react with this protein. The antigen was highly glycosylated since treatment with N–glycosidase F caused

a shift in mobility to 145 kDa. The deglycosylation of the antigen did not affect the reactivity for the antigen indicating that the binding of the antibodies is independent of glycosylation.

The identification of the target antigen was done by a western blot approach coupled to mass spectrometry: the area of interest after gel electrophoresis was excised, digested and the resulting peptides were analyzed by mass spectrometry. A list of candidate antigens was generated among which PLA2R1 was present. PLA2R1 was confirmed to be the genuine autoantigen when the recombinant PLA2R1 protein was expressed in HEK293 cells and found to react with the same patients' antibodies that also react to a similar band in the human kidney protein extract. Moreover, immunoprecipitation of the glomerular extract with the patients' serum revealed a 180 kDa band detected by anti–PLA2R1 specific antibodies in western blots.

Additionally, PLA2R1 colocalized with IgG4 staining in kidney biopsy from patients with MN and elution of glomerular immune complexes contained anti–PLA2R1 antibodies. In this study, the IgG4 subclass antibodies were predominant while other IgG subclasses were found in lower amounts. Of importance, the reactivity of anti–PLA2R1 autoantibodies was exclusively seen under non–reducing conditions, indicating that these autoantibodies only recognized conformational epitopes. This unique and relatively uncommon property of autoantibodies explains, at least in part, why it took so long to identify the MN autoantigen.

After this discovery, many studies confirmed that PLA2R1 is the main autoantigen in MN and that the predominant IgG subclass of anti–PLA2R1 autoantibodies is IgG4 (Beck, 2017; Ronco et al., 2010; Wetzels, 2018).

– Thrombospondin type–1 domain containing 7A (THSD7A)

After the identification of PLA2R1 as the major antigen in 70% of the patients with MN, investigation continued to identify the antigen(s) in the remaining 30% of patients. It began when Dr. Beck in Boston identified a unique case of a patient with MN and prostate cancer (Table 1.1) (Beck, 2010). This patient recognized by western blot of human kidney

glomerular extract a band of around 180 kDa, i.e. similar in size to that of PLA2R1 but clearly different based on immunoprecipitation and cross–reactivity studies.

At the same time, in our lab, we had started the identification of the second antigen by the same approach on human kidney extract but also by a candidate approach based on the hypothesis that the above antigen identified by Beck could be one of the paralogs of PLA2R1 which have similar molecular masses, i.e. the macrophage mannose receptor 1 (MRC1, 180 kDa), endo–180/c–type mannose receptor 2 (hMRC2, 180 kDa) or the dendritic cell receptor DEC–205/lymphocyte antigen 75 (hLY75, 205 kDa). Our strategy led us to pick up a first patient with MN and HIV from the Nice hospital. Like in Beck's experiments, the patient's serum recognized a similar band of around 200 kDa by western blot, slightly higher than that of PLA2R1.

In experiments aimed to exclude that the reactivity was not on a particular longer form of PLA2R1 but really different from PLA2R1 and specific, the antigen was found to have a more accurate molecular mass of around 250 kDa and was identified in both Lambeau and Beck laboratories by two related mass spectrometry approaches. In the first, the glomerular extract was treated with N–glycopeptidase F alone or with both N–glycopeptidase F and neuraminidase, and western blot analysis revealed three bands of 250 kDa, 225 kDa and 200 kDa. In the second strategy, the glomerular extract, with or without N–glycopeptidase F deglycosylation, was digested with trypsin. Western blot analysis and Coomassie staining were performed in parallel for the different fractions under non–reducing conditions. The corresponding bands were excised and analyzed by mass spectrometry. A list of potential candidates was generated and after validation of each protein by recombinant expression in HEK293 cells, thrombospondin type–1 domain containing 7A (THSD7A) was finally identified as the same autoantigen recognized by the two patients' sera (Figure 1.3) (Tomas et al., 2014).

A combined screening of 154 MN patients negative for anti–PLA2R1 extracted from a European cohort and a Boston cohort led to the detection of 15 patients with serum positive for anti–THSD7A reactivity, indicating a 2.5 to 5% prevalence in the general MN population and 8 to 14% in the PLA2R1–negative MN population. Importantly, none of the 15 patients were positive against PLA2R1, i.e. they were not double–reactive.

Immunofluorescence staining of kidney biopsies showed the colocalization of THSD7A and nephrin at the proximity of the foot processes, suggesting that THSD7A is expressed on the glomerular podocytes rather than at the glomerular basement membrane.

Also, similarly to what was found for PLA2R1–associated MN patients, anti–THSD7A antibodies were predominantly IgG4 and conformational as they reacted against THSD7A only under non–reducing conditions, and there was a colocalization of IgG4 antibodies and THSD7A on kidney biopsy. The structure of THSD7A is detailed in chapter 2.3.

– Double positivity for PLA2R1 and THSD7A

In 2016, Larsen and colleagues stained 258 kidney biopsies from patients with membranous nephropathy for PLA2R1 and THSD7A (Figure 1.5) (Larsen et al., 2016). The screening identified 2 patients (i.e. less than 1% of patients) with dual positivity for PLA2R1 and THSD7A. These dual positive MN patients showed enhanced granular staining for both PLA2R1 and THSD7A on the biopsy and circulating autoantibodies against both antigens in serological testing. Two additional patients with dual positivity (0.34%) were also identified by Wang and colleagues after screening 578 patients with MN (Wang et al., 2017). Here, the potential dual positivity was challenged by competition assays on ELISA and lysates from HEK293 expressing each of the two antigens. Competition with PLA2R1 did not inhibit binding of anti–THSD7A to THSD7A and vice versa for PLA2R1. These results further confirmed the absence of cross–reactivity of anti–THSD7A towards PLA2R1 and vice–versa. Additionally, immunofluorescence staining showed that PLA2R1 and THSD7A colocalized in the immune deposits in glomeruli. Finally, the two studies agreed on the importance of employing a "panel–based approach" during diagnosis of MN patients. This would avoid treating patients based on a single autoantibody type when a second autoantibody could be also driving the pathogenesis of the disease.

– Cytoplasmic antigens

In 1999, α–enolase, a glycolytic enzyme highly conserved among species, was reported as a new MN target autoantigen by probing sera from idiopathic MN patients against

human and porcine renal extracts in western blot assays performed under reducing conditions (Wakui et al., 1999). Anti–α–enolase antibodies were mainly IgG1 and IgG3. The presence of α–enolase antibodies was not however restricted to MN since antibodies have been detected in other diseases such as ANCA disease (Moodie et al., 1993) and systemic lupus erythematosus etc. (Pratesi et al., 2000).

More recently, in 2010, antibodies targeting aldose reductase (AR) and superoxide dismutase 2 (SOD2) (Bruschi et al., 2011; Prunotto et al., 2010) were found in sera and glomeruli of idiopathic MN patients. Antibodies against these cytoplasmic antigens were mainly IgG4 and colocalized with C5b–9 in electron–dense immune deposits from kidney biopsy.

In 2012, a study by Murtas et al. included a cohort of 186 MN patients to test for the different autoantibodies: PLA2R1, NEP, AR, SOD2 and α–enolase (Murtas et al., 2011). Antibodies against PLA2R1 were found in 60% of the cases while anti–AR, anti–SOD2 and anti–α–enolase were found in 34%, 28% and 43% respectively. Antibodies were mainly IgG4 and anti–PLA2R1 correlated significantly with the anti–AR, anti–SOD2 and anti – α – enolase. They also showed that only the absence of the four antibody types is associated with lower proteinuria at 1 year. It is important to mention that the coexistence of several autoantibodies in the serum from a single patient suggests a complex and progressive pathophysiological mechanism in MN.

– Other antigens like cationic BSA

In some rare cases of MN, the antigens detected in the subepithelial deposits are of exogenous origins (Table 1.1). This is the case for Hepatitis B or *Helicobacter Pylori* (Debiec et al., 2014; Nakahara et al., 2010). Many possibilities might explain these findings: the physiochemical properties can cause trapping of the antigen at the glomerular capillaries, as this was nicely shown for cationic BSA (cBSA) in early–childhood cases of MN (Figure 1.2) (Debiec et al., 2011). Also, non–precipitating immune complexes containing IgG4 and these antigens can be trapped at the GBM as it is documented in the chronic serum sickness model (Debiec et al., 2014).

– Common features of the main MN antigens

As presented above, different major and specific endogenous proteins have been identified as target antigens in MN. In Heymann nephritis, megalin was identified as the podocyte antigen but this is exclusively true in rats. Later, NEP was identified as the autoantigen in an alloimmune form of MN in neonates. Soon after, PLA2R1 was identified as the major autoantigen and THSD7A as the second antigen involved in idiopathic adult MN. Interestingly, these antigens share structural features that may explain their central role in the pathophysiology of MN in humans but also in animal models (Figure 1.3).

All four antigens are transmembrane glycosylated proteins that can be expressed in various areas of the kidney but at least to some extent in podocytes (NEP, PLA2R1 and THSD7A in human podocytes, and megalin in rat podocytes). Interestingly, these antigens can also be present in other tissues while the pathogenicity of MN seems to be "organ–specific", limited to the kidney. This suggests that the circulating autoantibodies cannot reach their antigen target in these tissues or that the formed immune complexes, if any, are not detrimental for the organ function.

I will further compare below PLA2R1 and THSD7A as the two main autoantigens in adult MN. In human glomeruli, both proteins are expressed in podocytes. PLA2R1 seems to be expressed on both foot processes and cell body while THSD7A is restricted to foot processes and the slit diaphragm (Gödel et al., 2015). It is important to note here that PLA2R1 is not expressed on podocytes in rodents contrary to THSD7A (Meyer-Schwesinger et al., 2015; Vindrieux et al., 2014).

PLA2R1 and THSD7A are both involved in MN, yet they belong to two different protein families: PLA2R1 belongs to the superfamily of C–type lectins and its ectodomain consists of an N–terminal cysteine–rich domain, a fibronectin type II domain and eight C–type lectin domains (Ancian et al., 1995). THSD7A on the other hand, belongs to the thrombospondin repeats superfamily and its extracellular domain consists of 21 domains of alternating TSP–1–like repeats and C6–like repeats (Except domain 1 and 2) (Figure 1.3) (Seifert et al., 2018).

To date, the function of the two proteins in the podocytes is not clear, yet they seem to be involved in cell and foot processes adhesion, and a soluble form generated by proteolysis or shedding of the full transmembrane protein have been documented for both antigens

(Higashino et al., 2002; Kuo et al., 2011). Furthermore, a splice variant directly coding for a soluble form of PLA2R1 has been identified in human kidney (Ancian et al., 1995). It is suggested that PLA2R1 might be implicated in cell adhesion and ECM remodeling by binding and internalization of collagens I and IV through the FNII domain (Takahashi et al., 2015). Additionally, adhesion of podocytes to collagen IV was inhibited when these latter were exposed to anti–PLA2R1 antibodies (Skoberne et al., 2014). The investigation of the specific function of PLA2R1 in podocytes *in vivo* is somewhat limited by the fact that PLA2R1 is not expressed in rodent podocytes.

THSD7A also plays a role in cellular adhesion in HUVEC cells (Wang et al., 2010) and primary podocytes *in vitro*. Incubation of podocytes with anti–THSD7A altered podocyte morphology by increasing stress fibers and stimulating focal adhesion signaling (Tomas et al., 2016). In a knockdown model of thsd7a in zebrafish larvae, THSD7A was shown to alter podocyte differentiation and impair the glomerular filtration barrier (GFB) function suggesting a role in the formation of the GFB (Tomas et al., 2017).

The ability of an antigen to shed into the GBM is likely an important factor for the formation of immune deposits (Beck, 2017). In addition to the splice variant coding for a soluble form of PLA2R1 (Ancian et al., 1995), transfection of the membrane–bound PLA2R1 in HEK293 cells leads to the constitutive shedding of the protein and secretion of the full soluble extracellular domain in the medium mediated by ADAM–10 and/or ADAM–17 proteolysis (Unpublished data). Similarly, a soluble form of THSD7A was detected in cell medium and found to promote endothelial cell migration and tube formation in angiogenesis assays (Kuo et al., 2011) (Chapter 5.3.2).

In the context of MN disease, although the development of the autoimmune response and the molecular details of the immune complex formation might be different for each autoantigen, it is remarkable that the severity of MN appears independent of the target antigen. Indeed, patients with either PLA2R1– or THSD7A–associated MN share the same renal disease characteristics, with no major differences in the clinical manifestations. Both PLA2R1 and THSD7A are predominantly targeted by IgG4 autoantibodies with small amounts of IgG1 and IgG3 detected more frequently at earlier stages of the disease or when a possible secondary cause is associated to MN (Huang et al., 2013). All autoantibodies recognize conformational epitopes, and many immunogenic epitopes are targeted on the two proteins linked by a mechanism of epitope spreading for PLA2R1 and may be for THSD7A

(Chapter 1.3.3 and 1.3.4). Indeed, we have obtained evidence that the immunodominant epitope on PLA2R1 is within the CysR domain and that after a second immunological event (like a boost), the autoimmune response would develop towards additional epitopes (C1 and C7) with worsening of the disease (Seitz-Polski et al., 2016). Such a two–step mechanism seems less obvious to occur in patients with THSD7A–associated MN as several epitopes were identified in most patients of a cohort of 31 patients, and in an apparently random manner (Seifert et al., 2018).

Finally, two important features appear to make differences between THSD7A– and PLA2R1–associated MN: First, the male to female ratio seems to differ between the two entities, with a higher female predominance for THSD7A–associated MN (Tomas et al., 2014). Second, THSD7A–associated MN was proposed to be more often associated with malignancy (Hoxha et al., 2017; Tomas et al., 2014). Hoxha and colleagues showed that contrary to PLA2R1, patients with THSD7A–associated MN were more prone to have an associated cancer. In line with these suggestions, THSD7A was detected in different cancerous tissues (Hoxha et al., 2017; Hoxha et al., 2016; Stahl et al., 2017) contrarily to PLA2R1 that is less frequently associated with cancer (Larsen et al., 2013; Qin et al., 2011). Nonetheless, it is important to note that PLA2R1 may play a role in cancer by acting as a kind of tumor suppressor gene (Augert et al., 2009; Augert et al., 2013; Vindrieux et al., 2013). The mechanism of epitope spreading in THSD7A–associated MN patients and their association with a higher risk of cancer development was further investigated in my thesis project, and results are described in chapter 4.1 and 4.2 of this manuscript.

1.3.2.3 The different antibodies in various forms of MN

– Generalities on IgG subclasses and complement pathways

Immunoglobulins G (IgG) are the most abundant immunoglobulin class among the five groups of immunoglobulins in humans (IgM, IgD, IgG, IgA, and IgE). IgG antibodies are one of the major components of the serum and their structure is composed of 82–96% of proteins and 4–18% of carbohydrates (Vidarsson et al., 2014). The IgGs antibodies are classified based on their decreasing order of frequency IgG1 (66%), IgG2 (23%), IgG3 (7%)

and IgG4 (4%) and differ in their heavy chain structure which is related to their distinct effector functions (Doi et al., 1984).

IgG1 response targets soluble and membrane protein antigens and is accompanied by low amounts of other IgGs mainly IgG3 and IgG4. The IgG2 response targets the polysaccharide–coated bacteria and this response can be restricted to IgG2. The IgG3 antibodies have a potent pro–inflammatory function and are effective in the induction of effector functions. Their shorter half–life may be important in limiting the excessive inflammatory reaction. Conversely, IgG4 antibodies have an anti–inflammatory function. They are produced following a long–term exposure to an antigen in a non–infectious setting where they may become predominant. They are also induced by allergens along with IgG1 and IgE (Vidarsson et al., 2014). Therefore, it appears that IgG4 antibodies have a protective role against the other IgG antibodies by competing with epitope recognition and prevent the effector function of the other subclasses of IgG antibodies. The IgG4 antibodies can also undergo Fab exchange by swapping a half of the molecule (heavy chain and attached light chain) with another molecule of IgG4 resulting in a bispecific antibody (van der Neut Kolfschoten et al., 2007). The IgG4 antibodies share 95% sequence homology in the constant domain with the other IgG isotypes. However, a few single amino acid mutations in the IgG4 constant region hamper these antibodies to exert most of the IgG pathogenic functions: P331S for binding to C1q (Tao et al., 1993) and L234F and P331S for binding to the Fc receptor (Canfield et al., 1991). As a result, IgG4 antibodies are unable to activate the classical complement pathway and immune cells. However, IgG4 antibodies may activate the lectin (MBL) complement pathway (Vidarsson et al., 2014).

Briefly, the complement cascade, composed of over 20 different proteins, is a part of the innate immunity required for host defense and inflammation (Figure 1.4). It is activated through the classical, the alternative and the lectin pathway that all lead to the cleavage of C3 and release of C3b opsonin by C3 convertase and to the C5 conversion. The generation of the C5b–9 or the membrane attack complex starts by the cleavage of C5 to produce the C5b which forms a stable complex by binding to C6 and forming C5b–6. This latter initiate pore formation by combining C7, C8 and multiple C9 molecules. The complement cascade is tightly regulated to prevent damaging the host cells (Sarma et al., 2011).

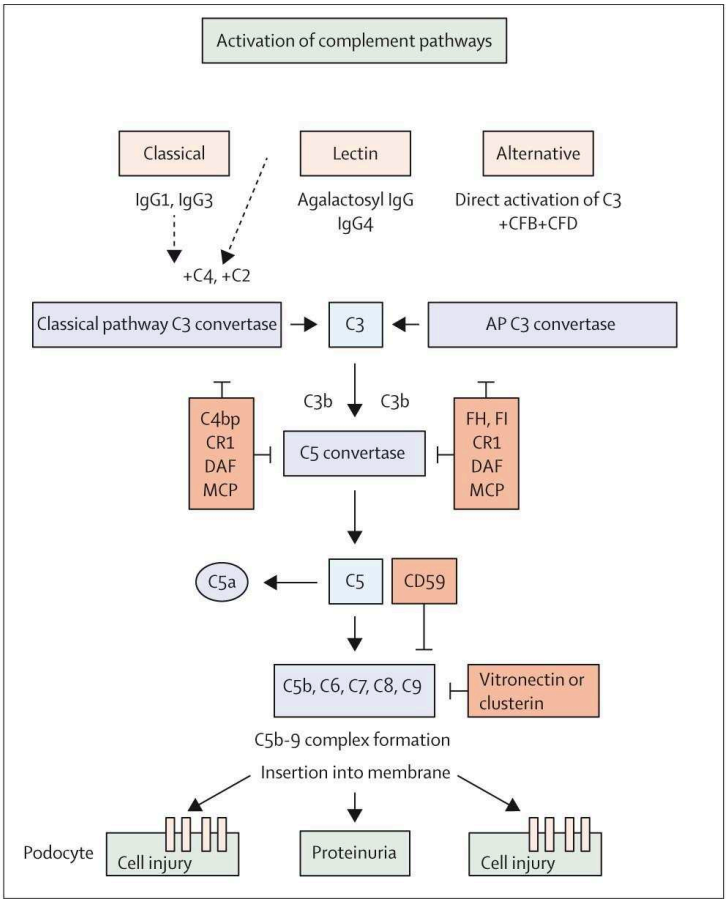

Figure 1.4 – Mechanism of activation of complement pathways. The complement system can be activated through three distinct pathways, each of which being stimulated by different IgG molecules. All the pathways converge towards the activation of C5 by C5 convertase and the formation of C5b. In combination with C6, C7, C8 and C9, the C5b for the C5b–9 also known as the membrane attack complex MAC. The MAC insertion on the podocyte membrane in sublytic levels can induce cellular injury and proteinuria in the absence of inflammation. This mechanism ma y be regulated by circulating and podocyte inhibitors. *Adapted from (Ronco et al., 2015) with copyright permission from "Elsevier".*

– Different predominant IgG subclasses in MN

Various subclasses of IgG autoantibodies can be found in different autoimmune diseases. For instance, in myasthenia gravis, the major antigen target is the acetylcholine receptor AchR and the autoantibodies are mainly IgG1 and variably IgG3, a second autoantigen is LRP4 with predominant IgG1 autoantibodies, and a third autoantigen is MuSK with predominantly but not exclusively IgG4autoantibodies. The reasons for the "switch" in IgG subclasses depending on the target autoantigen are not fully understand but is associated to a Th1/Th2 switch of the autoimmune response (Huang et al., 2013; Warren et al., 2003). Conversely, a growing subgroup of so–called "IgG4 autoimmune diseases", such as thrombotic thrombocytopenic purpura caused by autoantibodies against ADAMTS13 or Pemphigus caused by autoantibodies targeting desmogleins 1 and 3, the autoimmune response appears to be mostly driven by IgG4 autoantibodies (Cetin et al., 2018; Koneczny, 2018).

Long before the main antigen targets of MN were identified, primary (idiopathic) MN was defined by a predominant staining for IgG4 in kidney biopsy (Doi et al., 1984), a finding which is now consistent with the observations in PLA2R1– and THSD7A–associated MN (Beck, 2017; Beck et al., 2009; Tomas et al., 2014). The predominance of IgG4 anti–PLA2R1 and anti–THSD7A in idiopathic MN has been confirmed in many other studies (Table 1.1) (Cheng et al., 2018; Hofstra et al., 2012; Iwakura et al., 2015).

Conversely, IgG1 predominance or codominance with IgG4 is more common in various forms of secondary MN and alloimmune MN (Huang et al., 2013; Vivarelli et al., 2015). For instance, in various cases of cancer–associated MN with unknown antigens, kidney biopsy analysis shows more preponderant staining of IgG1 and IgG2 over IgG4 (Lönnbro-Widgren et al., 2015; Ohtani et al., 2004; Qu et al., 2012) . In secondary MN due to cBSA, both IgG1 and IgG4 antibodies have been found (Debiec et al., 2011). In alloimmune MN due to NEP, the ratio of IgG1 and IgG4 antibodies appear to be different among patients: some patients have mostly IgG1 anti–NEP while others show predominant IgG4 anti–NEP accompanied by low IgG1 antibodies (Table 1.1) (Vivarelli et al., 2015).

The predominance of IgG4 antibody subclass has been also shown to be dependent on the disease state. In stage I idiopathic MN, IgG1 subclass is predominant in the glomerular immune deposits while IgG4 becomes more predominant in later stages of the disease

(Huang et al., 2013). Such a mechanism of IgG subclass switch has been reported in many diseases including Malaria (Tongren et al., 2006) or Endemic Pemphigus Foliaceus (Warren et al., 2003). In this latter, before the onset of the clinical disease, the initial non–pathogenic anti–desmoglein–1 subclass is IgG1; the switch to IgG4 antibodies seems to be key as it is associated with the initiation of the clinical disease (Aoki et al., 2015).

1.3.3 Pathogenic effect of IgG4 antibodies versus other subclasses?

Studies on the pathogenicity of the different antibodies found in the various I and II form of human MN or of antibodies implicated in animal models is complex and I tried to summarize them below, in a step by step way.

Conceptually, after the different IgG subclasses of antibodies bind to their target antigen on the podocyte or its vicinity, the antibody may either directly alter the podocyte biology by blocking the antigen function (like for megalin, NEP, PLA2R1 or THSD7A), or induce complement–mediated podocyte injury (by activating either of the 3 pathways or several of them at the same time), in addition to forming immune complexes along the GBM. Antibodies accumulating in the subepithelial space can thus lead to the activation of the complement system and formation of C5b–9 also known as the membrane attack complex (MAC) (Figure1.4). Insertion of the C5b–9 on the surface lipid bilayer induces sublethal injury and phenotype change in the podocytes which in turn leads to foot process effacement, destruction of the slit diaphragm, and heavy proteinuria. Injured podocytes also produce more extracellular matrix proteins which lead to GBM expansion around the immune complexes and form the characteristic “spikes” visualized by silver staining (Ma et al., 2013; Nangaku et al., 2005).

Experimental animal models of MN and observations in MN patients have shown that the complement system likely plays a pivotal role in the pathogenesis. However, it is not clear which complement pathway is mainly activated in human MN and which of the three complement pathways has a major role or whether they cooperate to form C5b–9 and induce proteinuria. The activation of the complement is demonstrated by the deposition of C3, C4 and C5b–9 and by the urinary excretion of C5b–9 (Ma et al., 2013; Schulze et al., 1991) but these studies do not clarify which pathways is activated and by which IgGs. On the other hand, the absence of C1q is consistent with the inability of IgG4 antibodies to

activate the classical complement pathway, while the presence of C4d suggests an activation of the MBL pathway (Figure 1.4) (Brenchley et al., 1992; Ma et al., 2013; Val-Bernal et al., 2011). Finally, the staining of MBL in kidney biopsy from idiopathic MN patients suggests a role for the MBL pathway (Hayashi et al., 2018).

To sum up, in the major forms of idiopathic MN due to PLA2R1 and THSD7A, a still unresolved issue is thus whether the predominant IgG4 subclass plays a central pathogenic role (either direct or indirect via complement activation) or whether the low amounts of IgG1 or IgG3 are sufficient to activate the complement system, while IgG4 may in fact be protective against the other IgG subclasses (Salant, 2019).

– Anti–megalin antibodies

In the passive Heymann nephritis model, rats injected with rabbit anti–rat brush border antibodies developed a nephrotic syndrome similar to what occurred in rats actively immunized with rat kidney extracts, i.e. the active Heymann model (Heymann et al., 1959; Kerjaschki et al., 1996). These findings were the first to validate the pathogenicity of antibodies in MN. Furthermore, the main autoantigen of this model, megalin, is a multifunctional endocytic receptor and is present at the sole of podocyte foot processes in clathrin–coated pits. Antibodies against megalin block the uptake of apoE and apoB lipoproteins that bind to this receptor (Kerjaschki et al., 1997). This led to the local accumulation of these lipoproteins and the production of reactive oxygen species that potentially induce lipid peroxidation and cellular damage (Ronco et al., 2017).

The passive Heymann nephritis model has also provided important clues about the possible role of complement in MN. Indeed, the complement system is activated in passive HN as evidenced by the presence of C3 and C5b–9 in the immune deposits and detection of C5b–9 in podocytes from the urine (Figure 1.4) (Petermann et al., 2003). Also, depletion of serum C3 and C6 prevented development of proteinuria despite the accumulation of IgGs in the immune deposits (Baker et al., 1989; Salant et al., 1980). Additionally, pretreatment of rats with soluble human complement receptor 1 (it binds C4b and C3b and inhibits the enzymatic activity of C3 and C5) reduced complement–mediated proteinuria (Couser et al., 1995).

All together, these studies have demonstrated a major role of complement in passive HN induced by anti–megalin autoantibodies (Table 1.1). However, it is important to mention that anti–megalin autoantibodies do not belong to the IgG4 subclass, but to the "classical" rat IgG subclass able to bind complement, in contrast to the typical IgG4 subclass observed in the main idiopathic form of human MN (Ma et al., 2013).

– Anti–NEP antibodies

In the kidney, NEP is expressed in podocytes, at the brush border of tubular cells and in vessels. The proteolytic activity of NEP was assessed *in vitro* after incubation with IgG1 and IgG4 anti–NEP purified from serum (Table 1.1). IgG1 anti–NEP had much stronger inhibitory activity than IgG4 anti–NEP (Vivarelli et al., 2015). The biological consequences of the blocking effect of IgG1 anti–NEP antibodies on NEP is not yet understood. The direct binding of anti–NEP to its antigen can disturb the metabolism of regulatory peptides involved in glomerular hemodynamics, endothelial permeability, tubular function which may in turn induce podocyte injury (Hu et al., 2013; Ronco et al., 2017).

Regarding complement activation in antenatal alloimmune MN, two distinct patient case reports were described based on the IgG subclass predominance. For the Italian mother, the IgG1 anti–NEP, a complement–fixing antibody, was the predominant IgG subclass and was passively transmitted to the baby who experiences severe renal failure. C1q in addition to C3 and C5b–9 were detected in deposits suggesting activation of the classical complement pathway (Debiec et al., 2002; Debiec et al., 2004; Vivarelli et al., 2015). On the other hand, for the Moroccan mother producing only anti–NEP IgG4, proteinuria was not observed, suggesting that in alloimmune MN, anti–NEP IgG4 cannot induce the complement pathway.

– Anti–PLA2R1 antibodies

Ten years after the discovery of PLA2R1 as the major autoantigen in MN, the pathogenic effect of any anti–PLA2R1 IgGs, especially the predominant IgG4 subclass, is not definitely proven, yet suspected. This is in part due to the absence of a fairly relevant animal model of the PLA2R1–associated disease, since PLA2R1 is not expressed in mouse

podocytes (Table 1.1) (Meyer-Schwesinger et al., 2015), and since establishing a transgenic mouse line overexpressing human PLA2R1 has been impossible until now, despite several attempts (Salant, 2019). Nonetheless, the pathogenic role of anti–PLA2R1 in humans is supported by the higher risk of recurrence of MN after renal transplantation in patients having high anti–PLA2R1 titers in the circulation (Seitz-Polski et al., 2014; Stahl et al., 2010).

Also, several *in vitro* studies support both a direct and complement–mediated role of anti–PLA2R1 in podocyte injury (Figure 1.4). First, incubation of human podocytes expressing small amounts of PLA2R1 with patients' sera containing anti–PLA2R1 antibodies had much more effect on cell morphology when complement was added (Kistler et al., 2013) (and personal communication). Furthermore, addition of complement at sublytic doses to human podocytes overexpressing PLA2R1 and pretreated with serum or purified IgG4 anti–PLA2R1 antibodies induced degradation of synaptopodin and NEPH1 in a time and antibody–dependent manner, arguing for a role of IgG4 dependent on complement activation, especially via the MBL pathway (Haddad et al., 2017; Ma et al., 2011). Interestingly, it was found that the IgG4 fraction from MN patients (i.e. including anti–PLA2R1 antibodies) is hypogalactosylated and this would explain a strong activation of the MBL pathway through the Fc domain lacking a terminal galactose. Briefly, the MBL and ficolin components of the lectin complement pathway bind to acetylated glycans such as N–acetylglucosamine (GlcNAc) and N–acetylgalactosamine (GalNAc) and induce complex formation with the MBL–associated serine proteases (MASPs) to cleave and activate C4 (Chapter 5.3.3). In this context, the lack of the terminal galactose residue on the Fc domain of the IgG4 allows the activation of the lectin pathway by direct binding of the IgG and MBL (Malhotra et al., 1995).

As for a direct role of anti–PLA2R1 autoantibodies in interfering with the function of PLA2R1 as a possible adhesion protein on collagen type IV (Ancian et al., 1995), it has been shown that anti–PLA2R1 antibodies interfere with podocyte adhesion to collagen (Skoberne et al., 2014), while a soluble form of PLA2R1 inhibit the migration stimulated by the binding of collagen IV to human podocytes endogenously expressing membrane–bound PLA2R1 (Watanabe et al., 2018).

As for the activation of the complement system by anti–PLA2R1 antibodies *in vivo*, it appears that different pathways may be activated. In a well–characterized cohort of 117

patients with iMN, around 5% of the PLA2R1–associated MN patients were negative for the IgG4 subclass suggesting that IgG4 antibodies may not be always required for the development of the disease (Dähnrich et al., 2013; Hofstra et al., 2012). Interestingly, early stages of MN are characterized by IgG1 dominance contrary to IgG4 dominance and this is inversely correlated with C1q staining in the later stages of the disease (Huang et al., 2013).

These findings suggest that the IgG subclass switch may be associated with a complement pathway switch during the course of the disease, with the classical complement pathway mostly activated in the early stages of MN but other pathways are activated in later stages (Borza, 2016; Ma et al., 2013). Activation of the classical complement pathway is also illustrated in an allograft of recurrent PLA2R1–associated MN. Evaluation of both native and kidney graft biopsies revealed monotypic IgG3κ deposits together with C3, C1q, and C5b–9 (Debiec et al., 2012).

On the other hand, the activation of the alternative pathway in PLA2R1–associated MN patients is documented in rare cases of hyperactivation of this pathway following production of anti–CFH (complement factor H) autoantibodies, a complement regulatory protein known to inhibit the alternative pathway (Seikrit et al., 2018). Here, a patient developed progressive renal insufficiency even after diminution of IgG4 anti–PLA2R1 antibodies due IgG3 anti–CFH antibodies. The hyperactivation of the alternative pathway was demonstrated by the increase of properdin, known to stabilize the convertases in the alternative pathway. An additional proof for a role of the alternative pathway in PLA2R1–associated MN is shown by the intense staining of PLA2R, IgG4, C3, C5b–9, factor B, and properdin in rare patients with complete MBL deficiency (Bally et al., 2016).

Finally, in line with the above in vitro data, the staining of MBL in kidney biopsy from idiopathic MN patients suggests a role for the MBL pathway (Hayashi et al., 2018; Yang et al., 2016).

– Anti–THSD7A antibodies

THSD7A is a transmembrane protein proposed to mediate cell adhesion (Kuo et al., 2011) and is endogenously expressed at the foot processes of human and mouse podocytes

(Table 1.1) (Gödel et al., 2015). The pathogenic impact of anti–THSD7A in humans is supported by the rapid recurrence of MN after transplantation: anti–THSD7A detected before and after transplantation in addition to the enhanced THSD7A staining in the kidney allograft of the transplanted patient suggests that these antibodies are indeed pathogenic (Tomas et al., 2016). On the other hand, the effect of anti–THSD7A antibodies on the cellular function of THSD7A was assessed *in vitro* on primary glomerular epithelial cells (GEC) endogenously expressing THSD7A and HEK293 cells over–expressing THSD7A incubated with purified anti–THSD7A antibodies. Anti–THSD7A induced cytoskeleton rearrangement in GEC in addition to an alteration of the cell morphology with formation of stress fibers and increase of focal adhesions. Furthermore, anti–THSD7A antibodies induced cell detachment in HEK293 transfected cells (Tomas et al., 2016). In line with these observations, intravenous injection of purified anti–THSD7A antibodies from MN patients into BALB/c mice endogenously expressing THSD7A in podocytes causes a rapid formation of immune deposits and a transient increase of proteinuria that peaks at 17 days and declines thereafter. Furthermore, injection of concentrated but heat–decomplemented serum from THSD7A patients causes a more robust and sustained phenotype, with typical MN histopathological features and increase of albuminuria over a period of 70 days, with clear activation of the mouse complement system at late time points, when mice produce anti–human IgGs and activate the autologous phase, with C3 deposits at 70 days. In a parallel experiment, injection of purified polyclonal rabbit anti–THSD7A in BALB/c mice induced increasing proteinuria during a 14 days observation period yet lacked the ability to activate the complement in mice (Tomas et al., 2017). Together, these studies suggests that i) initial podocyte injury can result from direct binding of anti–THSD7A antibodies to THSD7A by a mechanism independent of complement activation highlighting a crucial localization and role of THSD7A in the podocytes at or next to the slit diaphragm and ii) further podocyte injury can be produced by anti–THSD7A antibodies upon activation of the complement pathway (Tomas et al., 2016).

However, the above experiments do not demonstrate which IgG subclass of anti–THSD7A antibodies are pathogenic, and especially whether the predominant IgG4 anti–THSD7A antibodies play a role. In the *in vivo* context of THSD7A–associated MN, activation of the lectin pathway was supported by the presence of MASP–1, MASP–2, MBL, C3a, C5a in kidney biopsies (Wang et al., 2018). Furthermore, additional *in vivo*

experiments in BALB/C mice as above with anti–THSD7A MN serum showed induction of MN with proteinuria and activation of the lectin pathway in mice. Finally, the activation of the classical and the alternative pathway by anti–THSD7A antibodies is not yet documented.

1.3.4 Epitopes recognized by anti–PLA2R1 and –THSD7A

After PLA2R1 was identified as the major autoantigen in 70% of MN patients in 2009, and then THSD7A as the second autoantigen in 2–5% of MN patients in 2014, many researchers embarked on searching for the epitopes in each antigen. Currently, a clearer map of the epitopes on PLA2R1 is available compared to THSD7A. However, many questions remain on the etiology and the course of the autoimmune response, including the identification of the genuine molecular epitopes recognized by the different IgG subclasses of autoantibodies.

– Epitopes in PLA2R1

Many groups investigated the immunogenic epitopes on PLA2R1 using different approaches. In 2013, Behnert et al. employed a "linear peptide mapping" approach and identified 7 peptides of 15 amino acids (a.a.) as putative epitopes recognized by MN patient antibodies (Behnert et al., 2013). In this approach, Behnert et al. synthetized 276 peptide sequences of 15 a.a. overlapping by 5 a.a. and spanning the full extracellular region of PLA2R1. By dot blot analysis, they identified 7 peptide sequences spanning all over PLA2R1, from the N– terminal CysR domain to the CTLD1, CTLD2, CTLD6 and CTLD8 domains, at the C–terminal end. However, these peptides were not confirmed to be bona fide epitopes when tested by ELISA since no significant difference in signal was observed when peptides were screened with various MN sera positive and negative for anti–PLA2R1. These negative results may be explained by the fact that this approach used a linear peptide scan while it was clearly demonstrated that patients' autoantibodies only recognized PLA2R1 under non–reducing conditions, indicating that the epitopes are conformational and that the recognized peptide sequences are likely discontinuous in the primary structure (Beck et al., 2009). Furthermore, the first peptide identified at the N–

terminal end of the CysR domain overlaps with the signal peptide, which is in fact cleaved and removed before routing of PLA2R1 to the plasma membrane or its secretion when expressed as a soluble protein (Lambeau et al., 1994; Rouault et al., 2007).

In 2014, a second group by Kao et al. proposed that the immunodominant epitope of PLA2R1 would consist of a relatively large region (about 50 kDa) of PLA2R1 comprising the first 3 domains CysR–FNII–CTLD1 and is sensitive to reducing agents. Further dissection of the epitope within this region was "catastrophic" and led to misleading results, which were not confirmed by others. In fact, the authors chose an apparently elegant strategy based on the insertion of a thrombin cleavage site between either the CysR and FNII domains or the FNII and CTLD1 domains followed by proteolysis, but they inserted the protease cleavage sites in a wrong place, between cysteines involved in disulfide bonds, and this messed up the strategy. Thus, the fact that they lost epitope recognition upon cleavage by thrombin while the CysR–FNII–CTLD1 fragment could not be apparently cleaved when analyzed under non–reducing conditions had nothing to do with their hypothesis of an "overlapping epitope between the 3 domains, as they claimed, but simply to the wrong design of their epitope mapping strategy (Kao et al., 2015). This strategy was carefully re–investigated in our lab and we could demonstrate that the CysR–FNII–CTLD1 region contains more than one "overlapping" epitope (Justino & Brglez et al, manuscript in preparation). Of note, only 10 sera from MN patients were tested, with most of the analysis performed with a single patient.

In 2015, a third group by Fresquet et al. used a strategy based on proteolysis of PLA2R1 followed by mass spectrometry analysis, and proposed that the immunodominant epitope resides in the N–terminal CysR ricin domain of PLA2R1 (Fresquet et al., 2015). They found that the reactivity to the entire CysR domain is sensitive to reduction and suggest that it is also sensitive to SDS denaturation on western blot versus slot blot analysis. By testing a few peptides within the CysR domain for antibody reactivity by biacore assays, they end up with a long peptide of 31 amino acids (WQDKGIFVIQSESLKKCIQAGKS–VLTLENCK) from the CysR domain which seemed to be sufficient to produce 85% inhibition of autoantibody binding to the CysR–CTLD3 of PLA2R1. Of note, only a pool of 5 patients' sera was used all over the above study to map this epitope. Finally, by ELISA assay on full PLA2R1 with competition by the CysR–CTLD3, they proposed that even though the CysR

domain (in fact they mostly used the CysR–CTLD3 region) contains the immunodominant epitope, other epitopes may be more distal, at least in some patients' sera.

Last, in 2016, Seitz–Polski & Dolla et al. in our laboratory described a more comprehensive picture of the anti–PLA2R1 epitopes, from the CysR to the distal domains of PLA2R1 (Seitz-Polski et al., 2016). Using a series of 10 successive deletion mutants of PLAR1 and a set of single domains as well as a cohort of 50 patients, we were able to identify three distinct and independent PLA2R1 domains containing one or several epitopes: CysR, CTLD1 and CTLD7 (Figure1.5). We also clarified the inaccurate conclusions proposed by Kao et al. based on insertion of a thrombin cleavage site between two cysteine bonds in the CTLD1 region, thus destabilizing the conformation of CTLD1 upon protease cleavage. In our hands, when we inserted the thrombin cleavage site at the correct position between FNII and CTLD1, we were able to cleave with thrombin and demonstrate a signal on both the CysR and CTLD1 cleaved domains with several patients, and therefore demonstrate that the CysR and CTLD1 contain independent epitopes. Using an extended cohort of 69 patients, we could demonstrate a mechanism of epitope spreading with worsening of the disease, as detailed below.

– Epitopes in THSD7A

THSD7A was identified as the second autoantigen in MN consisting of a new, largely unknown protein of 250 kDa, with little knowledge on the overall molecular architecture of its large extracellular region, and a suggested organization into 11 thrombospondin domains (TSDs) with many disulfide bonds, by homology with the prototypic thrombospondin–1 protein from the thrombospondin superfamily (Tomas et al., 2014). As for PLA2R1, the epitopes recognized by anti–THSD7A autoantibodies were sensitive to reducing conditions in western blot analysis, indicating that they are conformational. The location of the epitopes on THSD7A was first studied by Ma and colleagues using N– and C– Terminal truncation mutants of THSD7A along with constructs spanning one or more adjacent domains. Here, the sera recognized mostly 2 or more distinct domains on the C–terminal end of the antigen. An additional epitope region on the N–terminal end of THSD7A was recognized by a subset of patients (Hong et al., 2015).

Later, the domain organization of THSD7A was clarified by Seifert et al. with division of each of the 11 TSD domains into two variants of the TSP–1–like repeat (THBS1–like) and C6–like repeat, ending up with 21 repeated but not identical TSP–1–like domains in tandem (each containing 3 disulfides) and a coiled–coil domain with no disulfide bond between the D3 and D4 TSP–1 repeats (Figure 1.3) (Seifert et al., 2018). A detailed description of the structure of THSD7A is available in chapter 2.3 of this manuscript.

The mapping of domains containing epitopes was done in two steps: they first designed three large soluble fragments of the extracellular domain of the antigen (D1–D4, D5–D10 and D11–D21). Screening of 31 patients' sera by western blot under non–reducing conditions showed that several fragments were recognized by patients. These results suggested the presence of multiple epitopes spanning THSD7A from the N–terminal to the C–terminal end of the protein. To more precisely map the epitopes, smaller fragments were generated comprising two to three adjacent TSP–1–like/C6–like domains (D1–D2, D2–D3, etc.). All THSD7A domains except D3–D4 and D19–D21 were recognized by at least three patients.

These findings were validated in the recent *in silico* structural model of THSD7A (Figure 2.5) (Stoddard et al., 2018). Possible epitopes were determined based on epitope prediction algorithms combined with the extracellular domain model of THSD7A. Epitope prediction sites identified up to 18 epitope–containing domains of THSD7A while 3 domains showed no immunogenicity prediction. They also proposed that the coiled–coil domain and D4 contain epitopes, although this was not observed in the study by Seifert et al. Hydrophobic polar uncharged residues were suggested to be involved in the epitope sites and were found in 11 epitope containing domains. Five epitope domains contained mainly polar uncharged residues while an equal mixture of hydrophobic and polar uncharged residues was found in the last 2 epitope domains.

1.3.5 Epitope spreading in MN antigens

To elaborate the humoral immune response against a foreign or an endogenous protein (i.e. autoimmune response), the immune system initiates the response by producing antibodies recognizing a limited number of epitopes within that antigen then progresses by diversifying the antibody response towards additional epitopes (Cornaby et al., 2015). Over

time, this process happens in both T and B cells with a concerted mechanism of action with T and B cell epitopes and ends up with the production of multiple antibodies produced by B cells and targeting multiple epitopes on the same antigen or even on additional neighboring antigen molecules, each defined as immunodominant or non–immunodominant epitope. This mechanism is known as "epitope spreading" and is essential for an efficient humoral response. It can occur through various mechanisms including the interaction of B cells with T cells, endocytic processing of the antigens and somatic hypermutation in the B cells. Spreading can be directed against additional epitopes on the same molecule (known as "intramolecular" epitope spreading) or can diversify against two or more partners of the primary antigen (also known as "intermolecular" epitope spreading.

The mechanism of epitope spreading was documented in many autoimmune diseases such as pemphigus foliaceus and thyroid autoimmune disease and these examples may provide valuable insights for the investigation of the autoimmune response that occurs in MN (Aoki et al., 2015; Li et al., 2003; McLachlan et al., 2017). For instance, Pemphigus foliaceus is an autoimmune muco–cutaneous blistering characterized by skin acantholysis, where autoantibody binding to Desmoglein 1 and 3 (an epidermal cell adhesion molecule) leads to a loss of cell adhesion between keratinocytes. In a Brazilian population where the incidence of the disease is high, anti–Dsg1 autoantibodies were detected in healthy controls and in patients before the clinical onset of the disease. Antibodies from these patients recognized the non–pathogenic extracellular domain (EC5) of the protein. However, transition to the active disease is mediated by an intra–molecular epitope spreading and a rise of autoantibodies targeting the pathogenic region EC1 and EC2 of Dsg–1.

Such mechanism of epitope spreading has been also documented in the Heymann nephritis model by the presence of antibodies generated toward different epitopes in megalin and associated with the development of a nephrotic syndrome, glomerular immune deposits and proteinuria. The extracellular domain of megalin is composed of four main ligand binding domains (LBD–I to LBD–IV) (Figure 1.5). Initial immunization of rats with various fragments (L3 to L6) of the LBD I domain showed that the most N–terminal L6 recombinant protein (AA 1–236) was sufficient to induce a full–blown disease, as assessed by severity of proteinuria, whereas immunization with L4 and L3 produced only mild disease (Tramontano et al., 2006). Furthermore, immunization of rats with the L6 domain alone was sufficient to induce Heymann nephritis and epitope spreading towards

C – terminal domains. Four weeks post–injection, the rats produced antibodies against this L6 fragment but did not develop proteinuria. Eight weeks after immunization and with a boost at 4 weeks, epitope spreading occurs as evidenced by the presence of new antibodies against LBD–II, LBD–III and LBD–IV domains. The progression of the immune response and the reactivity against the other LBD fragments correlated with increased proteinuria (Shah et al., 2007).

PLA2R1–associated MN seem to follow a similar mechanism of epitope spreading (Seitz-Polski et al., 2016). In a study conducted in our laboratory, we showed that patients have autoantibodies against different epitopes in PLA2R1: CysR, CTLD1 and CTLD7 (Figure 1.5). Interestingly, screening of 69 patients for the different epitopes showed that 99% of patients had antibodies against CysR, suggesting that it is the immunodominant epitope. Patients were then stratified into three main groups according to the number of recognized epitopes in PLA2R1: CR patients with a "monoclonal" antibody profile targeting only the CysR (CR) domain, and CRC1 or CRC1C7 patients with a polyclonal profile targeting either CysR and CTLD1 (CRC1) or CysR, CTLD1 and CTLD7 (CRC1C7). Patients in these groups did not differ for sex, immunosuppressive treatment or full anti–PLA2R1 titers. Interestingly, we found that patients in the CR group were significantly younger than patients in the CRC1 and CRC1C7 groups, suggesting a progressive immune response with epitope spreading over time. We also found that patients with monoclonal reactivity (CR) had lower proteinuria and were more likely to go on spontaneous remission during follow–up. The validation of these findings and of the clinical significance of PLA2R1 epitope spreading *in vivo* and in MN cohorts is essential for better understanding of the pathophysiology of the disease and for improved personalized medicine, especially better prognosis and treatment efficacy (Chapter 4.3).

Contrary to what was described for megalin and PLA2R1, the mechanism of epitope spreading seems less obvious for THSD7A. The screening of 31 patients with THSD7A–associated MN revealed that 87% of patients had reactivity towards D1–D2 compared to 61% and 52% for D15–D16 and D9–D10. Serum from THSD7A–associated MN recognized more than one epitope domain and there was no specific trend for spreading on additional epitopes. Patients reacting to one or two epitopes tended to have lower proteinuria and were more likely to achieve remission compared to patients having more than two reactive epitopes (Seifert et al., 2018).

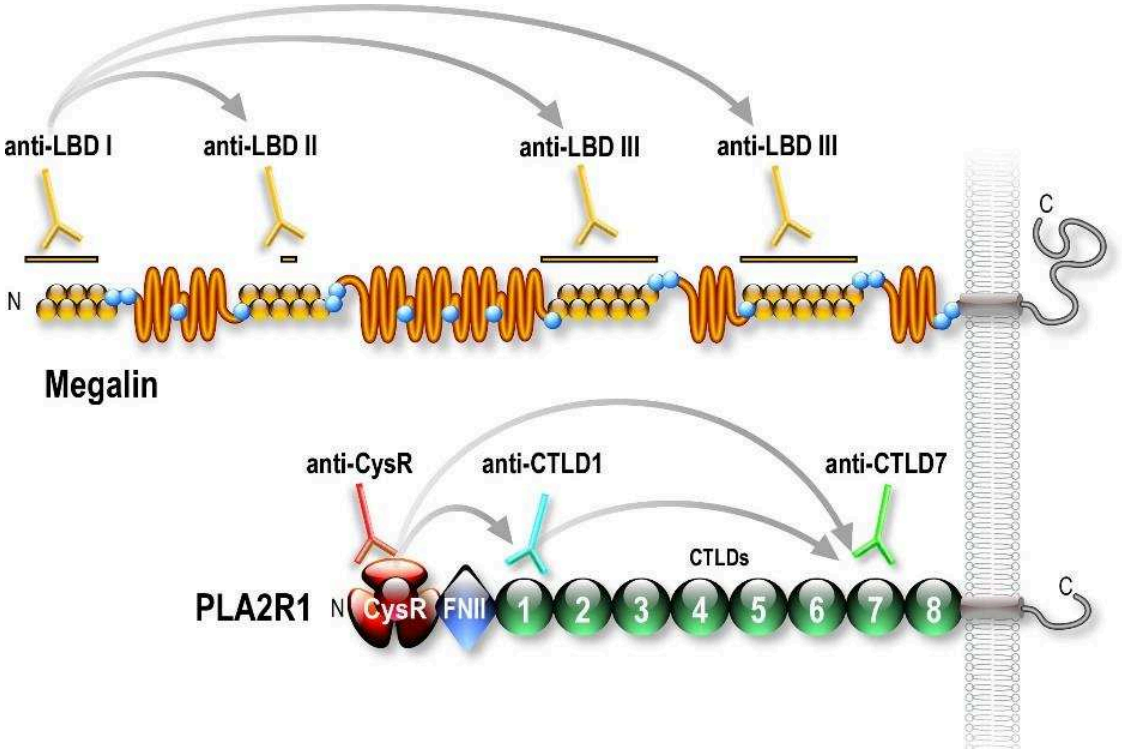

Figure 1.5 – Schematic representation of the epitope spreading mechanism on megalin and PLA2R1. Immunization of rats with the L6 fragment (comprising amino acids 1–236 from the LBD I domain) of megalin triggers glomerulonephritis like idiopathic MN with a mechanism of spreading of epitopes to the other domains in the protein (LBD II, III, IV). Patients with PLA2R1–associated MN were found to all exhibit an anti–CysR reactivity but can be stratified into a CR–only group, a CRC1 group and a CRC1C7 group, in accordance with a mechanism of epitope spreading and evolution towards a more severe form of MN.

To validate these findings, three rabbits were co–immunized with human and mouse THSD7A and were tested for epitope recognition. The sera from the three rabbits recognized the most N–terminal region of the protein (D1–D2) which was also recognized by most but not all patients. Of interest, rare cases of dual positivity for PLA2R1 and THSD7A have been documented. These cases might involve an intermolecular epitope spreading mechanism, but this is largely speculated at this point. This matter is further detailed in chapter 1.3.1.2 and in chapter 4.2.

1.3.6 Animal models of MN

In 1959, Heymann and colleagues established the first experimental model of membranous glomerulonephritis referred to as the Heymann nephritis model (Heymann et al., 1959) (Table 1.1). The active Heymann model is induced in male Sprague–Dawley rats by repeated immunization (once a week) with a crude renal extract (Fx1A) prepared from their own kidney in complete Freund adjuvant supplemented with additional Mycobacterium tuberculosis HRa37. After 6 to 12 weeks, proteinuria and immunohistological and clinical features resemble those seen of human membranous nephropathy. Rat IgG granular immune deposits and electron–dense subepithelial deposits were observed on the glomerular capillary walls, as well as appearance of strong proteinuria by 6– to 12–weeks post–injection.

In 1982, it was shown that the autoimmune response was mainly targeting megalin, a protein abundantly present in the crude kidney extracts (Kerjaschki et al., 1982). The same pathology can be reproduced in the passive HN model by injection of antibodies directed against brush border antigens produced in rabbits (anti–Fx1A) (Feenstra et al., 1975; Makker et al., 2011; Salant et al., 1988; Salant et al., 1989). Proteinuria in this model depends on the activation of the complement system (Petermann et al., 2003).

Studying Heymann nephritis offered great insights on the pathophysiology of the disease but the absence of megalin in the human immune deposits limited the use of this model in the research work on human MN.

After 2009, the identification of PLA2R1 and THSD7A as two main autoantigens in human MN opened a new era in the diagnosis of the disease (Beck et al., 2009; Tomas et al.,

2014). However, translating this knowledge into *in vivo* animal models was limited by the fact that PLA2R1 is not expressed in murine podocytes (Table 1.1) (Gödel et al., 2015).

It is important to note that recently a human PLA2R1 *knock–in* mouse model have been developed (Rhoden et al., 2018). These BL6/J mice showed no histological differences nor proteinuria differences when compared to wild–type mice under normal conditions. The ongoing work aims to induce MN using patients IgG antibodies and to validate the pathogenicity of anti–PLA2R1 antibodies.

On the other hand, thanks to the normal expression of THSD7A in mouse podocytes (Gödel et al., 2015; Meyer-Schwesinger et al., 2015) and the high level of identity between human and mouse THSD7A proteins, Tomas and colleagues could establish for the first time a THSD7A passive model of MN, similar in many ways to the passive HN rat model (Table 1.1) (Tomas et al., 2016). By injecting human serum containing anti–THSD7A antibodies or purified anti–THSD7A antibodies in wild–type BALB/c mice, they were able to induce proteinuria and histopathological features of MN. The injected antibodies bound specifically to THSD7A on the podocyte, induced the formation of immune deposits, and initiated proteinuria after 3 days of administration. Mice injected with full serum showed more persistent proteinuria due to the initiation of the autologous phase of the disease and the production of large amounts of mouse anti–human IgG antibodies. In contrast, mice receiving purified anti–THSD7A antibodies showed only transient proteinuria. At early time points, C3 and C5b–9 were undetectable in mice receiving the whole serum or the purified antibodies. At later time points such as day 70, C3 was detected in kidney biopsy when the whole serum was injected to mice.

This model was further validated by the injection of rabbit anti–THSD7A IgG in C57BL/6 and DBA/J1 mice as well as male Sprague–Dawley rats (Tomas et al., 2017). Injected antibodies bound to the glomerular filtration barrier of the rodents to form immune deposits. However, induction of proteinuria and full–blown disease was mouse strain specific and not seen in rats, suggesting that the genetic background may be crucial for the induction of proteinuria in this passive model of THSD7A–associated MN.

1.4 Diagnosis and prognosis of MN

Before 2009, treatment decision for biopsy–proven MN patients was mainly based on renal damage criteria including proteinuria and serum creatinine levels, sex, age and the presence of associated diseases (i.e. secondary MN) or not (idiopathic primary MN) rather than strong immunological criteria except for the type of IgG subclasses found in immune deposits (Cattran et al., 2008; Fervenza et al., 2008; Ruggenenti et al., 2009; Ruggenenti et al., 2013; Schieppati et al., 1993). Since about 30% of MN patients underwent spontaneous remission without immunosuppressive treatment, patients were treated with symptomatic medications for 6 months according to the KDIGO guidelines (Radhakrishnan et al., 2012). If nephrotic syndrome persisted beyond this period, the patients would have immunosuppressive treatment. However, this approach is not appropriate for many reasons including that patients, on average, reach spontaneous remission considerably later than 6 months and could exceed a 12–month period (Polanco et al., 2010; Reichert et al., 1998; van den Brand et al., 2014) and that around 40% of MN patients show progressive disease while 10–15% reach ESRD after a 10–15 years period (Dahan et al., 2017).

The identification of PLA2R1 and THSD7A as the autoantigens in 70% and 2–5% of MN patients induced a paradigm shift in healthcare of patients with MN. These events stimulated the interest in idiopathic MN and led to the development of many diagnostic tests and epitope investigations (Beck et al., 2014; Debiec et al., 2014; Francis et al., 2016; Ronco et al., 2012).

1.4.1 Biopsy staining

The expression of PLA2R1 and THSD7A is different in terms of localization and intensity from normal to MN kidney. In normal kidney, PLA2R1 appears on the external side of the GBM as a granular but weak staining while THSD7A is at the slit diaphragm in proximity to nephrin and show a linear and more intense staining (Beck et al., 2009; Tomas et al., 2014; von Haxthausen et al., 2018). In MN kidney biopsies, both PLA2R1 and THSD7A are trapped in the immune deposits and the staining intensity dramatically increases (Figure 1.6) (Debiec et al., 2011; Hoxha et al., 2012; Larsen et al., 2016).

This "enhanced biopsy staining" now allows the routine analysis of kidney biopsy for a differential diagnosis of MN due to either PLA2R1– or THSD7A–associated MN, yet it is far from being quantitative (Larsen et al., 2016; Larsen et al., 2013). Biopsy staining is still currently used in retrospective analysis of patients to document the type of MN while most of the studies now focused on evaluating the role of circulating autoantibodies to diagnose MN (Svobodova et al., 2013). Some authors however suggested that antigen detection on kidney biopsy provides additional information for diagnosis, treatment follow–up and relapse.

This technique can be used to diagnose MN patients with circulating PLA2R1– or THSD7A– antibodies in addition to patients that have low or undetectable antibody titers in serum (Debiec et al., 2011; Qin et al., 2016). The detection of antigens in kidney biopsies is more sensitive than the detection of circulating autoantibodies and the positive staining in glomeruli strongly correlates with the presence of circulating antibodies (Debiec et al., 2011; Hoxha et al., 2012; Pourcine et al., 2017; Qin et al., 2016; Ronco et al., 2015).

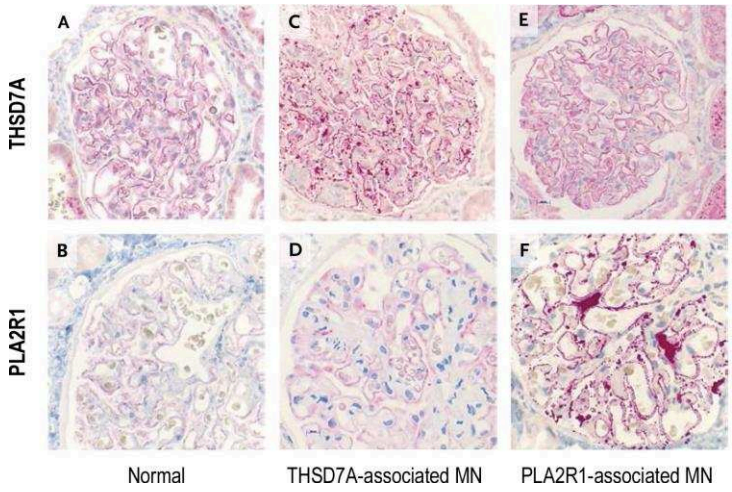

Figure 1.6 – Renal biopsy staining in PLA2R1– and THSD7A–associated MN and in a healthy control. (A–B) PLA2R1 and THSD7A staining of renal biopsy from a healthy control. (C–D) PLA2R1 and THSD7A staining of renal biopsy from a patient with PLA2R1–associated MN and (E–F) PLA2R1 and THSD7A staining of renal biopsy from a patient with THSD7A–associated MN. *Adjusted from (Tomas et al., 2014) and reproduced with permission from (scientific reference citation),"Copyright Massachusetts Medical Society".*

1.4.2 Detection of autoantibodies

– Anti–PLA2R1 detection

Circulating anti–PLA2R1 antibodies were detected in 70 to 80% of MN patients from Europe, USA and Asia except Japan where the prevalence seems to be only about 50% (Akiyama et al., 2014; Beck et al., 2009; Hihara et al., 2016; Hofstra et al., 2012; Hoxha et al., 2012; Qin et al., 2011). Currently, measurement of these antibodies is performed by three different assays: western blot, indirect immunofluorescence test (IIFT) and ELISA. Although all three techniques can detect anti–PLA2R1, the last two are more quantitative. The western blot was the first technique employed using human glomerular extracts containing endogenous PLA2R1 or HEK293 cells expressing recombinant human PLA2R1 (Beck et al., 2009). This technique is very sensitive but only semi–quantitative, requires non–reducing conditions and is not suitable for the evaluation of large cohorts.

The commercial IIFT is a cell–based assay consisting of biochips coated with HEK293 transfected with full–length membrane PLA2R1. Antibody titer is measured in serum by serial dilutions ranging from 1/10 to 1/1000 and is revealed by detection using total IgG (Hoxha et al., 2011). The IIFT was validated on a cohort of 117 patients with MN versus 153 healthy blood donors and 90 patients with non–membranous glomerulonephritis. Although only semi–quantitative, this assay showed 100% specificity and 52% sensitivity compared to biopsy–proven MN patients.

The first homemade ELISA to detect anti–PLA2R1 was established by Hofstra and colleagues. This assay was validated in a cohort of 117 patients with primary MN and is in 94% agreement with the IIFT (Hofstra et al., 2012). They showed that anti–PLA2R1 titers measured by ELISA barely correlated with proteinuria and could predict remission only. This correlation was lost when anti–PLA2R1 was measured by IIFT. Of note, there was a strong correlation between anti–PLA2R1 titers measured by total IgG or by the predominant IgG4 antibodies.

Finally, a standardized ELISA assay was developed by Euroimmun and consisted of the full extracellular domain of human PLA2R1 expressed in HEK293 and coated in the solid phase. The assay was validated with 200 patients with primary MN, 230 patients with various glomerular diseases, 316 patients with other autoimmune disease and 291 healthy

controls. It is quantitative and showed 99.9% specificity and 96.5% sensitivity with respect to the IIFT (Dähnrich et al., 2013). A cut–off value of >20 RU/mL was set above which anti–PLA2R1 titers are considered positive. This threshold however became a matter of debate since many studies suggested a reconsideration of this value for more accuracy of the diagnosis of PLA2R1–associated MN patients (Bobart et al., 2019; De Vriese et al., 2017; Liu et al., 2018; Tampoia et al., 2018).

Anti–PLA2R1 species–specific ELISA assays were developed in our laboratory based on the differential cross–reactivity of anti–PLA2R1 antibodies present in the serum from a cohort of 130 patients towards mouse, rabbit and human full–length PLA2R1 antigens. Results obtained with the rabbit PLA2R1 ELISA were in accordance with data obtained with the human ELISA, and thus validated the possible use of rabbit PLA2R1 as an alternative antigen to human PLA2R1 (Seitz-Polski et al., 2015). On the other hand, antibody cross–reactivity with mouse PLA2R1 was much lower, and interestingly, this mouse ELISA detected in fact only a subgroup of about 30% patients who had poor outcome. These results suggested that some epitopes but not all of them are conserved between human, rabbit and mouse PLA2R1, and that the ones conserved in the mouse antigen are the one more closely involved in MN pathogenesis. Finally, other specific assays have been described including the addressable laser bead immunoassay (ALBIA) technique, an assay based on the Luminex technology consisting of the antigen added to color–coded beads precoated with antigen specific antibodies and detected with biotinylated antibodies (Behnert et al., 2013).

– Anti–THSD7A detection

As said before, THSD7A was identified as a second MN autoantigen with a prevalence of approx. 2–5% of idiopathic MN patients in western countries and a higher prevalence of about 9% in Japan (Iwakura et al., 2015). The western blot detection conditions were similar to the ones used for the identification of PLA2R1 (Tomas et al., 2014). It was only a year after I started working on my PhD project that an IIFT methodology was published for screening patients with THSD7A–associated MN (Hoxha et al., 2017). Like for the available IIFT for detection of anti–PLA2R1, the IIFT consisted of biochips coated with either HEK293 cells overexpressing the full extracellular domain of THSD7A or non–transfected

cells. In their study, Hoxha and colleagues screened 1276 patients with MN and identified 40 patients with THSD7A–associated MN and showed a 2.6% prevalence of this disease. The assay had 92% specificity and 100% sensitivity compared to western blot.

As we saw for PLA2R1, the setup of an ELISA assay to measure anti–THSD7A antibody titers is essential for the diagnosis and prognosis of patients with THSD7A–associated MN, and this was one of the major focus during my PhD work (Chapter 4.1).

1.4.3 Comparison of the detection assays: Western Blot, IIFT and ELISA

Circulating autoantibodies against PLA2R1 or THSD7A are considered as highly specific and sensitive biomarkers of MN, especially for primary MN. Although screening by western blot or IIFT may be more sensitive than the current ELISA assays, the western blot assay is not suitable for the clinical routine and screening of large number of patients. Also, the IIFT allows only a semi–quantitative evaluation of antibody titers and is less appropriate for monitoring disease activity and response to treatment. Finally, the ELISA assay is less sensitive than the western blot and IIFT, but evaluation of antibody titer is quantitative and can be used in clinical settings for diagnosis and patient's follow–up (De Vriese et al., 2017; Ronco et al., 2015).

Studies have shown that ELISA and IIFT assays are in agreement to each other (94%) and that titers measured by ELISA correlate significantly with those by IIFT (Dähnrich et al., 2013; Hofstra et al., 2012). The ELISA is more suitable for follow–up measurement of anti–PLA2R1 while IIFT is more suitable for detection of very low anti–PLA2R1 or when ELISA results are not conclusive.

It is important to note that detection of autoantibodies in MN is mostly done by using secondary antibodies detecting human total IgG (commercial IIFT and ELISA) and rarely by using secondary antibodies detecting human IgG4 (mostly used in western blots and our homemade ELISAs), although it is the predominant IgG subclass (Dähnrich et al., 2013; Hofstra et al., 2012; Seitz-Polski et al., 2015). We have demonstrated that detection of human IgG4 is more sensitive than total IgG by ELISA (Seitz-Polski et al., 2015).

Finally, the detection of autoantibodies against PLA2R1 appear so far to be specific to MN as they have not been found in other autoimmune diseases nor healthy donors. Thus, there is now a debate between clinicians to reconsider the usefulness of kidney biopsy to document real cases of MN (i.e. "biopsy–proven") and substitute this latter by a serology–based assay (i.e. ELISA for anti–PLA2R1 or anti–THSD7A), especially for old patients or patients with life–threatening complications (Bobart et al., 2019; Pozdzik et al., 2018).

1.4.4 Diagnostic value of antibodies in MN

The identification of PLA2R1 and THSD7A as autoantigens in MN consists not only the major step for understanding the pathophysiological mechanisms but also for diagnosis and theragnosis of MN patients. Detection of circulating anti–PLA2R1 antibodies is very specific and sensitive biomarker of membranous nephropathy and is rarely detected in other patients with any kidney or systemic diseases. Specificity and sensitivity of anti–PLA2R1 antibodies was respectively 99% and 78% in a meta–analysis combining a total of 2212 patients from 15 studies (Du et al., 2014). The important diagnostic value of anti–PLA2R1 in diagnosis have even led clinicians to reconsider the necessity of kidney biopsy evaluation (Ronco et al., 2015).

It is noteworthy that although detection of PLA2R1 in the glomerular immune deposits do not allow a quantitative assessment of the progression of the disease yet sometimes it can be more sensitive for detection of additional PLA2R1–associated MN cases when no circulating autoantibodies are detected (Svobodova et al., 2013). In some cases, circulating anti–PLA2R1 are not detected while PLA2R1 antigen is detected in immune deposits (Debiec et al., 2011) and also circulating antibodies may not correlate with disease activity (De Vriese et al., 2017). This can be due to different scenarios. First, serum samples may be tested when the patient has reached immunological remission state, but proteinuria persists due to either the time lag between the immunological and clinical remission or the inability of the highly damaged podocytes to restore a fully functional filtration barrier (Beck et al., 2010). Second, the antibodies can be rapidly cleared from the blood circulation and are retained on the GBM. This concept is known as “kidney as a sink” and it is only when antibody production exceeds the buffering capacity of the kidney that the antibodies can be detected in serum (van de Logt et al., 2015).

Detection of anti–PLA2R1 antibodies in serum does not always discriminate between primary and secondary forms of MN. The prevalence for detection of anti–PLA2R1 in patients is high in idiopathic MN and much lower in secondary MN, depending on the tested cohorts and the secondary MN analyzed. In some cases, detection of anti–PLA2R1 antibodies of IgG4 subclass suggested a coincidental occurrence of other diseases such as cancer, sarcoidosis, Lupus, HBV and HIV (Garcia-Vives et al., 2019; Larsen et al., 2013; Qin et al., 2011; Stehlé et al., 2015; Xie et al., 2015). In other cases, treatment of the secondary diseases was independent of the evolution of anti–PLA2R1 antibodies: some patients went into remission without treatment or had persistent proteinuria after treatment of the associated disease (Iwakura et al., 2015; Qin et al., 2011). Additionally, staining for PLA2R1 antigens have been detected in patients with Hepatitis B and C suggesting a possible immune reaction against PLA2R1 in these diseases (Larsen et al., 2013; Xie et al., 2015). As for THSD7A, it was documented that a significant number of patients with anti–THSD7A positive MN are associated with cancer and that THSD7A can be stained in gallbladder carcinoma and in follicular dendritic cells in lymph nodes (Hoxha et al., 2011 ; Hoxha et al., 2016). In some of these cases, surgical removal of the tumor led to a decrease in anti–THSD7A antibodies and proteinuria, suggesting that THSD7A expressed in tumors may be seen as a new foreign (auto)antigen and is targeted by the immune system.

A new diagnosis algorithm by De Vriese et al. proposed a serology–based approach for MN avoiding a biopsy protocol and thus being "non–invasive" (Bobart et al., 2019; De Vriese et al., 2017). As a first step, anti–PLA2R1 titer in serum is evaluated in addition to thorough screen for secondary causes. If anti–PLA2R1 antibodies are positive and no association for associated diseases, patients are treated for the PLA2R1–associated MN. However, if anti–PLA2R1 antibodies are not detected in serum, kidney biopsy must be performed and here many possibilities are presented: positivity for PLA2R1 antigens of IgG4 dominance patients are considered PLA2R1–associated MN. Negativity for PLA2R1 antigens with an IgG–1, –2, –3 dominances, patients are classified with secondary MN and an intense screening for cancer or other underlying diseases is required. Finally, patients with negative PLA2R1 staining and IgG4 dominance are further tested for THSD7A antibodies and antigen staining in biopsy. In case a of THSD7A–associated MN an intensive screening for malignancies is required.

1.4.5 Monitoring value of antibodies in MN

The identification of anti–PLA2R1 as biomarker of disease activity in MN marks a paradigm shift in prognosis and theragnosis in this field (Beck et al., 2009). Anti–PLA2R1 titers are found to correlate with disease activity and proteinuria (Hofstra et al., 2011). High anti–PLA2R1 antibody titers reflect an active disease state while low or no titers correspond to spontaneous remission or a response to immunosuppressive treatment (Beck et al., 2011; Hoxha et al., 2011 ; Ruggenenti et al., 2015; Segarra-Medrano et al., 2014; Timmermans et al., 2014). And the subsequent re–increase in the anti–PLA2R1 titer is associated with disease recurrence (Seitz-Polski et al., 2014). The time lag between the immunologic and clinical remission is reflected by the decrease in anti–PLA2R1 titer before any detectable remission of proteinuria. Furthermore, reduction in antibody titer in untreated patients might can indicate a spontaneous remission and thus prevents unnecessary immunosuppressive treatment (Francis et al., 2016). The importance of evaluating anti–PLA2R1 titer for monitoring disease activity and after treatment is validated by several studies demonstrating that the antibody titer can indeed be qualified as an effective novel biomarker in MN (Perico et al., 2019).

Moreover, exciting progress has been made in the treatment of this disease. A selective depletion of B cells by treatment with rituximab, a monoclonal antibody against CD20 antigen present on B cell lymphocytes, emerged as a specific and safe treatment for patients with idiopathic MN and was first tested in 8 MN patients with long term proteinuria (Remuzzi et al., 2002). In a follow up period over 20 weeks, baseline proteinuria decreased by 62% while serum albumin increased by 31%. After one year, the reduction in proteinuria levels was maintained and was also associated with stable kidney function and a reduction in body weight, blood pressure, and serum cholesterol (Ruggenenti et al., 2003). Furthermore, among 35 patients with membranous nephropathy, 25 patients had detectable anti–PLA2R1 antibodies, and these antibodies decreased or disappeared in 17 patients with anti–PLA2R1 within 12 months after treatment with rituximab. The positive immunological response to treatment was accompanied by a complete or partial remission of proteinuria after 1 and 2 years (Beck et al., 2011). These pivotal findings were confirmed by subsequent studies (Dahan et al., 2017; Ruggenenti et al., 2015).

1.4.6 Prognosis value of antibodies in MN

The capacity to evaluate anti–PLA2R1 titer has added a substantial improvement in prognosis of MN patients. Measurement of anti–PLA2R1 titer is not only a biomarker of disease severity at the initial assessment but is also a predictor of long–term clinical outcome of MN patients (Hofstra et al., 2012; Kanigicherla et al., 2013; Seitz-Polski et al., 2015; van den Brand et al., 2014).

In a cohort study of 133 PLA2R1–associated MN patients with a follow–up period of 24 months, Hoxha and colleagues showed that patients reaching remission of proteinuria after 12 months had significantly lower anti–PLA2R1 antibody titer at the time of study inclusion. Also, patients with high antibody titers achieved remission of proteinuria much later than patients with lower titers. Patients with sustained high proteinuria levels had also high anti–PLA2R1 titers. This titer decreased in patients going on spontaneous remission (Hoxha et al., 2014). In this context, anti–PLA2R1 below 275 RU/mL measured at baseline by ELISA were shown as the only factor associated with remission within a 6 months period in the GEMRITUX clinical trial (Dahan et al., 2017). Similar findings were obtained in a 14–year retrospective study comprising 108 MN patients (Pourcine et al., 2017).

Furthermore, measuring anti–PLA2R1 titer at the end of treatment was shown to be predictive of clinical response. A study by Bech and colleagues analyzed a cohort of 48 patients following either cyclophosphamide or mycophenolate mofetil coupled with corticosteroids during a 12 month follow up period. They showed that anti–PLA2R1 titer at baseline did not predict response to treatment, yet after treatment this titer predicted the long–time outcome (Bech et al., 2014 ; Dahan et al., 2017).

We suggested that, in addition to anti–PLA2R1 titer, investigation of the epitope profile and spreading is important to stratify patients into subgroups with different prognosis (Seitz-Polski et al., 2016). Indeed, we showed that patients with antibodies targeting only the CysR domain (CysR) have a better outcome compared to patients with an epitope spreading profile (CysRC1, CysRC1C7). The increase in the number of epitopes correlated with increased proteinuria levels and high anti–PLA2R1 titer. Patients with a CysRC1 or CysRC1C7 profile had poor prognosis but some of them could have low anti–PLA2R1 titer, while patients with a CysR profile had better outcome, and some of them could have high

titer. This suggests that analysis of anti–PLA2R1 titer is not sufficient by itself to predict outcome, and that epitope profiling may help to better stratify patients into those at risk of poor outcome or not.

These results were found in a retrospective cohort but were recently confirmed in a well–characterized prospective and homogenous cohort of PLA2R1–associated MN patients. Indeed, screening of the GEMRITUX cohort for the different PLA2R1 epitopes suggests that epitope spreading at baseline can be a useful biomarker of outcome after treatment with rituximab versus conservative treatment with Renin Angiotensin system (RAS) blockers (Chapter 4.3).

As reviewed above, anti–PLA2R1 antibodies have been now widely used to diagnose, monitor and predict outcome in patients with PLA2R1–associated MN. This is not yet the case for anti–THSD7A antibodies first because of the more recent identification of THSD7A as the second antigen in MN (5 years later) and also because of the lower prevalence of the THSD7A–associated MN entity and finally the lack of quantitative detection assays. As for anti–PLA2R1, does anti–THSD7A titer correlate with the clinical state of the disease? Does this titer predict outcome of patients? What about THSD7A epitope profile and association with disease activity, etc.? These important questions will be answered in the chapter 4.1 and chapter 4.2 of this manuscript.

2 Introduction – THSD7A

THSD7A is a 250 kDa transmembrane protein that appears as a unique newly identified member of the thrombospondin (TSP) family (Wang et al., 2010). THSD7A shares with the 5 prototypic thrombospondin members (TSP1 to 5) a tandem of thrombospondin type 1 repeats (TSRs). TSRs are a unique structural motifs consisting of a three antiparallel ß–strand fold of about 60–70 amino acids maintained by 3 disulfide bonds, but with different assemblies (Figure 2.4–A) (Stoddard et al., 2018; Tucker, 2004). TSR folds are found not only in thrombospondins but also in many other "mosaic" multidomain proteins such as ADAMTS metalloproteases. Collectively, proteins with one or several TSR motif, irrespective of their other domains, would belong to the thrombospondin type 1 repeat superfamily of proteins (Figure 2.1).

I will make below a survey of the structure and function of the superfamily of proteins with TSR domains, then of the 5 members of the thrombospondin family, with focus on the prototypic TSR domain and the interacting molecules with TSRs, with the aim to extrapolate all of these findings to THSD7A and may be provide more hypotheses about the still largely unknown structure and function of THSD7A.

2.1 The thrombospondin type–1 repeat (TSR) superfamily

The thrombospondin type 1 repeat superfamily of proteins comprises numerous different families of proteins harboring one or several TSR motifs, irrespective of other domains present in these latter (Figure 2.1). Hence, thrombospondin type–1 repeats (TSR repeats) are found in many animal proteins including the complement component properdin, the binding protein TRAP, the ADAMTS family members, F–spondin, complement C6 and many others (Olsen et al., 2014).

The TSR fold is around 60 amino acids long and comprises 12 to 13 highly conserved amino acids: six cysteine residues (there are two pairing assemblies), two arginine and two glycine residues in addition to two or three tryptophan residues (Carlson et al., 2008).

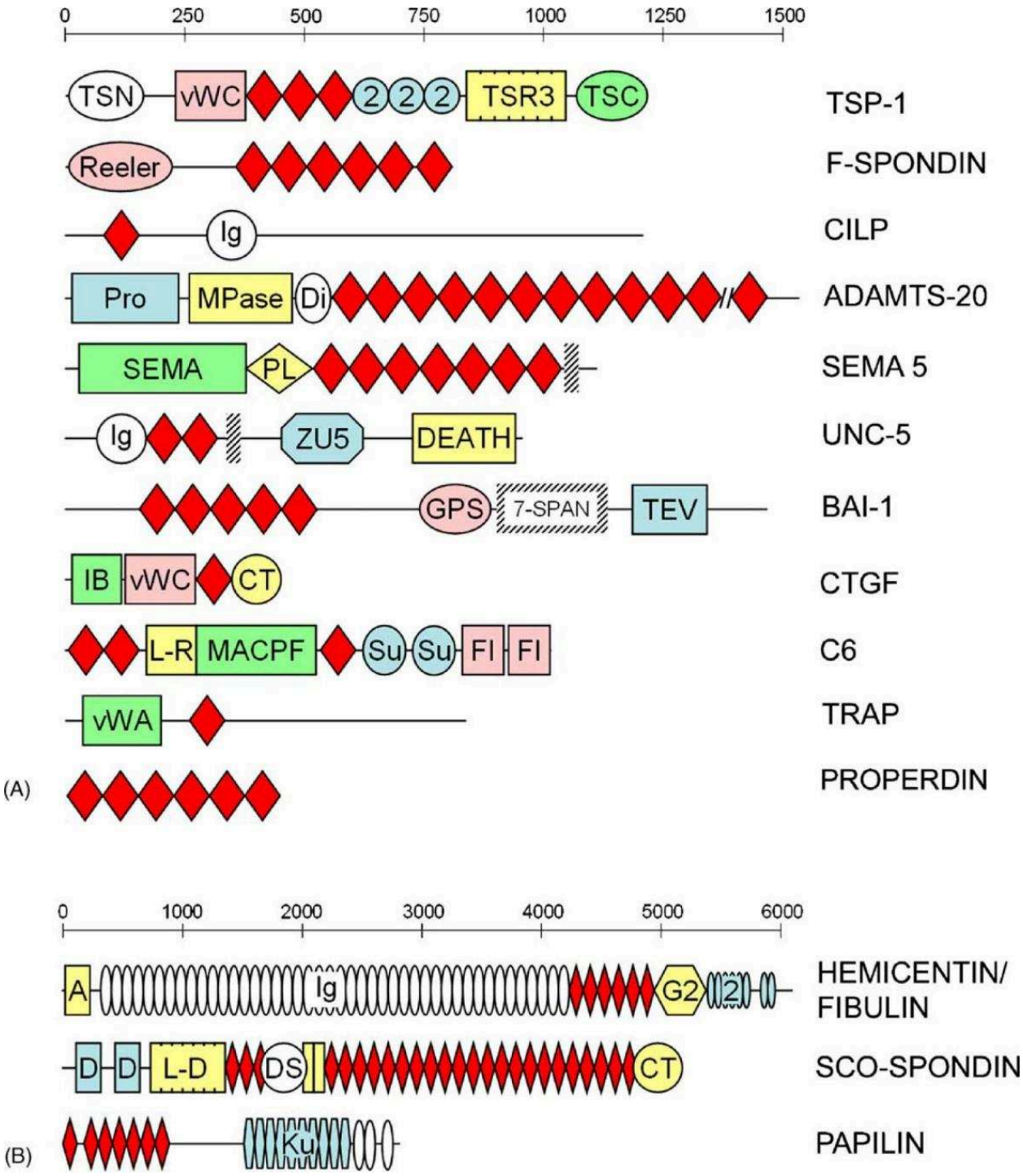

Figure 2.1 – Superfamily of thrombospondin repeats (TSR). Schematic illustration of the representative members of the TSR superfamily. The length of each protein is indicated by the amino acid scale above each group. TSRs are indicated by red diamonds and the transmembrane domains by shaded boxes. A full description of the different domains in each protein are available in the original reference (Tucker, 2004). *Adjusted from (Tucker, 2004) with copyright permission from "Elsevier".*

The crystal structure of the isolated three TSRs of human TSP–1 was first obtained by Tan and colleagues with the TSRs produced in *Drosophila S2* cells as expression system (Tan et al., 2002) and was later confirmed by Klenotic and colleagues with TSR–2 and TSR–3 produced in *E.coli* (Klenotic et al., 2011). This was the first high resolution crystal structure of a TSR domain providing a prototypic architecture of structural and functional study of the different TSR superfamily members. At a 1.9 Å resolution, TSRs of TSP–1 showed a three antiparallel ß strand (Tan et al., 2002). The two C–terminal strands (B and C) form a β-sheet structure while the N–terminal strand (A) connects to the second strand (B) by hydrogen bonds and Trp–ladder interactions (Figure 2.5–A). Jar handle structures are present in the loop between the B and C stands. Tryptophan residues located on the first strand A intercalate between the arginine residues on the second strand B. The conserved motifs WSXWS and R*R respectively in strand A and B create a Trp–ladder of six or more rungs. These rungs are stabilized by cation–π interactions between the guanidinium portion of the Arg and the indole portion of the Trp. The Trp–ladder is covered by disulfide bridges at both ends and an occasional substitution of its residues can occur (Olsen et al., 2014 ; Stoddard et al., 2018; Tucker, 2004). It is noteworthy that the lack of post–translational modifications such as glycosylation in the *E.coli* expression system do not influence the structure of the TSRs (Klenotic et al., 2011). In a boarder context, interaction of TSR and various ligands might be mediated through the "recognition" face consisting of a right–handed spiral, positively charged.

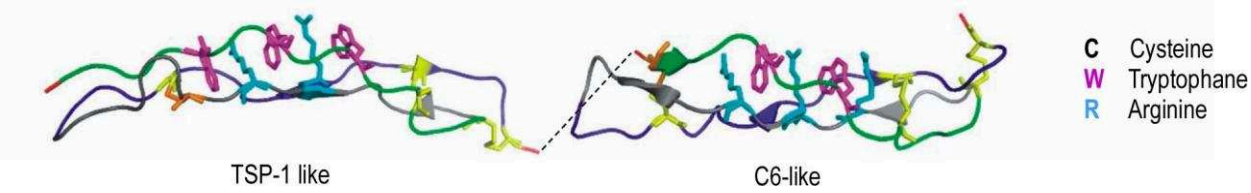

Figure 2.2 – Prediction of the three–dimensional structure of TSP–1–like and C6–like domains in THSD7A. Each domain consists of three antiparallel peptide strands stabilized by three disulfide bridges**.** The first strand of the domain contains two or three tryptophan residues that interlace with two or three arginine residues from the second strand. The first disulfide bond connects the first and the third strand of each domain (C1– C5), and the second disulfide bond connects the second strand and the third strand (C2– C6). The third disulfide bond differs between the TSP–1–like and the C6–like as it connects cysteines in the second and the third strand in TSP–1–like and cysteines in the first strand in C6–like domain. *Adjusted from (Seifert et al., 2018) with copyright permission from the "American Society of Nephrology".*

As detailed below, THSD7A is composed of an alternation of 21 TSRs domains (Figure 2.5–B). Seifert and colleagues suggest that the TSRs in THSD7A show high structural homology to TSP–1 TSRs (TSP–1–like or THBS1; PDB code 3r6b) and complement component 6 (C6–like; PDB code 3t5o) (Figure 2.2) (Seifert et al., 2018) whereas Stoddard and colleagues propose a model of THSD7A consisting of a mixture of TSP–1–like and F–spondin–like domains (Stoddard et al., 2018). Each of these 3 domains folds in three anti–parallel strands and is stabilized by three disulfide bridges. The distinction between the TSP–1–like and the C6–like domain (or F–spondin–like) resides in the position of the third disulfide bridge: the top disulfide is created between a cysteine in the B and C strand in TSP–1–like but in the A and C in C6–like domains or F–spondin–like (Figure 2.5–A) (Carlson et al., 2008).

2.2 The Thrombospondin family

In 1971, while studying the action of thrombin on human platelets, Baenziger and colleagues identified a glycoprotein released from the alpha–granules in response to thrombin stimulation, thereafter this protein was described as the first thrombospondin member (Thrombospondin–1 or TSP–1) (Figure 2.4) (Baenziger et al., 1971). Although some of the thrombospondin components have pre–metazoan origins, they remain exclusively expressed in metazoa (Adams et al., 2011) from drosophila to humans (Carlson et al., 2008; Shoemark et al., 2019).

2.2.1 Structure of Thrombospondins

Thrombospondins (TSPs) comprise a conserved family of extracellular glycoproteins which are oligomeric and multidomain, with various type 1, type 2 and type 3 repeats among other domains. In vertebrates, 5 genes encode for 5 distinct but similar thrombospondins (TSP1 to TSP5) which are all "matricellular" high molecular weight secreted glycoproteins (Figure 2.3). These proteins are further divided in two subgroups, based on the quaternary structure of the proteins into different oligomers: subgroup A comprises TSP–1 and TSP–2 which assemble in trimers while subgroup B comprises TSP–3,

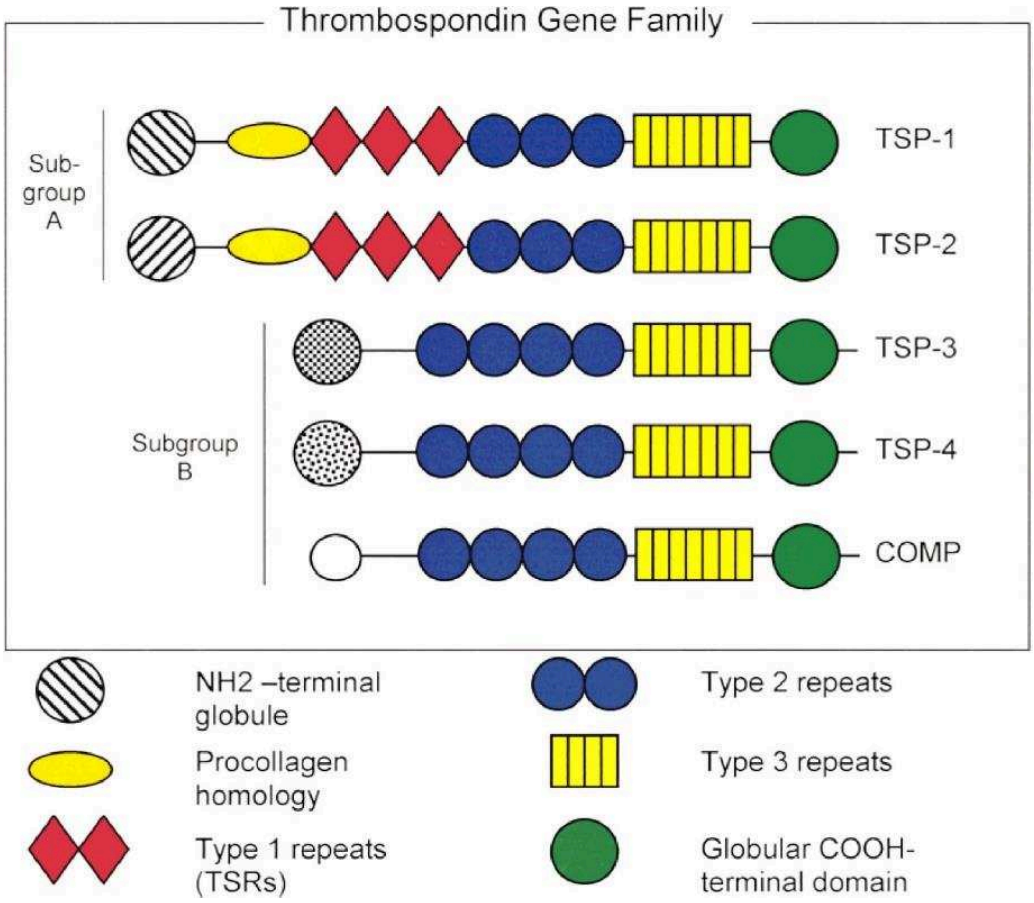

Figure 2.3 – Schematic illustration of the structural organization of the five members of the Thrombospondin family. TSP–1 and TSP–2 belong to the subgroup A while TSP–3, TSP–4 and TSP–5 (COMP) belong to the subgroup B. The domains represented in colors are similar between the different family members while the shaded domains at the N–terminal region share lower identity. *Adjusted from (Adams et al., 2000) with copyright permission from "Developmental Dynamics"*.

TSP–4 and TSP–5 (also known as cartilage oligomeric matrix protein COMP) which form pentamers (Farnoodian et al., 2018; Masli et al., 2014).

All 5 TSP members share the same structural domain organization in their C–terminal region, including 3 to 4 EGF–like domains called thrombospondin type 2 repeats, thirteen calcium binding domains called type 3 thrombospondin repeats and a globular C–terminal domain homologous to the L–type lectin domain (Figure 2.3). The TSP–1 and TSP–2 have a similar N–terminal structural organization consisting of a N–terminal globular domain, a von Willebrand type C domain and 3 thrombospondin type 1 repeats, i.e. TSR domains. In contrast, TSP–3, –4 and –5 have unique N–terminal domains and lack the von Willebrand

type C domain and the type 1 thrombospondin TSR domains (but do have the type 2 and type 3 thrombospondin repeats) (Adams, 2001; Adams et al., 2011).

2.2.2 Function of thrombospondins

TSP members are not only diverse in structure (Figure 2.3) but also in function, as each TSP member fulfills different ones. TSP–1 is implicated in platelet aggregation, regulation of the inflammatory response, angiogenesis and tumor growth. In addition to having these functions, the TSP–2 is also involved in extracellular matrix organization. The role of thrombospondins from subgroup B is less investigated. TSP–5 is expressed in the cartilage and plays a role in adhesion and differentiation of chondrocytes as well as extracellular cellular matrix assembly. TSP–4 and TSP–3 are the least studied thrombospondin members so far (Tucker, 2004).

2.2.3 Thrombospondin–1

Among the five thrombospondin family members, Thrombospondin–1 is the most well–known protein (Figure 2.4) (Lawler, 2002). It has an important role in angiogenesis (Lawler, 2002), cell proliferation, migration and attachment (Chen et al., 2000). Quite amazingly, thrombospondin–1 is known to interact with up 83 ligands comprising extracellular matrix proteins, cell receptors, cytokines and receptors. Heparin and local calcium concentration in the extracellular milieu are known to control thrombospondin–1 interactions by inducing conformational changes and surface exposure of specific binding sites (Resovi et al., 2014).

Thrombospondin–1 is a trimeric molecule of 420 kDa that consists of N– and C–terminal globular domains and 3 distinct types of thrombospondin repeats, one of them being TSR repeats (Tucker, 2004). In addition to the functions listed above, more functions have been attributed to the distinct domains (Figure 2.4) (Adams, 2001; Chen et al., 2000). The Laminin–G domain at N–terminal domain of TSP–1 is involved in heparin binding, disruption of focal contacts, platelet aggregation and TSP–1 endocytosis. The procollagen homology vWF type C domain inhibits angiogenesis. The type–1 repeats (TSRs) of TSP–1

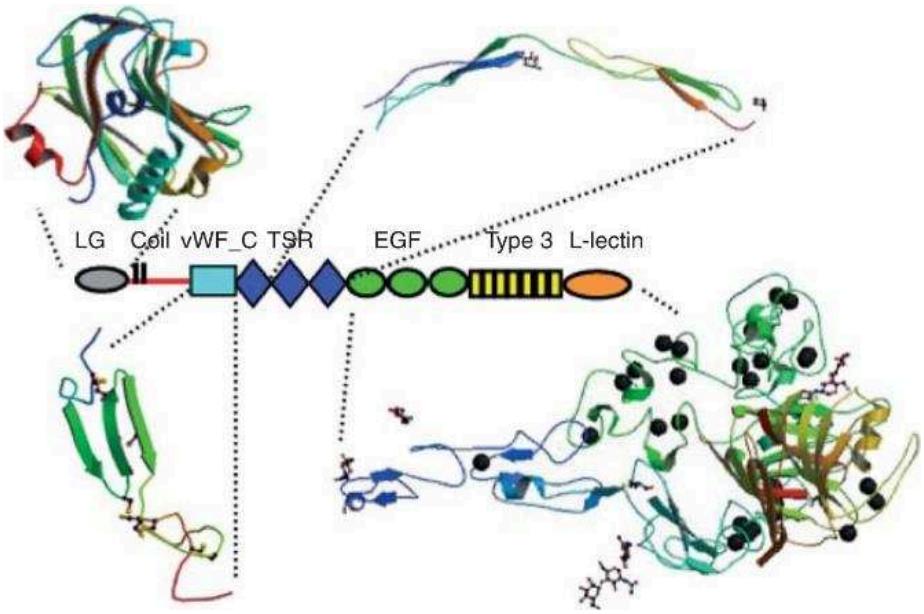

Figure 2.4 – Overall domain structure of thrombospondin–1. The crystal structure of the Laminin–G domain at N–terminal domain is represented in grey (PDB: 2ERF). The second to third TSRs of thrombospondin–1 are represented in dark blue (PDB: 1LSL). The C–terminal region of thrombospondin–1 is represented by the crystal structure of the C–terminal region of thrombospondin–2 (PDB: 1YO8). The black spheres represent Ca^{2+} ions. The vWF_C domain of thrombospondin–1 is represented by the crystal structure of the vWF_C domain of collagen IIA (PDB: 1U5M). The crystal structures are not shown at the same scale. *Adjusted from (Adams et al., 2011) with copyright permission from "Cold Spring Harbor Perspectives in Biology".*

participate in heparin binding, endothelial cell apoptosis and neurite outgrowth. These TSP type–1 repeats can bind CD36, fibronectin and TGF–β. These are followed by TSP type–2 repeats or epidermal–growth factor–like (EGF–like) binding integrins and calcium among other and type–3 calcium binding repeats with an RGD integrin binding domain. The protein ends with a globular–COOH terminal domain that can bind CD47.

– Thrombospondin –1 in kidney

In the kidney, thrombospondin–1 is expressed in various cells including mesangial cells, podocytes and tubular epithelial cells (Figure 2.4) (Hugo et al., 2009). Interestingly, thrombospondin–1 is weakly expressed in normal kidneys while its expression is upregulated in disease states where it may regulate levels of different cytokines, receptors

and proteases (Ponticelli et al., 2017). Various studies using *in vivo* models investigated the role of TSP–1 in the development of renal disease through the regulation of the fibrogenic TGF–β (Cui et al., 2013; Hugo et al., 2009; Maimaitiyiming et al., 2016; Zeisberg et al., 2014). Interestingly, TSP1 plays an important role in obesity–related kidney disease. While wild–type obese mice develop renal hypertrophy and albuminuria associated with increased kidney inflammation and activation of TGF–β signaling and fibrosis, TSP1 knock–out mice fail to develop any of these kidney damages (Cui et al., 2013). In several *in vivo* models of glomerulonephritis, thrombospondin–1 plays pro–apoptotic, pro–inflammatory and pro–fibrotic roles, and was found to be highly expressed in different inflammatory cells at the site of injury (Hugo et al., 2009). For instance, in rat Thy–1 nephritis, an animal model for human mesangio–proliferative glomerulonephritis, silencing of the TSP–1 gene in the animal renal tissues inhibited glomerular mesangial cell proliferation and decrease extracellular matrix production and proteinuria (Qiu et al., 2011).

2.3 Structure and biology of THSD7A

2.3.1 THSD7A family members

THSD7A is a type 1 transmembrane protein expressed in various organs including the cerebral cortex, lung, kidney, testis and the soft tissues. The architecture of this protein is highly conserved during vertebrate evolution starting from *Callorhinchus milii* known as the slowest evolving vertebrate (Seifert et al., 2018). The recently cloned zebrafish THSD7A showed a 69% homology with its human ortholog (hTHSD7A). Chicken, rat and mouse THSD7A orthologs respectively share 83, 90 and 92% of identity with the human THSD7A (Wang et al., 2011).

THSD7A belongs to the superfamily of proteins bearing a “Thrombospondin type–1 repeat or TSR”, present in around 90 other proteins in the human genome (Sims et al., 2015). The number of TSR varies among the different proteins in this superfamily for instance, the properdin contains 6 TSR motifs whereas Sco–spondin contains 25 TSR motifs (Figure 2.1) (Tucker, 2004). It is noteworthy that the structure of THSD7A domains (D1, D3, D6, D8, D12, D13, D12, D17) is highly conserved across species. This suggests a

conserved essential function mediated by these domains or by the full protein (Figure 2.5) (Stoddard et al., 2018).

THSD7B (~180 kDa) is the closest paralog of THSD7A and exhibits the same overall structural organization but only displays 52% of protein sequence identity. THSD7B gene is shown to be implicated in alcohol dependence disease (Wang et al., 2011), tooth agenesis (Haga et al., 2013) in addition to possible implication in non–small cell lung cancer (Lee et al., 2013) and tumor size in uterine leiomyoma (Aissani et al., 2015).

2.3.2 Structural properties of THSD7A

The thrombospondin type 1 domain–containing 7A (THSD7A) protein is encoded by a large gene (458 kb) mapped in chromosome 7p21.3 on the common fragile site (CFS) FRA7B in the terminal region of the short arm (Bosco et al., 2010). THSD7A is a type I transmembrane protein made up of 1,657 amino acids with an approximate molecular mass of 250 kDa for the mature protein (as estimated by SDS–PAGE analysis) (Tomas et al., 2014; Wang et al., 2010). It contains a long signal peptide of around 47 amino acids, a large N–terminal extracellular region with a high content of disulfides and 14 putative sites of N–glycosylation, a single–pass transmembrane domain and a short cytoplasmic tail (Tomas et al., 2014). When first described, the extracellular region was proposed to contain 10 thrombospondin type–1 repeats (TSRs), a coiled–coil domain, an arginine–glycine–aspartic acid motif (RGD), six tryptophan–rich sequences (WSXW), and a CD36 binding motif (Wang et al., 2010).

Recently, two new models of THSD7A were proposed: Seifert and colleagues based their prediction on alignments of THSD7A domains with TSP–1 type I repeats (TSRs) in the Protein Data Bank (PDB) (Seifert et al., 2018) while Stoddard and colleagues used *in silico* homology modeling to predict the detailed structure of THSD7A (Stoddard et al., 2018). The two studies predicted that the extracellular region of THSD7A comprises 21 domains with a combination of TSP–1–like repeats as found in TSP–1 (Klenotic et al., 2011) or in the related component 6 like domains (C6–like) (Figure 2.2) (Aleshin et al., 2012; Seifert et al., 2018) or the F–spondin (F–spondin–like) (Pääkkönen et al., 2006; Stoddard et al., 2018). In the first model of THSD7A, the protein starts with two TSP–1 like domains (D1 and D2)

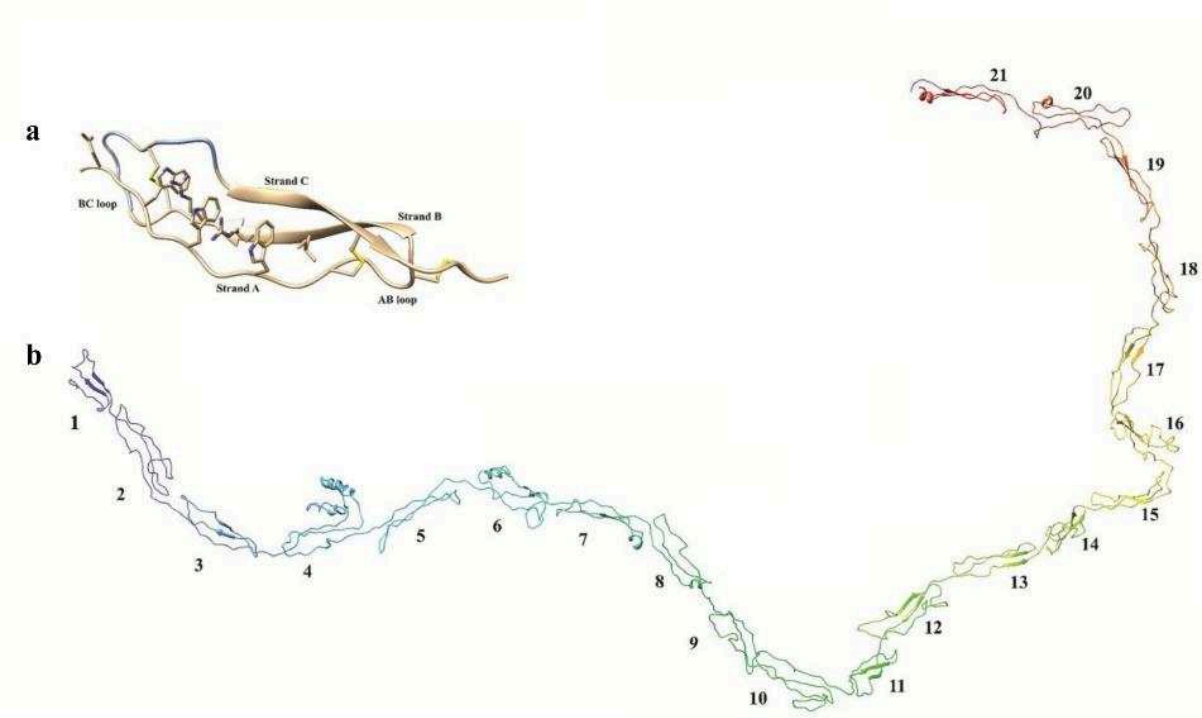

Figure 2.5 – In silico model structure of THSD7A. (a) Crystal structure of the second thrombospondin–1 repeat (PDB: 1LSL). The domain is formed by three anti–parallel strands with strands B and C forming a beta–sheet structure and one AB and BC loops. The three TRP and two arginine residues forming the Trp–ladder are shown. The three disulfide bonds as in TSP–1 like domain (C1–C5, C2–C6, and C3–C4) are shown in yellow. (b) An *in–silico* model structure of the extracellular domain of THSD7A showing 21 thrombospondins repeat domains with alternate THBS1–like or C6–like TSR repeats. *Adjusted from (Stoddard et al., 2018) with copyright permission from "Proteins".*

followed by two C6–like domains (D3 and D4) separated by a hydrophobic coiled–coil domain (CC). Beyond D4, the extracellular region (D5 to D21) consists of an alternating series of TSP–1–like and C6–like domains separated by short linkers of 1 to 9 amino acids (Figure 1.3). Six linker regions contain a proline residue based on the PDB where it is suggested to stabilize the angle between adjacent TSP–1–like and C6–like domains and therefore limit the flexibility of THSD7A (Seifert et al., 2018).

The structure of THSD7A proposed in the second model consists of an alternative series of TSP–1–like and F–spondin–like domains (Stoddard et al., 2018). The designation of this latter is based on the work of Tan K. and colleagues (Tan et al., 2002) where F–spondin serves as the prototype of the group 2 thrombospondin–1 repeats and also because the C strand in these domains are more similar to the F–spondin–like than to the analogous

domains in C6–like domains (Figure 2.2). Similar to what is found in the first model, the N–terminal region of THSD7A consists of two simultaneous TSP–1–like followed by an F–spondin–like domain. Here, they proposed that the coiled–coil structure previously described is in fact not a distinct entity but rather a coiled–coil insertion in one TSP–1 like domain and thus assigned this structure as the 4th domain (Figure 2.5). Subsequently, the rest of the extracellular region consists of alternating TSP–1–like and F–spondin–like domains. It is noteworthy that in this study, the sequence of domain 22 (D21 in (Seifert et al., 2018)) was unable to produce any thrombospondin model contrary to what was previously suggested. The linker regions in this model are limited to no more than one amino acid residue except for three domains (D1–D2, D3–D4 and D4–D5). An additional Trp–ladder structure was also identified in 20 of the 21 domains of THSD7A by Stoddard and colleagues.

Finally, the transmembrane region of THSD7A is a single alpha–helix and the cytoplasmic tail consists of a short coil with some alpha–helix characteristics. The cytoplasmic region contains positively charged residues on the inner side of the plasma membrane. It is suggested that this region might contain a calmodulin binding site (Stoddard et al., 2018).

Overall, the major distinction between these two models resides in the identification of the coiled–coil structure as a separate domain in Seifert et al. or as an insert in within a larger TSP–1–like domain in Stoddard et al. Nonetheless, we believe that both models bring valuable information on the structural design of THSD7A and that the differences between them is rather negligible.

2.3.3 Functional properties of THSD7A

Before the identification of THSD7A as a second autoantigen in MN, the number of studies investigating its function were very limited, with only 8 articles referred in PubMed with the keyword "THSD7A". Currently, most of the research is focused on the implication of THSD7A in MN and its expression within the glomerulus, with 52 articles in PubMed for "THSD7A and MN", among 68 in total.

– Hypothetical functions based on structural motifs

Many functions can be suggested based on the structural motifs present in the extracellular region of THSD7A. However, there is so far no strong biological data to support any of the following hypotheses.

Since the TSR domains of TSP1 have well–known binding function within the extracellular matrix, the homologous domains of THSD7A may fulfill similar adhesion functions. Similar to what is found in TSP–1, THSD7A contains six tryptophan–rich motifs (WSXW) in the C6–like (F–spondin–like) TSP1 domains (Figure 2.2). These motifs are known to bind the VLAL motif on the latent transforming growth factor– β complex (TGF–β) (Young et al., 2004) and to interact with fibronectin and promote cell adhesion by binding to glycoconjugates like heparin and sulfatides (Guo et al., 1992).

An RGD site may be located on the C–terminal of THSD7A (Wang et al., 2010). It is a cell adhesion site of many extracellular matrix proteins through the integrins on the cell surface. The specificity of interaction of different proteins is insured by a large number of integrins highly specific for one RGD–containing ligand. In addition to thrombospondins (Lawler et al., 1988), other ECM proteins contain one or more RGD sites including fibronectin (Pierschbacher et al., 1984), collagen type I and von Willebrand factor (Ruoslahti et al., 1987). Of note, this interaction can be fully lost by RGD containing peptides (Craig et al., 1995) or by a substitution of any amino acid as small as the exchange of alanine with glycine (Pierschbacher et al., 1984).

An additional CD36 binding motif CSQTCG was proposed by Wang and colleagues suggesting that it could promote activity toward CD36–expressing cells in the microvasculature (Wang et al., 2010).

– Role in cell adhesion

It is only until recently that THSD7A earned the “angioneurin” description due to its dual implication in angiogenesis and neurogenesis. It was first shown that THSD7A is preferentially expressed in the vasculature of placenta and in the human umbilical vein endothelial cells (HUVECs). In this context, THSD7A regulated endothelial cell migration and tube formation and engaged in organization of the cytoskeleton by forming clusters

with $\alpha_v\beta3$ integrin and paxillin at the focal adhesion sites (Wang et al., 2010). This endothelial tube formation and focal adhesion might likely be due to a soluble form available after cleavage of the transmembrane protein through the FAK–dependent signaling pathway (Kuo et al., 2011). (Chapter 5.3.2)

In developing zebrafish embryos, thsd7a is expressed at the ventral edge of the neural tube and is required for intra–segmental vessel patterning and neurovascular interaction (Wang et al., 2011). Further investigations discovered that thsd7a in developing zebrafish is expressed in the primary motor neurons and that a knockdown of its expression leads to the disruption of normal primary motor neuron formation and ISV sprouting via the Notch–dll4 signaling pathway (Liu et al., 2016).

Furthermore, the implication of thrombospondin–1 repeats and THSD7A in HUVECs in cell to extracellular matrix interactions suggests that THSD7A is likely to contribute to podocyte adhesion to the GBM (Kuo et al., 2011). THSD7A is expressed at the basal membrane of human and rodent podocytes. Evidence of its localization in the foot processes and the slit diaphragm were shown by EM imaging (Gödel et al., 2015). Glomerular cell extracts exposed to anti–THSD7A antibodies showed cytoskeleton rearrangement and focal adhesion alteration while binding of anti–THSD7A to THSD7A–overexpressing HEK293 induced cell detachment and apoptosis (Tomas et al., 2016). Finally, knockdown of THSD7A in zebrafish induced podocyte injury and disturbed the glomerular filtration barrier. These results demonstrated the importance of THSD7A for the structure of the glomerular filtration barrier (Tomas et al., 2017).

– Role in cancer

THSD7A is overexpressed in many tumor types including prostate, breast, renal, and colorectal cancers and this is due to a polysomy of the chromosome 7. The loss or gain of THSD7A expression is not consistent in the different tumors: low THSD7A expression in colorectal and renal cancers and overexpression in prostate cancer were associated with poor outcome (Stahl et al., 2017). Stahl and colleagues speculate that expression levels of THSD7A are linked with vascular invasion, metastasis and angiogenesis. Moreover, since FAK is overexpressed is cancer and is believed to play a role in tumor progression, they suggest that the soluble form of THSD7A can be involved in cancer development through

the FAK–signaling pathway (Kuo et al., 2011; Stahl et al., 2017). *In vitro*, cellular knock–down of THSD7A inhibits proliferation, invasion and migration activities of human Esophageal Squamous Cell Carcinoma (ESCC) cells (Hou et al., 2017).

In line with these studies, THSD7A may have a causal relationship in the development of THSD7A–associated MN (Hoxha et al., 2017; Hoxha et al., 2016; Lin et al., 2018; Stahl et al., 2017; Taguchi et al., 2019). The overexpressed THSD7A may be presented to the immune system as a new autoantigen, followed by a rise of the humoral response against THSD7A that eventually attacks the protein in the podocyte and causes MN (Stahl et al., 2017).

– Other functions

The SNP rs12673692 on THSD7A was shown to be significantly associated with lumbar and femoral bone mass density in adult Japanese women osteoporosis patients (Cao et al., 2012; Mori et al., 2008; Zhou et al., 2013). The TSP–1 present in THSD7A activates TGF–β which in turn stimulates bone matrix formation. This possibly suggests that THSD7A might play an important role in bone metabolism and the pathogenesis of osteoporosis through the modulation of TGF–β activity.

Also, THSD7A may contribute to preeclampsia, a common pregnancy disorder. The distribution pattern of THSD7A was similar to that of miR–210 (a small RNA with a predominant expression in preeclamptic placenta) in human placenta. MiR–210 binds to the 3'–UTR of THSD7A gene from 5182nt to 5189nt and suppresses THSD7A expression *in vitro*. Moreover, the inhibition of THSD7A expression attenuates the invasion–promoting effect of anti–miR–210 (Luo et al., 2016).

Finally, a genetic analysis showed that the SNP rs1526538 of THSD7A is linked to obesity or higher body mass index in Indian/south Asian populations. This may be consistent with the possible role of THSD7A in angiogenesis and the fact that angiogenesis is involved in obesity and adipose metabolism (Cao, 2007; Nizamuddin et al., 2015).

3 Aims of the study

The general aim of this thesis was to address the major molecular and clinical challenges raised after the identification of THSD7A as the second autoantigen in MN.

Only recently before the start of this PhD thesis project, THSD7A was identified as the second autoantigen in MN (Tomas et al., 2014). In that study, a limited number of patients (15) were identified, thus restricting the ability to answer many of the queries revolving around this discovery:

– What is the actual prevalence of THSD7A–associated MN disease? Which assay can be employed for diagnosis and prognosis of these patients?

– What are the clinical characteristics of THSD7A–associated MN patients? Are they specific for this subgroup or are they in accordance with those described for PLA2R1–associated MN patients? Are the levels of anti–THSD7A autoantibodies indicative of disease activity and response to treatment?

– Where are the epitope domains on the large THSD7A protein and are they linked by a mechanism of epitope spreading? Can the epitope profiling on THSD7A be used as a clinical biomarker of disease activity, like for PLA2R1?

The first objective was thus to develop the first ELISA assay that can be used in clinical settings for diagnosis of patients with THSD7A–associated MN. To establish the novel test, the main challenge was to produce and purify large amounts of folded THSD7A. It was indeed shown that anti–THSD7A antibodies only bind to conformational epitopes therefore conserving the three–dimensional structure of THSD7A is critical for the establishment of the ELISA assay. After the validation of our ELISA assay, we aimed to analyze a large cohort of THSD7A–associated MN patients to better document the clinical characteristics of THSD7A–positive patients. We screened 1012 patients with biopsy–proven MN from 6 cohorts and identified 49 patients with THSD7A–associated MN with specific clinical characteristics, suggesting etiologies different from those for PLA2R1–associated MN. We showed that measuring anti–THSD7A titer is useful to evaluate disease activity, response to treatment and clinical outcome.

The second objective concerned the physiopathological mechanism of MN and was focused on the identification of the THSD7A domains that contain conformational epitopes. For PLA2R1–associated MN, our laboratory recently identified several epitopes located in different PLA2R1 domains and linked by a mechanism of epitope spreading associated with worsening of the disease. Following one of the strategies previously used to identify epitopes in PLA2R1 (Fresquet et al., 2015; Roth et al., 2013) or other autoantigens, our initial attempt was to identify the THSD7A epitope domains by a proteolytic approach coupled to analysis by mass spectrometry. However, this method was unsuccessful because THSD7A is heavily disulfide–bonded and very resistant to proteolysis. To overcome this problem, we went back to the site–directed mutagenesis approach and identified autoantibodies targeting up to 6 distinct epitope regions on THSD7A. We further investigated the immunodominance of each epitope region and identified 4 groups of patients and analyzed their clinical characteristics.

Finally, I also participated in evaluating the predictive value of anti–PLA2R1 titer and epitope spreading in the GEMRITUX prospective cohort of 58 patients treated with rituximab. We showed that epitope spreading in PLA2R1–associated MN at baseline correlates with low clinical remission rate and suggested that epitope profiling may be considered for early therapeutic intervention.

4 Results

4.1 Development of an ELISA to identify THSD7A–associated MN patients (Article 1)

Following the identification of THSD7A as the second autoantigen in MN, it became important to develop a sensitive ELISA assay that will be useful in many aspects for patients with THSD7A–associated MN, starting from sensitive diagnosis and careful evaluation of the low prevalence of this disease entity. It was also important to screen such a population of MN patients with the hope to identify in the end a sufficient number of THSD7A–positive patients to analyze their specific characteristics. Screening of patients at a large scale requires a sensitive and performant method, faster and more quantitative than western blot and IIFT. Similar to what was done following the identification of PLA2R1 as the major autoantigen in MN, it was important to investigate the relationship between anti–THSD7A antibody titer and severity of the disease and its potential use as a prognosis factor.

In this context, the first aim of my project was to establish a reproducible ELISA test to screen a high number of MN patients. This assay will be used not only for the diagnosis of patients but also for follow–up of disease activity and prognosis.

4.1.1 Production of the recombinant protein

Little information about the detailed structure of THSD7A was available at the time we were developing the ELISA test. The amino acid sequence of the extracellular region of THSD7A is particularly rich in cysteines engaged into disulfide bonds, with a total number of disulfide bonds more than two–fold higher than in PLA2R1. Indeed, THSD7A contains 132 cysteines (8.5% of all amino acids) forming 66 disulfides while PLA2R1 has 54 cysteines (3.9%) forming 27 disulfides. With this information, we anticipated a robust and tightly packed conformation for THSD7A with a correct pairing of cysteine residues being crucial to maintain the structure of the protein. Additionally, it was predicted that THSD7A holds 14 glycosylation sites and this was in agreement with the important shift in the protein molecular mass after deglycosylation. Although patients' recognition of THSD7A was not

altered after deglycosylation of the protein by western blot (Tomas et al., 2014) we did not know whether glycosylation was crucial for antibody binding. The choice of the expression system was thus important to guarantee folding with appropriate cysteine pairing and glycosylation of THSD7A, similar to the endogenous protein present in kidney. For all these reasons, we chose to produce THSD7A in the eukaryotic system (HEK293 cells) rather than a prokaryotic (*E. coli*) system that lacks many of the mammalian post–translational modifications or an insect–cell system that produces proteins with different N–glycosylation motifs, possibly altering folding and solubility of the recombinant protein.

It is important to note that a soluble form of THSD7A of 200 kDa has been detected in the culture medium of HUVECs (native expression) and in HEK293 transfected with the full transmembrane protein (Kuo et al., 2011). Therefore, transfection of HEK293 with the full transmembrane THSD7A would produce both the soluble and the transmembrane. However, the epitopes on THSD7A and the proteolytic cleavage site(s) leading to the shedding of THSD7A are not yet identified. This prevented the use of the transmembrane form of THSD7A to generate the soluble form.

When I arrived in the lab, Guillaume Dolla had already designed and validated different constructs of membrane or soluble THSD7A with different tags added on the C–terminal end. The soluble form of THSD7A was designed with a 6x–Histidine tag at the C–terminal end and the transmembrane form was available with either a 6x–Histidine, an HA or a Flag tag at the C–terminal end. After transient transfection, the expression of the constructs of THSD7A detected by western blot showed that all four constructs had good expression levels. However, detection of the soluble form of THSD7A in medium was only possible for the soluble construct. For the membrane constructs, the generated soluble form was hardly detectable in medium, confirming the previous results obtained by Kuo et al. (Kuo et al., 2011). In their study, detection of the soluble form of THSD7A was only possible after concentrating the cell medium by about 100–fold. These results suggest an intracellular retention or uptake of the cleaved protein by the cell or even a possible degradation of the released fragments.

Based on these results, we decided to generate HEK293 cells expressing the soluble form of THSD7A with a 6x–Histidine tag at the C–terminal end subcloned into an expression plasmid allowing isolation of transfected cells by selection with antibiotics. The expression yield of recombinant proteins in transfected HEK293 cells depends on many

factors including the percentage of transfected cells within the population, the efficiency of gene transcription and translation, the level of post–translational modifications, etc. Additionally, the transiently transfected cells do not integrate the gene in their genome thus the expression is lost after a short period of time post–transfection. For this reason, we selected cells stably–expressing THSD7A after selection with neomycin and isolated single clones of HEK293 expressing soluble THSD7A–6xHis by limiting dilution. The production of soluble THSD7A–6xHis varied up to 10–folds among the 38 different clones analyzed. We selected the clone (D9) showing the highest production of THSD7A and amplify cells for the large–scale production of THSD7A up to a few liters in rollers. The recombinant protein was recovered from cell medium, purified by affinity chromatography on complete His–tag resin and the pure protein was used to develop the ELISA test described in the article 1 published in the Kidney International journal in which I am first author.

4.1.2 Identification of THSD7A–associated MN patients

We optimized our ELISA for detection of IgG4 anti–THSD7A antibodies by screening patients with "all cases of MN", i.e. expected to have THSD7A–associated MN or PLA2R1–associated MN or being double negative for both antigens, as well as other disease controls (Figure 1 of article 1). Using a ROC curve analysis, we set up a threshold for positivity at 16 RU/mL. We then used the ELISA to screen 1012 biopsy–proven MN patients from 6 national and international cohorts. This led to the identification of 28 cases of THSD7A–associated MN and demonstrates a prevalence of 2.8% for this disease entity. We also screened patients' serum that we received during a total period of 4 years and that were referred to our network of nephrology centers because of negativity for PLA2R1. This screening led to the inclusion of 21 additional patients constituting a cohort of 49 patients, which is relatively large when taking into consideration the rarity of this condition.

Only a couple of months after I arrived in the lab, Hoxha et al. published an IIFT for detection of anti–THSD7A antibodies in serum. We thus compared the positivity of the 49 patients using the three available detection techniques: ELISA, WB and IIFT (Figure 2 of article 1). It is important to note that the results obtained with our ELISA and the commercially available IIFT correlated significantly. We also found that the ELISA detection was more sensitive when using anti–IgG4 as compared to the anti–total IgG

detection. Finally, only 4 cases of MN double positivity for PLA2R1 and THSD7A were documented in the last two years (Larsen et al., 2016; Wang et al., 2017). The positivity for the antigens and antibody titers were not carefully investigated in these previous studies. Therefore, we could collect serum from these patients and examine in fact all the cases of MN patients which were reported in the world to be double positivity, i.e. a total of 8 MN patients (the 4 above previously published cases and 4 new cases obtained from our screening) (Figure 3 of article 1). We showed that levels of anti–PLA2R1 and anti–THSD7A can vary in any direction between the 8 patients and that patients can be positive or negative in serum but positive in biopsy, similar to what was already documented for MN patients with single positivity for PLA2R1 and THSD7A (Debiec et al., 2011; Hoxha et al., 2017). In our cohort, the 8 patients with double positivity did not differ clinically when compared to the other patients.

4.1.3 Clinical characteristics of THSD7A–associated MN patients

The study of this large cohort of 49 THSD7A–associated MN patients allowed for the first time a detailed analysis of the clinical characteristics of this particular group of patients. Interestingly, we observed that the male to female gender ratio of this cohort (1.3:1) contrasts with the typical ratio observed in the general MN population (2:1). We also identified a subgroup of young females below the age of menopause estimated at 51 years (Figure 4A of article 1). Apart from their age, the young female patients did not differ clinically from females above 51 years. Our data however suggest a possible etiology of MN with pregnancy or preeclampsia for this particular group of patients, in line with other case report studies (Iwakura et al., 2016; Luo et al., 2016).

Anti–THSD7A titers correlated with disease activity. We observed high antibody titer in patients with active disease and lower titers in patients on partial or complete remission. Anti–THSD7A titer appeared as a robust biomarker to monitor not only disease activity but also response to treatment. This was demonstrated by the illustration of 12 patients with available follow–up serum and different treatments (Figure 5 of article 1).

We were also able to demonstrate that anti–THSD7A titer at baseline can predict clinical outcome. By analyzing 36 patients for a median follow–up of 37 months, we

observed that patients with antibody titer below 134 RU/mL had a lower incidence of renal events as compared to patients with antibody titers above this value (Figure 6 of article 1).

Finally, many studies have suggested an implication of cancer in the development of THSD7A–associated MN (Hoxha et al., 2017; Hoxha et al., 2016; Stahl et al., 2017; Taguchi et al., 2019). We thus investigated the patients in our cohort for history of malignancy. Only 8/49 patients had a history of cancer, indicating a low prevalence in our cohort, and except for the fact that these patients had higher antibody titers, they did not show any clinical difference when compared with other patients in this cohort. Interestingly all patients with malignancy were significantly older than the rest of the population, suggesting that malignancy is likely co–incidental with MN disease rather than causative of MN in our cohort patients.

We conclude that our ELISA is a robust assay for the evaluation of anti–THSD7A antibodies and for monitoring disease activity and follow–up.

Article 1

Novel ELISA for thrombospondin type 1 domain-containing 7A autoantibodies in membranous nephropathy

Christelle Zaghrini[1], Barbara Seitz-Polski[1,2,3], Joana Justino[1], Guillaume Dolla[1], Christine Payré[1], Noémie Jourde-Chiche[4,5], Anne-Els Van de Logt[6], Caroline Booth[7], Emma Rigby[7], Jennie Lonnbro-Widgren[8], Jenny Nystrom[9], Christophe Mariat[10,11], Zhao Cui[12], Jack F.M. Wetzels[6], GianMarco Ghiggeri[13], Laurence H. Beck Jr[14], Pierre Ronco[15,16,17], Hanna Debiec[15,16] and Gérard Lambeau[1]

[1]*Université Côte d'Azur, Centre National de la Recherche Scientifique, Institut de Pharmacologie Moléculaire et Cellulaire, UMR7275 Valbonne Sophia Antipolis, France;* [2]*Laboratoire d'Immunologie, Centre Hospitalier Universitaire de Nice, Université Côte d'Azur, Nice, France;* [3]*Service de Néphrologie, Centre Hospitalier Universitaire de Nice, Université Côte d'Azur, Nice, France;* [4]*Aix-Marseille Université, Centre Recherche en Cardiovasculaire et Nutrition, Institut National de la Recherche Agronomique 1260, Institut National de la Santé et de la Recherche Médicale 1263, Marseille, France;* [5]*Assistance Publique–Hôpitaux de Marseille, Centre de Néphrologie et Transplantation Rénale, Hôpital de la Conception, Marseille, France;* [6]*Department of Nephrology, Radboud Institute for Health Sciences, Radboud University Medical Center, Nijmegen, the Netherlands;* [7]*Evelina London Children's Hospital, Lambeth, London, United Kingdom;* [8]*Institute of Medicine, Sahlgrenska University Hospital, University of Gothenburg, Gothenburg, Sweden;* [9]*Institute of Neuroscience and Physiology, University of Gothenburg, Gothenburg, Sweden;* [10]*Service de Néphrologie Dialyse, Transplantation Rénale, Hôpital Nord, Lyon, France;* [11]*CHU de Saint-Etienne, GIMAP, EA 3065, Université Jean Monnet, Saint-Etienne, Comue Université de Lyon, Lyon, France;* [12]*Renal Division, Department of Medicine, Peking University First Hospital, Beijing, China;* [13]*Division of Nephrology, Dialysis and Transplantation, Laboratory of Molecular Nephrology, G. Gaslini Children Hospital, Genoa, Italy;* [14]*Renal Section, Department of Medicine, Boston University School of Medicine, Boston, Massachusetts, USA;* [15]*Sorbonne Université, Université Pierre et Marie Curie, Université Paris 6, Paris, France;* [16]*Institut National de la Santé et de la Recherche Médicale, Unité Mixte de Recherche_S1155, Paris, France; and* [17]*Service de Néphrologie et Dialyses, Assistance Publique–Hôpitaux de Paris, Hôpital Tenon, Paris, France*

Autoantibodies against phospholipase A2 receptor 1 (PLA2R1) and thrombospondin type 1 domain-containing 7A (THSD7A) are emerging as biomarkers to classify membranous nephropathy (MN) and to predict outcome or response to treatment. Anti-THSD7A autoantibodies are detected by Western blot and indirect immunofluorescence test (IIFT). Here, we developed a sensitive enzyme-linked immunosorbent assay (ELISA) optimized for quantitative detection of anti-THSD7A autoantibodies. Among 1012 biopsy-proven MN patients from 6 cohorts, 28 THSD7A-positive patients were identified by ELISA, indicating a prevalence of 2.8%. By screening additional patients, mostly referred because of PLA2R1-unrelated MN, we identified 21 more cases, establishing a cohort of 49 THSD7A-positive patients. Twenty-eight patients (57%) were male, and male patients were older than female patients (67 versus 49 years). Eight patients had a history of malignancy, but only 3 were diagnosed with malignancy within 2 years of MN diagnosis. We compared the results of ELISA, IIFT, Western blot, and biopsy staining, and found a significant correlation between ELISA and IIFT titers. Anti-THSD7A autoantibodies were predominantly IgG4 in all patients. Eight patients were double positive for THSD7A and PLA2R1. Levels of anti-THSD7A autoantibodies correlated with disease activity and with response to treatment. Patients with high titer at baseline had poor clinical outcome. In a subgroup of patients with serial titers, persistently elevated anti-THSD7A autoantibodies were observed in patients who did not respond to treatment or did not achieve remission. We conclude that the novel anti-THSD7A ELISA can be used to identify patients with THSD7A-associated MN and to monitor autoantibody titers during treatment.

Kidney International (2019) **95,** 666–679; https://doi.org/10.1016/j.kint.2018.10.024

KEYWORDS: clinical outcome; ELISA; malignancy; membranous nephropathy; sex; THSD7A

The primary form of membranous nephropathy (MN) is an autoimmune kidney disease in which circulating autoantibodies target podocyte autoantigens, leading to deposition of immune complexes in the glomerular capillary wall, podocyte injury, and proteinuria.[1–3] Overall, MN affects more men than women (sex ratio 2:1), with a peak incidence at 50 to 55 years.[4,5] Clinical outcome varies from spontaneous remission to persistent proteinuria and end-stage renal disease in about 30% of cases.

Correspondence: *Gérard Lambeau, Institut de Pharmacologie Moléculaire et Cellulaire, Unité Mixte de Recherche 7275, Centre National de la Recherche Scientifique et Université Côte d'Azur, 660 Route des Lucioles, Sophia-Antipolis, 06560 Valbonne, France. E-mail: lambeau@ipmc.cnrs.fr*

Received 2 July 2018; revised 18 September 2018; accepted 11 October 2018

In 2009, phospholipase A2 receptor 1 (PLA2R1) was identified as the major target autoantigen with circulating autoantibodies present in about 70% of MN patients.[6] In 2014, thrombospondin type 1 domain-containing 7A (THSD7A) was identified as a second autoantigen for another group of 2% to 5% MN patients.[7] Most cases of PLA2R1- and THSD7A-associated MN are mutually exclusive, yet rare cases of dual positivity have been described.[8–10]

Both PLA2R1 and THSD7A autoantigens are expressed in human podocytes and are membrane-bound proteins (180 and 250 kDa, respectively) with a long extracellular region comprising multiple but distinct domains with disulfide bonds.[6,7] Anti-PLA2R1 and anti-THSD7A autoantibodies exclusively bind to conformational epitopes present in 1 or more respective domains and are predominantly of the IgG4 subclass.[11–16] Epitope spreading associated with disease worsening has been suggested for PLA2R1.[13,14]

Although the pathogenic role of anti-PLA2R1 autoantibodies is still a matter of debate, multiple studies have shown that anti-PLA2R1 autoantibodies are specific and sensitive biomarkers for 50% to 80% of MN patients, depending on the studied cohorts.[17,18] Anti-PLA2R1 autoantibodies are nowadays measured by robust biological assays such as indirect immunofluorescence test (IIFT)[19] and enzyme-linked immunosorbent assay (ELISA).[20,21] Furthermore, PLA2R1 antigen accumulated in glomerular immune deposits is detected by standardized biopsy staining protocols.[22–24] These assays are now routinely used in clinical practice to identify and diagnose patients with PLA2R1-associated MN, predict clinical outcome, and improve clinical management from conservative therapy to treatment with potent immunosuppressors.[20,25–36] Other specific assays have also been described.[37,38]

Concerning THSD7A, patients' autoantibodies have recently been shown to be pathogenic in a mouse model.[39,40] However, the detection of circulating autoantibodies is currently possible by Western blot (WB)[7] and IIFT,[41] which provide only semi-quantitative titers. As for PLA2R1-related MN, standardized biopsy staining protocols that can detect THSD7A antigen in glomerular immune deposits have been reported.[8,9,42,43] Developing more robust and rapid assays such as ELISA for the sensitive and quantitative measurement of autoantibody levels in THSD7A-associated MN patients would be helpful for both diagnosis and clinical follow-up.

In this study, we describe the setup of the first ELISA for the sensitive and quantitative detection of anti-THSD7A autoantibodies. We used the assay to screen a combined cohort of 1012 MN patients and identified 28 THSD7A-positive patients, indicating a prevalence of 2.8%. We also screened additional PLA2R1-negative patients and included in total 49 THSD7A-positive MN cases. We tested all cases by WB and IIFT, characterized the anti-THSD7A IgG subclasses and analyzed their reactivity for PLA2R1. We finally described the clinical characteristics of this population for age, sex, disease activity, and possible links to etiology including malignancy. Our results show that this ELISA is rapid, sensitive, and specific to measure anti-THSD7A autoantibodies and will be useful for better diagnosis and clinical follow-up of MN patients.

RESULTS

ELISA setup

We prepared the full extracellular domain of human THSD7A in human embryonic kidney (HEK) 293 cells (Supplementary Figure S1) as soluble antigen and set up an ELISA that can specifically detect anti-THSD7A autoantibodies in serum from a subset of patients with MN but not from patients with other diseases or from healthy donors (Figure 1). Because many studies have shown that IgG4 is the predominant IgG subclass in MN patients[6,7,20,21,24,42,44,45] and is more sensitive than total IgG to measure anti-PLA2R1 autoantibodies,[6,7,13,46,47] we optimized the ELISA for detection of IgG4 anti-THSD7A autoantibodies. Using the above-mentioned serum samples and receiver-operating characteristics curve analysis, we defined a cutoff value of 16 relative units (RU)/ml above which serum samples are considered positive for anti-THSD7A (Figure 1 and Supplementary Figure S2A). We also established a standard curve for conversion of optical density values into RU/ml (Supplementary Figure S2B).

Identification of THSD7A-positive patients

Screening by ELISA of baseline serum from a total of 1012 biopsy-proven MN patients from 6 national and international cohorts[14,20,32,33,48–51] led to the identification of 28 THSD7A-positive patients, indicating an overall prevalence of 2.8% for THSD7A-associated MN (Table 1). Three of these patients were also positive for anti-PLA2R1 autoantibodies, indicating a prevalence of about 0.3% for double-positive MN patients (Table 1).

Additionally, our consortium screened for THSD7A positivity in baseline serum or biopsy from other MN patients (mostly referred to our different nephrology centers because of PLA2R1-unrelated MN over the last 4 years) by any of the 4 techniques available to identify THSD7A-associated MN: ELISA, IIFT, WB, or enhanced THSD7A staining in biopsy.[8,9,14,33,41] This led to the inclusion of 21 additional THSD7A-positive patients, among which 5 were double positive. Collectively, our cohort thus included 49 THSD7A-positive MN patients (Figure 1, Supplementary Figure S3, Table 2, and Supplementary Table S1).

Comparison of THSD7A positivity by ELISA, WB, and IIFT and analysis of IgG subclasses

We then compared the positivity for THSD7A in baseline serum from the 49 patients by the 3 techniques: ELISA, WB, and IIFT (Figure 2, Supplementary Table S1). In total, 43 of 49 patients were fully positive by ELISA (Figure 1, Supplementary Table S1 for IgG4 detection), IIFT (Supplementary Figure S4, Supplementary Table S1 for total IgG detection), and WB (Supplementary Figure S5, Supplementary Table S1 for IgG4 detection). Among the 6

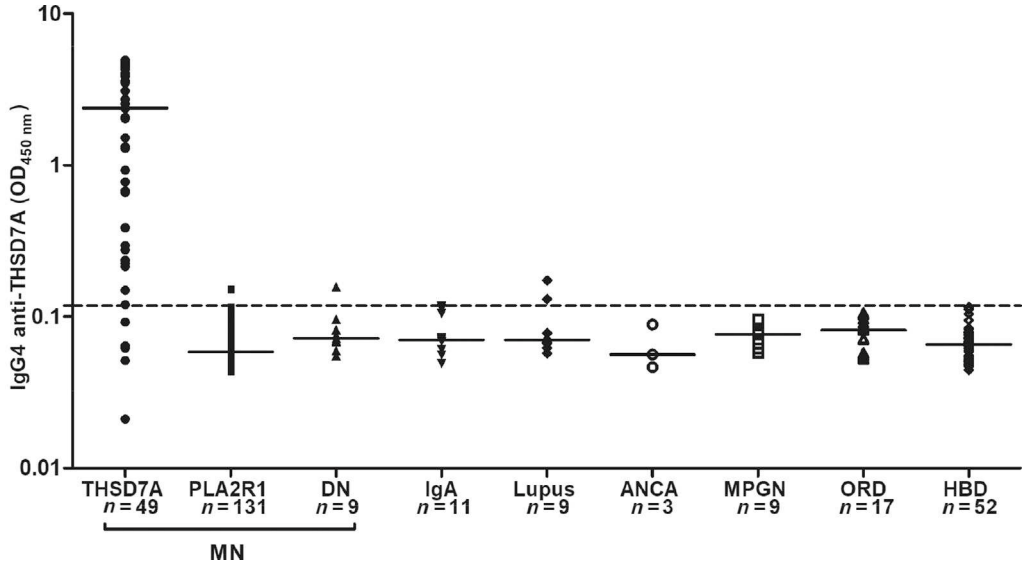

Figure 1 | Comparative analysis of IgG4 reactivity against thrombospondin type 1 domain-containing 7A (THSD7A) determined by enzyme-linked immunosorbent assay (ELISA). IgG4 anti-THSD7A reactivity was validated using THSD7A-positive membranous nephropathy (MN) patients (with respect to positivity by indirect immunofluorescence test and Western blot) versus THSD7A-negative MN patients (phospholipase A2 receptor 1 [PLA2R1]–positive and double-negative [DN] patients) and other control subjects (other diseases and healthy blood donors, $n = 101$). The data are expressed as optical density $(OD)_{450\ nm}$ and presented as medians. The dotted line represents the cutoff ($OD_{450\ nm}$ of 0.12 corresponding to 16 relative units/ml) at a defined specificity of 97% with respect to immunofluorescence test by receiver-operating characteristic curve analysis (Supplementary Figure S2). ANCA, anti-neutrophil cytoplasmic autoantibodies; HBD, healthy blood donor; IgA, IgA nephropathy; Lupus, lupus nephritis; MPGN, membranoproliferative glomerulonephritis; ORD, other renal diseases.

remaining patients, membranous nephropathy patient 40 (MN40) and MN41 were positive by IIFT when assayed at a 1:10 dilution with detection of total IgG (Supplementary Figure S4) but negative by WB and ELISA when detected for IgG4 (Supplementary Table S1). On the other hand, MN46 was positive by ELISA and WB but negative by IIFT (Figure 3). The last 3 patients (MN47, MN48, and MN49) were negative in serum by all 3 techniques but were positive based on THSD7A biopsy staining (Figure 3, Supplementary Figure S6).[9]

Because ELISA titers ranged over several logs (Figure 2, Supplementary Figure S3), we compared the different assays for 3 representative patients having low- to high-range anti-THSD7A titers and analyzed the correlation of titers measured by ELISA and IIFT for the whole cohort. Figure 2 shows that the 3 patients can be detected by ELISA at a 1:100 serum dilution (Figure 2a), by WB at the same dilution or lower (Figure 2b) and by IIFT, where appropriate dilution ranging from 1:10 to 1:1000 gave a specific signal (Figure 2c). The autoantibody titers measured by ELISA and IIFT correlated significantly ($r = 0.8592$, $P < 0.0001$) (Figure 2d for IgG4 ELISA and Supplementary Figure S3B for total IgG ELISA).

We also tested the positivity of the 49 patients by ELISA when detection of anti-THSD7A autoantibodies was performed with secondary antibodies specific for other IgG subclasses or total IgG. In our conditions, we detected IgG1, IgG2, and IgG3 anti-THSD7A autoantibodies in only 14%, 18%, and 20% of patients, respectively (Supplementary Figure S3C). As for total IgG, 38 of the 49 patients (78%) were positive, with autoantibody titers spanning 3 log units and correlating significantly with IgG4 titers ($r = 0.925$,

Table 1 | THSD7A and PLA2R1 reactivity of patients' sera from the different MN cohorts screened in this study

	Patients				THSD7A-positive		THSD7A-negative	
Cohort	All	Male	Female	THSD7A-positive	PLA2R1-positive	PLA2R1-negative	PLA2R1-positive	PLA2R1-negative
Nice	275	183 (67)	92 (33)	8 (2.9)	1	7	150 (54.6)	117 (42.5)
Saint-Etienne	68	45 (66)	23 (34)	2 (2.9)	0	2	41 (60.3)	25 (36.8)
Gemritux	75	52 (69)	23 (31)	2 (2.7)	0	2	61 (81.3)	12 (16.0)
Sweden	25	16 (64)	9 (26)	1 (4.0)	0	1	16 (64.0)	8 (32.0)
Italy	251	175 (70)	76 (30)	6 (2.4)	2	4	182 (72.5)	63 (25.1)
Netherlands	318	219 (69)	99 (31)	9 (2.8)	0	9	234 (73.6)	75 (23.6)
Total	1012	690 (68.2)	322 (31.8)	28 (2.8)	3 (0.3)	25 (2.5)	684 (67.6)	300 (29.6)

MN, membranous nephropathy; PLA2R1, phospholipase A2 receptor 1; THSD7A, thrombospondin type 1 domain-containing 7A.
Values are shown as *n* (%).
The main clinical characteristics of each cohort can be found elsewhere: Nice,[14] Saint-Etienne,[49] Gemritux,[32] Sweden,[50] Italy,[48] and the Netherlands.[51]

Table 2 | Epidemiological and clinical baseline characteristics of anti-THSD7A positive patients

Characteristics of THSD7A-positive patients	All (n = 49)	Male (n = 28)	Female (n = 21)	P value
Sex, M/F	28/21	28 (57)	21 (43)	
Age at diagnosis (yr)	59.9 (48.5–75.0)	67.0 (54.3–75.0)	48.8 (36.5–64.5)	0.003
Proteinuria (g/d)	6.1 (4.1–10.2)	6.6 (5.3–11.2)	5.0 (3.0–7.7)	0.106
Serum creatinine (μmol/l)	89.0 (70.7–121.0)	112.0 (88.0–145.0)	70.7 (64.7–86.6)	0.0004
eGFR (CKD-EPI) (ml/min per 1.73 m^2)	76.5 (49.8–90.0)	60.0 (39.8–80.0)	85.5 (64.5–91.8)	0.017
Serum albumin (g/l)	21.0 (16.5–25.3)	21.0 (15.3–25.8)	22.2 (17.5–25.3)	0.681
Anti-THSD7A titer (RU/ml)	278.0 (40.5–835.0)	256.0 (27.5–857.8)	302 (55.5–1035.0)	0.585
Cancer incidence	8 (16)	6 (21)	2 (10)	0.264

CKD-EPI, Chronic Kidney Disease Epidemiology Collaboration; eGFR, estimated glomerular filtration rate; RU, relative units; THSD7A, thrombospondin type 1 domain-containing 7A.
Values are n (%) or median (interquartile range).
The 49 patients were positive for THSD7A by at least 1 technique of detection: enzyme-linked immunosorbent assay (44 of 49 positive patients with IgG4 detection and 1 additional patient with total IgG detection), indirect immunofluorescence test (45 of 49 positive patients, total IgG detection), Western blot (44 of 49 positive patients, IgG4 detection), or biopsy staining (11 of 11 positive patients).

$P < 0.0001$) (Supplementary Figure S3D and E). More careful analysis showed that 37 of the 38 patients positive with total IgG were among the 44 patients positive for IgG4 while the last patient was negative for IgG4. Among the 7 patients negative for total IgG but positive for IgG4, 6 had low IgG4 anti-THSD7A titers and were negative for IgG1, IgG2, and IgG3 subclasses while the last one was positive for both IgG4 and IgG3. The higher number of patients detected with anti-IgG4 secondary antibodies is likely due to the better signal-to-noise ratio of these antibodies as compared with that of anti-total IgG (Supplementary Figure S3) and the fact that anti-THSD7A autoantibodies are mostly IgG4, like for anti-PLA2R1 autoantibodies.[7,46,47,52,53]

Among the 5 patients negative with IgG4 detection, 4 were also negative for total IgG, IgG1, IgG2, and IgG3. However, the last patient, MN40, illustrated a unique case in our cohort because it was negative for IgG4 but positive for total IgG. We carefully double-checked the positivity of this patient when using total IgG versus IgG4 and other IgG subclasses by ELISA, WB, and IIFT, and we confirmed that this patient was clearly positive for anti-THSD7A total IgG as well as IgG1, but not IgG2, IgG3, and IgG4 (Supplementary Figures S3, S4, and S5).

MN patients double positive for THSD7A and PLA2R1

We carefully evaluated the 49 patients for their double positivity for THSD7A and PLA2R1 by detection of anti-THSD7A and anti-PLA2R1 autoantibodies in baseline serum by ELISA, WB, and IIFT, and of THSD7A and PLA2R1 antigens in immune deposits (when biopsies were available). In total, 8 patients (MN42 to MN49) were found to be double positive

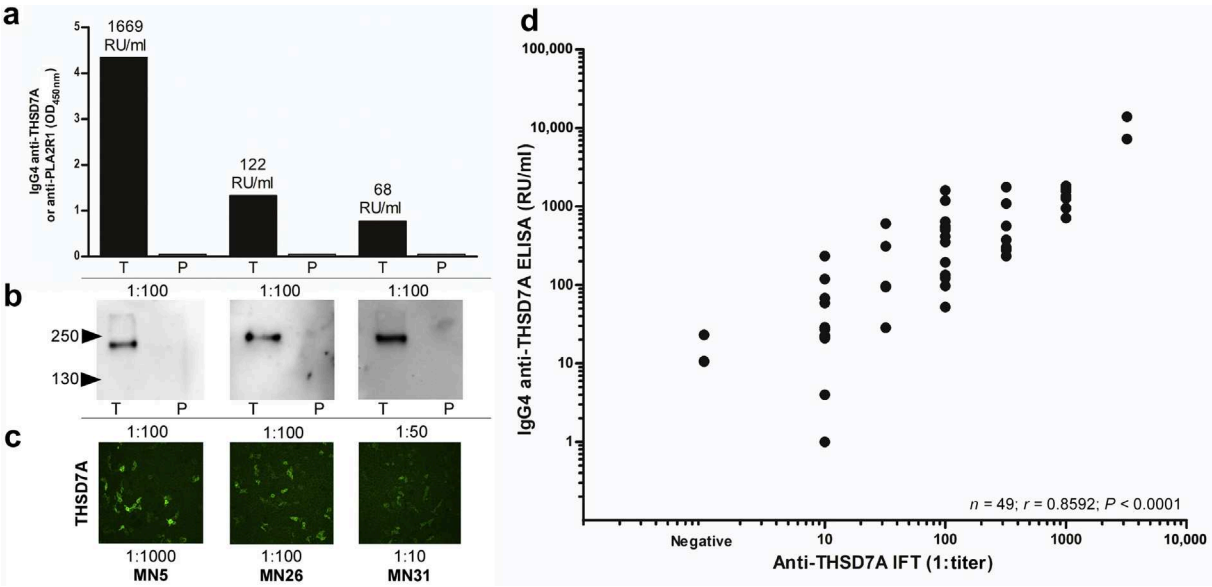

Figure 2 | Comparison of anti-thrombospondin type 1 domain-containing 7A (THSD7A) detection in serum by enzyme-linked immunosorbent assay (ELISA), Western blot, and indirect immunofluorescence test (IIFT). (**a**) ELISA reactivity for 3 membranous nephropathy (MN) patients (MN5, MN26, and MN31) with low- to high-range titers detected at a dilution of 1:100. MN5 was further diluted to determine the ELISA titer with accuracy. (**b**) Western blot reactivity of the same patients tested at optimal serum dilution against purified recombinant THSD7A (T) and phospholipase A2 receptor 1 (PLA2R1) (P) (50 ng each). Blots were exposed for different times. (**c**) IIFT reactivity at optimal serum dilution. (**d**) Correlation between anti-THSD7A levels of MN patients (n = 49) as measured by IIFT (detection for total IgG) and ELISA (detection for IgG4). The correlation is significant (r = 0.8592, $P < 0.0001$). OD, optical density; RU, relative units. To optimize viewing of this image, please see the online version of this article at www.kidney-international.org.

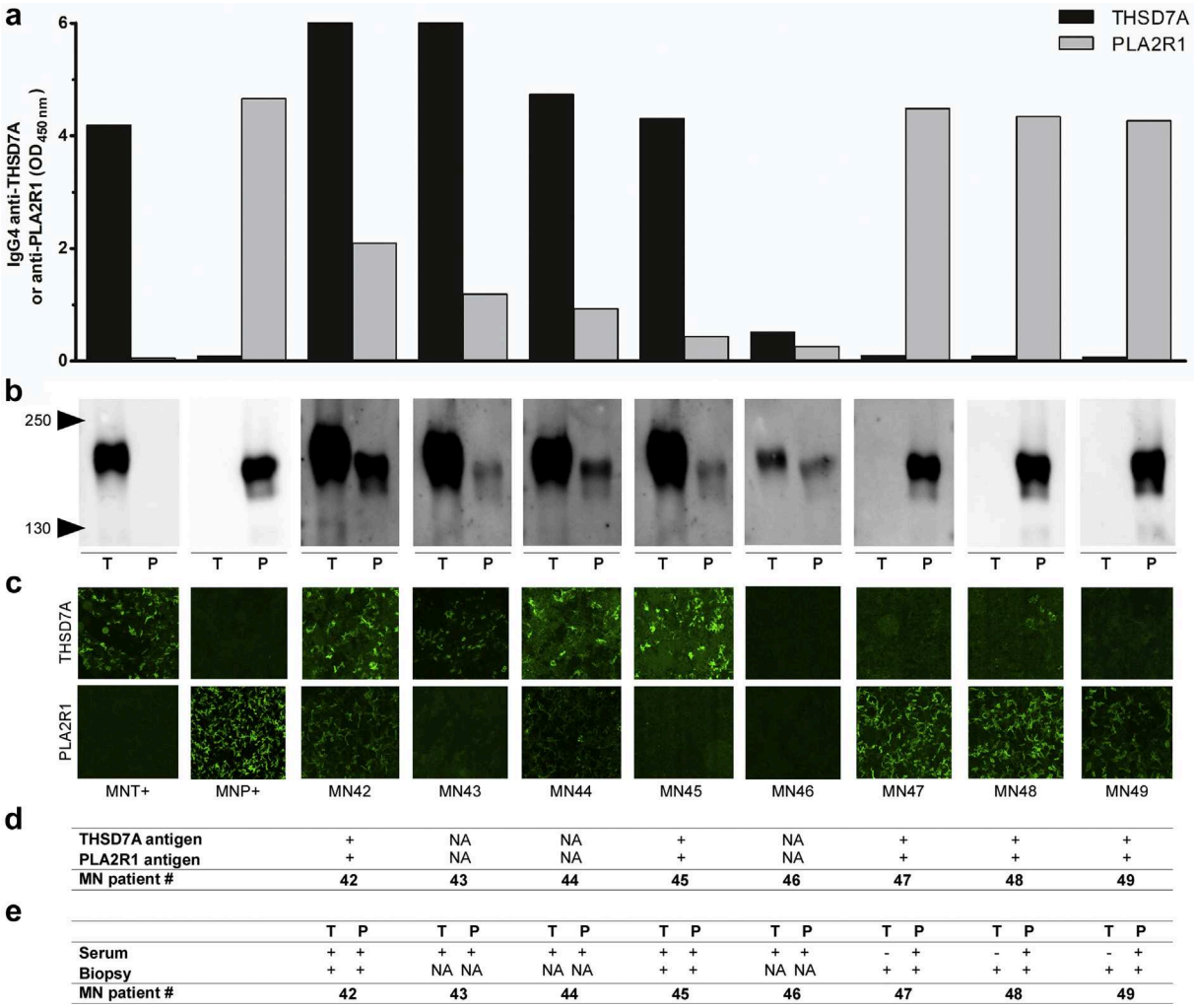

Figure 3 | Detection of anti-thrombospondin type 1 domain-containing 7A (THSD7A) and anti-phospholipase A2 receptor 1 (PLA2R1) autoantibodies in double-positive membranous nephropathy (MN) patients. (**a**) Reactivity of sera from double-positive MN patients (MN42 to MN49) and single-positive MN control subjects (MNT+ and MNP+) against THSD7A and PLA2R1 antigens in enzyme-linked immunosorbent assay (ELISA). All sera were diluted at 1:100 except MN46 (1:25). (**b**) Western blot reactivity of sera from double-positive MN patients (MN42 to MN49) against THSD7A (T) and PLA2R1 (P) antigens (50 ng each) loaded on sodium dodecylsulfate polyacrylamide gel electrophoresis (SDS-PAGE) (6%) under nonreducing conditions. All sera were used at a dilution of 1:25. Soluble forms of THSD7A and PLA2R1 have molecular masses of about 230 kDa and 170 kDa, respectively. (**c**) Indirect immunofluorescence test showing the reactivity of MN42 to MN49 against HEK 293 cells transfected with THSD7A or PLA2R1 expression vectors. Sera were tested at a dilution of 1:10 or higher depending on titer. (**d**) Summary of positivity by biopsy staining for THSD7A and PLA2R1 antigens (biopsies were available for 5 patients: MN49 staining is shown in Supplementary Figure S6; for other patients, the original data can be found elsewhere[8,9]). (**e**) Summary of positivity for THSD7A and PLA2R1 autoantibody or antigen in serum or on biopsy, respectively. NA, not available; OD, optical density. To optimize viewing of this image, please see the online version of this article at www.kidney-international.org.

(Figure 3). Four of these patients were previously reported from an American cohort (MN42 and MN45)[8] and a Chinese cohort (MN47 and MN48),[9] but none of them were compared for levels of anti-THSD7A and anti-PLA2R1 autoantibodies by quantitative ELISA. Analysis with baseline serum showed that double-positive patients can have different titers of anti-THSD7A and anti-PLA2R1 autoantibodies (Figure 3a). Four patients had relatively higher titers of anti-THSD7A than anti-PLA2R1; 1 patient had low titers of both autoantibodies; and the last 3 patients had no detectable levels of anti-THSD7A but high anti-PLA2R1 titers. The first 5 patients (MN42 to MN46) were clearly double positive in serum by ELISA and WB (Figure 3a and b), but some of them appeared less positive by IIFT, which may be explained, at least in part, by the low titers measured by ELISA (Figure 3c). The last 3 patients (MN47, MN48, and MN49) were positive in serum by all 3 techniques (ELISA, WB, and IIFT) for PLA2R1 but not for THSD7A (Figure 3a to c).

Among the 49 patients, renal biopsies were available for a total of 11 patients and were tested for THSD7A and PLA2R1 staining. This includes data previously published for MN42, MN45, MN47, and MN48.[8,9] In agreement with ELISA, 6 patients (MN5, MN6, MN13, MN26, MN34, and MN41) were positive for THSD7A but negative for PLA2R1 on biopsy

(Supplementary Figure S6). The other 5 patients had enhanced staining for both THSD7A and PLA2R1 (for MN42, MN45, MN47, MN48, and MN49, see Larsen *et al.*[8] and Wang *et al.*[9]; see also Supplementary Figure S6 for MN49; data for MN42 to MN49 are summarized in Figure 3d).

Taken together, we conclude that 8 patients are double positive for THSD7A and PLA2R1 (Figure 3e). Our analyses also illustrate the need of using all available techniques for detection of anti-THSD7A and anti-PLA2R1 in serum and antigen staining in biopsy to identify these rare cases of double-positive MN patients.

Clinical characteristics of THSD7A-associated MN patients

Overall, the baseline clinical characteristics of the 49 THSD7A-associated MN patients (Table 2, Supplementary Table S1) did not strongly differ from patients with PLA2R1-associated MN including those from the cohorts listed in Table 1.[23,27,33,34,41,49,54] At baseline, the median age of the 49 anti-THSD7A-positive patients was 59.9 years. Median proteinuria and estimated glomerular filtration rate (eGFR) were 6.1 g/d (interquartile range [IQR]: 4.1–10.2) and 76.5 ml/min per 1.73 m^2 (IQR: 49.8–90.0), respectively. There was no significant correlation between anti-THSD7A titer and proteinuria (Supplementary Figure S7).

Because we previously observed a high proportion of women in THSD7A-positive patients as compared to PLA2R1-positive patients,[7] we investigated the influence of sex on the clinical parameters and anti-THSD7A titers in our cohort (Table 2). Among the 49 patients, 28 were male (57%) and 21 were female (43%), giving a sex ratio of 1.3:1, which contrasts with the 2:1 ratio typically observed in the general MN population (e.g., it is 2.1:1 in our combined cohort of 1012 patients) (Table 1) or the PLA2R1-associated MN-specific subgroup.[15] Interestingly, female patients were significantly younger than male patients (48.8 vs. 67.0 years, $P = 0.003$). Data for age of menopause were lacking in our cohort. The average age at menopause of women with CKD is 51 years,[55,56] which suggests that a significant number of women developed MN before menopause (Figure 4a, Table 2). However, the levels of anti-THSD7A titers did not significantly differ between male and female patients, nor with age when analyzed by tertiles or when female patients were compared as 2 subgroups, below and above 51 years (Figure 4b, Supplementary Figure S8A, Supplementary Table S2). Titers separated by sex did not correlate with proteinuria (Supplementary Figure S7). Proteinuria and serum albumin did not differ between male and female patients, irrespective of age (Table 2, Supplementary Figure S8B). Serum creatinine was higher and eGFR was lower in male patients, which might be partly age-related or due to more severe disease in these men (Table 2).

It has been reported that THSD7A-associated MN may be linked to malignancy.[41] In our cohort, only 8 patients (16%) had a history of malignancy, including 6 male and 2 female patients (Table 2, Supplementary Table S3). Clinical parameters were similar between these patients and others, except for serum albumin, which was lower, possibly due to superimposed malnutrition.[57] Interestingly, all 8 patients with malignancy were significantly older, and only 3 of them were diagnosed for malignancy within 2 years of MN diagnosis (Supplementary Tables S3 and S4). Titers of anti-THSD7A autoantibodies tended to be higher in patients with associated malignancy but the difference did not reach statistical significance (Supplementary Table S3). Although the pattern of IgG subclass may differ between primary and secondary MN associated with malignancy,[24,45,58] no differences in the relative levels of anti-THSD7A IgG subclasses were observed between patients with and without malignancy (Supplementary Table S5).

We finally compared the clinical characteristics of patients with single positivity to THSD7A ($n = 41$) versus double positivity to THSD7A and PLA2R1, which included 4 male and 4 female patients ($n = 8$). No significant differences were observed for age, sex, and baseline clinical values nor for percentage of malignancy-associated MN between the 2 groups (Supplementary Table S6).

Association of anti-THSD7A titer with disease activity

We compared anti-THSD7A titers at baseline and during follow-up to test the association between anti-THSD7A titers and disease activity, including response to treatment or spontaneous remission. Overall, we observed higher titers of anti-THSD7A autoantibodies in patients with active disease as compared to those in partial or complete remission (Figure 5a). We only had follow-up sera for 12 patients with a median follow-up of 17 months (IQR: 7.0–31.3), but this number was sufficient to demonstrate that the anti-THSD7A titer is a relevant biomarker of the immunological autoimmune response and helps to monitor response to treatment (Figure 5b and c). At baseline, the 12 patients had nephrotic to subnephrotic range proteinuria (median: 5.9 g/d [IQR: 3.0–6.6]) and relatively high anti-THSD7A titers (median: 206 RU/ml [IQR: 68.8–472.8]). At the last follow-up of patients with available serum samples, patients who had reached spontaneous remission or remission after conservative or immunosuppressive treatment had non-nephrotic proteinuria levels (median: 1 g/d [IQR: 0.8–2.7]) and no detectable or strongly decreased anti-THSD7A titers (IQR: 16–26.5 RU/ml). In contrast, patients who did not reach remission, either untreated or resistant to immunosuppressive treatment, had nephrotic range proteinuria (median: 10.8 g/d [IQR: 6.5–14.0]) and persistently high anti-THSD7A titers (median: 709 RU/ml [IQR: 381.3–993.3]).

The utility of anti-THSD7A titer to monitor disease activity and response to treatment was further illustrated by the clinical follow-up of patient MN13, a 4-year-old girl treated twice with rituximab over 27 months (Supplementary Figure S9). At baseline, the patient had high proteinuria (6.1 g/d) and anti-THSD7A titer (715 RU/ml). Treatment with rituximab led to a progressive decrease of anti-THSD7A titer that was followed by fluctuating but finally decreasing proteinuria down to the subnephrotic range at month 18. Between months 18 and 27, anti-THSD7A titer and

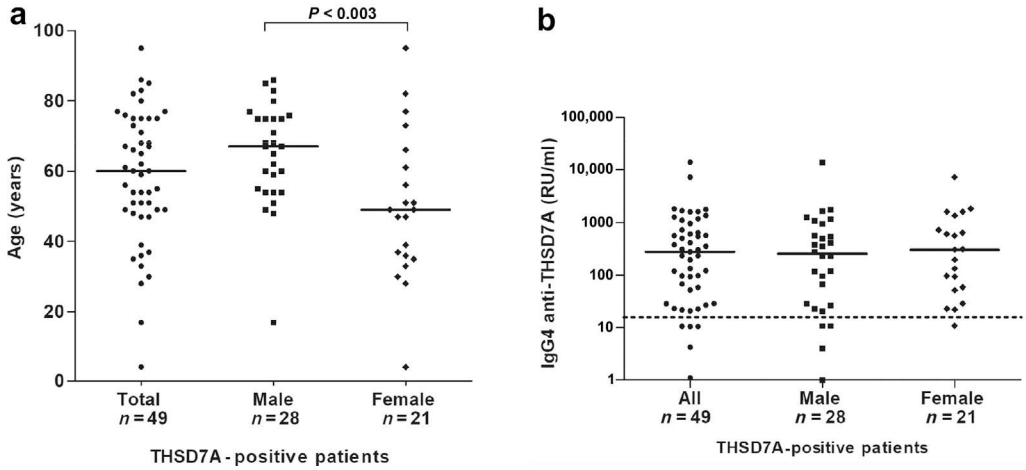

Figure 4 | Distribution of age and anti-thrombospondin type 1 domain-containing 7A (THSD7A) titers among THSD7A-positive patients as a whole or by sex. (**a**) Age distribution of anti-THSD7A-positive patients ($n = 49$). The data are presented as medians. Female patients were significantly younger than male patients using the Mann-Whitney *U* test ($P < 0.003$). (**b**) Distribution of anti-THSD7A titers for THSD7A-positive patients, as measured with anti-IgG4 secondary antibodies. The dotted line represents the threshold value for IgG4 detection. RU, relative units.

proteinuria increased again, suggesting an ongoing relapse. Comparison of anti-THSD7A autoantibody levels by ELISA, WB, and IIFT showed that ELISA was the most accurate assay to detect subtle changes of anti-THSD7A levels, with IgG4 and IgG3 appearing as the most relevant IgG subclasses to monitor disease activity.

Anti-THSD7A titer and clinical outcome of THSD7A-associated MN patients

Among the 49 THSD7A-associated MN patients, we had clinical outcome and detectable anti-THSD7A autoantibodies at baseline for 36 patients during a median follow-up of 37 months (range 6.5–180 months) (Supplementary Tables S1 and S7). During follow-up, 10 patients (28%) were untreated or treated with antiproteinuric therapy (angiotensin-converting enzyme inhibitors or angiotensin 2 receptor blockers and diuretics or all 3) while 24 (67%) patients received an additional immunosuppressive treatment (cyclosporine A, cyclophosphamide, rituximab, or adrenocorticotropic hormone). Treatment information was not available for 2 patients. Twelve patients (33%) remained in active disease among which 2 reached end-stage kidney disease, while 24 (67%) reached complete ($n = 16$) or partial ($n = 8$) remission. Two patients (MN29 and MN33) experienced relapse after partial remission (one after spontaneous remission and the other after treatment with cyclosporine A). Among the 12 patients who remained in active disease, 10 patients (83%) had received an immunosuppressive treatment (Supplementary Tables S1 and S7). Among the 24 patients who reached remission, 14 (58%) had received an immunosuppressive treatment (Supplementary Tables S1 and S7).

We evaluated the association between anti-THSD7A titer at baseline and clinical outcome. Overall, baseline anti-THSD7A titer significantly differs between patients reaching remission or not during follow-up (134 [IQR: 52; 955] vs. 536 [IQR: 250; 1671] RU/ml, respectively, $P = 0.04$) (Figure 6a), while these 2 groups were comparable for age, sex ratio, proteinuria, albuminemia, eGFR, and immunosuppressive treatment (Supplementary Table S7).

We then divided the patients into tertiles based on anti-THSD7A titer and analyzed outcome. Patients in the lowest tertile (titers 23–122 RU/ml) tended to have a higher rate of remission (11 of 12, 92%) compared with patients in the middle (titers 134–566 RU/ml) and highest (titers 606–13,920 RU/ml) tertiles (6 of 12, 50% and 7 of 12, 58%, respectively, $P = 0.07$), while persistent proteinuria and renal failure tended to be more frequent in patients with high anti-THSD7A titer, but none of these trends reached statistical significance (not shown). Because of the small sample size, we combined the middle and highest tertiles and compared renal survival during the first 3 years after diagnosis to the lowest tertile. Patients from the lowest tertile had better renal survival with more remission compared with patients from the medium and highest tertiles (Figure 6b, $P = 0.006$).

DISCUSSION

This study had 2 major aims: (i) the development of a robust ELISA allowing the sensitive and quantitative measurement of anti-THSD7A autoantibodies, and (ii) the analysis of a relatively large retrospective cohort of THSD7A-positive patients from which we may identify clinical characteristics specific for THSD7A-associated MN.

We set up an ELISA to detect anti-THSD7A autoantibodies in serum with characteristics and performance similar to those previously reported for PLA2R1, using the purified full extracellular region of THSD7A as antigen for the solid-phase assay, validation of the ELISA with MN patients versus negative control subjects and detection for either total IgG or IgG4 secondary antibodies.[20,21] Using this ELISA to screen a combined cohort of 1012 MN patients, we identified 28

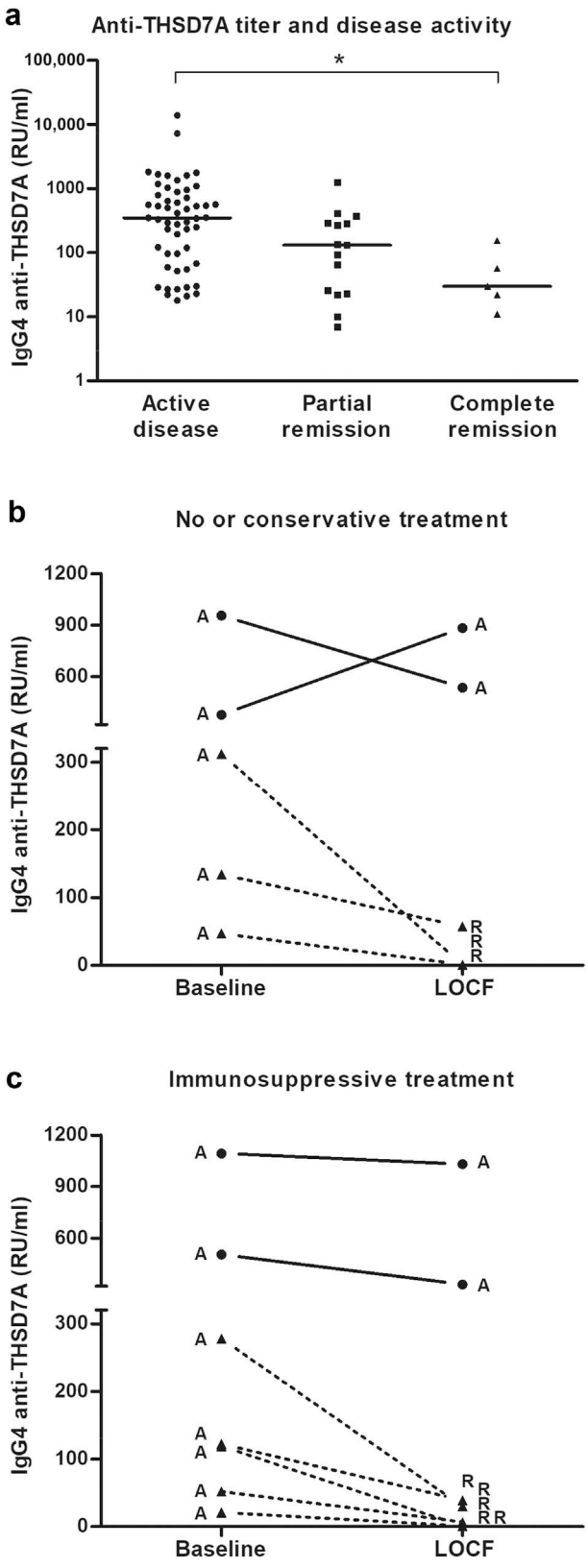

Figure 5 | Relationships between anti-thrombospondin type 1 domain-containing 7A (THSD7A) titers and clinical status in THSD7A-positive patients. (**a**) Anti-THSD7A titers were measured from baseline and follow-up sera of anti-THSD7A patients with active disease (53 baseline and follow-up serum samples with a mean proteinuria of 7.4 g/d), partial remission (15 follow-up serum samples with a mean proteinuria of 1.9 g/d), or complete remission (5 follow-up serum samples with a mean proteinuria of 0.3 g/d). The anti-THSD7A titer was significantly lower in patients with complete remission than in those in active disease. The difference in titer between patients in active disease versus partial remission did not reach significance. (**b**) Anti-THSD7A titers during follow-up of patients who received no or conservative treatment and (**c**) immunosuppressive treatment. Anti-THSD7A titers of patients who reached remission are shown with dotted lines. A, active disease; LOCF, last observation carried forward; R, remission; RU, relative units.

patients, indicating a prevalence of 2.8%, in accordance with the prevalence range of 2% to 5% previously reported for Caucasian or Asian cohorts (data are summarized in Supplementary Table S8).[7,9,41–43,59,60] By screening additional patients mostly referred because of PLA2R1-unrelated MN, we included 21 more cases, providing a cohort of 49 patients with THSD7A-associated MN. We validated the novel ELISA by comparing its sensitivity against the 49 MN patients with the original WB method[7] and the commercially available IIFT assay.[41] We found similar levels of sensitivity by ELISA and WB, and a significant correlation between anti-THSD7A titers measured by IIFT and ELISA. Among the 49 patients, 43 were positive by the 3 techniques: ELISA (IgG4 detection), WB (IgG4 detection), and IIFT (total IgG detection). One was positive by ELISA, WB, and IIFT (total IgG detection). One was only positive by ELISA (IgG4 detection) and WB (IgG4 detection). One was only positive by IIFT (total IgG detection). The last 3 were negative in serum by all 3 techniques. These discrepancies may be explained by the different autoantibody detection systems and presentation of antigens in solid-phase ELISA, WB, and IIFT cell-based assay. We also found that the ELISA is more sensitive when detection of anti-THSD7A autoantibodies is made with anti-IgG4 as compared to anti-total IgG. Indeed, 6 patients could be detected only with anti-IgG4 while 1 patient could be detected only with anti-total IgG. It is thus preferable to use anti-IgG4 as a secondary antibody to detect the highest number of MN patients with THSD7A-associated disease and avoid false-negative cases, yet further screening with anti-total IgG may help to identify additional patients.

The 3 patients who had no circulating anti-THSD7A autoantibodies detected by ELISA, WB, and IIFT were positive on biopsy with the presence of immune deposits containing the THSD7A antigen. Such discrepancies have been initially observed for PLA2R1-associated MN[22] and more recently for THSD7A-associated MN.[41] We conclude that the new ELISA is reliable and in accordance with available methods of detection such as WB and IIFT.[7,41]

Among the 49 patients, we identified 8 patients who were double positive for THSD7A and PLA2R1. No major clinical differences were observed between the single- and double-positive patients. Four double-positive cases were novel and from Europe while 2 were already reported from an American cohort[8] and two from a Chinese cohort.[9] Three of the new cases were identified from the screening of 1012 MN patients,

indicating an overall prevalence of about 0.3%. However, these 3 double-positive cases actually represent about 10% of the 28 THSD7A-positive patients (identified from 1012 patients) but only about 0.4% of the 684 patients identified with PLA2R1-associated MN (Table 1). With the observed respective prevalence of about 70% and 3% for PLA2R1 and THSD7A in our combined cohort, and assuming that the respective production of anti-PLA2R1 and anti-THSD7A autoantibodies is a random event, one would have expected many more double-positive patients in the PLA2R1-positive group than in the negative one, suggesting a negative association between the 2 events. However, we could not determine from these studies whether the presence of both anti-PLA2R1 and anti-THSD7A autoantibodies is coincidental or associated one to another (for instance by intermolecular epitope spreading),[61] nor could we determine what autoantibody would precede the other during the natural history of the disease.

Careful analysis of the 8 double-positive patients led us to make 2 additional observations. First, the respective circulating levels of anti-THSD7A and anti-PLA2R1 could be very different between patients, with all scenarios observed, that is, lower titer of anti-THSD7A than anti-PLA2R1 and vice versa, or similar titers of both autoantibodies. Second, among the 5 patients with available serum and biopsy, 2 were fully positive, in other words, for both antigens in serum and biopsy (MN42 and MN45), while 3 (MN47, MN48, and MN49) were positive in both serum and biopsy for PLA2R1 but only positive for THSD7A in biopsy. This different pattern of positivity in serum versus biopsy is reminiscent of what was previously observed for MN patients with single positivity for PLA2R1 or THSD7A.[22,41]

In this study, we also present the clinical analysis of the largest cohort of patients with THSD7A-associated MN with quantitative analysis of anti-THSD7A titers for the different IgG subclasses. First, we observed that the titer of anti-THSD7A autoantibodies is heterogeneous and can vary by up to 3 orders of magnitude in both sexes. Second, we showed that IgG4 is the predominant IgG subclass for anti-THSD7A autoantibodies in most patients, regardless of coincidental diseases. Third, we observed no strong correlation between anti-THSD7A titer and levels of proteinuria, as previously observed for PLA2R1-associated MN.[20] Nonetheless, the anti-THSD7A titer appears to be a relevant biomarker to monitor disease activity during follow-up and treatment with immunosuppressors, as exemplified for the 12 patients with available follow-up. Fourth, we showed that patients with low anti-THSD7A titer at baseline had better clinical outcome, as was previously observed for PLA2R1-associated MN.[20,25,27,28,31,35,62] In addition to anti-PLA2R1 titer, PLA2R1 epitope spreading was recently identified as a prognosis biomarker to predict outcome in MN.[14,34] Despite the recent identification of several epitopes in THSD7A,[16] it remains to determine whether epitope spreading also occurs in patients with THSD7A-associated MN and may be a relevant biomarker of disease activity and clinical outcome.

The relatively large size of our cohort allowed stratification of patients by sex and comparison of their epidemiological and clinical parameters. First, we observed a male-female ratio of 1.3:1 that contrasts with the 2:1 ratio typically reported when considering all MN cases or PLA2R1-associated MN.[2–5,63] Second, we observed that female patients were younger than male patients at diagnosis, suggesting different etiologies. To confirm our findings, we compiled the available data on sex and age from all previous studies identifying cases of THSD7A-associated MN (Supplementary Table S8) and observed that female patients were indeed more preponderant and younger in THSD7A-associated MN than in PLA2R1-associated MN. Third, we observed that female patients had on average similar levels of anti-THSD7A autoantibodies, yet the levels seemed to vary with age. However, we could not find evidence of significant differences in disease activity, response to treatment, and clinical outcome between male and female patients.

The underlying etiologies leading to PLA2R1- and THSD7A-associated MN are currently unknown.[2,3,64] We observed many associated diseases in our cohort of THSD7A-associated diseases (Supplementary Table S1). Recent studies reported that 8 of 40 THSD7A-positive MN patients (20%) had an associated malignancy within a median time of 3 months from diagnosis of MN, suggesting that THSD7A-positive patients are at higher risk of having an underlying malignant disease and may be intensively screened for cancer as a possible etiology.[41,65] In our cohort, we found that 8 of the 49 THSD7A-positive MN patients (16%) had a history of cancer, including 1 double-positive patient. However, only 3 patients had cancer (gastric, colonic, and prostatic) within 2 years of MN diagnosis. Furthermore, we observed that 7 of the 8 patients were older than 65 years, with 6 male and 2 female patients. These observations are in line with the study by Hoxha *et al.*[41] where 5 of the 8 patients were older than 65 years, with 5 male and 3 female patients. We also observed that the 8 THSD7A-positive patients with associated cancer tended to have higher anti-THSD7A titers, but no significant differences in IgG subclasses. Earlier studies reported that the prevalence of malignancy in MN patients is higher than in the general population, while it increases with age,[66–69] but our data converge to the point that most cases of THSD7A-associated MN with malignancy were likely coincidental in our subgroup of 8 patients.

Another cause of MN may be associated with pregnancy and preeclampsia,[70–73] including recent observations for THSD7A-associated MN.[74,75] In line with this hypothesis, we observed a significant subgroup of young THSD7A-positive female patients (before menopause) (Figure 4b) in our cohort but we could not find evidence of a relationship between MN and pregnancy or preeclampsia.

We also described 2 cases of pediatric and adolescent MN with no associated underlying disease: a 4-year-old girl who was treated with rituximab and reached partial remission, and a 17-year-old boy who had high anti-THSD7A titer at baseline and was resistant to rituximab.

In conclusion, we have reported a novel ELISA that is useful to diagnose MN patients for THSD7A-associated disease, to

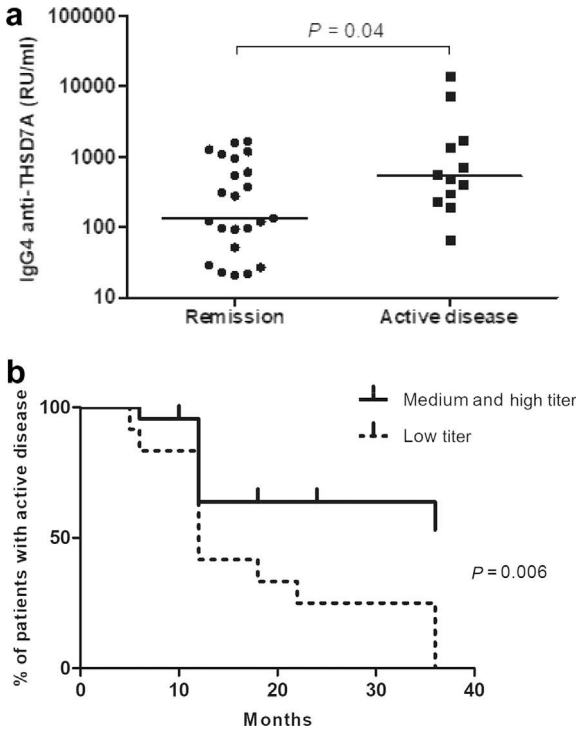

Figure 6 | Anti-thrombospondin type 1 domain-containing 7A (THSD7A) titer at baseline predicts clinical outcome. (**a**) Anti-THSD7A titers at baseline significantly differ between patients with remission versus active disease at last follow-up ($n = 36$, $P = 0.04$). (**b**) Renal survival at last follow-up. Renal event is defined by partial or complete remission within 3 years after anti-THSD7A enzyme-linked immunosorbent assay (ELISA) measured at baseline. Patients with a low titer of anti-THSD7A (titers 23–122 relative units [RU]/ml, first tertile) had a higher incidence of renal events as compared to patients with medium and high titer (titers 134–13,920, middle and high tertiles together) ($n = 36$, $P = 0.006$).

carefully monitor disease activity and response to treatment during follow-up, and predict clinical outcome. We also described new cases of patients with THSD7A-associated MN supporting the hypothesis that THSD7A-associated MN differs from PLA2R1-associated MN in the natural history and epidemiological features, such as sex, age at onset, and associated etiologies.[15,76] Interestingly, this situation appears reminiscent to that observed for myasthenia gravis, a neuromuscular autoimmune disease with multiple autoantigens and different paths and etiologies toward the same disease entity.[77,78]

METHODS

Patients

Because the prevalence of THSD7A-associated MN is low, we included patients from several national and international nephrology centers. Baseline serum samples of patients with biopsy-proven MN were collected within 6 months from renal biopsy. A total of 1012 patients originating from 6 independent retrospective cohorts and additional patients who were referred to us mostly for PLA2R1-unrelated MN were screened for anti-THSD7A autoantibodies. eGFR was calculated by applying the Chronic Kidney Disease Epidemiology Collaboration (CKD-EPI) formula. Disease activity was defined as no remission of nephrotic syndrome. Partial remission was defined as proteinuria lower than 3.5 g/d and at least 50% reduction from the time of inclusion in the study with normalization of the serum albumin concentration and stable serum creatinine. Complete remission of proteinuria was defined as proteinuria lower than 0.5 g/d, normal albuminemia, and stable eGFR. Remissions were classified as spontaneous if they were occurring without the administration of immunosuppressive agents during follow-up. The negative control groups included serum samples from patients with other diseases such as lupus nephritis ($n = 9$), membranoproliferative glomerulonephritis ($n = 9$), anti-neutrophil cytoplasmic autoantibodies vasculitis ($n = 3$), IgA nephropathy ($n = 11$), other renal diseases ($n = 18$) and from healthy blood donors ($n = 52$). The studies were approved by the relevant institutional review boards in the different countries and were conducted according to the principles of the Declaration of Helsinki. Written informed consent was obtained from participants in all studies.

ELISA for the detection of anti-THSD7A and anti-PLA2R1 autoantibodies

Purified recombinant THSD7A protein (prepared as described in the Supplementary Methods) or the full extracellular domain of human PLA2R1 prepared as described[21] were used as antigens to coat 96-well ELISA microplates (Thermo Fisher Scientific, Waltham, MA) in 20 mmol/l tris(hydroxymethyl)-aminomethane pH 8.0 overnight at 4 °C. Plates were blocked with SeramunBlock (Seramun Diagnostica, Heidesee, Germany) for 2 hours. Patients' serum samples diluted at 1:100 in 0.1% low-fat dry milk phosphate-buffered saline were incubated for 2 hours. Plates were washed 3 times with phosphate-buffered saline–Tween 0.02%. Bound human antibodies were detected with either anti-human horseradish peroxidase–conjugated IgG1, IgG2, IgG3, IgG4, or total IgG (Southern Biotech, Birmingham, AL) diluted in SeramunStab ST (Seramun Diagnostica) at 1:5000, 1:5000, 1:20,000, 1:30,000, and 1:200,000, respectively. Secondary antibodies were all incubated for 1 hour. After washes, tetramethylbenzidine peroxidase substrate was added and developed for 15 minutes. The reaction was stopped by adding 1.2 N HCl. All incubation steps were carried out at room temperature on a plate shaker. The optical density was read at 450 nm using a plate reader. A standard curve for IgG4 detection was made using a highly THSD7A-positive serum that was assigned a value of 99,000 RU/ml when not diluted. A standard curve consisting of 8 dilutions covering the range from 990 RU to 9.9 RU/ml was plotted using the GraphPad Prism software and applied to each plate to convert optical density values into RU/ml (Supplementary Figure S2B). Samples that were out of range were diluted at 1:500 and 1:1000 and reanalyzed. The interassay variation was measured by incorporating a borderline positive serum sample on each plate. Results from 10 different plates showed a coefficient of interassay variation lower than 20% (not shown). Normal range for IgG1, IgG2, IgG3, and total IgG detection were defined using serum samples from disease control subjects and healthy donors (not shown).

WB and IIFT for the detection of circulating anti-THSD7A and anti-PLA2R1 autoantibodies and kidney biopsy staining for THSD7A and PLA2R1 antigens

Detailed procedures for WB[7] and biopsy staining[22] are provided in the Supplementary Methods. We used the commercial cell-based IIFT kit from Euroimmun AG containing a mosaic biochip of formalin-fixed HEK293 cells overexpressing full-length human THSD7A or PLA2R1 or mock-transfected HEK293 as a negative control.

Statistical analysis

Baseline characteristics of the patients in the study were expressed as percentages for qualitative variables and medians and IQRs for quantitative variables. Nonparametric correlations between several parameters were calculated using the Spearman test. Quantitative variables were compared by Mann-Whitney U or 1-way analysis of variance (ANOVA) tests and categorical variables were compared by a Pearson chi-squared test or a Fisher exact test. P values lower than 0.05 were considered as statistically significant. Statistics were performed using the GraphPad Prism version 6 software. Renal survival curves were calculated using Kaplan-Meyer estimates for survival distribution. The endpoint was the time where patients entered into remission (partial or complete) from baseline. Differences between groups based on tertiles of anti-THSD7A titer were analyzed with the log-rank test.

DISCLOSURE

Some coauthors are coinventors on the patents "Diagnostics for membranous nephropathy" (LHB and GL), "Methods and kits for monitoring membranous nephropathy" (BSP and GL), and "Prognosis and monitoring of membranous nephropathy based on the analysis of PLA2R1 epitope profile and spreading" (BSP, GD, and GL).

ACKNOWLEDGMENTS

We are grateful to the following physicians who participated in the inclusion of patients in this study: Vincent L. M. Esnault (Centre Hospitalier Universitaire [CHU], Nice, France); Stéphane Burtey, Laurent Samson, Laurent Daniel, and Sophie Jego-Desplat (CHU la Conception, Marseille, France); Karine Dahan (Hôpital Tenon, Paris, France); Aude Servais (Hôpital Necker, Paris, France); Michel Delahousse (Hôpital Foch, Suresnes, France); Corinne Bagnis (Hôpital de la Pitié-Salpêtrière, Paris, France); Thomas Crépin, Nadège Devillard, and Cécile Courivaud (CHU de Besançon, France); Arnaud Lionet (Centre Hosptialier Régional Universitaire, Lille, France); Coralien Vink (Radboudumc, Nijmegen, The Netherlands); Christopher Larsen (Arkana Laboratories, Little Rock, AR, USA); Meryl Waldman (National Institutes of Health/National Institute of Diabetes and Digestive and Kidney Diseases, Bethesda, MD, USA); Jai Radhakrishnan (Columbia University, New York, NY, USA); Tanuja Mishra (Baltimore, MD, USA); and Ming-Hui Zhao (University of Peking, China). HD and PR thank the Centre de Ressources Biologiques (Hôpital Tenon) for the preparation and storing of samples.

Supported by grants to GL from Centre National de la Recherche Scientifique, the Fondation Maladies Rares (LAM-RD_20170304), the National Research Agency (grants MNaims ANR-17- CE17-0012-01), and "Investments for the Future" Laboratory of Excellence SIGNALIFE, a network for innovation on signal transduction pathways in life sciences (ANR-11-LABX-0028-01) with allocated PhD fellowships for CZ and JJ), and the Fondation de la Recherche Médicale (DEQ20180339193 to GL and FDT201805005509 to JJ); grants from the Centre Hospitalier Universitaire de Nice and the Direction Générale de l'Offre de Soins of the French Ministry of Health (PLA2R1 autoantibodies in Membranous Nephropathy in Kidney Transplantation Programme, PRAM-KT PHRC2011-A01302-39, NCT01897961) to GL and BSP; grants from the European Research Council ERC-2012 ADG_20120314 no. 322947 and the Seventh Framework Programme of the European Community contract no. 2012-305608 (European Consortium for High-Throughput Research in Rare Kidney Diseases) to PR; grants from the Dutch Kidney Foundation (Nierstichting Nederland 17PhD12 program) to JFMW and AEvdL; grants from the National Institutes of Health/National Institute of Diabetes and Digestive and Kidney Diseases (R01 DK097053) to LHB; and grants from the Sahlgrenska University Hospital ALF, The Swedish Kidney Foundation and The Swedish Medical Research Council grant 14764 to JN and JLW.

SUPPLEMENTARY MATERIAL

Supplementary Methods.

Figure S1. Cloning, expression, and purification of recombinant human soluble thrombospondin type 1 domain-containing 7A 6X histidine (THSD7A-6xHis). (**A**) Schematic representation of the pCMV6-entry expression vector coding for human soluble THSD7A-6xHis. The cDNA insert encodes for the signal peptide followed by the full extracellular region of THSD7A (from Met-1 to Thr-1606, Uniprot Q9UPZ6) and a C-terminal 6xHis Tag. (**B**) Western blot after HisTag purification from human embryonic kidney 293 cell medium containing soluble THSD7A-6xHis and probed with membranous nephropathy patient 8 (MN8) under nonreducing conditions at a 1:100 dilution. We loaded 400 ml of cell medium onto 4 ml of Ni-NTA resin. The resin was washed once with 40 ml of washing equilibrium buffer and then with 40 ml of washing buffer containing 10 mmol/l imidazole. Bound protein was eluted with 28 ml (in 7 fractions) of elution buffer containing 400 mmol/l imidazole. Aliquots of cell medium (CM), flow-through (FT), washes (W), and eluate (1 to 7) fractions were separated by sodium dodecylsulfate polyacrylamide gel electrophoresis (10%), transferred to polyvinylidene difluoride membranes and analyzed by Western blot. (**C**) Silver staining of the purified THSD7A-6xHis (100 ng) after buffer exchange with 1X phosphate-buffered saline. (**D**) Western blots to validate the purified THSD7A-6xHis as a native folded protein. Purified recombinant THSD7A-6xHis (50 ng) was loaded on sodium dodecylsulfate polyacrylamide gel electrophoresis (10%) under reducing or nonreducing conditions and probed with 2 commercially available anti-THSD7A antibodies and 2 representative anti-THSD7A-positive patients (MN8 and MN10; dilution 1:100).

Figure S2. Receiver-operating characteristic curve and calibration curve for IgG4 anti-thrombospondin type 1 domain-containing 7A (THSD7A) enzyme-linked immunosorbent assay (ELISA). (**A**) Receiver-operating characteristic curve analysis of IgG4 anti-THSD7A detection in 44 anti-THSD7A-positive patients and 242 negative control subjects by ELISA. The area under the curve was 0.9982 (95% confidence interval: 0.9957–1.0, $P < 0.0001$). (**B**) Calibration curve covering the range of 9.9 relative units (RU)/ml to 990 RU/ml used to convert optical density (OD) values into RU/ml.

Figure S3. Levels of IgG subclasses and total IgG for anti-thrombospondin type 1 domain-containing 7A (THSD7A) autoantibodies, and correlation between anti-THSD7A titers by enzyme-linked immunosorbent assay (ELISA) and indirect immunofluorescence test (IIFT). (**A**) Scatter plot showing the distribution of anti-THSD7A titers for the 49 THSD7A-positive patients, as measured with total IgG as a secondary antibody. Titer for membranous nephropathy patient (MN40) is shown with asterisk (*). (**B**) Correlation between total IgG anti-THSD7A titers measured by IIFT versus ELISA. The correlation is highly significant ($n = 49$, $r = 0.8359$, $P < 0.0001$). (**C**) Distribution of anti-THSD7A IgG subclasses measured by ELISA for the THSD7A-positive patients ($n = 49$) versus control subjects (other diseases and healthy donors, $n = 101$). The anti-THSD7A titer for IgG3 and IgG4 subclasses was significantly different from that of control subjects using 1-way analysis of variance test (**<0.01, ***<0.001). Optical density (OD) values for MN40 are shown with asterisk (*). (**D**) Correlation between anti-THSD7A titers measured by ELISA using IgG4 and total IgG secondary antibodies ($n = 49$, $r = 0.9251$, $P < 0.0001$). (**E**) Zoom on the low to middle range titers of anti-THSD7A titers measured by ELISA using IgG4 and total IgG secondary antibodies ($n = 47$).

Figure S4. Indirect immunofluorescence test (IIFT) data for thrombospondin type 1 domain-containing 7A (THSD7A)-positive patients. Autoantibody titers were estimated by the fluorescence intensity at various dilutions. Data are shown at the dilution titer. Data for membranous nephropathy patient 5 (MN5), MN13, MN26, MN31, and MN42 to MN49 are presented in the main figures.

Figure S5. Western blot analysis of purified recombinant thrombospondin type 1 domain-containing 7A (THSD7A) and

phospholipase A2 receptor 1 (PLA2R1) antigens (50 ng each) probed with all sera from THSD7A-positive patients under nonreducing conditions. Serum reactivity of patients was tested at optimal serum dilution (1:10 to 1:100). The blots were exposed for different times. Results for membranous nephropathy patient 5 (MN5), MN13, MN26, MN31, and MN42 to MN49 are presented in the main figures.

Figure S6. Immunofluorescence staining of thrombospondin type 1 domain-containing 7A (THSD7A) and phospholipase A2 receptor 1 (PLA2R1) antigens for available patients' biopsies. (**A**) Available immunofluorescence biopsy staining for THSD7A antigen for the anti-THSD7A-positive patients included in this study (membranous nephropathy patient 5 [MN5], MN6, MN13, MN26, MN34, MN41) and for 1 double-positive patient (MN49). An anti-PLA2R1 positive serum (MNP+) was used as a positive control for PLA2R1 staining. Bar = 50 μm.

Figure S7. Correlation of proteinuria with IgG4 and total IgG anti-thrombospondin type 1 domain-containing 7A (THSD7A) titers measured by enzyme-linked immunosorbent assay for anti-THSD7A-positive patients as a whole or by sex. (**A**) Correlation between proteinuria and IgG4 anti-THSD7A titers for all ($n = 49$, $r = 0.2767$, $P = 0.0542$), male or female THSD7A-positive patients. (**B**) Correlation between proteinuria and total IgG anti-THSD7A titers for all ($n = 49$, $r = 0.2711$, $P = 0.0595$), male or female THSD7A-positive patients. Proteinuria levels show no significant correlation with anti-THSD7A titers.

Figure S8. Relationship between anti-thrombospondin type 1 domain-containing 7A (THSD7A) titer, proteinuria, and age of anti-THSD7A-positive patients by tertiles. (**A**) Relationship between anti-THSD7A median titer (relative units [RU]/ml) and age of patients in tertiles for all, male, or female THSD7A-positive patients. (**B**) Relationship between proteinuria levels (g/d) and age of patients in tertiles for all male or female THSD7A-positive patients. Anti-THSD7A and proteinuria levels show no significant correlation with age.

Figure S9. Anti-thrombospondin type 1 domain-containing 7A (THSD7A) titer and proteinuria levels during clinical follow-up for membranous nephropathy patient 13, a THSD7A-positive pediatric patient (4 years old at baseline) treated with rituximab. The patient had nephrotic range proteinuria at baseline and received 2 courses of rituximab (RTX) at months 2 and 7. See more clinical details in the Supplementary Methods. (**A**) Respective levels of anti-THSD7A autoantibodies measured by enzyme-linked immunosorbent assay for the different IgG subclasses and proteinuria during a follow-up of 27 months. (**B,C**) Anti-THSD7A levels measured by Western blot and indirect immunofluorescence test. Enzyme-linked immunosorbent assay and indirect immunofluorescence test detect the fluctuation of serum anti-THSD7A levels more quantitatively than Western blot. Bar = 70 μm. There is a significant correlation between anti-THSD7A titers measured by enzyme-linked immunosorbent assay and indirect immunofluorescence test (not shown). (**D**) IgG4 anti-THSD7A titer shown in relative units (RU)/ml while it is shown as optical density (OD) values in panel A.

Table S1. Detailed clinical characteristics of the 49 thrombospondin type 1 domain-containing 7A (THSD7A)-associated membranous nephropathy patients, ranked by titers from highest to lowest and by sex. Double-positive patients are listed at the end for each sex. Enzyme-linked immunosorbent assay (ELISA) titer <16 relative units (RU)/ml were measured at dilution 1:25 or 1:10 when serum was available. A, active disease; CR, complete remission; CP, cyclophosphamide; ESKD, end-stage kidney disease; NA, not available; PR, partial remission; RTX, rituximab.

Table S2. Clinical characteristics of females below and above 51 years (chosen as average age for menopause).[55,56] No differences were observed.

Table S3. Clinical characteristics of anti-thrombospondin type 1 domain-containing 7A (THSD7A)-positive patients with and without associated malignancy. Values are shown as *n* or median (interquartile range).

Table S4. Time gap between malignancy and membranous nephropathy (MN) diagnosis. *Negative values indicate prior diagnosis of malignancy.

Table S5. Distribution of anti-thrombospondin type 1 domain-containing 7A (THSD7A) IgG subclasses in THSD7A-positive patients. Values are shown as *n* (%).

Table S6. Clinical baseline characteristics of double-positive patients. No major difference was observed between patients with single positivity for anti-THSD7A versus double positivity for anti-thrombospondin type 1 domain-containing 7A (THSD7A) and anti-phospholipase A2 receptor 1 (PLA2R1). Values are shown as *n* (%) or median (interquartile range).

Table S7. Baseline characteristics of thrombospondin type 1 domain-containing 7A (THSD7A)-positive patients in remission versus active disease during follow-up. Only anti-THSD7A titer differs between the 2 subgroups of patients.

Table S8. Characteristics of all anti-thrombospondin type 1 domain-containing 7A (THSD7A)-positive patients published to date. Values are shown as *n* and mean (or median [*][S1,S2]) for age. ND, not defined.

Supplementary material is linked to the online version of the paper at www.kidney-international.org.

REFERENCES

1. Ponticelli C, Glassock RJ. Glomerular diseases: membranous nephropathy—a modern view. *Clin J Am Soc Nephrol*. 2014;9:609–616.
2. Beck LH Jr, Salant DJ. Membranous nephropathy: from models to man. *J Clin Invest*. 2014;124:2307–2314.
3. Ronco P, Debiec H. Pathophysiological advances in membranous nephropathy: time for a shift in patient's care. *Lancet*. 2015;385:1983–1992.
4. Schieppati A, Mosconi L, Perna A, et al. Prognosis of untreated patients with idiopathic membranous nephropathy. *N Engl J Med*. 1993;329:85–89.
5. Cattran DC, Reich HN, Beanlands HJ, et al. The impact of sex in primary glomerulonephritis. *Nephrol Dial Transplant*. 2008;23:2247–2253.
6. Beck LH Jr, Bonegio RG, Lambeau G, et al. M-type phospholipase A2 receptor as target antigen in idiopathic membranous nephropathy. *N Engl J Med*. 2009;361:11–21.
7. Tomas NM, Beck LH Jr, Meyer-Schwesinger C, et al. Thrombospondin type-1 domain-containing 7A in idiopathic membranous nephropathy. *N Engl J Med*. 2014;371:2277–2287.
8. Larsen CP, Cossey LN, Beck LH. THSD7A staining of membranous glomerulopathy in clinical practice reveals cases with dual autoantibody positivity. *Mod Pathol*. 2016;29:421–426.
9. Wang J, Cui Z, Lu J, et al. Circulating antibodies against thrombospondin type-I domain-containing 7A in Chinese patients with idiopathic membranous nephropathy. *Clin J Am Soc Nephrol*. 2017;12:1642–1651.
10. Hayashi N, Okada K, Matsui Y, et al. Glomerular mannose-binding lectin deposition in intrinsic antigen-related membranous nephropathy. *Nephrol Dial Transplant*. 2018;33:832–840.
11. Kao L, Lam V, Waldman M, et al. Identification of the immunodominant epitope region in phospholipase A2 receptor-mediating autoantibody binding in idiopathic membranous nephropathy. *J Am Soc Nephrol*. 2015;26:291–301.
12. Fresquet M, Jowitt TA, Gummadova J, et al. Identification of a major epitope recognized by PLA2R autoantibodies in primary membranous nephropathy. *J Am Soc Nephrol*. 2015;26:302–313.
13. Seitz-Polski B, Dolla G, Payre C, et al. Cross-reactivity of anti-PLA2R1 autoantibodies to rabbit and mouse PLA2R1 antigens and development of two novel ELISAs with different diagnostic performances in idiopathic membranous nephropathy. *Biochimie*. 2015;118:104–115.
14. Seitz-Polski B, Dolla G, Payre C, et al. Epitope spreading of autoantibody response to PLA2R associates with poor prognosis in membranous nephropathy. *J Am Soc Nephrol*. 2016;27:1517–1533.
15. Beck LH Jr. PLA2R and THSD7A: disparate paths to the same disease? *J Am Soc Nephrol*. 2017;28:2579–2589.

16. Seifert L, Hoxha E, Eichhoff AM, et al. The most N-terminal region of THSD7A is the predominant target for autoimmunity in THSD7A-associated membranous nephropathy. *J Am Soc Nephrol*. 2018;29:1536–1548.
17. Du Y, Li J, He F, et al. The diagnosis accuracy of PLA2R-AB in the diagnosis of idiopathic membranous nephropathy: a meta-analysis. *PLoS One*. 2014;9:e104936.
18. Hu SL, Wang D, Gou WJ, et al. Diagnostic value of phospholipase A2 receptor in idiopathic membranous nephropathy: a systematic review and meta-analysis. *J Nephrol*. 2014;27:111–116.
19. Hoxha E, Harendza S, Zahner G, et al. An immunofluorescence test for phospholipase-A2-receptor antibodies and its clinical usefulness in patients with membranous glomerulonephritis. *Nephrol Dial Transplant*. 2011;26:2526–2532.
20. Hofstra JM, Debiec H, Short CD, et al. Antiphospholipase A2 receptor antibody titer and subclass in idiopathic membranous nephropathy. *J Am Soc Nephrol*. 2012;23:1735–1743.
21. Dahnrich C, Komorowski L, Probst C, et al. Development of a standardized ELISA for the determination of autoantibodies against human M-type phospholipase A2 receptor in primary membranous nephropathy. *Clin Chim Acta*. 2013;421C:213–218.
22. Debiec H, Ronco P. PLA2R autoantibodies and PLA2R glomerular deposits in membranous nephropathy. *N Engl J Med*. 2011;364:689–690.
23. Hoxha E, Kneissler U, Stege G, et al. Enhanced expression of the M-type phospholipase A2 receptor in glomeruli correlates with serum receptor antibodies in primary membranous nephropathy. *Kidney Int*. 2012;82:797–804.
24. Larsen CP, Messias NC, Silva FG, et al. Determination of primary versus secondary membranous glomerulopathy utilizing phospholipase A2 receptor staining in renal biopsies. *Mod Pathol*. 2013;26:709–715.
25. Beck LH Jr, Fervenza FC, Beck DM, et al. Rituximab-induced depletion of anti-PLA2R autoantibodies predicts response in membranous nephropathy. *J Am Soc Nephrol*. 2011;22:1543–1550.
26. Hofstra JM, Fervenza FC, Wetzels JF. Treatment of idiopathic membranous nephropathy. *Nat Rev Nephrol*. 2013;9:443–458.
27. Kanigicherla D, Gummadova J, McKenzie EA, et al. Anti-PLA2R antibodies measured by ELISA predict long-term outcome in a prevalent population of patients with idiopathic membranous nephropathy. *Kidney Int*. 2013;83:940–948.
28. Hoxha E, Thiele I, Zahner G, et al. Phospholipase A2 receptor autoantibodies and clinical outcome in patients with primary membranous nephropathy. *J Am Soc Nephrol*. 2014;25:1357–1366.
29. Ruggenenti P, Debiec H, Ruggiero B, et al. Anti-phospholipase A2 receptor antibody titer predicts post-rituximab outcome of membranous nephropathy. *J Am Soc Nephrol*. 2015;26:2545–2558.
30. van de Logt AE, Hofstra JM, Wetzels JF. Pharmacological treatment of primary membranous nephropathy in 2016. *Expert Rev Clin Pharmacol*. 2016;9:1463–1478.
31. Ruggenenti P, Fervenza FC, Remuzzi G. Treatment of membranous nephropathy: time for a paradigm shift. *Nat Rev Nephrol*. 2017;13:563–579.
32. Dahan K, Debiec H, Plaisier E, et al. Rituximab for severe membranous nephropathy: a 6-month trial with extended follow-up. *J Am Soc Nephrol*. 2017;28:348–358.
33. Pourcine F, Dahan K, Mihout F, et al. Prognostic value of PLA2R autoimmunity detected by measurement of anti-PLA2R antibodies combined with detection of PLA2R antigen in membranous nephropathy: a single-centre study over 14 years. *PLoS One*. 2017;12:e0173201.
34. Seitz-Polski B, Debiec H, Rousseau A, et al. Phospholipase A2 receptor 1 epitope spreading at baseline predicts reduced likelihood of remission of membranous nephropathy. *J Am Soc Nephrol*. 2018;29:401–408.
35. De Vriese AS, Glassock RJ, Nath KA, et al. A proposal for a serology-based approach to membranous nephropathy. *J Am Soc Nephrol*. 2017;28:421–430.
36. Cattran DC, Brenchley PE. Membranous nephropathy: integrating basic science into improved clinical management. *Kidney Int*. 2017;91:566–574.
37. Behnert A, Schiffer M, Muller-Deile J, et al. Antiphospholipase A(2) receptor autoantibodies: a comparison of three different immunoassays for the diagnosis of idiopathic membranous nephropathy. *J Immunol Res*. 2014;2014:143274.
38. Huang B, Wang L, Zhang Y, et al. A novel time-resolved fluoroimmunoassay for the quantitative detection of antibodies against the phospholipase A2 receptor. *Sci Rep*. 2017;7:46096.
39. Tomas NM, Hoxha E, Reinicke AT, et al. Autoantibodies against thrombospondin type 1 domain-containing 7A induce membranous nephropathy. *J Clin Invest*. 2016;126:2519–2532.
40. Tomas NM, Meyer-Schwesinger C, von Spiegel H, et al. A heterologous model of thrombospondin type 1 domain-containing 7A-associated membranous nephropathy. *J Am Soc Nephrol*. 2017;28:3262–3277.
41. Hoxha E, Beck LH Jr, Wiech T, et al. An indirect immunofluorescence method facilitates detection of thrombospondin type 1 domain-containing 7A-specific antibodies in membranous nephropathy. *J Am Soc Nephrol*. 2017;28:520–531.
42. Iwakura T, Ohashi N, Kato A, et al. Prevalence of enhanced granular expression of thrombospondin type-1 domain-containing 7A in the glomeruli of Japanese patients with idiopathic membranous nephropathy. *PLoS One*. 2015;10:e0138841.
43. Sharma SG, Larsen CP. Tissue staining for THSD7A in glomeruli correlates with serum antibodies in primary membranous nephropathy: a clinicopathological study. *Mod Pathol*. 2018;31:616–622.
44. Huang CC, Lehman A, Albawardi A, et al. IgG subclass staining in renal biopsies with membranous glomerulonephritis indicates subclass switch during disease progression. *Mod Pathol*. 2013;26:799–805.
45. Lonnbro-Widgren J, Ebefors K, Molne J, et al. Glomerular IgG subclasses in idiopathic and malignancy-associated membranous nephropathy. *Clin Kidney J*. 2015;8:433–439.
46. Liu Y, Li X, Ma C, et al. Serum anti-PLA2R antibody as a diagnostic biomarker of idiopathic membranous nephropathy: the optimal cut-off value for Chinese patients. *Clin Chim Acta*. 2018;476:9–14.
47. Tampoia M, Migliucci F, Villani C, et al. Definition of a new cut-off for the anti-phospholipase A2 receptor (PLA2R) autoantibody immunoassay in patients affected by idiopathic membranous nephropathy. *J Nephrol*. 2018;31:899–905.
48. Murtas C, Bruschi M, Candiano G, et al. Coexistence of different circulating anti-podocyte antibodies in membranous nephropathy. *Clin J Am Soc Nephrol*. 2012;7:1394–1400.
49. Jullien P, Seitz Polski B, Maillard N, et al. Anti-phospholipase A2 receptor antibody levels at diagnosis predicts spontaneous remission of idiopathic membranous nephropathy. *Clin Kidney J*. 2017;10:209–214.
50. Lonnbro-Widgren J, Molne J, Haraldsson B, et al. Treatment pattern in patients with idiopathic membranous nephropathy-practices in Sweden at the start of the millennium. *Clin Kidney J*. 2016;9:227–233.
51. van den Brand JA, van Dijk PR, Hofstra JM, et al. Long-term outcomes in idiopathic membranous nephropathy using a restrictive treatment strategy. *J Am Soc Nephrol*. 2014;25:150–158.
52. Obrisca B, Ismail G, Jurubita R, et al. Antiphospholipase A2 receptor autoantibodies: a step forward in the management of primary membranous nephropathy. *BioMed Res Int*. 2015;2015:249740.
53. Dou Y, Zhang L, Liu D, et al. The accuracy of the anti-phospholipase A2 receptor antibody in the diagnosis of idiopathic membranous nephropathy: a comparison of different cutoff values as measured by the ELISA method. *Int Urol Nephrol*. 2016;48:845–849.
54. Akiyama S, Akiyama M, Imai E, et al. Prevalence of anti-phospholipase A2 receptor antibodies in Japanese patients with membranous nephropathy. *Clin Exp Nephrol*. 2015;19:653–660.
55. Baker FC, de Zambotti M, Colrain IM, et al. Sleep problems during the menopausal transition: prevalence, impact, and management challenges. *Nat Sci Sleep*. 2018;10:73–95.
56. Vellanki K, Hou S. Menopause in CKD. *Am J Kidney Dis*. 2018;71:710–719.
57. Gyan E, Raynard B, Durand JP, et al. Malnutrition in patients with cancer: comparison of perceptions by patients, relatives, and physicians—results of the NutriCancer2012 Study. *JPEN J Parenter Enteral Nutr*. 2018;42:255–260.
58. Ohtani H, Wakui H, Komatsuda A, et al. Distribution of glomerular IgG subclass deposits in malignancy-associated membranous nephropathy. *Nephrol Dial Transplant*. 2004;19:574–579.
59. Lin L, Wang WM, Pan XX, et al. Biomarkers to detect membranous nephropathy in Chinese patients. *Oncotarget*. 2016;7:67868–67879.
60. Qin HZ, Zhang MC, Le WB, et al. Combined assessment of phospholipase A2 receptor autoantibodies and glomerular deposits in membranous nephropathy. *J Am Soc Nephrol*. 2016;27:3195–3203.
61. Vanderlugt CL, Miller SD. Epitope spreading in immune-mediated diseases: implications for immunotherapy. *Nat Rev Immunol*. 2002;2:85–95.
62. Bech AP, Hofstra JM, Brenchley PE, et al. Association of anti-PLA2R antibodies with outcomes after immunosuppressive therapy in idiopathic membranous nephropathy. *Clin J Am Soc Nephrol*. 2014;9:1386–1392.

63. Dai H, Zhang H, He Y. Diagnostic accuracy of PLA2R autoantibodies and glomerular staining for the differentiation of idiopathic and secondary membranous nephropathy: an updated meta-analysis. *Sci Rep*. 2015;5:8803.
64. Xu X, Wang G, Chen N, et al. Long-term exposure to air pollution and increased risk of membranous nephropathy in China. *J Am Soc Nephrol*. 2016;27:3739–3746.
65. Hoxha E, Wiech T, Stahl PR, et al. A mechanism for cancer-associated membranous nephropathy. *N Engl J Med*. 2016;374:1995–1996.
66. Ronco PM. Paraneoplastic glomerulopathies: new insights into an old entity. *Kidney Int*. 1999;56:355–377.
67. Lefaucheur C, Stengel B, Nochy D, et al. Membranous nephropathy and cancer: epidemiologic evidence and determinants of high-risk cancer association. *Kidney Int*. 2006;70:1510–1517.
68. Beck LH Jr. Membranous nephropathy and malignancy. *Semin Nephrol*. 2010;30:635–644.
69. Cambier JF, Ronco P. Onco-nephrology: glomerular diseases with cancer. *Clin J Am Soc Nephrol*. 2012;7:1701–1712.
70. Malik GH, Al-Harbi AS, Al-Mohaya S, et al. Repeated pregnancies in patients with primary membranous glomerulonephritis. *Nephron*. 2002;91:21–24.
71. Surian M, Imbasciati E, Cosci P, et al. Glomerular disease and pregnancy: a study of 123 pregnancies in patients with primary and secondary glomerular diseases. *Nephron*. 1984;36:101–105.
72. Al-Rabadi L, Ayalon R, Bonegio RG, et al. Pregnancy in a patient with primary membranous nephropathy and circulating anti-PLA2R antibodies: a case report. *Am J Kidney Dis*. 2016;67:775–778.
73. O'Shaughnessy MM, Jobson MA, Sims K, et al. Pregnancy outcomes in patients with glomerular disease attending a single academic center in North Carolina. *Am J Nephrol*. 2017;45:442–451.
74. Luo R, Wang Y, Xu P, et al. Hypoxia-inducible miR-210 contributes to preeclampsia via targeting thrombospondin type I domain containing 7A. *Sci Rep*. 2016;6:19588.
75. Iwakura T, Fujigaki Y, Katahashi N, et al. Membranous nephropathy with an enhanced granular expression of thrombospondin type-1 domain-containing 7A in a pregnant woman. *Intern Med*. 2016;55:2663–2668.
76. Hoxha E, von Haxthausen F, Wiech T, et al. Membranous nephropathy—one morphologic pattern with different diseases. *Pflugers Arch*. 2017;469:989–996.
77. Phillips WD, Vincent A. Pathogenesis of myasthenia gravis: update on disease types, models, and mechanisms. *F1000Res*. 2016;5:F1000. Faculty Rev-1513.
78. Berrih-Aknin S, Frenkian-Cuvelier M, Eymard B. Diagnostic and clinical classification of autoimmune myasthenia gravis. *J Autoimmun*. 2014;48–49:143–148.

SUPPLEMENTARY INFORMATION

Novel ELISA for Thrombospondin type 1 domain-containing 7A autoantibodies in membranous nephropathy: analysis of a cohort of 49 patients

Christelle Zaghrini, Barbara Seitz-Polski, Joana Justino, Guillaume Dolla, Christine Payré, Noémie Jourde-Chiche, Anne-Els Van de Logt, Caroline Booth, Emma Rigby, Jennie Lonnbro-Widgren, Jenny Nystrom, Christophe Mariat, Zhao Cui, Jack F. M. Wetzels, GianMarco Ghiggeri, Laurence H. Beck Jr, Pierre Ronco, Hanna Debiec and Gérard Lambeau

SUPPLEMENTARY METHODS

Cloning and expression of recombinant soluble human THSD7A in HEK293 cells — The entire extracellular domain of human THSD7A (NP_056019, a. a. 47-1606) was produced in HEK293 cells essentially as described for full-length membrane-bound THSD7A [1]. The full-length cDNA coding for human THSD7A with a Myc-Flag tag and inserted into the pCMV6-entry expression vector (Origene RC213616) was used as a PCR template to delete the transmembrane domain and replace the Myc-Flag tag by a 6x histidine tag (Figure S1A) using the Phusion Site-Directed Mutagenesis Kit (Thermo Fisher Scientific). The THSD7A-6xHis insert was fully sequenced. For production of recombinant soluble THSD7A protein, HEK293 cells were cultured in DMEM medium containing 10% heat-inactivated FBS, 50 units/mL penicillin G, 100 µg/mL streptomycin (all from Gibco) at 37°C in a humidified atmosphere of 5% CO_2. The pCMV6-entry vector coding for soluble THSD7A-6xHis was transfected in HEK293 cells using Exgen (Biomol GmbH) according to the manufacturer's instructions. Transfected cells were selected with 1 mg/mL geneticin (Gibco). Single cell cloning was done by serial dilution in 96-well plates and the best expressing cell clones were selected. For large-scale production, cell clones were cultured to sub-confluency in complete medium, then switched to serum-free medium and the cell culture medium was harvested after expression for 7 days. The recombinant protein was purified by affinity chromatography on complete His-tag purification beads according the manufacturer's protocol (Roche). Cell culture medium containing the recombinant THSD7A protein was incubated with the beads for capture at 4°C overnight on a rocker. The column was washed with equilibrium buffer (300 mM NaCl, 20 mM Tris pH 7.4) followed by washes with equilibrium

buffer containing 10 mM imidazole. The bound protein was eluted stepwise with 400 mM imidazole (Figure S1B). The yield of production was 1 mg of purified soluble THSD7A/L of cell medium. Elutions were concentrated and buffer-exchanged with 1X PBS using an ultrafiltration cell system (Amicon) equipped with an YM-30 membrane. The purity and folding of THSD7A was validated by SDS-PAGE silver staining and WB with commercially available anti-THSD7A antibodies and THSD7A-associated MN sera (Figure S1C and D).

WB analysis for the detection of anti-THSD7A and anti-PLA2R1 autoantibodies — The detection of anti-THSD7A and anti-PLA2R1 autoantibodies was evaluated by WB after running SDS-PAGE (6 or 10%) under reducing or non-reducing conditions as specified in figure legends. Fifty ng/well of THSD7A or PLA2R1 antigens were run on SDS-polyacrylamide gel and transferred to methanol-soaked polyvinylidene difluoride membranes (Bio-Rad) under semi-dry conditions with 0.05% SDS in the transfer buffer using Trans-blot Turbo (Bio-Rad) at 25 V constant for 30 min. Membranes were blocked for 1 hour at RT with 5% milk in PBS-Tween 0.05%. The primary and secondary antibodies (diluted with 0.5% milk in PBS-T or PBS-T, respectively) were incubated at room temperature for 2 and 1 h, respectively. The purity and folding of the purified recombinant THSD7A antigen was initially validated using two commercial antibodies (a rabbit polyclonal THSD7A antibody from Atlas antibodies AB, Sweden, working dilution 1:500; and a goat polyclonal THSD7A antibody from Santa Cruz Biotechnologies, working dilution 1:250) and 2 THSD7A-positive MN sera at a working dilution of 1:100 (Figure S1D). The secondary antibodies used were HRP-conjugated goat anti-rabbit IgG (working dilution 1:5000, Southern Biotech, Birmingham, USA), rabbit anti-goat (working dilution 1: 20,000, Southern Biotech, Birmingham, USA) and HRP-conjugated mouse anti-human IgG4 (working dilution 1:30,000, Southern Biotech, Birmingham, USA), respectively. To test the positivity of the

THSD7A-associated MN patients, 50 ng/well of THSD7A and PLA2R1 antigens were loaded on a 10% SDS-polyacrylamide gel under non-reducing conditions. Membranes were probed with serum samples at a dilution ranging from 1:10 to 1:100 depending on the anti-THSD7A titer measured by ELISA (Figure S5). Serum samples from double positive patients were tested at a 1:25 dilution by WB from 6% SDS-polyacrylamide gel loaded with 50 ng/well of THSD7A and PLA2R1 antigens under non-reducing conditions. The secondary antibody was HRP-conjugated mouse anti-human IgG4 at 1:7,500 dilution. The detection of protein bands was performed with an enhanced chemiluminescent substrate (Perkin Elmer) and a Fuji LAS3000 digital imager.

IIFT for the detection of anti-THSD7A and anti-PLA2R1 autoantibodies — We used the cell–based IIFT kit from Euroimmun AG containing a mosaic biochip of formalin-fixed HEK293 cells overexpressing full-length human THSD7A or PLA2R1 or mock-transfected HEK293 as a negative control. Anti-THSD7A and anti-PLA2R1 titers were measured in a semi-quantitative manner by diluting serum samples at 1:10, 1:100 and 1: 1,000 in PBS-Tween 0.2% and incubating them with the biochip for 30 min. Bound IgG antibodies were then detected using a fluorescein isothiocyanate-conjugated goat anti-human IgG antibody (Euroimmun) as secondary antibody. Slides were examined using a confocal microscope at 460-490 nm LED excitation. Antibody titers were estimated by the fluorescence intensity at each dilution according to the manufacturer's instructions.

Kidney biopsy staining for THSD7A and PLA2R1 antigens — Patients' kidney biopsies were fixed in a solution containing ethanol (75%), formol (3%) and acetic acid (5%). Fixed biopsy specimens were paraffin-embedded according to standard techniques. Dewaxed sections (4-µm thickness) were hydrated and antigens were retrieved by Heat Induced Epitope Retrieval (HIER) at pH 6.0 and 95°C (Diagnostic BioSystems ref KO35). HIER was followed by 5 min incubation

with HistoReveal (Abcam). Biopsies were stained by immunofluorescence using rabbit polyclonal anti-THSD7A at x100 or anti-PLA2R1 at x500 (both from Atlas antibodies AB, Sweden) as primary antibodies and goat conjugated rabbit Fab IgG antibody Alexa 488 (Molecular Probes) at 1:250 (Invitrogen) as secondary antibody.

Detailed follow-up for patient MN13 — At baseline, the patient had high proteinuria (6.1 g/day) associated with high anti-THSD7A titer (especially for IgG4 and IgG3 subclasses) detected by both ELISA and IIFT At month 2, the patient was treated with rituximab (2 doses at 375 mg/m^2), which led to a rapid decrease of anti-THSD7A titers for both IgG3 and IgG4 subclasses followed by gradually decreasing levels of proteinuria from months 3 to 7 (5.2 to 1.4 g/day). At month 7, proteinuria suddenly increased up to 5.5 g/day at months 10 to 13. A renal biopsy performed at month 13 showed enhanced staining of THSD7A antigen on the glomerular basement membrane suggesting a still active MN disease (Figure S9). The patient was treated with a second course of rituximab (2 doses at 375 mg/m^2) which led to further decrease but not disappearance of anti-THSD7A autoantibodies at month 10, as measured by ELISA and IIFT, and was followed by decreased proteinuria to the sub-nephrotic range at month 18, down to 1.9 g/day. Overall, we concluded that the first and second rituximab treatments were effective and led to partial immunological remission, with a significant but slow decrease of anti-THSD7A autoantibodies. This was followed by a global decrease of proteinuria from months 0 to 18, despite a transient increase of proteinuria over 5 months. Finally, between months 18 and 27, there was a slight increase in anti-THSD7A titer with a concomitant increase in proteinuria up to 3.4 g/day, suggesting a possible MN relapse associated with anti-THSD7A autoantibodies. We also compared anti-THSD7A autoantibody levels by ELISA, WB and IIFT during follow-up and treatment (Figure S9). By WB, anti-THSD7A levels were also detected throughout the follow-up

period but it was difficult to evaluate the titer variation over time. Both IIFT and ELISA could measure the change in titer, yet ELISA was more accurate to detect subtle changes. We also monitored by ELISA the changes in anti-THSD7A IgG subclasses. Levels of anti-THSD7A IgG1 and IgG2 were barely detectable at baseline and during follow-up and were thus not useful to monitor the anti-THSD7A immunological response. In contrast, both IgG3 and IgG4 autoantibodies could be robustly monitored throughout follow-up, and both IgG subclasses appeared to vary simultaneously, yet ELISA assay measuring IgG4 anti-THSD7A titers was more reliable (Figure S9).

Table S1: Detailed clinical characteristics of the 49 THSD7A-associated MN patients, ranked by titers from highest to lowest and by sex. Double-positive patients are listed at the end for each gender. ELISA titer <16 RU/mL were measured at dilution 1:25 or 1:10 when serum was available. A, active disease; CR, complete remission; CP, cyclophosphamide; ESKD, end stage kidney disease; NA, not available; PR, partial remission; RTX, rituximab.

Patient ID	ELISA (RU/mL)	WB	IIFT	Anti-PLA2R1	Gender	Age (years)	UProt. (g/day)	SAlb. (g/L)	Screat. (µmol/L)	eGFR (CKD-EPI) (mLmin/1.73 m^2)	Associated disease	Follow-up (months)	Treatment	Outcome
	Anti-THSD7A													
1	13920	+	3200	–	M	68	25.9	13	88	77	Colon adenocarcinoma	5	RTX	A
4	1776	+	320	–	M	71	14.6	14	108	59	None	54	None	A
5	1669	+	1000	–	M	54	9.1	15	89	84	None	150	Prednisone ACTH Cyclosporine A, RTX	CR
9	1270	+	1000	–	M	17	2.7	29	120	76	None	6.5	RTX	PR
10	1188	+	100	–	M	85	3.0	14	80	77	Prostate cancer	36	RAS blockers	PR
11	1092	+	320	–	M	67	10.6	NA	116	56	Diabetes Mellitus	85	CP Prednisone	PR
12	955	+	1000	–	M	59	5.9	23	89	81	None	84	None	CR
14	505	+	100	–	M	55	12.2	15	235	26	Hypothyroidism, diabetes, psoriasis	10	RTX	ESKD
15	566	+	320	–	M	49	9.0	NA	212	31	Discoid lupus	NA	Alternating months of prednisone and CP followed by RTX	A
17	545	+	100	–	M	68	6.0	16	88	77	Cheek intra-epidermal carcinoma Pityriasis rosea, Biermer's disease	48	RAS blockers	PR
18	416	+	100	–	M	62	5.5	18	115	58	None	180	Steroids + CP	ESKD
19	376	+	320	–	M	54	2.9	27	131	53	None	102	CP Prednisone	CR

Patient ID	ELISA (RU/mL)	WB	IIFT	Anti-PLA2R1	Gender	Age (years)	UProt. (g/day)	SAlb. (g/L)	Screat. (μmol/L)	eGFR (CKD-EPI) (mLmin/1.73 m^2)	Associated disease	Follow-up (months)	Treatment	Outcome
	Anti-THSD7A													
21	278	+	320	–	M	80	5.9	26	80	80	Parotitis, Warthin's tumor	14	ACTH	CR
22	234	+	10	–	M	76	8.0	25	150	38	None	NA	Steroids + CP diuretics	CR
23	233	+	320	–	M	75	10.3	NA	89	73	COPD	24	CP Prednisone	A (Persistent proteinuria)
26	122	+	100	–	M	67	5.4	19	122.8	53	Polymyalgia rheumatica,	18	RTX	CR
27	119	+	10	–	M	75	12.0	24	152	38	Pancreatic carcinoma	90	Cyclosporine A, CP Prednisone	CR
28	97	+	100	–	M	75	5.3	31	103	61	None	37	None	CR
31	68	+	10	–	M	75	6.3	20	120	51	None	32	NA	A
35	29	+	32	–	M	83	14.5	15	202.4	25	None	NA	NA	NA
36	27	+	10	–	M	60	10.0	21	90	80	HBV	NA	Steroids + CP RAS blockers diuretics	CR
39	21	+	10	–	M	51	4.0	26	87	88	HIV, HCV	62	RTX	CR
40	<16	–	10	–	M	77	7.0	21	129.9	45	Prostate cancer, diabetes	3	RAS blockers	A
41	<16	–	10	–	M	60	13.2	5	184	34	Gastric carcinoma,	NA	None	NA (Death)
45	353	+	100	+	M	54	11.4	19	72.5	100	NA	NA	NA	NA
46	23	+	–	+	M	86	5.3	21	190	27	None	NA	NA	PR
47	<16	–	–	+	M	48	4.0	25	47	125	NA	NA	ACE and RAS blockers	A
48	<16	–	–	+	M	65	6.0	28	52	106	None	NA	ACE and RAS blockers	CR

Patient ID	ELISA (RU/mL)	WB	IIFT	Anti-PLA2R1	Gender	Age (years)	UProt. (g/day)	SAlb. (g/L)	Screat. (µmol/L)	eGFR (CKD-EPI) (mLmin/1.73 m^2)	Associated disease	Follow-up (months)	Treatment	Outcome
		Anti-THSD7A												
2	7255	+	3200	–	F	95	6.5	10	67	67	Breast cancer, hypothyroidism	12	Corticosteroids Cyclosporine A	A
3	1827	+	1000	–	F	61	20.0	17	66.3	86	Hypothyroidism	NA	NA	NA
6	1605	+	100	–	F	73	4.3	18	74	69	None	72	RAS blockers	CR
7	1586	+	1000	–	F	51	14.9	NA	NA	NA	None	NA	NA	NA
8	1354	+	1000	–	F	37	7.0	18	59	113	Monoclonal IgG Kappa, multiple sclerosis	10	RTX	A
13	715	+	1000	–	F	4	6.1	22	NA	NA	Haemolytic anaemia, thrombocytopenia	32	RTX	A
16	606	+	32	–	F	49	19.6	10	71	86	None	23	CP, Prednisone	CR
20	302	+	320	–	F	66	3.5	24	141.4	33	None	29	Cyclosporine A Prednisone Tacrolimus	A
24	194	+	100	–	F	36	5.0	25	80	82	None	NA	ACTH, RAS blockers	A
25	134	+	100	–	F	33	1.57	39	82.2	81	Hypothyroidism, alopecia areata, latent tuberculosis	44	RAS blockers	CR
29	97	+	32	–	F	51	3.0	36	70.7	86	NA	50	Cyclosporine A plasmapheresis RTX	PR
30	94	+	32	–	F	35	1.8	26	53	119	NA	12	RAS blockers	PR
32	59	+	10	–	F	30	3.7	NA	NA	NA	NA	NA	None	NA

Patient ID	ELISA (RU/mL)	WB	IFT	Anti-PLA2R1	Gender	Age (years)	UProt. (g/day)	SAlb. (g/L)	Screat. (µmol/L)	eGFR (CKD-EPI) (ml/min/1.73 m^2)	Associated disease	F-up (Months)	Treatment	Outcome
	Anti-THSD7A													
33	52	+	100	–	F	47	3.0	NA	70.7	88	Iritis	120	Cyclosporine A Prednisone RTX Tacrolimus ACTH, CP	PR
34	29	+	10	–	F	47	6.6	24	69	91	NA	12	RAS blockers	A
37	23	+	10	–	F	82	1.0	23	110	40	None	46	None	NA
38	22	+	10	–	F	39	6.5	21	70	94	None	22	RAS blockers Steroids + CP	CR
42	642	+	100	+	F	56	3.0	NA	114.9	46	NA	NA	NA	NA
43	561	+	100	+	F	49	8.4	14	100	57	None	NA	Steroids diuretics	NA
44	312	+	32	+	F	77	10	22	60	85	Rectal cancer and thymoma, Goujerot-Sjogren syndrome, monoclonal IgG lambda, HBV	60	None Tumorectomy	CR
49	<16	–	–	+	F	28	4.7	26	53	124	Goujerot-Sjogren syndrome	38	ACE blockers	CR

Table S2. Clinical characteristics of females below and above 51 years (chosen as average age for menopause).[55-56] No differences were observed

Clinical characteristics	Females <51 (n=14)	Females >51 (n=7)	P Value
Age at diagnosis (year)	38.0 [32.3–49.0]	73.0 [61.0–82.0]	0.003
Proteinuria (g/day)	5.6 [3.0–7.4]	4.3 [3.0–10.0]	0.881
Serum Albumin (g/L)	24.0 [18.0–26.0]	20.1 [15.3–23.0]	0.208
Serum Creatinine (µmol/L)	70.7 [59.0–80.0]	74.0 [66.3–115.0]	0.319
eGFR (CKD-EPI) (mL/min/1.73 m^2)	88.0 [82–113.0]	67.0 [40.0–85.0]	0.145
Anti-THSD7A titer (RU/mL)	115.5 [46.3–633.3]	642.0 [302.0–1827.0]	0.079

References

55. Baker FC, de Zambotti M, Colrain IM, et al. Sleep problems during the menopausal transition: prevalence, impact, and management challenges. Nature and science of sleep 2018; **10:** 73-95.

56. Vellanki K, Hou S. Menopause in CKD. Am J Kidney Dis 2018; **71:** 710-719.

Table S3: Clinical characteristics of anti-thrombospondin type 1 domain-containing 7A (THSD7A)-positive patients with and without associated malignancy. Values are shown as n or median (interquartile range).

Clinical characteristics	No malignancy (n=41)	Malignancy (n=8)	P value
Gender M/F (n)	22/19	6/2	0.264
Age at diagnosis (year)	54 [47–69]	76 [69–83]	0.002
Proteinuria (g/day)	6.0 [3.9–9.6]	8.5 [6.1–12.9]	0.117
Serum creatinine (µmol/L)	89.0 [70.7–120.0]	88.0 [70.3–146.0]	0.873
eGFR (CKD-EPI) (mL/min/1.73 m^2)	78.0 [52.5–88.0]	72.0 [39.8–77.0]	0.296
Serum albumin (g/L)	22.3 [18.0–26.0]	15.0 [10.9–21.9]	0.016
Anti-THSD7A titer (RU/mL)	234.0 [40.5–679.0]	429.0 [32.8–5738]	0.635

Table S4: Time gap between malignancy and membranous nephropathy (MN) diagnosis. *Negative values indicate prior diagnosis of malignancy.

MN patient	Gender	Age (year)	Malignancy	Time of diagnosis of tumor to MN diagnosis (months)*
1	M	68	Colon adenocarcinoma	-18*
10	M	85	Prostate cancer	0
17	M	68	Cheek intra-epidermal cancer	96
27	M	75	Pancreatic cancer	84
40	M	77	Prostate cancer	-22
41	M	60	Gastric cancer	0
2	F	95	Breast cancer	-108*
44	F	77	Rectal cancer and thymoma	0

Table S5: Distribution of anti-thrombospondin type 1 domain-containing 7A (THSD7A) IgG subclasses in THSD7A-positive patients. Values are shown as n(%).

Anti-THSD7A IgG subclass	No malignancy (n=41)	Malignancy (n=8)	P value
IgG1 n (%)	5 (12.2)	1 (12.5)	0.981
IgG2 n (%)	8 (19.5)	0 (0)	0.172
IgG3 n (%)	7 (17.0)	2 (25.0)	0.596
IgG4 n (%)	38 (93.0)	6 (75.0)	0.131

Table S6: Clinical baseline characteristics of double-positive patients. No major difference was observed between patients with single positivity for anti-THSD7A versus double positivity for anti-thrombospondin type 1 domain-containing 7A (THSD7A) and anti-phospholipase A2 receptor 1 (PLA2R1). Values are shown as n (%) or median (interquartile range).

Clinical characteristics	THSD7A positive (n=41)	Double positive (n=8)	P value
Gender M/F (n)	24/17	4/4	0.655
Age at diagnosis (year)	60.0 [48.0–75.0]	55.0 [48.3–74.0]	0.828
Proteinuria (g/day)	6.3 [3.9–10.4]	5.7 [4.2–9.6]	0.715
Serum creatinine (µmol/L)	89.0 [73.3–125.0]	66.3 [52.3–111.0]	0.082
eGFR (CKD-EPI) (mL/min/1.73 m^2)	74.5 [49.5–84.5]	92.5 [48.8–120.0]	0.159
Serum albumin (g/L)	21.0 [15.0–25.0]	22.2[19.0–25.6]	0.591
Anti-THSD7A titer (RU/mL)	278.0 [63.5–1140.0]	167.5 [16.0–509.0]	0.136
Cancer incidence n (%)	7 (17)	1 (13)	0.748

Table S7. Baseline characteristics of thrombospondin type 1 domain-containing 7A (THSD7A)-positive patients in remission versus active disease during follow-up. Only anti-THSD7A titer differs between the 2 subgroups of patients.

Clinical characteristics	Remission n=24	Active n=12	P value
Age (years)	59.6 ± 3.928	57.8 ± 6.868	0.82
Sex ratio F/M	9/15	5/7	1.00
Proteinuria (g/day)	5.7 [3–8.825]	6.8 [5.7–11.71]	0.06
Serum creatinine (µmol/L)	87.5 [70.8–119.0]	108.0 [80.0–141.4]	0.33
Serum albumin (g/L)	23.4 [18.8–26.3]	18.0 [13.4–22.5]	0.03
Time of Follow-up (months)	48.0 [18.0–85.0]	29.0 [11.0–43.0]	0.196
Treatment with immunosuppressors	14*	9*	0.27
Anti-THSD7A titer (RU/mL)	134.0 [52.0–955.0]	536.0 [250.0–1671.0]	0.04

*Data for treatment was unavailable for 1 patient in each subgroup.

Table S8: Characteristics of all anti-thrombospondin type 1 domain-containing 7A (THSD7A)-positive patients published to date. Values are shown as n and mean (or median [*] [S1-S13]) for age. ND, not defined.

Reference	Year	Origin	All		Male		Female		Cancer (n)
			Patients (n)	Age (years)	Patients (n)	Age (years)	Patients (n)	Age (years)	
s3	2014	USA, France, Germany	17	49.9	6	54	11	47	1
s4	2015	Japan	5	42.4	2	–	3	–	0
s5	2016	Japan	1	–	–	–	1	30	0
s6	2016	China	5	39.8	2	54	3	32	1
s7	2016	China	4	–	–	–	–	–	ND
s8	2016	USA	9	62	7	–	2	–	ND
s1	2017	USA, Germany	40	60.5*	17	–	23	–	8
s9	2017	France	2	–	–	–	–	–	0
s10	2017	China	12	51.5	8	62.5	4	44.5	1
s11	2017	Japan	2	–	–	–	–	–	ND
s12	2017	USA	31	62.0	19	–	12	–	2
s13	2017	France	2	–	–	–	–	–	1
s2	2018	Germany	31	37*	19	–	12	–	9
This study	2018	France	49	58.4	28	67	21	48.8	8

References

s1. Hoxha E, Beck LH, Jr., Wiech T, et al. An Indirect Immunofluorescence Method Facilitates Detection of Thrombospondin Type 1 Domain-Containing 7A-Specific Antibodies in Membranous Nephropathy. J Am Soc Nephrol 2017; **28:** 520-531.

s2. Seifert L, Hoxha E, Eichhoff AM, et al. The Most N-Terminal Region of THSD7A Is the Predominant Target for Autoimmunity in THSD7A-Associated Membranous Nephropathy. J Am Soc Nephrol 2018.

s3. Tomas NM, Beck LH, Jr., Meyer-Schwesinger C, et al. Thrombospondin type-1 domain-containing 7A in idiopathic membranous nephropathy. N Engl J Med 2014; **371:** 2277-2287.

s4. Iwakura T, Ohashi N, Kato A, et al. Prevalence of Enhanced Granular Expression of Thrombospondin Type-1 Domain-Containing 7A in the Glomeruli of Japanese Patients with Idiopathic Membranous Nephropathy. PloS one 2015; **10:** e0138841.

s5. Iwakura T, Fujigaki Y, Katahashi N, et al. Membranous Nephropathy with an Enhanced Granular Expression of Thrombospondin Type-1 Domain-containing 7A in a Pregnant Woman. Internal medicine (Tokyo, Japan) 2016; **55:** 2663-2668.

s6. Lin L, Wang WM, Pan XX, et al. Biomarkers to detect membranous nephropathy in Chinese patients. Oncotarget 2016; **7:** 67868-67879.

s7. Qin HZ, Zhang MC, Le WB, et al. Combined Assessment of Phospholipase A2 Receptor Autoantibodies and Glomerular Deposits in Membranous Nephropathy. J Am Soc Nephrol 2016; **27:** 3195-3203.

s8. Larsen CP, Cossey LN, Beck LH. THSD7A staining of membranous glomerulopathy in clinical practice reveals cases with dual autoantibody positivity. Mod Pathol 2016; **29:** 421-426.

s9. Dahan K, Debiec H, Plaisier E, et al. Rituximab for Severe Membranous Nephropathy: A 6-Month Trial with Extended Follow-Up. J Am Soc Nephrol 2017; **28:** 348-358.

s10. Wang J, Cui Z, Lu J, et al. Circulating Antibodies against Thrombospondin Type-I Domain-Containing 7A in Chinese Patients with Idiopathic Membranous Nephropathy. Clin J Am Soc Nephrol 2017; **12:** 1642-1651.

s11. Hayashi N, Okada K, Matsui Y, et al. Glomerular mannose-binding lectin deposition in intrinsic antigen-related membranous nephropathy. Nephrol Dial Transplant 2017.

s12. Sharma SG, Larsen CP. Tissue staining for THSD7A in glomeruli correlates with serum antibodies in primary membranous nephropathy: a clinicopathological study. Mod Pathol 2017.

s13. Pourcine F, Dahan K, Mihout F, et al. Prognostic value of PLA2R autoimmunity detected by measurement of anti-PLA2R antibodies combined with detection of PLA2R antigen in membranous nephropathy: A single-centre study over 14 years. PloS one 2017; **12:** e0173201.

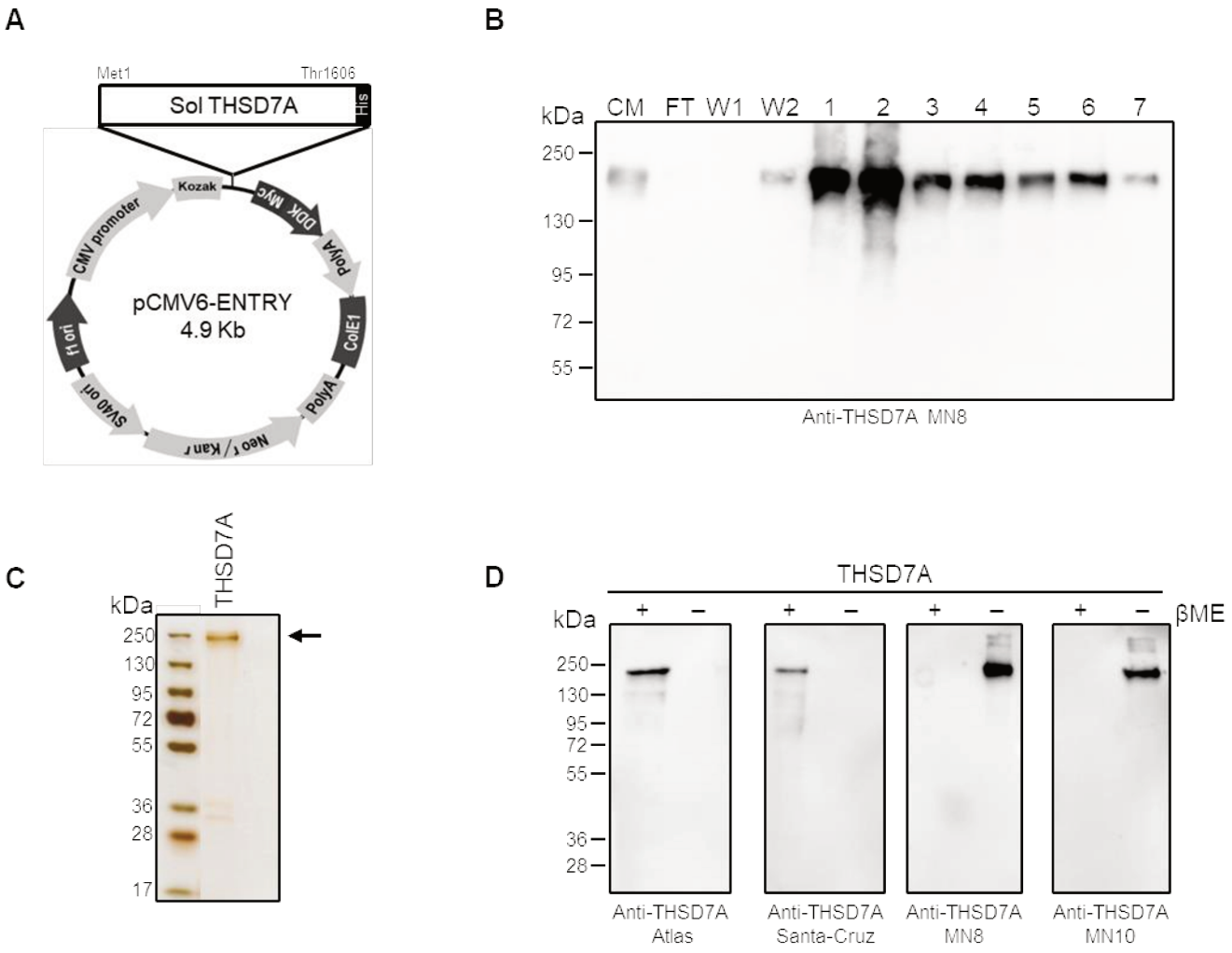

Figure S1: Cloning, expression, and purification of recombinant human soluble thrombospondin type 1 domain-containing 7A 6X histidine (THSD7A-6xHis). (A) Schematic representation of the pCMV6-entry expression vector coding for human soluble THSD7A-6xHis. The cDNA insert encodes for the signal peptide followed by the full extracellular region of THSD7A (from Met-1 to Thr-1606, Uniprot Q9UPZ6) and a C-terminal 6xHis Tag. **(B)** Western blot after His Tag purification from human embryonic kidney 293 cell medium containing soluble THSD7A-6xHis and probed with membranous nephropathy patient 8 (MN8) under nonreducing conditions at a 1:100 dilution. We loaded 400 ml of cell medium onto 4 ml of Ni-NTA resin. The resin was washed once with 40 ml of washing equilibrium buffer and then with 40 ml of washing buffer containing 10 mmol/l imidazole. Bound protein was eluted with 28 ml (in 7 fractions) of elution buffer containing 400 mmol/l imidazole. Aliquots of cell medium (CM), flow-through (FT), washes (W), and eluate (1 to 7) fractions were separated by sodium dodecylsulfate polyacrylamide gel electrophoresis (10%), transferred to polyvinylidene membranes and analyzed by Western blot. **(C)** Silver staining of the purified THSD7A-6xHis (100 ng) after buffer exchange with 1X phosphate-buffered saline. **(D)** Western blots to validate the purified THSD7A-6xHis as a native folded protein. Purified recombinant THSD7A-6xHis (50 ng) was loaded on sodium dodecylsulfate polyacrylamide gel electrophoresis (10%) under reducing or nonreducing conditions and probed with 2 commercially available anti-THSD7A antibodies and 2 representative anti-THSD7A-positive patients (MN8 and MN10; dilution 1:100).

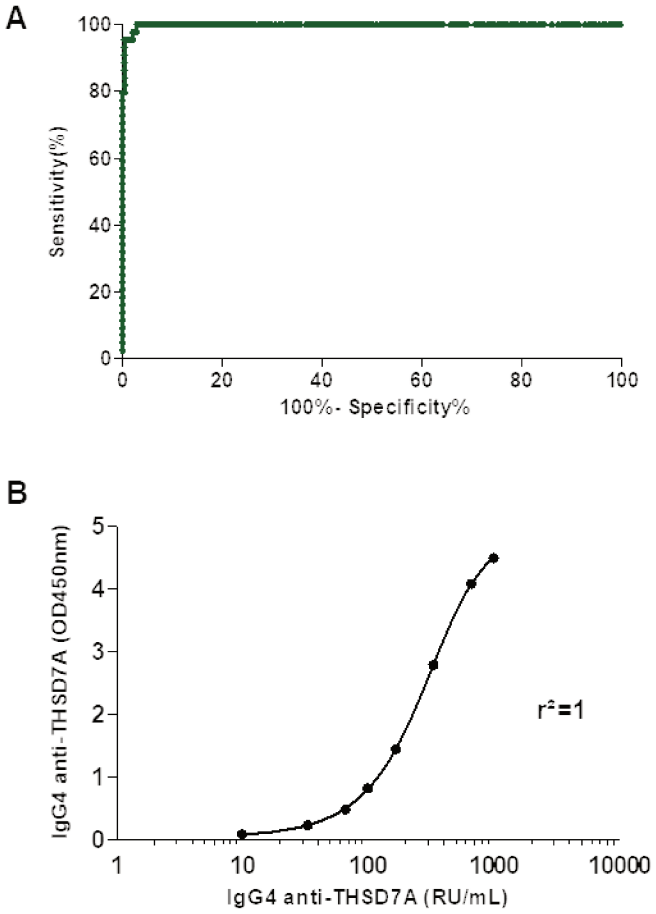

Figure S2: Receiver-operating characteristic curve and calibration curve for IgG4 anti-thrombospondin type 1 domain-containing 7A (THSD7A) enzyme-linked immunosorbent assay (ELISA). (A) Receiver-operating characteristic curve analysis of IgG4 anti-THSD7A detection in 44 anti-THSD7A-positive patients and 242 negative control subjects by ELISA. The area under the curve was 0.9982 (95% confidence interval: 0.9957–1.0, $P < 0.0001$). **(B)** Calibration curve covering the range of 9.9 relative units (RU)/ml to 990 RU/ml used to convert optical density (OD) values into RU/ml.

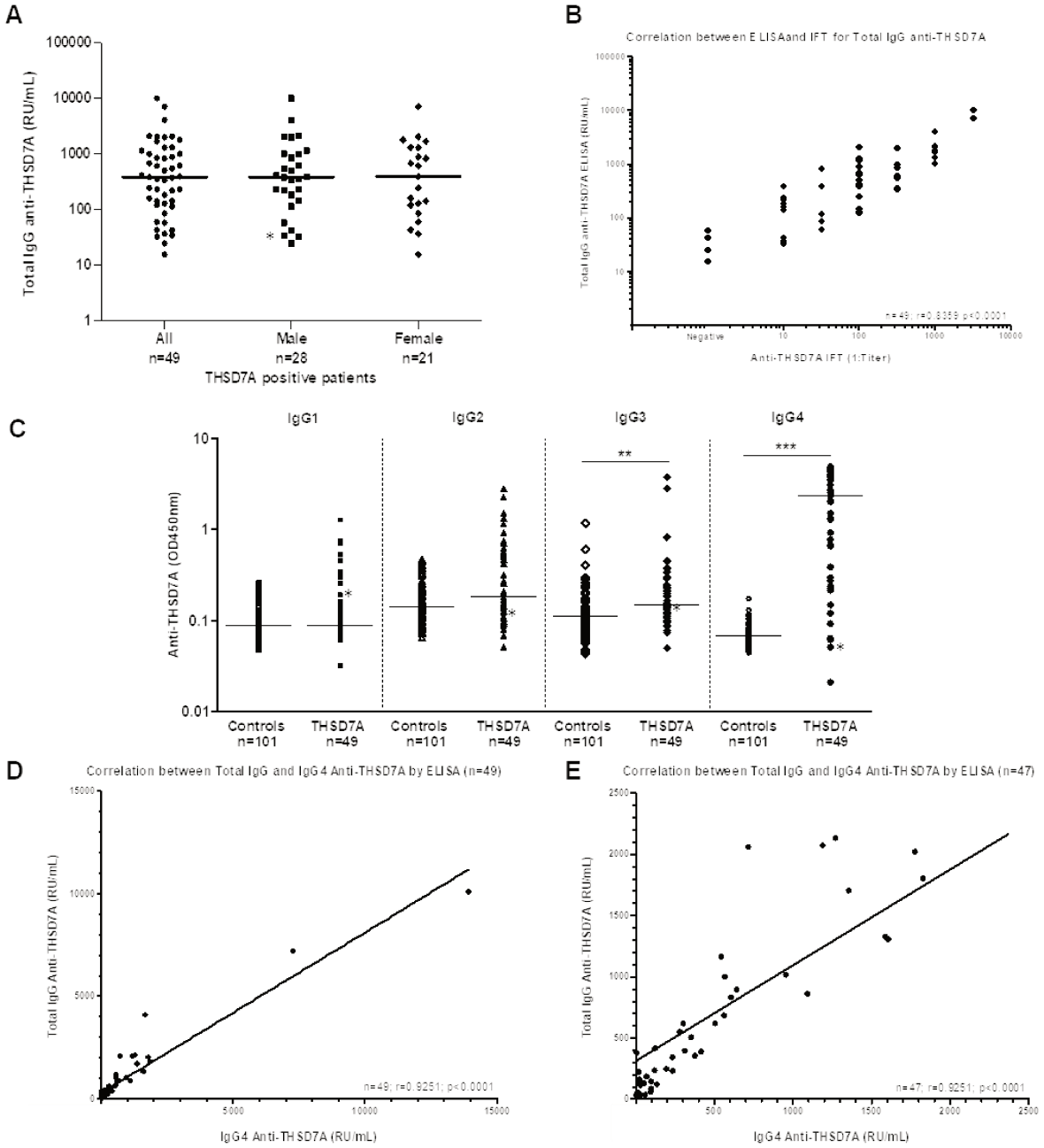

Figure S3: Levels of IgG subclasses and total IgG for anti-thrombospondin type 1 domain-containing 7A (THSD7A) autoantibodies, and correlation between anti-THSD7A titers by enzyme-linked immunosorbent assay (ELISA) and indirect immunofluorescence test (IIFT). (A) Scatter plot showing the distribution of anti-THSD7A titers for the 49 THSD7A-positive patients, as measured with total IgG as a secondary antibody. Titer for membranous nephropathy patient (MN40) is shown with asterisk (*). **(B)** Correlation between total IgG anti- THSD7A titers measured by IIFT versus ELISA. The correlation is highly significant (n=49, r=0.8359, $P < 0.0001$). **(C)** Distribution of anti-THSD7A IgG subclasses measured by ELISA for the THSD7A-positive patients (n=49) versus control subjects (other diseases and healthy donors, n=101). The anti-THSD7A titer for IgG3 and IgG4 subclasses was significantly different from that of control subjects using one-way analysis of variance test (**<0.01, ***<0.001). Optical density (OD) values for MN40 are shown with asterisk (*). **(D)** Correlation between anti-THSD7A titers measured by ELISA using IgG4 and total IgG secondary antibodies (n = 49, r = 0.9251, $P < 0.0001$). (E) Zoom on the low to middle range titers of anti-THSD7A titers measured by ELISA using IgG4 and total IgG secondary antibodies (n = 47).

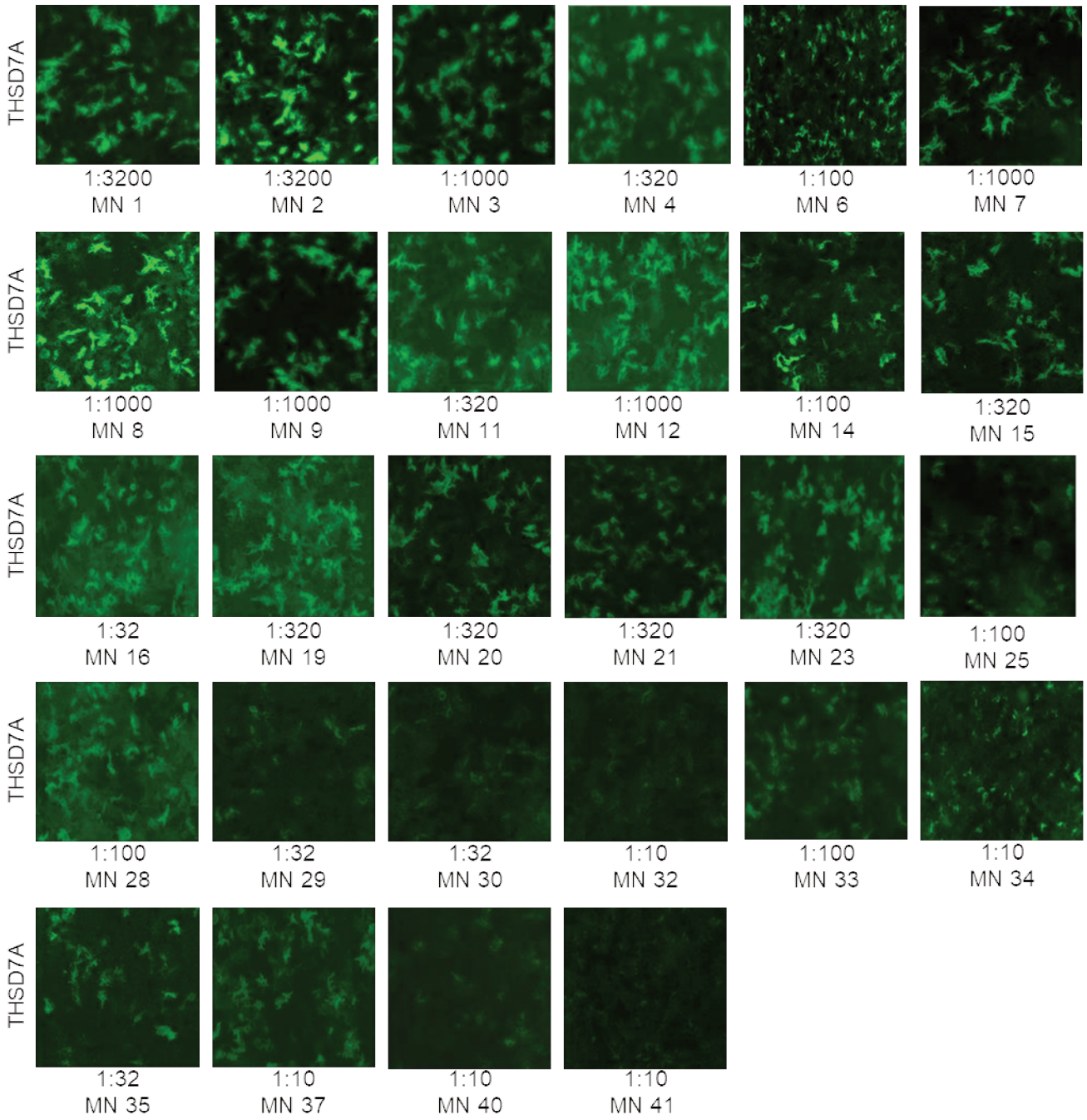

Figure S4: Indirect immunofluorescence test (IIFT) data for thrombospondin type 1 domain-containing 7A (THSD7A)-positive patients. Autoantibody titers were estimated by the fluorescence intensity at various dilutions. Data are shown at the dilution titer. Data for membranous nephropathy patient 5 (MN5), MN13, MN26, MN31, and MN42 to MN49 are presented in the main figures.

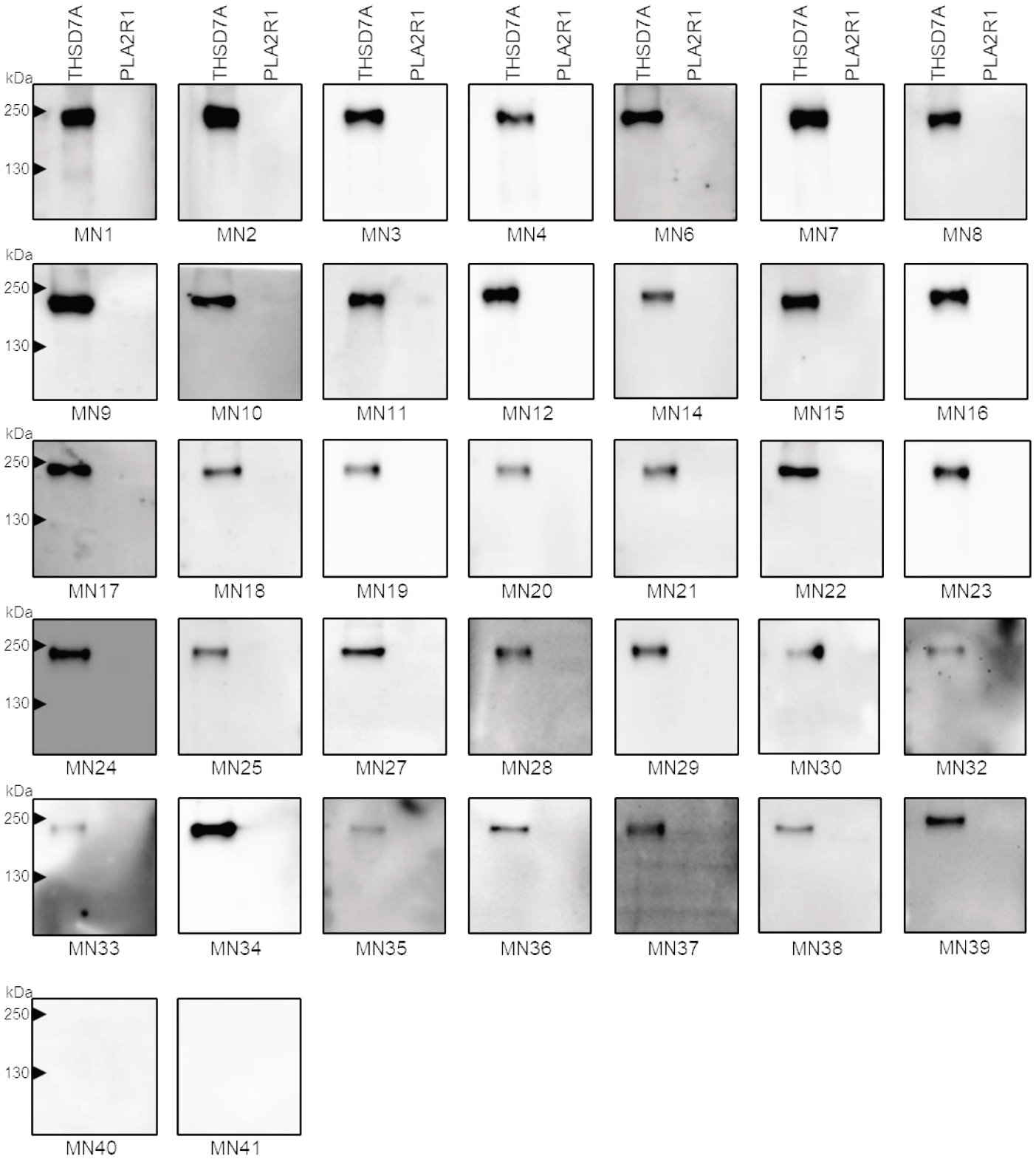

Figure S5: Western blot analysis of purified recombinant thrombospondin type 1 domain-containing 7A (THSD7A) and phospholipase A2 receptor 1 (PLA2R1) antigens (50 ng each) probed with all sera from THSD7A-positive patients under nonreducing conditions. Serum reactivity of patients was tested at optimal serum dilution (1:10 to 1:100). The blots were exposed for different times. Results for membranous nephropathy patient 5 (MN5), MN13, MN26, MN31, and MN42 to MN49 are presented in the main figures.

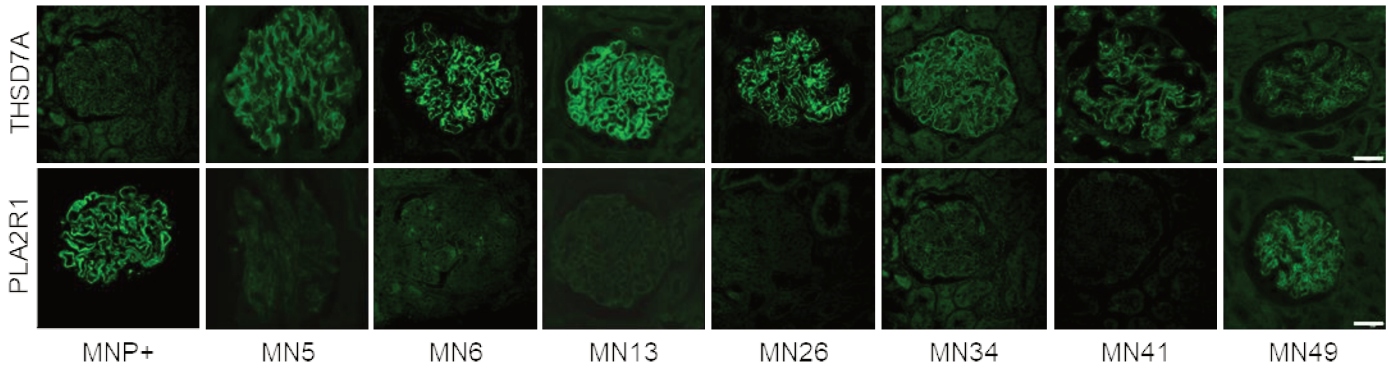

Figure S6: Immunofluorescence staining of thrombospondin type 1 domain-containing 7A (THSD7A) and phospholipase A2 receptor 1 (PLA2R1) antigens for available patients' biopsies. **(A)** Available immunofluorescence biopsy staining for THSD7A antigen for the anti-THSD7A-positive patients included in this study (membranous nephropathy patient 5 MN5, MN6, MN13, MN26, MN34, MN41) and for 1 double-positive patient (MN49). An anti-PLA2R1 positive serum (MNP+) was used as a positive control for PLA2R1 staining. Bar=50 µm.

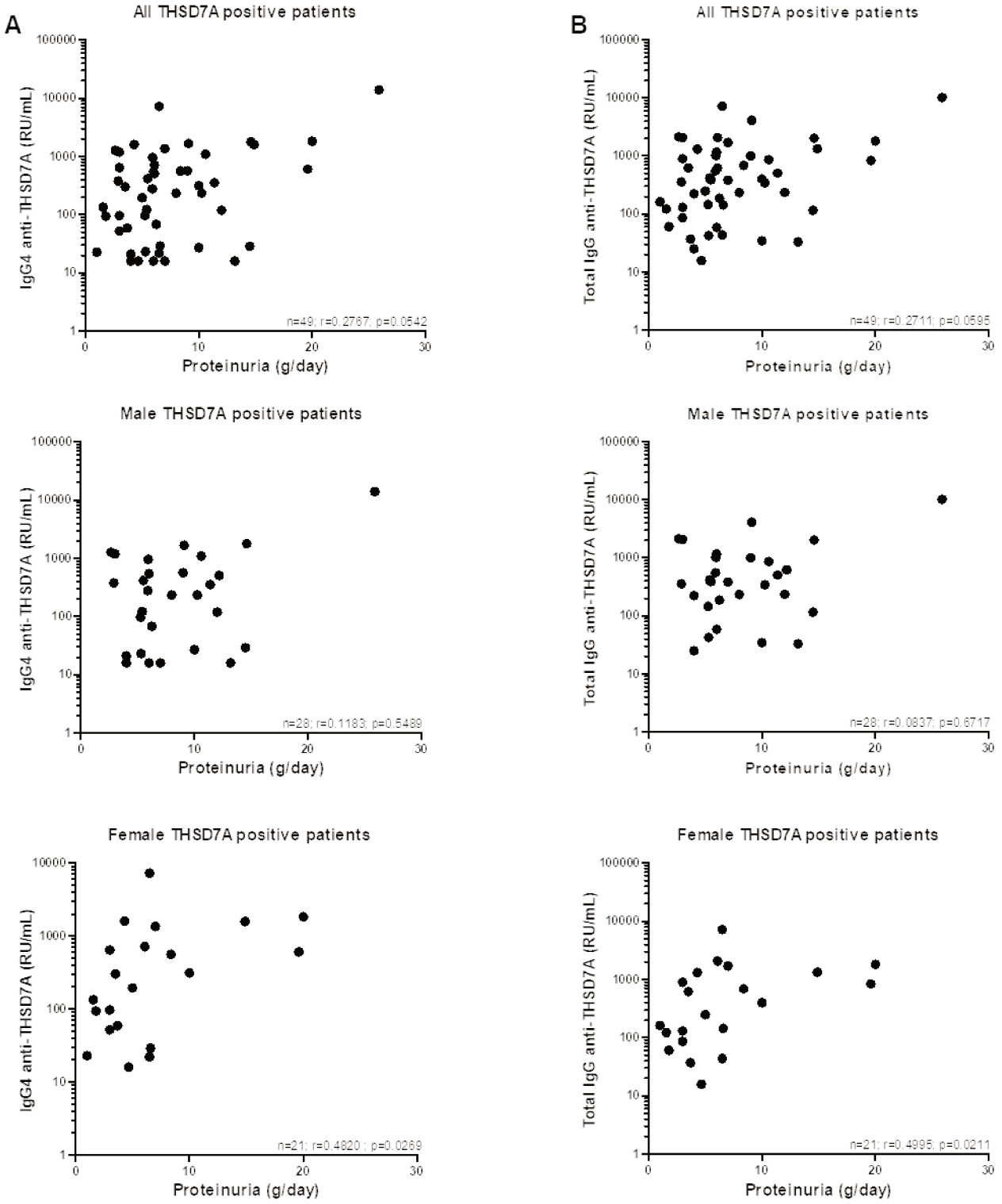

Figure S7: Correlation of proteinuria with IgG4 and total IgG anti-thrombospondin type 1 domain-containing 7A (THSD7A) titers measured by enzyme-linked immunosorbent assay for anti-THSD7A-positive patients as a whole or by sex. (A) Correlation between proteinuria and IgG4 anti-THSD7A titers for all (n=49, r=0.2767, P=0.0542), male or female THSD7A-positive patients. **(B)** Correlation between proteinuria and total IgG anti-THSD7A titers for all (n=49, r=0.2711, P=0.0595), male or female THSD7A-positive patients. Proteinuria levels show no significant correlation with anti-THSD7A titers.

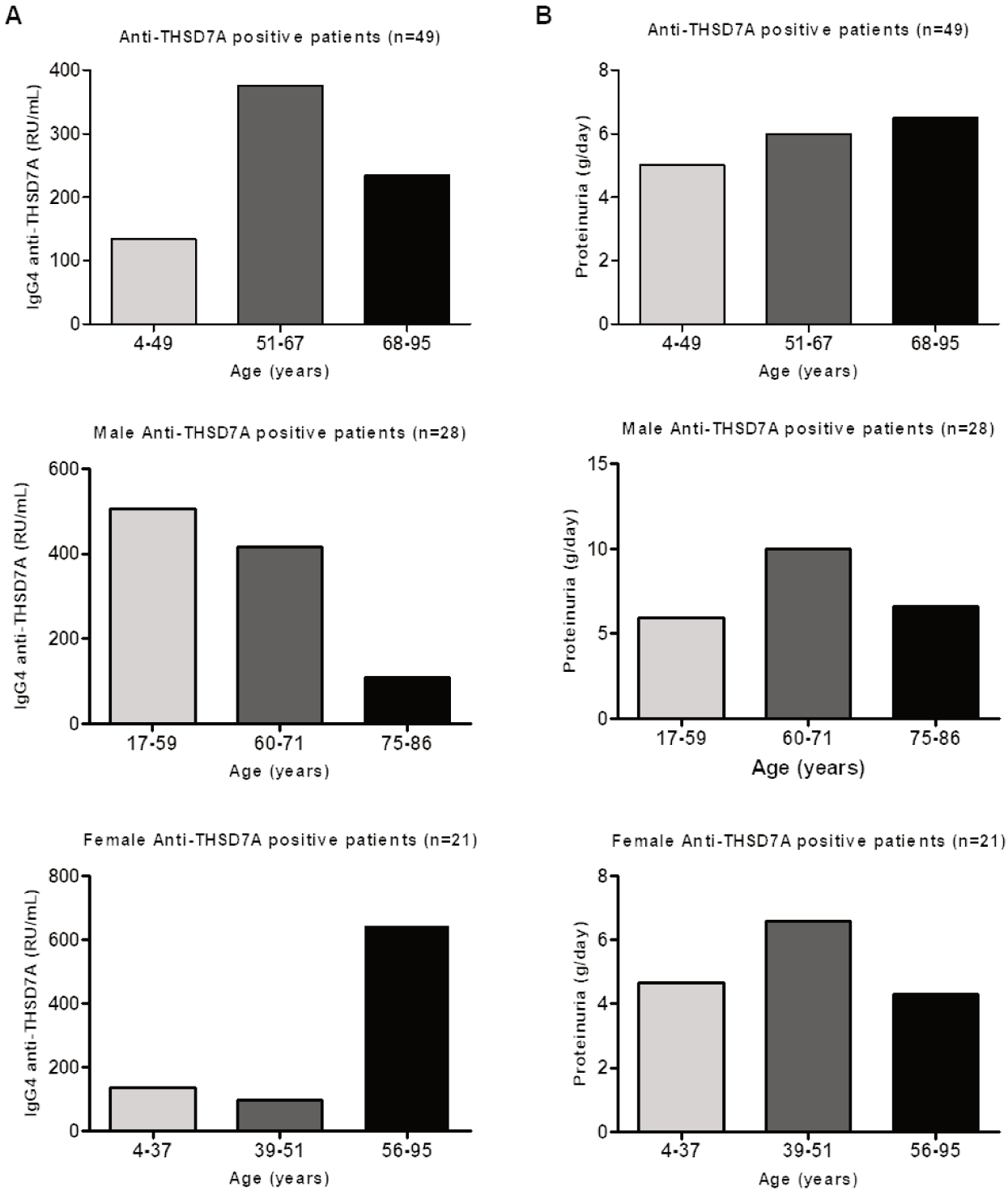

Figure S8: Relationship between anti-thrombospondin type 1 domain-containing 7A (THSD7A) titer, proteinuria, and age of anti-THSD7A-positive patients by tertiles. (A) Relationship between anti-THSD7A median titer (relative units [RU]/ml) and age of patients in tertiles for all, male, or female THSD7A-positive patients. **(B)** Relationship between proteinuria levels (g/d) and age of patients in tertiles for all, male, or female THSD7A-positive patients. Anti-THSD7A and proteinuria levels show no significant correlation with age.

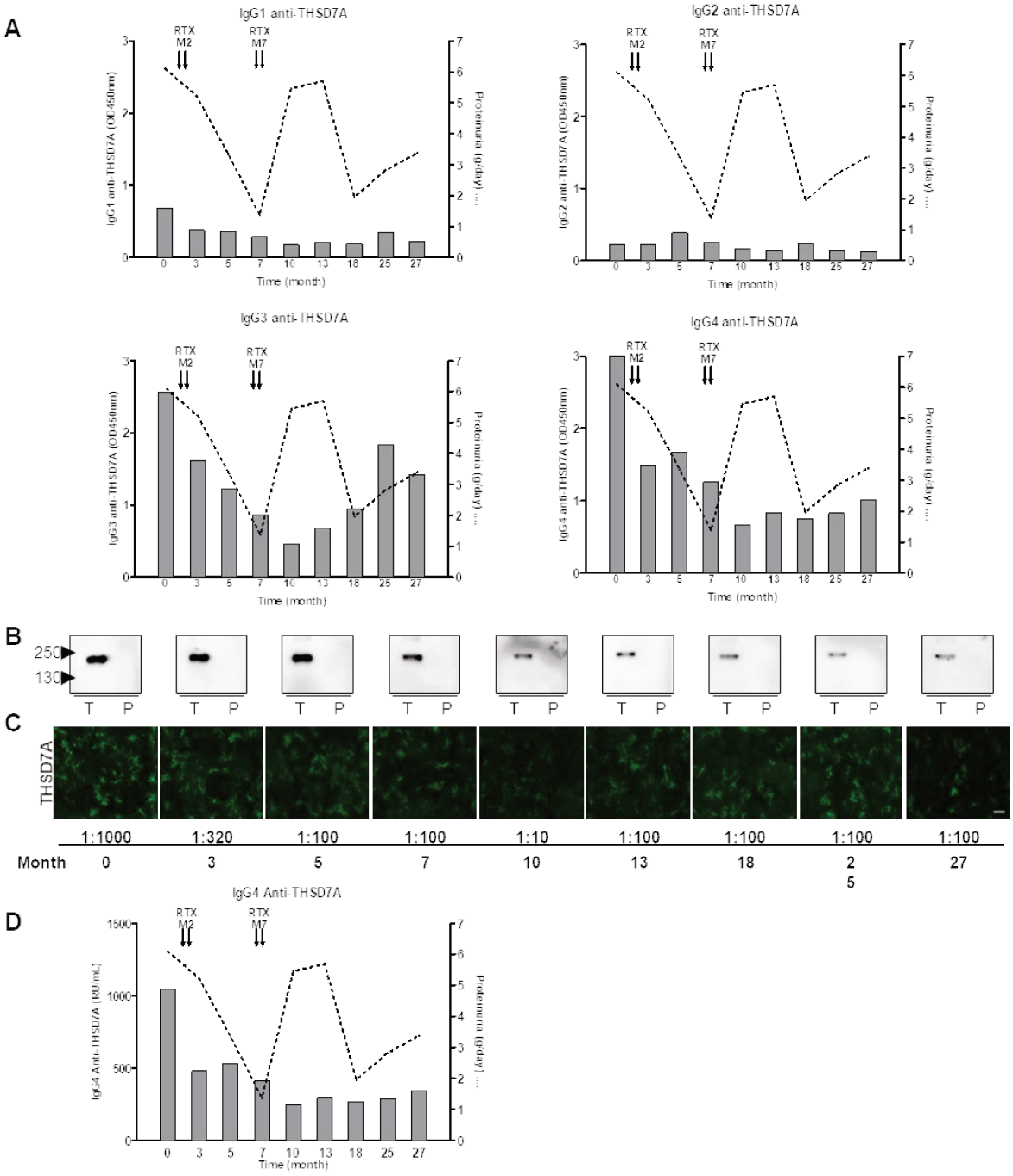

Figure S9: Anti-thrombospondin type 1 domain-containing 7A (THSD7A) titer and proteinuria levels during clinical follow-up for membranous nephropathy patient 13, a THSD7A-positive pediatric patient (4 years old at baseline) treated with rituximab. The patient had nephrotic range proteinuria at baseline and received 2 courses of rituximab (RTX) at months 2 and 7. See more clinical details in the Supplementary Methods. **(A)** Respective levels of anti-THSD7A autoantibodies measured by enzyme-linked immunosorbent assay for the different IgG subclasses and proteinuria during a follow-up of 27 months. **(B,C)** Anti-THSD7A levels measured by Western blot and indirect immunofluorescence test. Enzyme-linked immunosorbent assay and indirect immunofluorescence test detect the fluctuation of serum anti-THSD7A levels more quantitatively than Western blot. Bar=70 um. There is a significant correlation between anti-THSD7A titers measured by enzyme-linked immunosorbent assay and indirect immunofluorescence test (not shown). **(D)** IgG4 anti-THSD7A titer shown in relative units (RU)/ml while it is shown as optical density (OD) values in panel A.

4.2 Identification of THSD7A epitopes in MN (Unpublished data)

While establishing the ELISA test for detection of all anti–THSD7A autoantibodies, the second main aim of my thesis project was to identify the epitope domains targeted by these antibodies and investigate whether a mechanism of epitope spreading may occur in THSD7A–associated MN, as it was proposed for PLA2R1–associated MN.

When I started this study, a preliminary study just came out as an abstract in the Kidney week 2015 congress by Hong Ma & Laurence Beck and colleagues, showing that most patients' autoantibodies target multiple epitope regions in THSD7A, throughout the entire molecule (Hong et al., 2015). They generated multiple N– and C–terminal truncation mutants comprising single or multiple adjacent domains and tested the reactivity of patients' sera by western blot, dot blot and immunoprecipitation. Most patients reacted with 2 or more domains, mainly on the C–terminal region. However, an additional N–terminal epitope region was recognized by a smaller group of patients. They confirmed that binding of anti–THSD7A autoantibodies to the different epitope regions was always conformation–dependent.

At the time I started investigating the epitope regions in THSD7A, little was known about the detailed domain organization of the large extracellular region of THSD7A. The protein was thought to contain 10 or 11 thrombospondin domains in addition to 14 glycosylation sites and an RGD motif (Tomas et al., 2014; Wang et al., 2010). A first approach would have been to identify THSD7A epitopes by generation of multiple transmembrane and soluble deletion mutants (from the full protein to single domains in a sequential way), as previously done for PLA2R1 epitopes. However, because of the large effort of molecular biology required to prepare such constructs on a large protein (more than 100 have been made for PLA2R1) and because of the limited information on the THSD7A domain organization (especially the delimitation between domains and the pairing of the numerous disulfides which is crucial to preserve the conformational structure of the domains), we first considered an alternative strategy expected to be more straightforward. This strategy was based on the limited proteolysis of the full THSD7A antigen that we had just produced in large amounts and as a pure protein, followed by testing of the resulting fragments by western blot for reactivity with patients' antibodies and identification by mass spectrometry. A similar strategy was used previously to identify

the different epitope regions recognized by autoantibodies against myeloperoxidase in ANCA vasculitis disease (Roth et al., 2013) and for the identification of the major epitope region on PLA2R1 in MN (Fresquet et al., 2015).

4.2.1 Identification of THSD7A epitopes by limited proteolysis

– Digestion of THSD7A with proteases and denaturants.

Because of our insufficient knowledge on the delimitation of the multiple THSD7A domains in the early days of work with THSD7A, we decided to use a strategy similar to the above one, trying to identify THSD7A epitopes by generating small fragments of the full THSD7A recombinant protein under conditions of limited proteolysis, and looking for reactivity with patients' antibodies. The digestion of THSD7A by enzymes in the presence of chemical compounds on limited cleavage sites would produce fragments of the full protein and increase the chance to preserve the conformational epitopes recognized by patients' sera. The reactive fragments would then be identified by mass spectrometry. In our strategy, we tried to cut THSD7A with many proteases including trypsin, proteinase K, furin, kallikrein, urokinase, etc.).

Digestion of THSD7A was assayed with different proteases in various conditions of incubation, including deglycosylation before protease treatment and digestion in the presence of urea. Digestions were also performed at various temperatures and time of incubation (data not shown). We aimed to set up conditions with only limited digestion of THSD7A to generate short fragments of the protein but not complete digestion. Digestion of THSD7A was mainly evaluated using an anti–THSD7A commercial antibody (Sigma) and a patient's serum (MN17) which we had in sufficient amounts, under reducing and non–reducing conditions, respectively. Of note, the commercial anti–THSD7A antibody recognized one or more epitope(s) between Val250 and Cys355 at the N–terminal region the molecule in a non–conformational manner, i.e. in western blot under reducing conditions.

It was previously shown that THSD7A is highly glycosylated and that treatment with neuraminidase and N–glycopeptidase–F leads to a shift in its molecular weight evidenced by western blot (Tomas et al., 2014). Similar findings were observed when we treated 1 μg THSD7A with the same enzymes (data not shown). Also, treatment of THSD7A

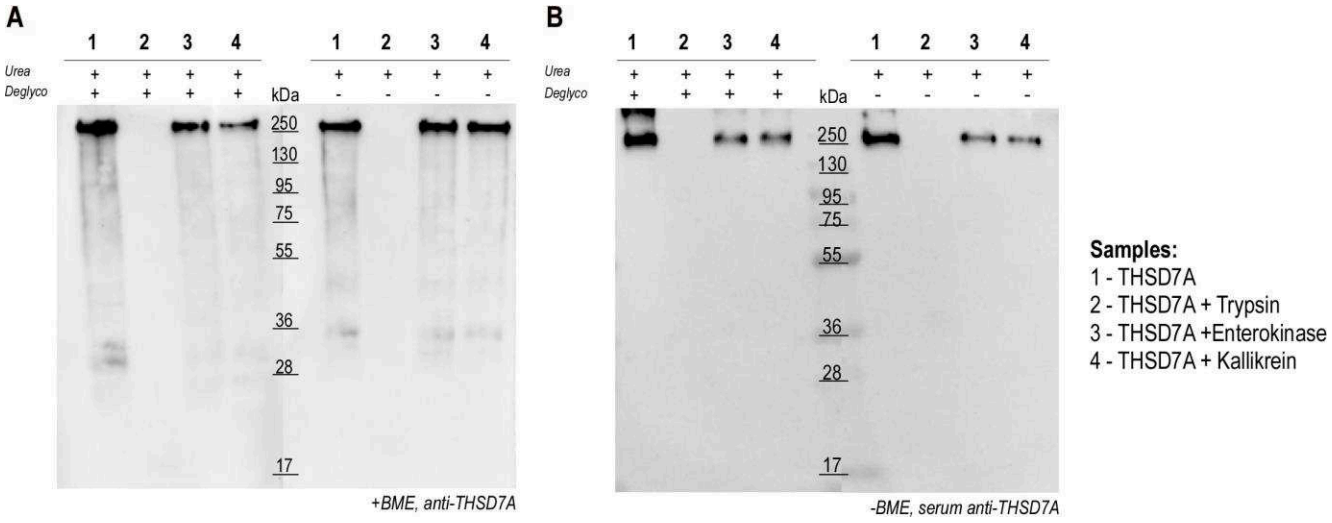

Figure 4.1 – Western blot of proteolysis of THSD7A by three proteases. THSD7A (1 μg/condition) was deglycosylated overnight at 37°C with neuraminidase and N–glycopeptidase–F. The protein was then digested with trypsin or Enterokinase or kallikrein in the presence of 2 M Urea. Proteolysis of THSD7A by trypsin was incubated for 6 hours at 50°C while Enterokinase and kallikrein were incubated with THSD7A for 6 hours at 37°C. (A) The western blot was analyzed under reducing conditions (+BME) with commercial anti–THSD7A and (B) under non–reducing conditions (–BME) with serum from patient MN17. Incubation of THSD7A with 2 M urea alone (i.e. no proteases added) did not alter the structure of the protein nor its recognition by antibodies under reducing and non–reducing conditions (data not shown). The shift in size between glycosylated and deglycosylated THSD7A is not evident due to the poor separation of high molecular weight proteins in the gel conditions chosen to resolve possible THSD7A fragments (i.e. 10% SDS–PAGE). Proteolysis of THSD7A by trypsin was complete as evidenced by western blot under reducing and non–reducing conditions. Evidence for limited proteolysis of THSD7A by Enterokinase or Kallikrein is deduced from the less intense staining of intact THSD7A when assayed with serum anti–THSD7A.

with 2 M urea alone did not alter protein reactivity by commercial and patient's antibodies. Despite numerous assay conditions with varying amounts of proteases and different denaturants (heat, urea, detergents), we could not identify conditions generating short fragments of THSD7A of interest, and the reactions were "all or none", either cleaving the protein in too small pieces or likely peptides no longer reactive with patients' antibodies, or apparently not cleaving THSD7A in fragments visible by gel analysis under non–reducing conditions and reactive with patients' antibodies. Representative results are shown in figure 4.1. For instance, digestion of THSD7A with trypsin in the presence of urea and after deglycosylation induced total proteolysis as evidenced by the loss of reactivity for both commercial and patient antibodies by western blot under the appropriate conditions.

On the other hand, digestion with Enterokinase and Kallikrein in the same conditions induced only a partial digestion (as indicated by the decrease in intensity of the full THSD7A band) but did not produce cleaved fragments of THSD7A still reactive with either of the antibodies.

– Digestion of THSD7A by combined treatment with proteases and dithiothreitol

The above apparent "all or none" results of digestion with the different proteases may at least in part be explained by the presence of many disulfides in THSD7A. These disulfides would still maintain the protein as an apparently single chain full protein when analyzed under non–reducing conditions, even if the protease (Enterokinase or kallikrein) was cleaving the protein at different reactive sites, thereby altering the reactivity of antibodies to conformational epitopes. It is only after extensive cleavage (like with trypsin) that the full protein would disappear but would then become cut into too small and non–reactive fragments.

With this possible scenario in mind, and as described in previous studies (Suckau et al., 1990), we aimed to identify the THSD7A epitopes by coupling optimized amounts of reducing agent and protease like trypsin. Of note, we knew that reduction of THSD7A under strong reducing conditions leads to full loss of patients' autoantibody reactivity (Beck et al., 2009; Tomas et al., 2014). However, we reasoned that a mild and well–defined reduction of the protein would maintain the reactivity to some THSD7A domains (i.e. still folded) while this reduction would provide a better cleavage condition with proteases and hence would produce detectable fragments of THSD7A still harboring some conformational epitopes.

As a first step toward this goal, we incubated THSD7A in the absence of proteases, but with increasing concentrations of dithiothreitol (DTT) overnight at 50°C. The aim was to determine the maximal DTT concentration at which THSD7A is still reactive with patients' autoantibodies but at least partially reduced. A total loss of conformation of THSD7A will prevent reactivity of anti–THSD7A autoantibodies with the short fragments after digestion and therefore hamper the identification of the epitopes of interest.

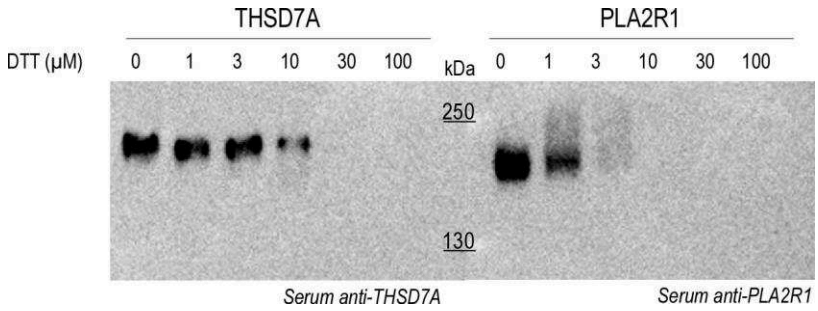

Figure 4.2 – Patients' autoantibody reactivity of THSD7A and PLA2R1 after treatment with increasing concentrations of DTT by western blot. The purified THSD7A and rbPLA2R1 (1 μg/condition) were incubated overnight at 50°C with increasing concentrations of DTT ranging from 1 µM to 100 μM. The western blot was performed under non–reducing conditions and probed with anti–THSD7A MN serum (left) and anti–PLA2R1 MN serum (right).

Interestingly, and despite the numerous disulfides, we found that the reactivity of anti–THSD7A autoantibodies towards full THSD7A was completely lost at relatively low concentrations of DTT higher than 10 μM (Figure 4.2). In the same conditions, anti–PLA2R1 antibodies lost the recognition for PLA2R1 at concentrations higher than 3 μM DTT (Figure 4.2). The higher resistance of THSD7A to the reduction by DTT compared to PLA2R1 might be due to the "apparent titration" of disulfides at these low concentrations of DTT, with THSD7A contains about twice the number of cysteine residues and disulfide bonds compared to rbPLA2R1. These results allowed us to determine the maximal concentration of DTT that can be used in combination with proteases to cleave THSD7A and possibly identify epitope domains.

In a second experiment, we combined the digestion by kallikrein or trypsin with the low range concentrations of DTT to ensure a partial/mild reduction of THSD7A (Figure 4.3). However, in the presence of DTT concentrations as low as 5 μM, THSD7A was apparently fully digested by kallikrein or trypsin. We thus could not probe any epitope region when using the MN patients' antibodies (MN13). Two hypotheses might explain the results we obtained using this approach:

– The epitope domains were cleaved by the digestion and therefore anti–THSD7A autoantibodies were unable to bind since the conformational epitope was no longer available.

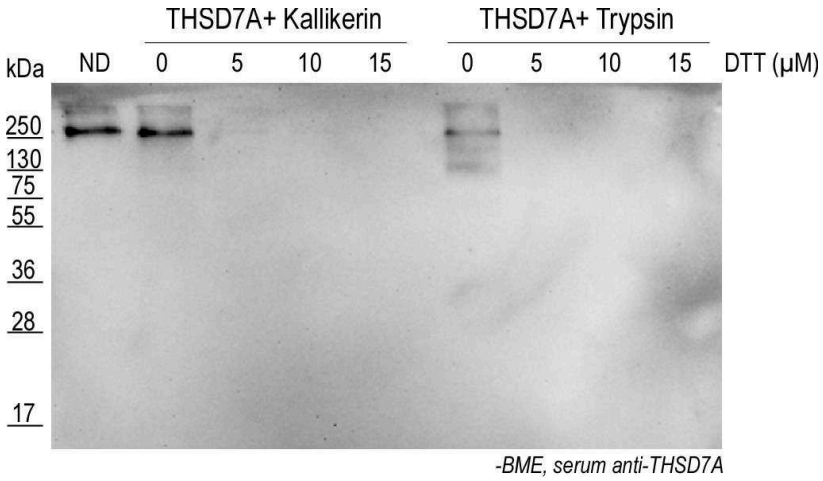

Figure 4.3 – Strong proteolysis of THSD7A by combining DTT and enzymes. Purified THSD7A (2 μg/condition) was first deglycosylated overnight at 37°C followed by enzyme digestion in the presence of different DTT concentrations by kallikrein or trypsin for 6 hours at 37°C or 50°C, respectively. Western blot was probed under non–reducing conditions with anti–THSD7A MN serum. No fragments reactive with patients' antibodies could be detected after digestion with DTT as low as 5 μM.

– The protein was successfully cut i.e. the fragments were still containing epitopes, but the transfer conditions of the western blot were not optimal, and the fragments were not retained on the PVDF membrane.

Because these experiments were time–consuming and largely unsuccessful, we decided to stop this proteolytic approach and moved back to the site–directed mutagenesis approach. Of note, probing the possible different reactivity of partially reduced THSD7A with a ramp of increasing DTT concentration with different patients' sera would have allowed us to determine if there is a common major epitope recognized by all or many patients or whether there are different discrete epitopes with different sensitivities to DTT, and possibly not recognized by all patients, i.e. suggesting a mechanism of epitope spreading (data not shown). We however did not test these hypotheses, for lack of time.

4.2.2 Identification of THSD7A epitopes by site–mutagenesis

The investigation of the epitope domains on THSD7A using the proteolysis strategy was unsuccessful. We therefore switched to a site–directed mutagenesis approach. In a collaborative work with Dr. Laurence Beck in Boston, we obtained the cDNA for 17 mutants

of THSD7A used in their preliminary study mentioned above (Hong et al., 2015). These mutants (mostly soluble) spanned mainly the N–terminal region of the antigen and comprised 2 to 12 adjacent domains. Of note, these constructs were designed based on the preliminary observation suggesting a predominance of the N–terminal region of THSD7A. It has been shown that culture of HEK293 cells at low temperature (30°C in our settings) reduces the growth rate of cells but increases the folding and production of difficult to express or mutant recombinant proteins (Bernier et al., 2004; Gora et al., 2009; Lin et al., 2015). Therefore, we optimized the protein yield of the THSD7A soluble constructs in culture medium by incubating transiently transfected HEK293 cells either at 37 °C or at 30 °C during the period of production. Then we tested by western blot the reactivity of 2 patients with high anti–THSD7A titer for reactivity against the different mutants. Even though the western blot technique is known to be a highly sensitive technique for protein detection, we were not able to evidence any epitope region when probing the 17 THSD7A mutants with high titer anti–THSD7A titer serum (data not shown). We thus chose to screen for the positivity on these mutants by ELISA.

By the time we expressed the different mutants in sufficient amounts and started analyzing the epitope profiles of THSD7A–associated MN patients, Seifert et al. published the first complete study on the THSD7A epitopes identified by western blot and dot blot (Seifert et al., 2018). They reevaluated the structure of THSD7A using the position–sensitive alignment search tool and structure–based alignments of THSD7A with the thrombospondin–1 domain. They aligned the conserved cysteine, tryptophan, and arginine residues and showed that the structure of THSD7A consists of 21 TSR–like domains (D1–D21), with each domain most similar to either the TSP–1 like (THSB1) fold found in thrombospondin–1 (PDB ID 3r6b) or the C6–like fold found in complement component 6 (PDB ID 3t5o) and F–spondin (PDB ID 1szl). They also showed that the domains are separated by very short linker regions with and without a proline residue, indicating a quite limited flexibility between the adjacent domains. In total, THSD7A consisted of 11 TSR–like domains with the TSP–1 like (D1, 2, 5, 7, 9, 11, 13, 15, 17, 19 and 21) (Figure 4.5), with most of these domains alternating with 10 TSR–like domains with the C6–like fold (i.e. D3, 4, 6, 8, 10, 12, 14, 16, 18 and 20). The coiled–coil domain was between D3 and D4 TSR–like domains. The detailed information that we obtained on the structure of the extracellular domain of THSD7A allowed us to prepare additional mutants to obtain a full

set of soluble mutants. We thus designed the mutants D1–D2, D2–D3, D5–D6, D7–D8, D11–D12, D17–D18 and D19–D21 based on the domain delimitation available in this study by Seifert et al. (Seifert et al., 2018).

– Epitopes in THSD7A as identified by Seifert et al.

The identification of the epitope regions on THSD7A by Seifert and colleagues was done by western blot and native blot in a two–steps manner (Seifert et al., 2018). They first designed three large fragments spanning the full extracellular region of THSD7A and tested their reactivity with 31 THSD7A–associated MN patients. The first construct encoded for the N–terminal region from D1 to D4, thus comprising 2 TSP–1–like and 2 C6–like domains and the coiled–coil region. The second construct encoded for the region between D5 and D10 comprising 3 pairs of TSP–1–like and C6–like domains. The last construct encoded for the C–terminal extracellular region from D11 to D21, comprising 11 alternating TSP–1–like and C6–like domains. Patient's sera reacted with at least one of the three fragments, with D1–D4 being the most recognized, followed by D11–D21, and with 42% of patients recognizing all 3 fragments of THSD7A. In a second experiment, they designed 11 smaller THSD7A deletion mutants to narrow down the epitope regions. The fragments contained 2 or 3 adjacent TSP–1–like or C6–like domains. As a result, the patients' sera had different reactivities, but all together, they recognized with different prevalence up to 9 out of the 11 epitope regions while none of them could recognize D3–D4 and D19–D21 regions. The domain D1–D2 was the most prevalent domain, recognized by 87% of the patients followed by D15–D16, D9–D10 and D13–D14 recognized by 61, 52 and 45% of patients, respectively.

– Design and expression of THSD7A constructs

Designing and defining domain borders of soluble THSD7A mutants is a very delicate process to obtain correctly folded constructs. Omitting a single amino acid residue at either the N–terminal or C–terminal part of the construct can increase the risk of misfolding of the domain or even the loss of its conformation.

Figure 4.4 – Alignment of TSP–1 like and C6–like domains in THSD7A. The alignment of the TSP–1 like domains and the C6–like domains of THSD7A was done by FASTA sequence alignment on Multiple Sequence Comparison by Log–Expectation (MUSCLE). The specific but conserved residues that define the structure of either of the two different folds of thrombospondin repeats (TSR–like or TSP–1–like repeats) are indicated at the top of the sequence alignments. Note the low percentage of identity between the different domains in each group indicating the high sequence variability between the repeated domains forming THSD7A, hence the presence of distinct not cross–reactive epitopes in each domain.

This has been observed previously for PLA2R1 (Seitz-Polski et al., 2016) where we could successfully express several soluble forms while others failed to express the protein of interest (Kao et al., 2015), by messing up the disulfide bond pairing and loosing folding of the protein (Justino et al., unpublished data). We designed the different THSD7A constructs as follows: D1–D2 (from Ala–48 to Asp–194), D2–D3 (from Asp–116 to Glu–250), CC–D4 (from Tyr–253 to Thr–424), D5–D6 (from Ala–423 to Asp–575), D7–D8 (from Asp–575 to Val–696), D9–D10 (from Thr–695 to Gln–831), D11–D12 (from Ser–832 to Asp–959), D13–D14 (from Tyr–961 to Asn–1095), D15–D16 (from Gln–1096 to His–1221), D17–D18 (from His–1221 to Arg–1342), D19–D21 (from Arg–1342 to Thr–1606). The cysteine and the tryptophan residues aligned between TSP–1–like domains and C6–like domains (Figure 4.4). The constructs CC–D4, D9–D10, D13–D14 and D15–D16 were C–terminally tagged with 3xFlag while mutants D1–D2, D2–D3, D5–D6, D7–D8, D11–D12, D17–D18, D19–D21 were tagged with both HA and 6xHis tags (Figure 4.5).

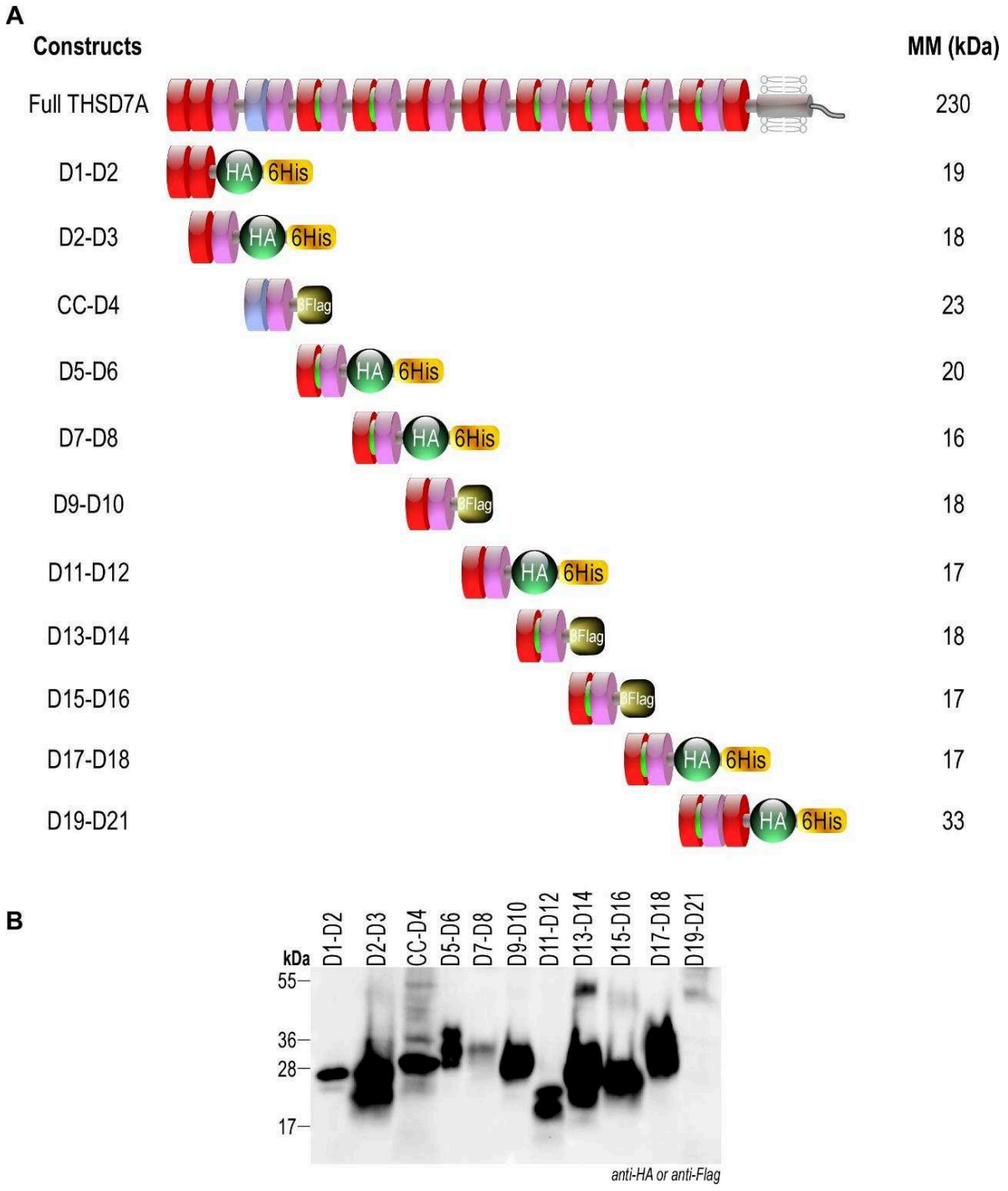

Figure 4.5 – Design and expression of soluble constructs of THSD7A. (A) Schematic diagram of wild–type THSD7A and the 11 soluble constructs of THSD7A with either HA and 6xHis tags or 3xFlag at the C–terminal end. Cylinders in red represent TSP–1–like (THBS1–like) domains whereas those in pink represent C6–like domains. The precise location of domain borders is found in Figure 4.4. (B) Validation of expression of THSD7A constructs in HEK293 cells on 10% SDS–PAGE under reducing conditions using anti–HA or anti–Flag antibodies.

We transfected all mutants in HEK293 cells, generated stable cell populations for each construct after antibiotic selection and collected large volumes of cell medium containing the soluble proteins after culture at 30°C to increase the production of folded proteins. We validated the expression of the constructs by western blot under reducing conditions using the anti–HA and anti–Flag antibodies (Figure 4.5).

– Identification of THSD7A epitope domains

Our previous experience with PLA2R1 epitopes has shown that it is important to test the reactivity of patients' autoantibodies by both ELISA and western blot, each technique having advantages and drawbacks, such as different reactivity, sensitivity and detection limits, titration, etc. Of note, one PLA2R1 epitope could be detected by ELISA but not by western blot (Justino et al., unpublished data).

We thus first screened the reactivity of a total of 38 THSD7A–associated MN patients with serum samples available at baseline against 11 different constructs of THSD7A by our homemade ELISA technique based on capture of the antigen using the tag antibody first coated on the ELISA plate. Eleven THSD7A constructs were captured by immobilized anti – HA or anti–Flag coated on ELISA wells. Serum from patients was added at a dilution of 1:100. Based on previous studies (Tomas et al., 2014) and the results we obtained recently with our full THSD7A ELISA (Chapter 4.1), we decided to detect patients' antibodies from the IgG4 subclass as it is the predominant IgG subclass in THSD7A–associated MN. Only the domain CC–D4 was not reactive with any patient. Among the 11 domains, 10 were reactive with at least one patient, and several were recognized by many patients. The D1–D2 was the most prevalent epitope domain with 74% (n=28) of positive patients followed by D9–D10 and D13–D14 with 58 (n=22) and 47% (n=18) of positive patients, respectively (Figure 4.6). We identified a unique patient with antibodies targeting the D19–D21 domain. Overall, 13% (n=5) of the patients showed single epitope positivity against either D1–D2, D9–D10 or D11–D12. The remaining patients showed multiple epitope positivity for 2, 3, 4, 5 and up to 6 epitopes in 24 (n=9), 30 (n=11), 18 (n=7), 5 (n=2) and 10% (n=4) of patients, respectively.

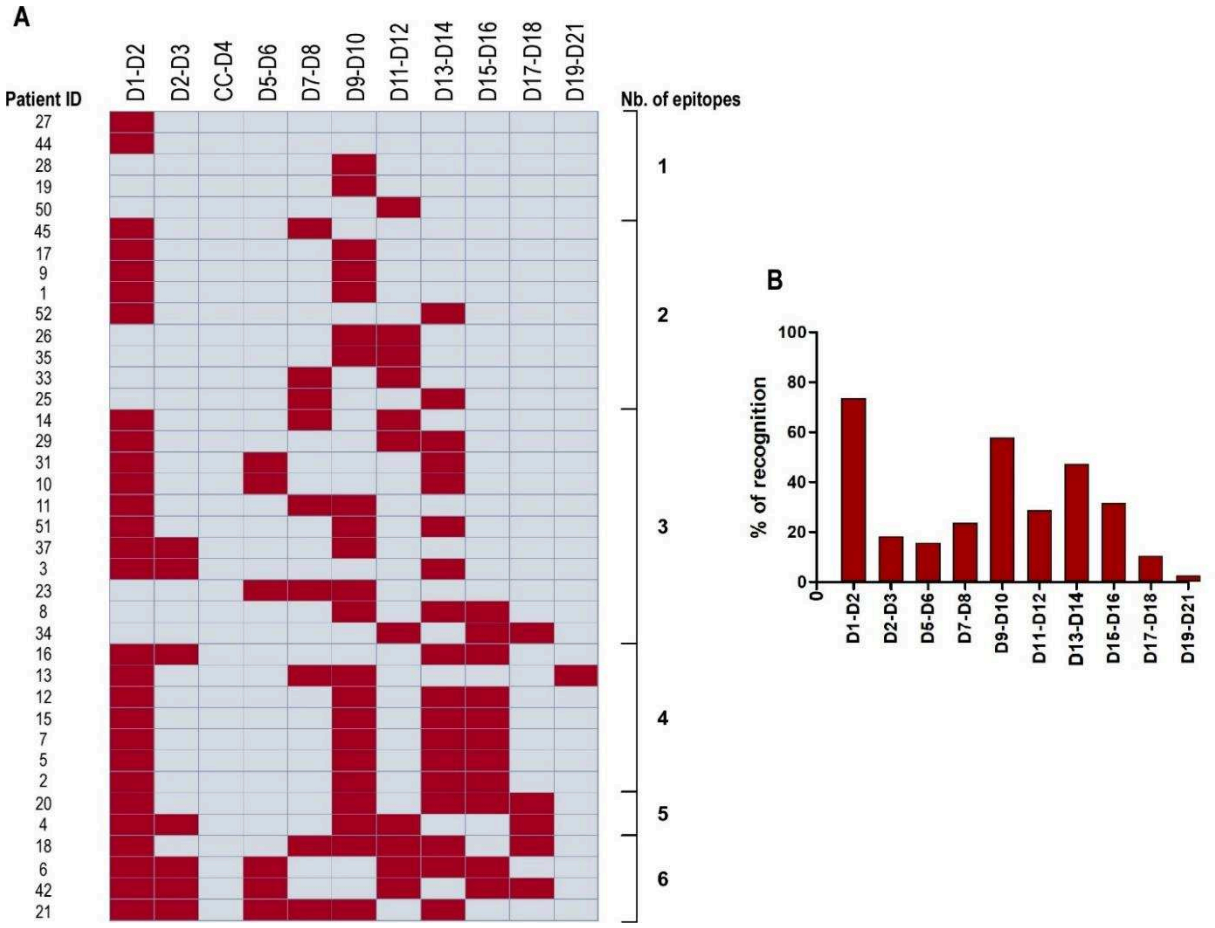

Figure 4.6 – Epitopes regions recognized by autoantibodies of THSD7A–associated MN patients. (A) Heat map illustrating the reactivity of the 38 patients with THSD7A–associated MN with the different THSD7A constructs. The reactivity for the distinct constructs was evaluated by ELISA with affinity–captured soluble constructs of THSD7A on immobilized anti–HA or anti–Flag antibodies. The yellow areas indicate positive reactivity to the domain while the blue areas indicate no reactivity. The patients' profiles are ordered first by epitope domain number from N–terminal to C–terminal of THSD7A and second by the number of epitopes recognized by each patient (patient ID). (B) Prevalence for reactivity of the 38 THSD7A–associated MN patients to THSD7A constructs represented in percentage of recognition. Most of the patients recognized either the epitope region D1–D2 (74%) or D9–D10 (58%) but none of them recognized the domain CC–D4 (not shown).

These results were in accordance with the recent findings by Seifert and colleagues obtained by western blot. They found that the N–terminal region of THSD7A containing D1–D2 contains the predominant epitope in THSD7A–associated MN. In their study, serum samples from 31 MN patients recognized mostly D1–D2 followed by D15–D16, D9–D10 and D13–D14 (Seifert et al., 2018).

– Association of epitope profiles with clinical characteristics

The 38 patients screened for THSD7A epitopes were a subset of our retrospective cohort of 49 patients plus new patients (n=3) for which both sufficient serum samples were available to identify epitopes and clinical data were collected for analysis of the clinical relevance of epitope profile versus anti–THSD7A titer.

We first compared the number of epitopes recognized by the patients' sera (n=38) with anti–THSD7A titers. The number of recognized THSD7A epitopes varied between 1 and 6 epitopes per patient. Anti–THSD7A titer increased as the number of epitope positivity increased until reaching a plateau between 4 and 6 epitopes (Figure 4.7–A). Patients with a single epitope profile (D1–D2 or D9–D10 or D11–D12) had a lower anti–THSD7A titer, as compared to the rest of the population, i.e. patients with more than one epitope. The patients with positivity against 2 or 3 epitopes seemed to have an intermediate anti–THSD7A titer while patients with 4, 5 and 6 epitopes had slightly higher antibody titers reaching a plateau. The titer of anti–THSD7A significantly correlated with the number of recognized epitopes on THSD7A (n=38, r=0.3991, p= 0.013) (not shown). Interestingly, we observed discrepancies for some patients between the epitope profile and the antibody titers. For instance, patients MN1 and MN17 recognized 2 epitope regions (D1–D2 and D9–D10) but had largely different anti–THSD7A titers of 13,920 RU/mL vs. 545 RU/mL respectively. On the hand, patients MN19 and MN20 had comparable anti–THSD7A titer (376 RU/mL and 302 RU/mL respectively) but had different epitope profiles (1 epitope vs. 5 epitopes).

We suggested in a previous study that for PLA2R1–associated MN mechanism of intramolecular epitope spreading could be associated with worsening of the disease (Seitz-Polski et al., 2016). In our cohort of THSD7A–associated MN, the analysis of epitope positivity did not reveal an obvious path suggesting a sequential and specific mechanism of

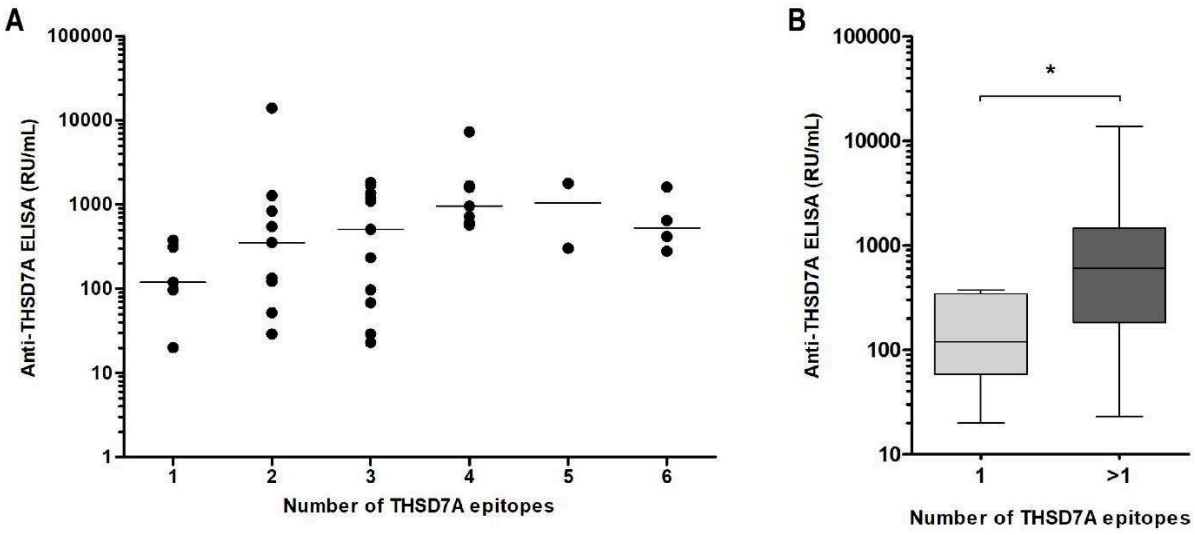

Figure 4.7 – Relationship between anti–THSD7A titer and positivity towards increasing number of epitopes. (A) Distribution of anti–THSD7A titer measured by the novel THSD7A ELISA and the corresponding number of epitopes on THSD7A for each patient (n=38). The correlation between anti–THSD7A titer and the epitope profile is significant (data not shown). (B) Comparison of the anti–THSD7A titer in patients with single versus multiple epitope positivity. Patients with antibodies targeting multiple epitopes have significantly higher anti–THSD7A titer compared to patients with single epitope profile (p= 0.04). The data for anti–THSD7A titers is represented as dot for each patient and medians for each subgroup.

	All	Single epitope positivity	Multiple epitope positivity	p Value
No. of patients n (%)	38	5	33	
Sex				0.374
Male (%)	22 (58.0)	4 (80.0)	18 (54.5)	
Female (%)	16 (42.0)	1 (20.0)	15 (45.5)	
Age at diagnosis (yr)	61.5 (49.0–75.0)	75.0 (58.5–76.0)	59.0 (48.0–72.0)	0.180
Proteinuria (g/day)	6.2 (3.1–11.2)	5.3 (2.5–11.0)	6.3 (3.5–11.4)	0.410
Serum albumin (g/L)	19.5 (15.0–24.5)	27.2 (23.1–29.7)	18.0 (15.0–23.4)	0.023
Serum creatinine (µmol/L)	89.0 (72.1–120.0)	103.0 (78.5–141.5)	89.0 (71.7–118.0)	0.527
eGFR (mL/min/1.73m^2)	74.5 (52.5–84.3)	61.0 (45.5–84.0)	76.0 (52.0–85.0)	0.752
Anti-THSD7A titer (RU/mL)	524.8 (121.3–1291.0)	119.0 (58.5–344.0)	605.6 (183.5–1470.0)	0.040

Table 4.1 – Epidemiological and clinical characteristics of patients stratified according to their epitope profile. Values are shown as n (%) or median (IQR). eGFR was calculated using the CKD–EPI formula.

epitope spreading from a single predominant epitope to other epitopes. In other words, a spreading reaction from 1 epitope to 2 or more epitopes seemed to occur rather randomly and did not follow a defined sequence of targeted epitopes. Based on these results, we combined the patients with multiple epitope positivity (i.e. 2 to 6) (n=33) as a single group and we compared them to patients with single epitope positivity (n=5). We observed a significant increase in anti–THSD7A titer between patients with single epitope positivity compared to multiple epitopes (p=0.04) (Figure 4.7–B). Overall, the clinical characteristics of the THSD7A–associated MN patients did not differ between the two groups (Table 4.1). There was no obvious gender effect on the distribution of epitopes in this cohort (p= 0.374). The patients were also comparable for median age at baseline, proteinuria and estimated glomerular filtration rate (p= 0.180; p= 0.410, p= 0.752, respectively).

4.2.3 From immunodominant epitopes to epitope spreading in THSD7A

Autoantibodies from our cohort of 38 THSD7A–associated MN patients recognize almost equally the D1–D2 and D9–D10 epitope regions, as indicated by the slight difference in prevalence for the two epitopes (74% vs. 58% for D1–D2 and D9–D10, respectively) (Figure 4.6). Additionally, we found that among the 5 patients with single epitope positivity, two targeted D1–D2 while two others targeted D9–D10, the last one targeting D11–D12. Based on the above findings, we raised the possibility that THSD7A–associated MN patients could have two immunodominant epitope regions, i.e. D1–D2 and D9–D10 while other domains would harbor "non–immunodominant" epitopes, possibly illustrating a mechanism of epitope spreading.

To test this hypothesis, we assessed the immunodominant binding properties of each epitope domain as defined by the strength of signal towards this epitope relative to full THSD7A antigen. This can be best evaluated by the percentage of inhibition on full THSD7A by ELISA competition assays with each epitope domain. We thus designed an assay consisting of pre–incubating the patients' serum sample with a saturating amount of each recombinant soluble epitope domain (Figure 4.5) then add the antigen–antibody pre–incubated immune complex to an ELISA plate coated with full THSD7A antigen. If the antibody targets an epitope domain responsible for most of the signal measured on full THSD7A antigen (i.e. the full titer) we should observe a high decrease of the ELISA signal.

In contrast, if the antibody targets an epitope representing only a small percentage of the total signal on the full antigen, we should observe little inhibition. Thus, evaluation of the remaining signal for each patient serum towards the full THSD7A antigen by competition with different epitope domain should identify which epitope domain is the most immunodominant, in addition to possibly being the most prevalent, as assessed by direct ELISA on the different domains (as determined above).

– Optimization of the competition assay with THSD7A epitopes

We first optimized the conditions of the competition assay for the signal on the full antigen and for the different competing domain constructs, including full THSD7A antigen as a positive control (medium from 0.1 μL to 100 μL) by performing dose–response experiments. Based on the titer determined by the full THSD7A ELISA, we diluted patients' serum to obtain an OD value in the linear range of the assay when testing serum against the full THSD7A. We then pre–incubated the serum with increasing amounts (i.e. volumes of cell medium) of each soluble THSD7A construct for 30 minutes prior to loading on the ELISA wells coated with the full antigen.

Figure 4.8 shows representative results for the patients MN5, MN1 recognizing the epitopes D1–D2 and D9–D10 respectively and for MN8 recognizing the epitopes D13–14 and D15–D16. As expected, the percentage of inhibition by full soluble THSD7A antigen (used as a positive control) was maximal and reached 100%. For D1–D2 and D9–D10, the inhibition was maximal with 3 μL of medium and reached 50% and 75%, respectively.

Increasing the volume of medium shows a plateau of inhibition for both epitopes, indicating that the serum antibody was already saturated with 30 μL of medium containing the epitope domain. The same was observed for other domains such as D13–D14 and D15–D16, with a maximal inhibition also reaching a plateau at 3 μL of medium, but here the maximal percentage of inhibition was limited to 25% and 13%, respectively. We could not detect a significant competition with the other domains D5–D6, D7–D8, D11–D12, D17–D18 or D19–D21 with the few patients that we tested (data not shown). These results indicate that for the above patient MN5, MN1 and MN8, the autoantibodies targeting D1–D2 and D9–D10 are responsible for most of the signal measured by ELISA on full THSD7A (i.e. mostly responsible for the measured titer) while antibodies targeting the other domains

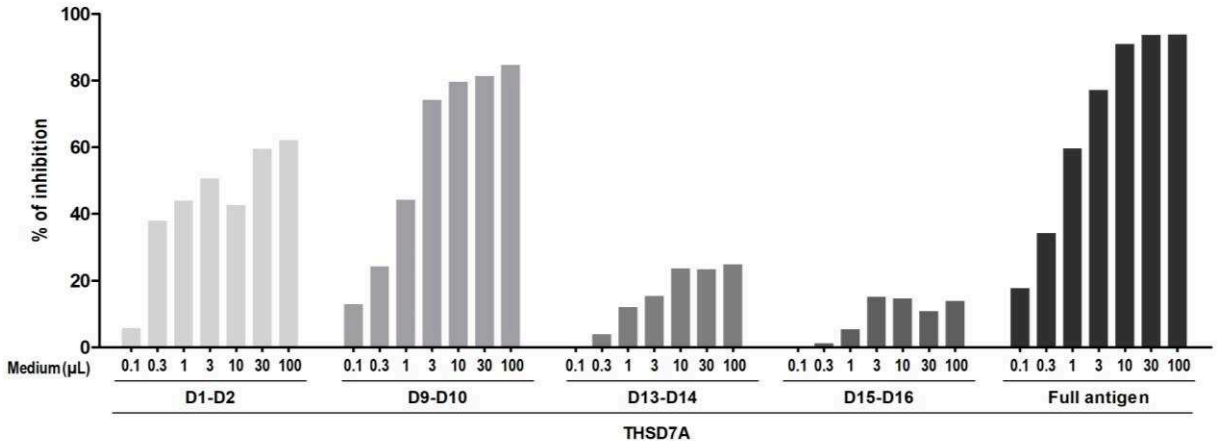

Figure 4.8 – Optimization of the competition assay for THSD7A. Bar graph displaying the percentage of inhibition of full THSD7A by the full antigen or each THSD7A constructs. The competition assay is performed by preincubation of serum from MN1, MN5 patients with increasing amounts of D1–D3, D9–D10 respectively and MN8 patient with increasing amounts of D13–D14 and D15–D16 for 30 minutes followed by incubation on the ELISA well coated with full THSD7A. The competition with full THSD7A served as a positive control. The percentage of inhibition reached a plateau with volume of medium higher than 3 μL for each epitope domain. The data are expressed as percentage of inhibition calculated based on the specific OD values.

D11–D12, D13–D14 and D15–D16 are responsible for a minor fraction of the signal. Based on these experiments, we decided to use 100 μL of medium containing each recombinant THSD7A epitope domains in competition experiments to investigate the immunodominant binding properties of the different THSD7A epitope domains. We then tested 13 THSD7A–associated MN patients by competition with the full antigen and the different THSD7A constructs. As expected, the full THSD7A antigen inhibited almost 100% of the signal for all patients. Furthermore, for 8 patients, competition with the construct D1–D2 resulted in up to 80% inhibition while competition with D9–D10 was much weaker, and it was the opposite case for another set of 6 patients. Finally, D13–D14 was a strong competitor for one patient, with a maximal inhibition of 60% while D1–D2 and D9–D10 were weaker competitors (Figure 4.9). A weaker percentage of inhibition was observed with all other epitopes (percentage of inhibition below 30%). In summary, we observed that D1–D2 and/or D9–D10 inhibit most of the signal of the anti–THSD7A antibodies when assayed against the full antigen, suggesting that these two domains are the most immunodominant ones. This result was in accordance with the fact that D1–D2 and D9–D10 are the most prevalent domains, as measured by direct ELISA with each different epitope domains (Figure 4.6).

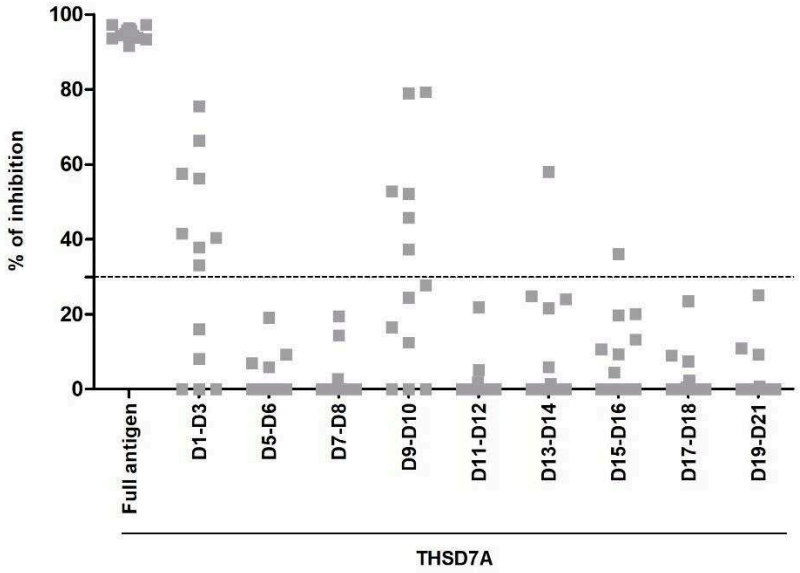

Figure 4.9 – Immunodominant epitope competition assays with THSD7A epitope domains by ELISA using full THSD7A for 13 THSD7A–positive patients. The graph shows the percentage of inhibition with the full THSD7A antigen or the 9 THSD7A soluble constructs by competition ELISA on full THSD7A antigen for 13 THSD7A–associated MN patients. The data are expressed as percentage of inhibition calculated from the specific OD values. The dotted line represents an arbitrary cut–off value of 30%, above which the percentage of inhibition by the competing epitopes may be considered as "immunodominant". These assays thus identify the immunodominant domains, i.e. those inhibiting most of the ELISA signal on full THSD7A. For these patients, the major immunodominant epitopes are either within D1–D3 (for 8 patients), D9–D10 (for 6 patients) or D13–D14 (for one patient).

To confirm our results of competition by ELISA, we performed competition assays by western blot for the patient MN1 (Figure 4.10). This patient had the highest anti–THSD7A antibody titer (13,920 RU/mL) and its epitope profile was D1–D2 and D9–D10 as determined by direct ELISA (Figure 4.6). For competition by western blot, we preincubated the serum sample with medium containing an excess of full THSD7A antigen or the D1–D2 or D9–D10 constructs. Western blot results showed that most of the signal on full THSD7A is blocked by preincubation with D9–D10. On the other hand, antibodies targeting D1–D2 slightly inhibit the signal against the full antigen. In summary, these results demonstrate that although patient MN1 has antibodies targeting both D1–D2 and D9–D10, the signal on the full antigen is mostly coming from reactivity of antibodies against the D9–D10 epitope domain, suggesting that it is the immunodominant epitope region for this patient.

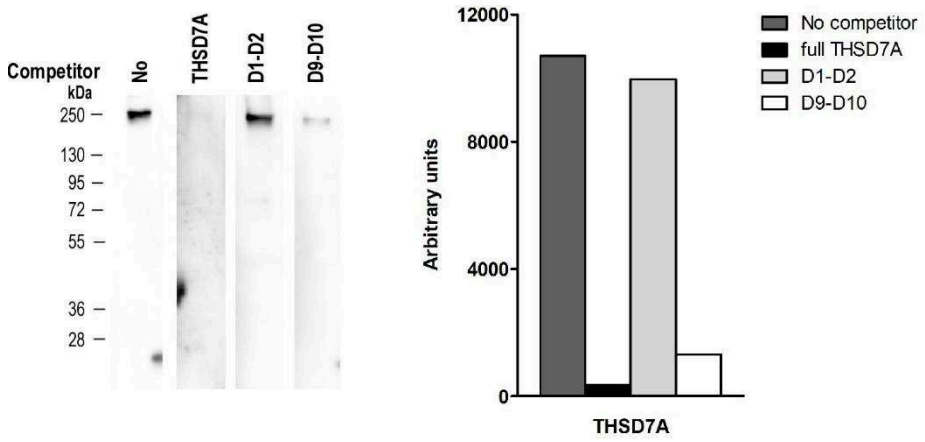

Figure 4.10 – Competition assay between THSD7A full antigen and the THSD7A constructs D1–D2 and D9–D10 for patient MN1. The western blot reactivity of MN1 was tested at optimal serum dilution against 1 μg of purified recombinant THSD7A. The serum samples were preincubated with control medium without competitor or medium containing an excess of full THSD7A or D1–D2 or D9–D10 domains. The four blots were run in parallel and revealed for the same exposure time. The bar graph in the right panel represents the quantification of THSD7A signal detected by western blot.

– Cross–reactivity between D1–D2 and D9–D10 THSD7A constructs

Despite the apparently low amino acid sequence identity between the D1–D2 and the D9–D10 domains suggesting no cross–reactivity, we wanted to verify that the competition by either D1–D2 or D9–D10 is domain–specific and that a single class of anti–THSD7A autoantibody does not recognize the same epitope in the two different domains. We thus tested the cross–reactivity between the two domains by competition ELISA (Figure 4.11).

We selected two patients (MN1 and MN3) having immunodominant autoantibodies targeting almost exclusively either D1–D2 or D9–D10. We preincubated the serum with different amounts of D1–D2 or D9–D10 in a dose response manner (volume of cell medium ranging from 0.001 μL to 100 μL). The incubation was then loaded on ELISA wells coated with either D1–D2 or D9–D10. For the patient MN3 with autoantibodies mainly targeting D1–D2, preincubation of the serum sample with an increasing volume of medium containing D1–D2 led to a percentage of inhibition reaching 100% (Figure 4.11–A). Conversely, competition with increasing amounts of D9–D10 did not show any inhibition. Results in mirror were found for the patient MN1. Preincubation with an increasing volume of medium containing D9–D10 led to a percentage of inhibition reaching 100% while

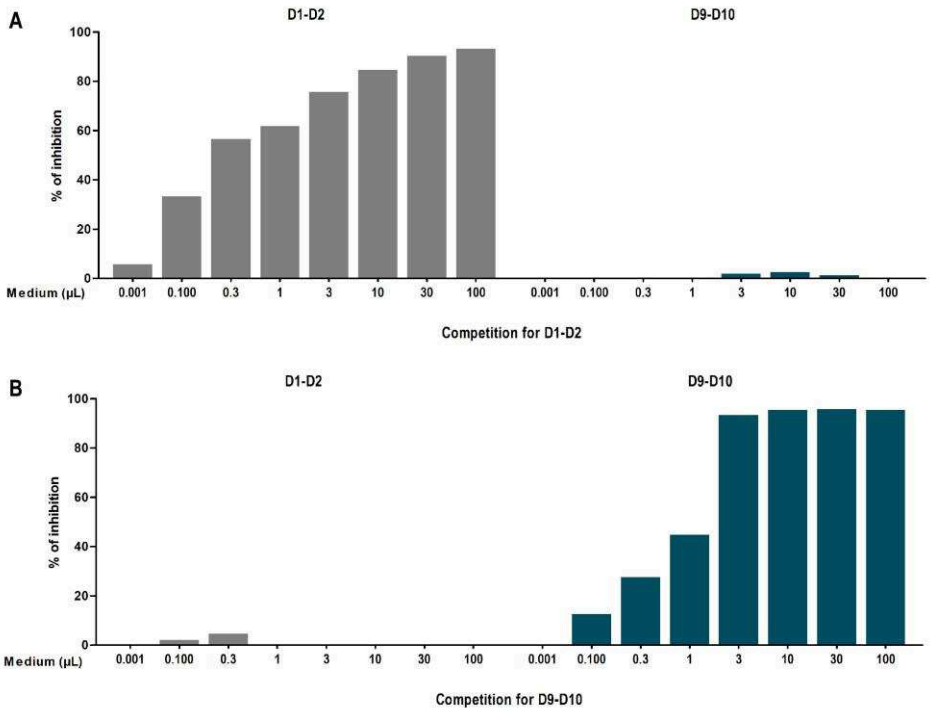

Figure 4.11 – Absence of cross–reactivity between D1–D2 and D9–D10. (A–B) Bar graphs showing the percentage of inhibition by each D1–D2 or D9–D10 on both domains. The competition assay was performed by preincubation of THSD7A–associated MN patients' sera containing autoantibodies mostly targeting either D1–D2 (Panel A) or D9–D10 (Panel B) (as measured by competition on full THSD7A antigen, see above) with increasing volumes of medium containing D1–D2 or D9–D10 domains for 30 minutes followed by incubation on the ELISA well coated with either D1–D2 or D9–D10. The domains D1–D2 and D9–D10 bound exclusively to anti–D1–D2 and anti–D9–D10, indicating no cross–reactivity between the two domains.

competition with D1–D2 did not show any inhibition (Figure 4.11–B). These results were in accordance with the low percentage of protein identity between these THSD7A domains (Figure 4.4). Collectively, our results show that serum autoantibodies of patients with THSD7A–associated MN are polyclonal, target different epitope regions of THSD7A but can be immunodominant or not, with the full titer measured by ELISA being due to only some of these autoantibodies, the most prevalent and immunodominant ones.

– Identification of immunodominant epitope groups

Due to the limited volume of serum available versus the large volume of serum required to investigate the immunodominance in THSD7A–associated MN, it was reasonable to limit

the competition assays with only the domains shown to contain epitopes based on the epitope profile determined above for each serum by direct ELISA on the above 11 epitope domains (Figure 4.6).

We set a threshold value of 50% inhibition above which the domain is considered as an immunodominant epitope. We screened 35 patients among the 49 patients with THSD7A–associated MN previously described in the chapter 4.1. The competition assay led to the stratification of patients into four groups with different immunodominant epitope profiles based on the percentage of inhibition with the different domains (Figure 4.12). For twelve patients (34%), the percentage of inhibition was above 50% after competition with D1–D2 but not with other domains, including D9–D10 (Figure 4.12–A). For another group of fourteen patients (40%), the total signal against the full THSD7A was considerably inhibited by preincubation with D9–D10, but not by D1–D2 (Figure 4.12–B). In a third group of 3 patients (9%), the signal for the full antigen was equally inhibited by competition with either D1–D2 or D9–D10 (Figure 4.12–C). Finally, the last group consisted of 6 patients (17%) for which no strong inhibition was observed with the so–called immunodominant epitopes, i.e. D1–D2 or D9–D10, with inhibition by these domains below 30%, while more inhibition was observed with another domain, i.e. D11–D12 for 3 patients, D13–D14 for 2 patients and D7–D8 for the last patient (Figure 4.12–D). We thus considered this group as the "non–immunodominant" group.

Overall, we concluded that our THSD7A–associated MN population are distributed into four groups based on their epitope immunodominance or absence of immunodominance, yet the patients were positive for the so–called immunodominant epitopes.

– Clinical relevance of immunodominant epitope groups

Next, we analyzed the association between the immunodominant epitope profile and the clinical parameters. The clinical characteristics of patients with a D1–D2 immunodominance did not differ from those with a D9–D10 or D1–D2/D9–D10 immunodominance (Table 4.2). The three groups were comparable for age, kidney function and anti–THSD7A titer.

Based on these results, we combined patients from the three immunodominant epitope groups as a single larger group (n=29) and we compared this latter with the group of patients qualified as "non–immunodominant" (n=6) (Table 4.3). The median age between the patients in the immunodominant epitope group was 67 years compared to 49 years in the non–immunodominant epitope group yet this did not reach statistical significance (p=0.273). Among patients in the immunodominant epitope group (n=29), 69% were males (n=20) and 31% females (n=9). In the non–immunodominant epitope group, 17% were males (n=1) compared to 83% females (n=5).

There was thus an apparently significant switch in gender distribution between the immunodominant and the non–immunodominant epitope group (p=0.028). Proteinuria in patients with "non–immunodominance" (3 g/day) tended to be lower than that in the immunodominant group (7 g/day) (p=0.087). Patients in the non–immunodominant group also had significantly higher estimated glomerular filtration rate (p=0.040). Of note, anti–THSD7A titer was significantly lower in the non–immunodominant group than in the immunodominant group (p=0.046) suggesting that the difference in the previous clinical characteristics might be linked to the antibody titer.

	All	D1–D2	D9–D10	D1–D2 and D9–10	p Value
No. of patients n (%)	35	12 (34)	14 (40)	3 (9)	
Sex					0.137
Male (%)	21 (60.0)	6 (28.5)	11 (52.5)	3 (14.3)	
Female (%)	14 (40.0)	6 (42.8)	3 (21.4)	0 (0)	
Age at diagnosis (yr)	62.2 (49.0–75.0)	74.0 (54.0–79.3)	60.5 (44.5–69.8)	67.0 (49.0–71.0)	0.306
Proteinuria (g/day)	6.3 (3.6–11.0)	9.1 (4.3–12.0)	6.0 (5.3–12.4)	10.6 (9.0–14.6)	0.450
Serum albumin (g/L)	19.5 (15.3–25.5)	19.0 (15.0–22.6)	19.0 (16.0–27.2)	13.6 (13.6 –13.6)	0.332
Serum creatinine (µmol/L)	89.0 (71.0–116.0)	80.0 (71.0–110.0)	103.0 (88.0–122.8)	116.0 (108.0–212.0)	0.075
eGFR (mL/min/1.73m2)	77.0 (56.0–85.0)	80.0 (51.0–86.0)	73.0 (53.0–77.0)	56.0 (31.0–59.0)	0.188
Anti-THSD7A titer (RU/mL)	544.5(119.0–1354.0)	479.5 (158.8–1501.0)	629.7 (205.3–1412.0)	1091.5 (566–1776)	0.524
No. of epitopes	3.0 (2.0–4.0)	3.0 (2.0–4.0)	2.5 (2.0–4.0)	4.0 (3.0–5.0)	0.316
Disease outcome					0.188
Active disease	10	1	5	2	
Remission	19	7	7	1	

Table 4.2 – Clinical characteristics of THSD7A–associated patients from different immunodominant epitope groups.

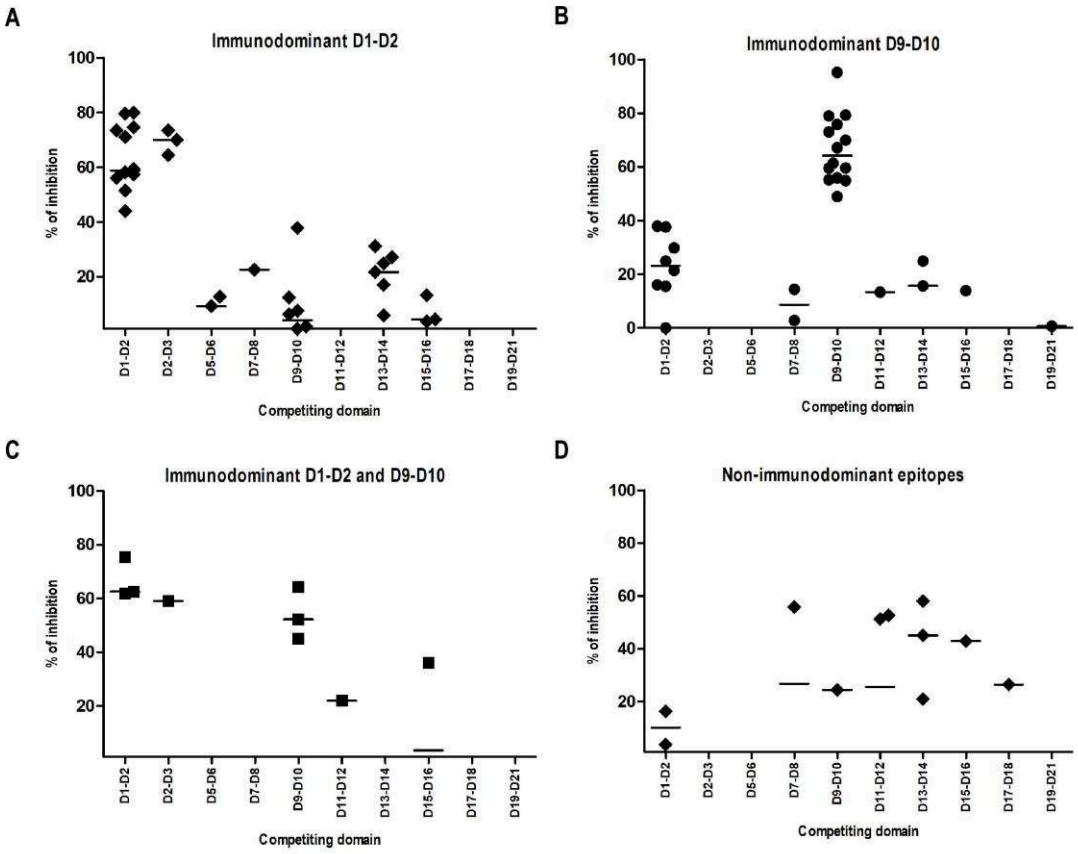

Figure 4.12 – Distribution of epitope immunodominance in THSD7A–associated MN patients. (A–D) Graphs showing the percentage of inhibition by the different THSD7A epitope domains in competition assays with the full antigen for the 35 patients. Patients were stratified into 4 groups (panels A to D) based on the most immunodominant epitope domain or a "non–immunodominant" profile. The data are expressed as percentage of inhibition calculated from the specific OD values.

	All	Immunodominant epitopes	Non-immunodominant epitopes	p Value
No. of patients n (%)	35	29(83)	6 (17)	
Sex				0.028
Male (%)	21 (60.0)	20 (69)	1 (16.7)	
Female (%)	14 (40.0)	9 (31)	5 (83.3)	
Age at diagnosis (yr)	62.2 (49.0–75.0)	67.0 (50.0–75.0)	49.0 (43.5–71.0)	0.273
Proteinuria (g/day)	6.3 (3.6–11.0)	7.0 (5.4–12.0)	3.0 (1.9–6.5)	0.087
Serum albumin (g/L)	19.5 (15.3–25.5)	19.0 (15.0–22.8)	28.0 (17.0–37.5)	0.099
Serum creatinine (µmol/L)	89.0 (71.0–116.0)	89.0 (77.0–120.0)	70.7 (68.5–85.9)	0.038
eGFR (mL/min/1.73m2)	77.0 (56.0–85.0)	73.0 (53.0–82.5.0)	84.5 (77.5–88.8)	0.040
Anti-THSD7A titer (RU/mL)	544.5(119.0–1354.0)	605.6(255.5–1470.0)	74.5 (26.7–1914.0)	0.046
No. of epitopes	3.0 (2.0–4.0)	3.0(2.0–4.0)	2.5 (1.8–3.3)	0.432
Disease outcome				
Active disease	10	8	2	>0.999
Remission	19	15	4	

Table 4.3 – Comparison of the clinical characteristics of THSD7A–associated MN patients from the combined immunodominant group (D1–D2 or D9–D10 or both) and the "non–immunodominant" epitope group.

– Clinical characteristics of low titer THSD7A–associated MN patient

We compared the distribution of anti–THSD7A titers among the immunodominant and non–immunodominant groups. We observed that only patients from the immunodominant epitope groups (i.e. D1–D2, D9–D10 and D1–D2/D9–D10) can have high anti–THSD7A titer while all but one patient from the "non–immunodominant" group have low antibody titer (Figure 4.13).

In our previous study (Chapter 4.1 and article 1), we demonstrated that patients with anti–THSD7A titer below 134 RU/mL showed better clinical outcome. Therefore, we set this threshold value here and we compared the clinical characteristics of patients with antibody titer below 134 RU/mL from the immunodominant group versus the non–immunodominant group. Patients with an antibody titer below 134 RU/mL in the immunodominant and non–immunodominant groups had comparable levels of proteinuria (5.8 g/day vs 3.0 g/day) and serum albumin (21.3 g/L vs 28.0 g/L) while eGFR levels were significantly different between the 2 groups (45.5 mL/min/1.73m^2 vs 84.0 mL/min/1.73m^2, respectively) (Table 4.4).

Based on these data, we speculated that patients belonging to the non–immunodominant epitope group are less likely to develop high anti–THSD7A titers during follow–up as compared to patients from the immunodominant groups. This is supported by the absence of high antibody titer in patients from the non–immunodominant group (with the exception MN2) in comparison with patients in the immunodominant groups (Figure 4.13). Finally, and may be of clinical relevance, this suggests that the only way to have patients with high titers is to promote the autoimmune response on the autoantibodies targeting the immunodominant epitopes, i.e. either D1–D2 or D9–D10 or both. This would suggest a mechanism of epitope spreading where D1–D2 and D9–D10 are the immunodominant epitopes that drives the autoimmune response and the full titer, while the other epitopes are non–immunodominant epitopes, but with their positivity being an indicator of epitope spreading per se for most patients as well as an indirect indicator of epitope spreading within the immunodominant epitopes. These results will be the material for a manuscript in preparation.

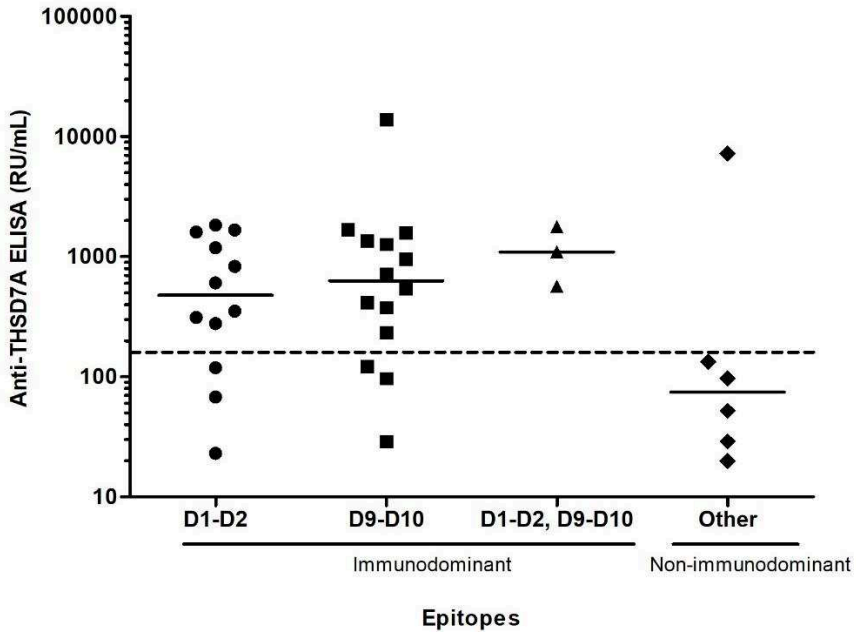

Figure 4.13 – Distribution of anti–THSD7A titer according to the type of immunodominance or not. The graph represents the relationship between the anti–THSD7A titer of patients in comparison with the various immunodominance groups. The data are shown as titer in RU/mL with median values. The dotted line represents the cut–off value (134 RU/mL) defined in the previous study as the threshold for a differential clinical outcome.

	All	Immunodominant low titer	Non-immunodominant	p Value
No. of patients n (%)	35	6	6	
Sex				0.080
Male (%)	21 (60.0)	5 (83)	1(17)	
Female (%)	14 (40.0)	1 (17)	5 (83)	
Age at diagnosis (yr)	62.2 (49.0–75.0)	75 (73.0–82.3)	49.0 (43.5–71.0)	0.064
Proteinuria (g/day)	6.3 (3.6–11.0)	5.8 (4.2–12.6)	3.0 (1.9–6.5)	0.393
Serum albumin (g/L)	19.5 (15.3–25.5)	21.3 (18.0–25.8)	28.0 (17.0–37.5)	0.272
Serum creatinine (µmol/L)	89.0 (71.0–116.0)	121.4 (108.3–164.6)	70.7 (68.5–85.9)	0.002
eGFR (mL/min/1.73m2)	77.0 (56.0–85.0)	45.5 (34.7–55.0)	84.5 (77.5–88.8)	0.002
Anti-THSD7A titer (RU/mL)	544.5(119.0–1354.0)	82.7 (27.5–119.8)	74.4 (26.7–1914.0)	0.936
No. of epitopes	3.0 (2.0–4.0)	2.0 (1.0–3.0)	2.5 (1.8–3.3)	0.451
Disease outcome				>0.999
Active disease	10	1	2	
Remission	19	3	4	

Table 4.4 – Comparison of the clinical characteristics of patients with low antibody titer in the immunodominant and non–immunodominant epitope groups.

4.3 Epitope profiling of PLA2R1 at baseline predicts outcome of MN (Article 2)

Anti–PLA2R1 antibodies are important biomarkers of MN. Standardized assays are now commercially–available for measurement and quantification of anti–PLA2R1 titers. Although the pathogenic role of anti–PLA2R1 antibodies is not yet proven, many groups have shown that antibody titer correlates with disease activity and response to treatment(Beck et al., 2011; Hofstra et al., 2011; Hofstra et al., 2012). At baseline, low antibody titer predicted spontaneous remission while high antibody titers predicted poor prognosis (Bech et al., 2014 ; Hoxha et al., 2014). In 2016, our laboratory suggested that analysis of the targeted epitopes in PLA2R1 is an important tool for monitoring of disease activity and for prognosis of MN (Seitz-Polski et al., 2016). Using a retrospective cohort of 69 patients with PLA2R1–associated MN, three epitopes were identified in the CysR, CTLD1 and CTLD7 domains of PLA2R1 and patients were stratified based on their epitope profile: CR, CRC1 and CRC1C7. Patients with single reactivity against the CysR domain were younger, had lower proteinuria and reached spontaneous remission more often. Epitope spreading beyond CysR indicated poor renal prognosis. During follow–up, epitope spreading was associated with progression and worsening of the disease while reverse spreading towards CysR suggested favorable outcome. These results were obtained in a retrospective cohort with patients differing in baseline disease activity, follow–up period and various treatments. We aimed to confirm these findings by analyzing epitope profiling of patients from GEMRITUX, a well–characterized prospective cohort established by the group of Pr. Pierre Ronco and colleagues at the Hôpital Tenon in Paris. The results of this study are now published in the *Journal of American Society of Nephrology* where I am the fifth author.

The GEMRITUX is the first randomized clinical trial (Clinicaltrial.gov identifier: NCT01508468) for the evaluation of Rituximab treatment in "all cases" of idiopathic MN, i.e. with patients either positive or negative for anti–PLA2R1 or anti–THSD7A (Dahan et al., 2017). The cohort comprises 75 patients divided in two treatment groups: the first group comprised 38 patients receiving antiproteinuric treatment (NIAT) while the second group comprises 37 patients treated with Rituximab in addition to antiproteinuric agents (RITUX). For our specific study with the aim to analyze the impact of PLA2R1 epitope

spreading on efficacy of Rituximab treatment, we included only the subset of patients with PLA2R1–associated MN, which represents 58 out of the 75 patients (77%). For these 58 patients, 29 patients were from the NIAT group and 29 patients were from the RITUX group. Serial samples of serum were available at baseline and during follow–up for at least 18 months (primary endpoint), as detected by IIFT and/or ELISA.

Full anti–PLA2R1 titer was measured with the commercial ELISA from Euroimmun AG (Lübeck, Germany) according to the protocol previously described (Dähnrich et al., 2013). We assessed the reactivity of patients for the different PLA2R1 epitopes with our homemade ELISA assays for CysR, CTLD1 and CTLD7 epitopes. The three epitope domains were expressed in HEK293 as secreted soluble forms with an HA tag at the C–terminal end. The full ELISA conditions were previously described (Seitz-Polski et al., 2016).

First, we evaluated the epitope profiling of patients at baseline. Among the 58 patients, 65% (n=38) had epitope spreading defined by additional reactivity against CTLD1 or CTLD7 or both (qualified as "spreaders") (Table 1 of article 2). Contrary to what was observed previously (Seitz-Polski et al., 2016), we did not find an association between the epitope profiling and age or proteinuria at the time of assay. On the other hand, we found that the anti–PLA2R1 titer significantly correlates with epitope spreading beyond CysR. However, some patients can have anti–PLA2R1 titer in the low tertile range and can be spreaders or non–spreaders, and vice–versa, i.e. mid–range and high titer patients can be non–spreaders, yet all patients are "spreaders" when the antibody titer is higher than 369.5 RU/mL. Collectively, these observations indicate a "global" correlation between epitope profile and the likelihood of spreading with full anti–PLA2R1 titer, but that discrepancies between can be observed among patients within the same range of antibody titer.

Secondly, we evaluated the effect of Rituximab treatment on the epitope profiling of PLA2R1 during follow–up. At baseline, 62.1% (n=18) and 68.9% (n=20) of patients in the NIAT and the RITUX group had epitope spreading, respectively. At months 3 and 6, we observed a significant decrease in the number of epitope reactivity indicating that Rituximab induced reversal of epitope spreading and a decrease in the anti–PLA2R1 titers. (Figure 2 of article 2) For instance, reverse spreading occurred in 58.8% of patients in the RITUX group in contrast to 25% in the NIAT group at month 6.

Finally, we investigated whether epitope spreading could be a stronger indicator of remission than full anti–PLA2R1 titer. The combined analysis of the two populations of patients, NIAT and RITUX, indicated that weaker reactivity against CTLD7 and lower rate of epitope spreading at baseline increased the likelihood of early remission and response to treatment. Lower anti–PLA2R1 titers correlated with higher remission rate only at month 6 but not at month 3. Additionally, patients with a CysR profile at baseline showed 60% of remission at month 6. These results were further confirmed on a median follow–up period of 23 months (Figure 1 of article 2).

In summary, epitope spreading at baseline is a powerful prognostic tool and is associated with a lower remission rate at 6 and 23 months of follow–up. Based on the results obtained in this study, we suggest that both epitope profiling and full anti–PLA2R1 titer should be monitored at diagnosis. Patients with low anti–PLA2R1 titer but a "spreader" profile should be treated with Rituximab early after diagnosis to avoid worsening of the disease before treatment. In contrast, patients with high anti–PLA2R1 titer but no evidence for spreading may be monitored and leave untreated until evidence for spreading would occur. Patients with very high titers should be all spreaders and be treated immediately.

Article 2

BRIEF COMMUNICATION www.jasn.org

Phospholipase A2 Receptor 1 Epitope Spreading at Baseline Predicts Reduced Likelihood of Remission of Membranous Nephropathy

Barbara Seitz-Polski,*†‡ Hanna Debiec,§‖ Alexandra Rousseau,¶ Karine Dahan,** Christelle Zaghrini,* Christine Payré,* Vincent L.M. Esnault,‡ Gérard Lambeau,* and Pierre Ronco§‖**

*Institut de Pharmacologie Moléculaire et Cellulaire, Centre National de la Recherche Scientifique, Université Côte d'Azur, Sophia Antipolis, Valbonne, France; †Laboratoire d'Immunologie and ‡Service de Néphrologie, Centre Hospitalier Universitaire de Nice, Université Côte d'Azur, Nice, France; §Université Pierre et Marie Curie, Sorbonne Universités, Paris, France; ‖Unité Mixte de Recherche 1155, Institut National de la Santé et de la Recherche Médicale, Paris, France; ¶Unité de Recherche Clinique de l'Est Parisien, hôpital Saint-Antoine, Assistance Publique Hôpitaux de Paris, Paris, France; and **Department of Nephrology and Dialysis, hôpital Tenon, Assistance Publique Hôpitaux de Paris, Paris, France

ABSTRACT

The phospholipase A2 receptor (PLA2R1) is the major autoantigen in primary membranous nephropathy. Several PLA2R1 epitopes have been characterized, and a retrospective study identified PLA2R1 epitope spreading as a potential indicator of poor prognosis. Here, we analyzed the predictive value of anti-PLA2R1 antibody (PLA2R1-Ab) titers and epitope spreading in a prospective cohort of 58 patients positive for PLA2R1-Ab randomly allocated to rituximab (n=29) or antiproteinuric therapy alone (n=29). At baseline, the epitope profile (CysR, CysRC1, CysRC7, or CysRC1C7) did not correlate with age, sex, time from diagnosis, proteinuria, or serum albumin, but epitope spreading strongly correlated with PLA2R1-Ab titer ($P<0.001$). Ten (58.8%) of the 17 patients who had epitope spreading at baseline and were treated with rituximab showed reversal of epitope spreading at month 6. In adjusted analysis, epitope spreading at baseline was associated with a decreased remission rate at month 6 (odds ratio, 0.16; 95% confidence interval, 0.04 to 0.72; P=0.02) and last follow-up (median, 23 months; odds ratio, 0.14; 95% confidence interval, 0.03 to 0.64; P=0.01), independently from age, sex, baseline PLA2R1-Ab level, and treatment group. We propose that epitope spreading at baseline be considered in the decision for early therapeutic intervention in patients with primary membranous nephropathy.

J Am Soc Nephrol 29: ●●●–●●●, 2017. doi: https://doi.org/10.1681/ASN.2017070734

Primary membranous nephropathy is an autoimmune disease against a podocyte antigen. Antibodies to the phospholipase A2 receptor 1 (PLA2R1-Ab) and thrombospondin type 1 domain containing 7A (THSD7A) are associated with 70%–80% and about 2%–3% of cases, respectively.[1,2] Although the pathogenic role of anti-THSD7A has been established,[3] that of PLA2R1-Ab is not yet proven. However, it is strongly suggested by the observation that PLA2R1-Ab titers usually rise during clinically active phases and decrease before normalization of proteinuria.[4] Spontaneous remission occurs in up to 50% of patients, and ESRD occurs in about 30%.[5] High titers of PLA2R1-Ab at presentation and their persistence predict poor clinical outcome.[6,7] Therefore, reducing PLA2R1-Ab level has become an important goal of therapy. Although the identification of PLA2R1-Ab has been paradigm shifting in the diagnosis and management of patients, there are cases that call for additional biomarkers. Indeed, antibodies may persist during apparent clinical remission, and conversely, a drop in antibody titer may not be associated with a clinical remission.[7,8]

PLA2R1 is a 180-kDa membrane receptor with a large extracellular region

Received July 6, 2017. Accepted September 20, 2017.

B.S.-P., H.D., and A.R. contributed equally to this work.

G.L. and P.R. contributed equally to this work.

Published online ahead of print. Publication date available at www.jasn.org.

Correspondence: Prof. Pierre Ronco, Institut National de la Santé et de la Recherche Médicale Unit 1155, Hôpital Tenon, 4 rue de la Chine, F–75020 Paris, France, or Dr. Gérard Lambeau, Institut de Pharmacologie Moléculaire et Cellulaire, Unité Mixte de Recherche 7275, Centre National de la Recherche Scientifique et Université Côte d'Azur, Sophia-Antipolis, Valbonne, France. E-mail: pierre.ronco@upmc.fr or lambeau@ipmc.cnrs.fr

comprising ten distinct globular domains, including a cysteine-rich domain (CysR), a fibronectin type II domain, and eight distinct C-type lectin domains (CTLD1–8).[9] Each domain is separated by a small linker sequence of less than ten amino acids. An immunodominant epitope was first identified in a region spanning the Cystein rich domain (CysR)-fibronectin type II-C-type lectin domain 1 (CTLD1) domains,[10] which was further restricted to the CysR domain alone.[11] In a previous study,[12] we became interested in epitope spreading, which is a common process of immune response to infectious agents and self-antigens. It usually first involves the so-called immunodominant epitope recognized by most antibodies (CysR for PLA2R1), then extends to noncross-reactive epitopes on the same protein (intramolecular epitope spreading, CTLD1 and/or CTLD7 for PLA2R1) or to dominant epitopes on neighboring molecules (intermolecular epitope spreading). The result is an increase in the antibody repertoire diversity, responsible for an enhanced overall immune response. Epitope spreading is a primary immunopathogenic event in autoimmune diseases.[13–17] In this previous study, we identified reactive epitopes in the CysR, CTLD1, and CTLD7 domains, and we further showed that patients with anti-CysR–restricted activity were younger, had lower proteinuria, and exhibited a higher rate of spontaneous remission and a lower rate of renal failure progression.[12] Conversely, high PLA2R1-Ab activity and epitope spreading beyond the CysR epitope were independent risk factors for poor renal prognosis in a collection of 69 sera from five French nephrology centers. Because these patients were analyzed retrospectively, they differed by the severity of the nephrotic syndrome, duration of follow-up, management of antiproteinuric therapy, and indications for immunosuppressive treatment.

The first aim of this study was to test the reactivity of PLA2R1-Ab against the three previously characterized PLA2R1 epitope domains (CysR, CTLD1, and CTLD7) in a well defined prospective cohort (Evaluate Rituximab Treatment for Idiopathic Membranous Nephropathy [GEMRITUX]) of patients with severe nephrotic syndrome at treatment onset. The GEMRITUX cohort is part of a French multicenter, randomized, controlled trial (Clinicaltrial.gov identifier: NCT01508468) testing rituximab added to antiproteinuric therapy (RITUX) against antiproteinuric therapy alone (NIAT), (Supplemental Appendix).[18] Among the 75 patients (38 in the NIAT group and 37 in the RITUX group) who were enrolled in the GEMRITUX study,[18] 58 patients (29 in each group) showed PLA2R1-Ab reactivity by IFTA and/or ELISA and had available serum at baseline for analysis of epitope reactivity.

Table 1 depicts the characteristics of the whole population versus randomization groups at baseline (M0) and at month 3 (M3) and month 6 (M6) after treatment onset. Epitope reactivity toward CysR, CTLD1, and CTLD7 domains was measured by specific ELISAs that defined four epitope groups (CysR, CysRC1, CysRC7, and CysRC1C7).[12] All patients reactive with CTLD1 and/or CTLD7 were also reactive with CysR. Spreading of the immune response, as defined by addition of CTLD1 and/or CTLD7 reactivity to CysR, was identified in 38 out of 58 (65.5%) patients at baseline. There was no association between the epitope group (CysR, CysRC1, CysRC7, or CysRC1C7) and age, sex, time from diagnosis (kidney biopsy) to inclusion, proteinuria, or serum albumin. Conversely, there was a strong correlation between PLA2R1-Ab titer and epitope group ($P<0.001$), with the higher titers being associated with reactivity beyond CysR (Supplemental Table 1). Similar results were observed when patients were categorized according to the presence or absence of spreading ($P<0.001$ for PLA2R1-Ab titer) (Supplemental Table 2). Spreading was constant for a PLA2R1-Ab titer >369.5 RU/ml (Supplemental Figure 1), but because of the small size of the cohort, this threshold will need confirmation in future studies. The lack of association of epitope group and spreading with age and proteinuria is at odds with the observations made by Seitz-Polski *et al.*[12] who found that patients from the CysR group were significantly younger and had lower proteinuria. These discrepancies may be explained by a more advanced disease in the GEMRITUX cohort, where all patients had persistent nephrotic syndrome (mean value of 8.2 g/g for the whole cohort; Table 1) after a 6-month run-in period of optimized antiproteinuric therapy, whereas proteinuria was <3 g/g in 22 out of 69 (32%) patients in the study by Seitz-Polski *et al.*[12,18]

Our second objective was to investigate the effect of rituximab on epitope profiles and spreading. No difference at baseline was observed between randomization groups (NIAT versus RITUX) regarding age, sex, serum creatinine, serum albumin, proteinuria, PLA2R1-Ab titer, and epitope reactivity or spreading (Table 1). Epitope spreading was observed at baseline in 18 out of 29 (62.1%) and 20 out of 29 (68.9%) patients treated with NIAT and rituximab, respectively. At M3, there was a trend of lower rate of spreading in the rituximab group as compared with the NIAT group (42.3% versus 69.6%). This trend was maintained at M6 (26.9% versus 50%). There was a significant effect of rituximab on epitope profile at M3 and M6, being characterized by a drop in the number

Significance Statement

About 80% of patients with primary membranous nephropathy (pMN) have PLA2R1 auto-antibodies (PLA2R1-Ab). Although Ab titers are associated with disease activity, predicting clinical outcome is challenging. In retrospective studies both high PLA2R1-Ab titer and PLA2R1 epitope spreading have correlated with poor outcome. This paper analyzes the predictive value of PLA2R1-Ab titer and epitope spreading in a prospective cohort of 58 patients treated with rituximab or control (GEMRITUX). The results suggest that epitope spreading at baseline predicts a reduced likelihood of clinical remission independently of PLA2R1-Ab titer. We propose that epitope spreading be considered in the decision for early therapeutic intervention in pMN patients. These findings should be confirmed in larger cohorts of patients.

Table 1. Demographic and immunopathologic characteristics of the patients of the GEMRITUX cohort, according to therapeutic intervention at M0, M3, and M6

Characteristics	Whole Cohort, *n*=58	NIAT, *n*=29	RITUX, *n*=29	*P* Value
Age	56.5 [42.0–63.0]	59.0 [44.0–63.0]	52.0 [41.0–63.0]	0.5
Sex				0.4
Men	42 (72.4)	19	23	
Women	16 (27.6)	10	6	
Proteinuria at M0, g/g of serum creatinine	8.2 [4.8–10.0]	7.4 [6.2–9.0]	8.4 [4.4–11.0]	0.51
Serum albumin at M0, g/dl	2.2 [1.9–2.5]	2.2 [2.0–2.5]	2.2 [1.8–2.5]	0.52
Serum creatinine at M0, mg/L	10.8 [9.0–13.8]	10.4 [8.7–13.8]	11.5 [9.4–13.1]	0.48
PLA2R1-Ab at M0, RU/ml	101.5 [31.2–481.2]	199.5 [24.2–480.0]	100.5 [35.4–481.2]	0.85
CysR at M0, RU/ml	1423.5 [369.0–3240.0]	1572.0 [494.0–3240.0]	1256.0 [270.0–3114.0]	0.52
CTLD1 at M0, RU/ml	157.0 [0.0–2334.0]	12.0 [0.0–1190.0]	471.0 [0.0–2334.0]	0.33
CTLD7 at M0, RU/ml	220.5 [23.0–609.0]	136.0 [36.0–662.0]	223.0 [13.0–604.0]	0.65
Group M0				0.74
CysR	20 (34.48)	11 (37.93)	9 (31.03)	
CysRC1	8 (13.79)	4 (13.79)	4 (13.79)	
CysRC7	10 (17.24)	6 (20.69)	4 (13.79)	
CysRC1C7	20 (34.48)	8 (27.59)	12 (41.38)	
Spreading M0	38/58 (65.6)	18 (62.1)	20 (68.9)	0.78
Proteinuria at M3, g/g of serum creatinine[a]	5.1 [3.2–7.6]	5.0 [3.0–8.5]	5.1 [3.5–7.4]	0.86
Serum albumin at M3, g/dl[b]	2.6 [2.0–2.9]	2.3 [1.8–2.7]	2.7 [2.1–3.1]	0.12
Serum creatinine at M3, mg/L[a]	11.5 [9.4–13.6]	11.5 [9.7–13.9]	11.8 [9.0–13.6]	0.99
PLA2R1-Ab at M3, RU/ml[c]	43.1 [0–102.5]	70.5 [30.3–325.9]	0.0 [0.0–60.5]	0.002
Group M3[d]				0.002
Negative	12 (24.5)	0 (0.0)	12 (46.2)	
CysR	10 (20.4)	7 (30.4)	3 (11.5)	
CysRC1	9 (18.4)	6 (26.1)	3 (11.5)	
CysRC7	6 (12.2)	3 (13.1)	3 (11.5)	
CysRC1C7	12 (24.5)	7 (30.4)	5 (19.2)	
Spreading M3[d]	27/49 (55.1)	16 (69.6)	11 (42.3)	0.09
Proteinuria at M6, g/g of serum creatinine[e]	4.4 [2.0–7.3]	6.2 [2.2–7.5]	3.7 [1.8–6.5]	0.21
Serum albumin at M6, g/dl[e]	2.6 [2.1–3.3]	2.4 [2.0–2.9]	2.9 [2.5–3.4]	0.07
Serum creatinine at M6, mg/L[e]	11.9 [9.4–14.8]	12.0 [9.4–14.4]	11.9 [9.8–14.8]	0.71
PLA2R1-Ab at M6, RU/ml[f]	30.1 [0–98.5]	57.2 [16.5–298.0]	0 [0–57.0]	0.01
Group M6[c]				
Negative	17 (34.0)	0 (0.0)	17 (65.4)	
CysR	14 (28.0)	12 (50.0)	2 (7.7)	<0.001
CysRC1	5(10.0)	4 (16.7)	1 (3.9)	
CysRC7	2 (4.0)	2 (8.3)	0 (0.0)	
CysRC1C7	12 (24.0)	6 (25.0)	6 (23.1)	
Spreading M6[c]	19/50 (38.0)	12/24 (50.0)	7/26 (26.9)	0.15

Data are shown as *n* (%) or median [interquartile range].
[a]One missing value.
[b]Two missing values.
[c]Eight missing values.
[d]Nine missing values.
[e]Four missing values.
[f]Five missing values.

of patients with CysRC1C7 reactivity concomitant with a dramatic increase in those with CysR reactivity only and in those negative for all epitope domains ($P<0.001$ and $P<0.001$, respectively) (Supplemental Table 3). When individually considering the patients who spread at baseline, ten out of 17 (58.8%) patients treated with rituximab and only four out of 16 (25%) patients treated with NIAT showed a "reverse" spreading (CysRC1 and/or CysRC7 to CysR only or negative for all epitope domains) at M6. These results indicate that rituximab favors reversal of epitope spreading in parallel with a decrease in PLA2R1-Ab titers. Among spreaders at baseline treated with rituximab, results at last follow-up showed a significant gradient of response ($P=0.01$), with the lower response rate being observed in patients with persistent reactivity versus two or three epitopes (one out of seven), and the higher response rate in patients with no reactivity (seven out of eight) or those with CysR reactivity only (two out of two). Although persistence of

spreading is associated with a much lower rate of remission, it does not seem necessary to become nonreactive to all three epitopes for clinical remission to occur. Among the seven spreaders treated with rituximab who did not respond clinically at last follow-up, only one had lost epitope reactivity, and six remained spreaders. Among the 13 patients in the NIAT group who initially showed epitope spreading and did not respond clinically at last follow-up, ten remained spreaders. Therefore, the spreaders who did not respond clinically remained spreaders, except for three. In the NIAT group, among the 11 patients with CysR-only reactivity at baseline, five achieved spontaneous remission at M6 (83.3% of all remissions) and eight (61.5%) achieved spontaneous remission at last follow-up; among the 18 spreaders at baseline, only one (16.7% of all remissions) achieved spontaneous remission at M6, and five achieved spontaneous remission (38.5%) at last follow-up. Although these findings should be taken with caution, given the small size of the cohort, and would require confirmation in future studies, physicians should consider delaying immunosuppressive treatment in patients with CysR-only reactivity.

Our third aim was to establish whether epitope spreading was a more potent predictor of remission than PLA2R1-Ab titer, in the context of a randomized trial with strict criteria of eligibility (for definition of remissions, see Supplemental Appendix). At M6, 15 patients had reached clinical remission with (n=9) or without (n=6) rituximab, whereas 43 patients had not. Lower levels of CTLD7 reactivity ($P<0.01$) and lower rate of epitope spreading (P=0.03), (Figure 1A, Supplemental Table 4) were the only factors at baseline associated with higher remission rates at M6, whereas PLA2R1-Ab titers did not reach statistical significance. At M3, lower titers of PLA2R1-Ab ($P<0.01$) and lower rate of epitope spreading (P=0.001) were associated with higher remission rates (Figure 1A). Patients with CysR-only reactivity at baseline accounted for 60.0% of remissions and 25.6% of no remissions at M6. Distribution of remissions was different according to treatment group combined with spreading at baseline (Figure 2). In adjusted analysis (Table 2), spreading at baseline was associated with a decreased rate of remission (odds ratio, 0.16; 95% confidence interval, 0.04 to 0.72; P=0.02) independently from age, sex, treatment group, and baseline PLA2R1-Ab titer. We then assessed whether these results could be confirmed during the extended period of follow-up (median, 23 months; interquartile range, 22–25)

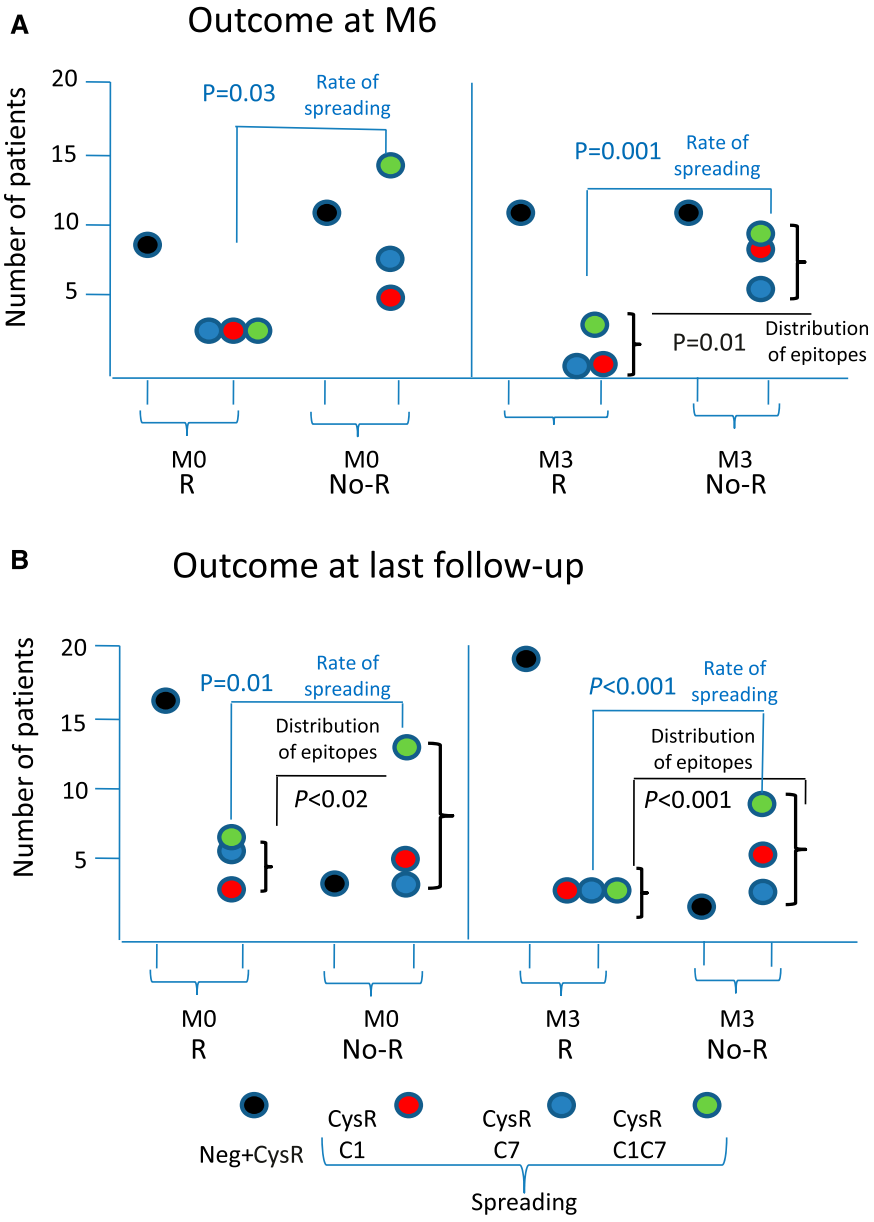

Figure 1. Clinical outcome is predicted by epitope distribution and spreading at baseline and month 3. Epitope distribution is shown at baseline (M0) and month 3 (M3) according to outcome at (A) M6 (full cohort including both treatment groups) and (B) last follow-up (full cohort). Patients are divided into those who achieved remission (R) and those who did not achieve remission (No-R) at M6 and last follow-up, respectively. Reactivity with the various epitope domains is shown by color codes. "Neg" means lack of reactivity with any epitope domain at M3. Note that the rate of epitope spreading significantly differs from baseline between R and No-R patients.

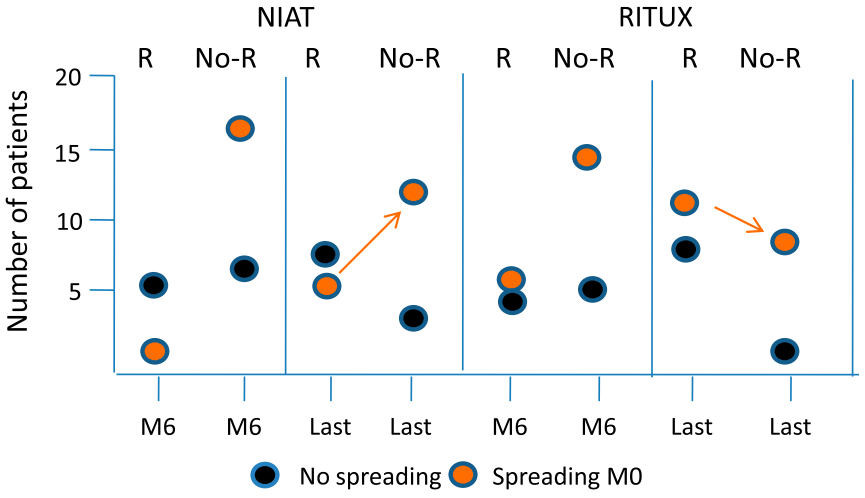

M6	Remission (n=15)	No Remission (n=43)	P value
NIAT - NO spreading M0	5 (33.33)	6 (13.95)	0.0374
NIAT - Spreading M0	1 (6.67)	17 (39.53)	
RITUX - NO spreading M0	4 (26.67)	5 (11.63)	
RITUX - Spreading M0	5 (33.33)	15 (34.88)	

Last follow-up	Remission (n=32)	No Remission (n=26)	P value
NIAT - NO spreading M0	8 (25)	3 (11.54)	0.0118
NIAT - Spreading M0	5 (15.63)	13 (50)	
RITUX - NO spreading M0	8 (25.00)	1 (3.85)	
RITUX - Spreading M0	11 (34.38)	9 (34.62)	

Figure 2. Absence of spreading and rituximab treatment are associated with better clinical outcome. Combined effect of treatment group and spreading at baseline on clinical outcome is shown at M6 and last follow-up before modification of treatment (Last). Absence or presence of epitope spreading at baseline (M0) is shown by color codes. Results suggest that rituximab tends to blunt the effect of spreading on clinical remission at last follow-up. Note the higher number of spreaders with no remission (No-R) compared with those with remission (R) in the NIAT group (arrow), contrasting with the lower number of spreaders with No-R versus R in the RITUX group. Exact numbers and percentages are shown in the table.

before any treatment modification. At the end of that period, 32 patients had entered remission whereas 26 patients had not. The level of CysR (P=0.04), CTLD1 (P<0.01), and CTLD7 reactivity (P=0.01), the distribution of epitope profiles (P=0.02) and the rate of epitope spreading (P=0.01) at baseline were associated with remission (Figure 1B, Supplemental Table 5). The titer of PLA2R1-Ab (P<0.001), the distribution of epitope groups (P<0.001), and the rate of epitope spreading (P<0.001) at M3 were also associated with remission (Supplemental Table 4). Patients with CysR-only reactivity at baseline accounted for 50.0% of remissions and 15.4% of no remissions at last follow-up. Distribution of remissions before any treatment modification was different according to treatment arm combined with spreading at baseline (Figure 2). In adjusted analysis, epitope spreading at baseline was associated with a decreased rate of remission at last follow-up (odds ratio, 0.14; 95% confidence interval, 0.03 to 0.64; P=0.01), independently from age, sex, treatment group, and baseline PLA2R1-Ab titer. To further support the possible preeminence of epitope spreading over PLA2R1-Ab titer, we generated a variable combining PLA2R1-Ab titer <50 RU/ml (considered as low level) versus ≥50 RU/ml and spreading at baseline, and examined clinical response at last follow-up. The results show a significantly different distribution of remissions among the groups (P=0.03). Among the patients with low levels of PLA2R1-Ab (<50 RU/ml), 11 out of 15 (73%) of those with no spreading at baseline achieved clinical remission whereas only four out of nine (44%) of those with spreading did so. Among the patients with higher levels of PLA2R1-Ab (≥50 RU), all patients with no spreading achieved remission whereas only 12 out of 29 (41%) of those with spreading did so. Although these numbers are small, the data suggest that spreading may drive the absence of remission more than PLA2R1-Ab level at baseline (Supplemental Figure 2).

In our initial GEMRITUX study, we showed that remission was associated with PLA2R1-Ab level <275 RU/ml at baseline.[18] We now add an important, independent prognostic factor, epitope spreading at baseline, which is associated with low remission rates both at M6 and at last follow-up in a well phenotyped population of patients with severe clinical presentation. Our data suggest that if a patient has only a low level of anti-PLA2R1 but significant spreading, he/she should be treated with rituximab at the time of diagnosis. If a patient has high anti-PLA2R1 levels but no spreading, he/she could be watched and not treated. However, these potentially important results have to be confirmed in further studies.

This study has several limitations. We did not measure epitope-specific IgG subclasses because in our previous study, we did not observe an anti-CTLD7 antibody different from IgG4, and we rarely detected IgG1, IgG2, and IgG3 anti-CysR and anti-CTLD1 antibodies.[12] Because of the sample size of PLA2R1-positive patients in the GEMRITUX cohort, we could not perform a multivariate analysis in the RITUX group only, to identify epitope spreading as a predictor of response to rituximab.

Table 2. Unadjusted and adjusted odd ratios for clinical remission at M6 and last follow-up of baseline indicators (M0)

Effect	Unadjusted				Adjusted			
	Odds Ratio	95% Wald Confidence Limits		Type 3 Analysis *P* Value	Odds Ratio	95% Wald Confidence Limits		Type 3 Analysis *P* Value
M6								
Age, yr	1.02	0.98	1.07	0.38	1.02	0.97	1.07	0.37
Sex				0.93				0.96
Men	1				1			
Women	0.94	0.25	3.53		1.04	0.24	4.54	
PLA2R1-Ab at M0, RU/ml	1.00	0.99	1.00	0.67	1.00	0.99	1.00	0.44
Treatment				0.37				0.21
NIAT	1				1			
NIAT and RITUX	1.73	0.52	5.69		2.37	0.62	9.06	
Spreading M0				0.02				0.02
No	1				1			
Yes	0.23	0.07	0.79		0.16	0.04	0.72	
Last follow-up								
Age, yr	1.01	0.98	1.05	0.51	1.02	0.98	1.07	0.38
Sex								
Men	1			0.92	1			0.54
Women	1.06	0.33	3.39		1.54	0.4	5.99	
PLA2R1-Ab at M0, RU/ml	1.00	0.99	1.00	0.22	1.00	0.99	1.00	0.86
Treatment								
NIAT	1			0.12	1			0.04
NIAT and RITUX	2.34	0.81	6.74		3.72	1.05	13.2	
Spreading M0								
No	1			0.01	1			0.01
Yes	0.18	0.05	0.65		0.15	0.03	0.64	

Note that spreading at baseline is the only predictor of remission at M6, and it also predicts remission at last follow-up before any treatment modification, independently from PLA2R1-Ab titer.

Despite these defects, our study suggests that the absence of epitope spreading at onset is an independent factor of remission at M6 and last follow-up in patients with persisting nephrotic syndrome despite full renin-angiotensin system blockade. We propose that baseline epitope spreading should be carefully considered in the decision for early therapeutic intervention in patients with primary membranous nephropathy. Although treatment may be delayed in patients with CysR-only reactivity, epitope spreading and its persistence after 3 months should be added to the therapeutic algorithm. Additional studies are needed to further define the therapeutic window opportunity on the basis of epitope reactivity. As long as epitope-specific assays for PLA2R1-Ab are not commercially available, a high titer of total PLA2R1-Ab (by ELISA) at baseline is the best surrogate currently available for detection of epitope spreading.

CONCISE METHODS

Study Population

This study presents the results of an ancillary study to the GEMRITUX randomized controlled trial (Clinicaltrial.gov identifier: NCT01508468).[18] Eligibility criteria, study treatments and monitoring, and definition of clinical and immunologic remission are given in the Supplemental Appendix and detailed elsewhere.[18] The GEMRITUX study was approved by a national ethical committee. In this study, eligible patients were those positive by IFTA or ELISA and with serum available during follow-up for epitope profiling (n=58).

Anti-PLA2R1 Assays with Full-Length Antigen

PLA2R1-Ab (total IgG) toward the full-length PLA2R1 antigen were assessed using IFTA and the quantitative ELISA test commercialized by EuroImmun AG (Lübeck, Germany) as previously described.[19] For ELISA, sera were diluted to 1:100 and incubated with PLA2R1 (full extracellular domain of PLA2R1) already coated onto microplates and detected by incubation with anti-human IgG horseradish peroxidase conjugate. The final titer for each sample was calculated from the calibration curve extinction values plotted against the concentration for each calibrator. ELISA cutoff values were established according to the manufacturer's protocol, and the results were considered as negative for values $<$14 RU/ml and positive for values $\geq$14 RU/ml. In our laboratory, the calculated intra- and inter-assay variations are $<$4% and $<$9%, respectively.

ELISA using Isolated PLA2R1 Domains

The three PLA2R1 domains CysR (Ala-26 to Lys-164), CTLD1 (Thr-223 to Asn-359), and CTLD7 (Thr-1102 to Glu-1237) were produced in HEK293 cells as secreted proteins harboring an HA tag.[12] The reactivity of sera toward these domains was analyzed essentially as previously described.[12] Briefly, plates were coated with anti-HA antibody (Sigma-Aldrich) diluted at 1:5000 in

20 mM Tris (pH 8.0; 100 μl per well) at 4°C overnight. Plates were then blocked for 2 hours with Seramun Block (Seramun Diagnostica). Cell medium from HEK293 cells transfected with the soluble forms of the three PLA2R1 domains (10–100 μl per well, depending on protein expression) were then added and incubated for 1 hour. Plates were washed and patients' sera, diluted at 1:100 (or higher as needed) in PBS/0.1% dry milk, were added in duplicate (100 μl per well) to the ELISA plates, which also contained a serial dilution of an MN standard serum and a quality control calibrator (between plates). After 2 hours incubation at room temperature on a plate shaker, plates were washed four times with PBS/0.02% Tween 20. Anti-human IgG4 horseradish peroxidase conjugate (#9200–05; Southern Biotech) diluted at 1:7500 in Seramun Stab ST plus was added (100 μl per well; Seramun Diagnostica) and incubated for 1 hour at room temperature on a plate shaker. After four washes, tetramethylbenzidine was added, and the reactions were developed for 15 minutes and then stopped with HCl 1.2 N. The plates were read at 450 nm. The cutoff was optimized by receiver-operating characteristics curve analysis. A highly positive index patient serum was used in each plate to generate a standard curve and a negative control.

An ELISA index value for each antigen was obtained for patients or controls as follows (mean test result−mean domain negative control)/(mean domain positive control−mean domain negative control)×domain correction factor×100. The domain correction factor was determined for each domain as the mean of all of the positive controls for that domain on all plates minus the mean of the negative controls, divided by the cutoff for that domain assay, as described by Warren *et al.*[20] Results were expressed as relative units per milliliter.

Statistical Analyses

Characteristics of patients were described with frequencies and percentages for categorical data, and with medians and interquartile ranges for quantitative data. Categorical data were compared using Fisher exact test, whereas quantitative data were compared using Wilcoxon–Mann–Whitney nonparametric test. Adjusted analysis was performed using logistic regression. Because of the small number of patients analyzed, adjustment was limited to age, sex, treatment group, and PLA2R1 titer. All tests were two-sided and a P value <0.05 indicated statistical significance. Analyses were performed using SAS v.9.3 software (SAS Institute, Cary, NC).

ACKNOWLEDGMENTS

This research is supported by European Research Council ERC-2012 ADG_20120314 grant 322947 (to P.R.), the Seventh Framework Programme of the European Community contract no. 2012-305608 (European Consortium for High-Throughput Research in Rare Kidney Diseases) (to P.R.), and by grants from CNRS, the National Research Agency to G.L. through the "Investments for the Future" Laboratory of Excellence SIGNALIFE, a network for innovation on signal transduction pathways in life sciences, (programme reference ANR-11-LABX-0028-01), and to G.L. and P.R. (grant MNaims ANR-17-CE17-0012-01) the Fondation pour la Recherche Médicale (ING20140129210 and SPF20150934219), and the Centre Hospitalier Universitaire de Nice and the Direction générale de l'offre de soins of the French Ministry of Health (Phospholipase A2 Receptor (PLA2R1) Autoantibodies in Membranous Nephropathy in Kidney Transplantation Programme, PHRC2011-A01302-39, NCT01897961) to G.L., B.S.-P., and V.L.M.E. Principal Investigator. This work has been developed and supported through the Fédération Hospitalo-Universitaire *Oncoage* (Nice, France) with V.L.M.E. as PI.

DISCLOSURES

None.

REFERENCES

1. Beck LH Jr., Bonegio RG, Lambeau G, Beck DM, Powell DW, Cummins TD, Klein JB, Salant DJ: M-type phospholipase A2 receptor as target antigen in idiopathic MN. *N Engl J Med* 361: 11–21, 2009
2. Tomas NM, Beck LH Jr ., Meyer-Schwesinger C, Seitz-Polski B, Ma H, Zahner G, Dolla G, Hoxha E, Helmchen U, Dabert-Gay AS, Debayle D, Merchant M, Klein J, Salant DJ, Stahl RAK, Lambeau G: Thrombospondin type-1 domain-containing 7A in idiopathic membranous nephropathy. *N Engl J Med* 371: 2277–2287, 2014
3. Tomas NM, Hoxha E, Reinicke AT, Fester L, Helmchen U, Gerth J, Bachmann F, Budde K, Koch-Nolte F, Zahner G, Rune G, Lambeau G, Meyer-Schwesinger C, Stahl RA: Autoantibodies against thrombospondin type 1 domain-containing 7A induce membranous nephropathy. *J Clin Invest* 126: 2519–2532, 2016
4. Ronco P, Debiec H: Pathophysiological advances in membranous nephropathy: Time for a shift in patient's care. *Lancet* 385: 1983–1992, 2015
5. Glassock RJ: Diagnosis and natural course of membranous nephropathy. *Semin Nephrol* 23: 324–332, 2003
6. Kanigicherla D, Gummadova J, McKenzie EA, Roberts SA, Harris S, Nikam M, Poulton K, McWilliam L, Short CD, Venning M, Brenchley PE: Anti-PLA2R antibodies measured by ELISA predict long-term outcome in a prevalent population of patients with idiopathic membranous nephropathy. *Kidney Int* 83: 940–948, 2013
7. Hoxha E, Thiele I, Zahner G, Panzer U, Harendza S, Stahl RA: Phospholipase A2 receptor autoantibodies and clinical outcome in patients with primary membranous nephropathy. *J Am Soc Nephrol* 25: 1357–1366, 2014
8. Seitz-Polski B, Payré C, Ambrosetti D, Albano L, Cassuto-Viguier E, Berguignat M, Jeribi A, Thouret MC, Bernard G, Benzaken S, Lambeau G, Esnault VL: Prediction of membranous nephropathy recurrence after transplantation by monitoring of anti-PLA2R1 (M-type phospholipase A2 receptor) autoantibodies: A case series of 15 patients. *Nephrol Dial Transplant* 29: 2334–2342, 2014
9. Ancian P, Lambeau G, Mattéi MG, Lazdunski M: The human 180-kDa receptor for secretory phospholipases A2. Molecular cloning, identification of a secreted soluble form, expression, and chromosomal localization. *J Biol Chem* 270: 8963–8970, 1995
10. Kao L, Lam V, Waldman M, Glassock RJ, Zhu Q: Identification of the immunodominant epitope region in phospholipase A2 receptor-mediating autoantibody binding in idiopathic membranous nephropathy. *J Am Soc Nephrol* 26: 291–301, 2015
11. Fresquet M, Jowitt TA, Gummadova J, Collins R, O'Cualain R, McKenzie EA, Lennon R, Brenchley PE: Identification of a major epitope recognized by PLA2R autoantibodies in primary membranous nephropathy. *J Am Soc Nephrol* 26: 302–313, 2015
12. Seitz-Polski B, Dolla G, Payré C, Girard CA, Polidori J, Zorzi K, Birgy-Barelli E, Jullien P, Courivaud C, Krummel T, Benzaken S, Bernard G, Burtey S, Mariat C, Esnault VL, Lambeau G: Epitope spreading of autoantibody response to PLA2R associates with poor prognosis in membranous nephropathy. *J Am Soc Nephrol* 27: 1517–1533, 2016

13. Cornaby C, Gibbons L, Mayhew V, Sloan CS, Welling A, Poole BD: B cell epitope spreading: Mechanisms and contribution to autoimmune diseases. *Immunol Lett* 163: 56–68, 2015
14. Chen JL, Hu SY, Jia XY, Zhao J, Yang R, Cui Z, Zhao MH: Association of epitope spreading of antiglomerular basement membrane antibodies and kidney injury. *Clin J Am Soc Nephrol* 8: 51–58, 2013
15. Li N, Aoki V, Hans-Filho G, Rivitti EA, Diaz LA: The role of intramolecular epitope spreading in the pathogenesis of endemic pemphigus foliaceus (fogo selvagem). *J Exp Med* 197: 1501–1510, 2003
16. McRae BL, Vanderlugt CL, Dal Canto MC, Miller SD: Functional evidence for epitope spreading in the relapsing pathology of experimental autoimmune encephalomyelitis. *J Exp Med* 182: 75–85, 1995
17. Naserke HE, Ziegler AG, Lampasona V, Bonifacio E: Early development and spreading of autoantibodies to epitopes of IA-2 and their association with progression to type 1 diabetes. *J Immunol* 161: 6963–6969, 1998
18. Dahan K, Debiec H, Plaisier E, Cachanado M, Rousseau A, Wakselman L, Michel PA, Mihout F, Dussol B, Matignon M, Mousson C, Simon T, Ronco P; GEMRITUX Study Group: Rituximab for severe membranous nephropathy: A 6-month trial with extended follow-up. *J Am Soc Nephrol* 28: 348–358, 2017
19. Ruggenenti P, Debiec H, Ruggiero B, Chianca A, Pellé T, Gaspari F, Suardi F, Gagliardini E, Orisio S, Benigni A, Ronco P, Remuzzi G: Anti-phospholipase A2 receptor antibody titer predicts post-rituximab outcome of membranous nephropathy. *J Am Soc Nephrol* 26: 2545–2558, 2015
20. Warren SJ, Arteaga LA, Rivitti EA, Aoki V, Hans-Filho G, Qaqish BF, Lin MS, Giudice GJ, Diaz LA: The role of subclass switching in the pathogenesis of endemic pemphigus foliaceus. *J Invest Dermatol* 120: 104–108, 2003

This article contains supplemental material online at http://jasn.asnjournals.org/lookup/suppl/doi:10.1681/ASN.2017070734/-/DCSupplemental.

Supplementary appendix

Supplementary Note #1: Patients' inclusion and non-inclusion criteria in the GEMRITUX study [11]

Eligible patients were 18 years of age or older and had a biopsy-proven primary MN (pMN). Patients were enrolled from January 2012 to July 2014 in 31 French centers if they had a urinary protein excretion or a urinary protein/creatinine ratio greater than, or equal to, 3.5 g/day or 3,500 mg/g, respectively, and a serum albumin lower than 30 g/L for at least 6 months despite full dose of Non Immunosuppressive, Antiproteinuric Treatment (NIAT) (angiotensin-converting enzyme inhibitors and/or angiotensin-2 receptor blockers, diuretics and statin). The estimated GFR by MDRD formula had to be above 30 mL/min/1.73m^2. Exclusion criteria were secondary MN, pregnancy, breast-feeding, immunosuppressive treatment in the three preceding months, and active infectious disease.

Supplementary Note #2: Clinical and immunological remission

Clinical remission was defined accordingly to 2012 KDIGO (KDIGO clinical practice guideline for glomerulonephritis. Kidney Int Suppl.2: 186-197, 2012) as 1) complete in case of urinary protein excretion less than 500 mg per day or 500 mg/g creatinine; 2) partial in case of urinary protein excretion <3.5 g per day or 3,500 mg/g creatinine and ≥500 mg/g creatinine with at least 50% reduction compared to baseline. Antibody depletion was defined as complete disappearance of antibodies in PLA2R1-Ab positive patients.

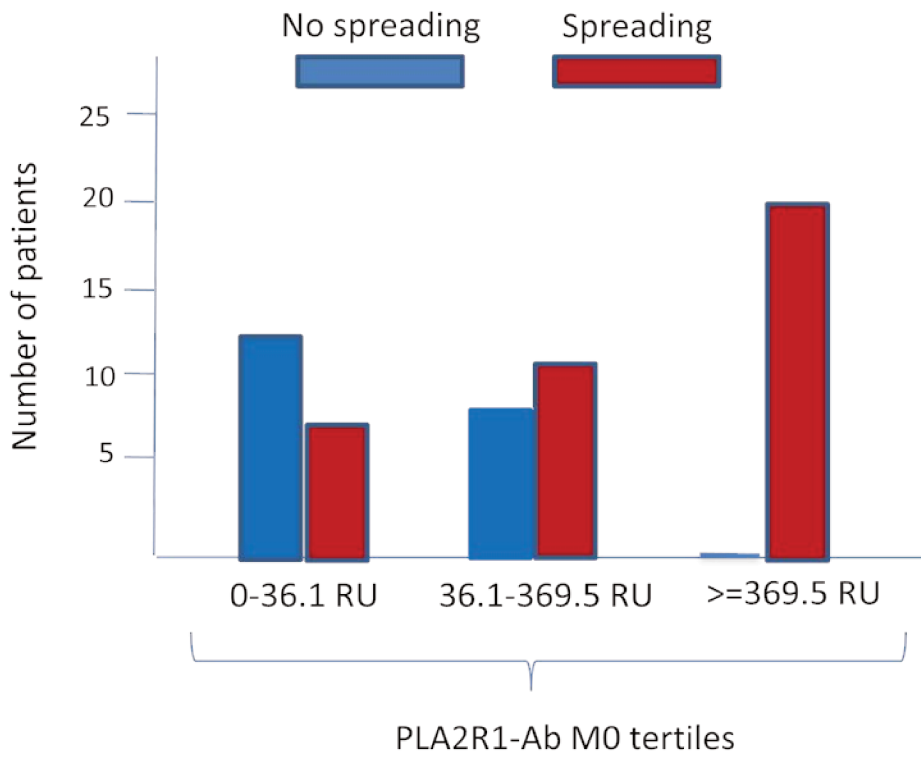

Supplementary Figure 1: Rate of spreading according to PLA2R1-Ab titer.

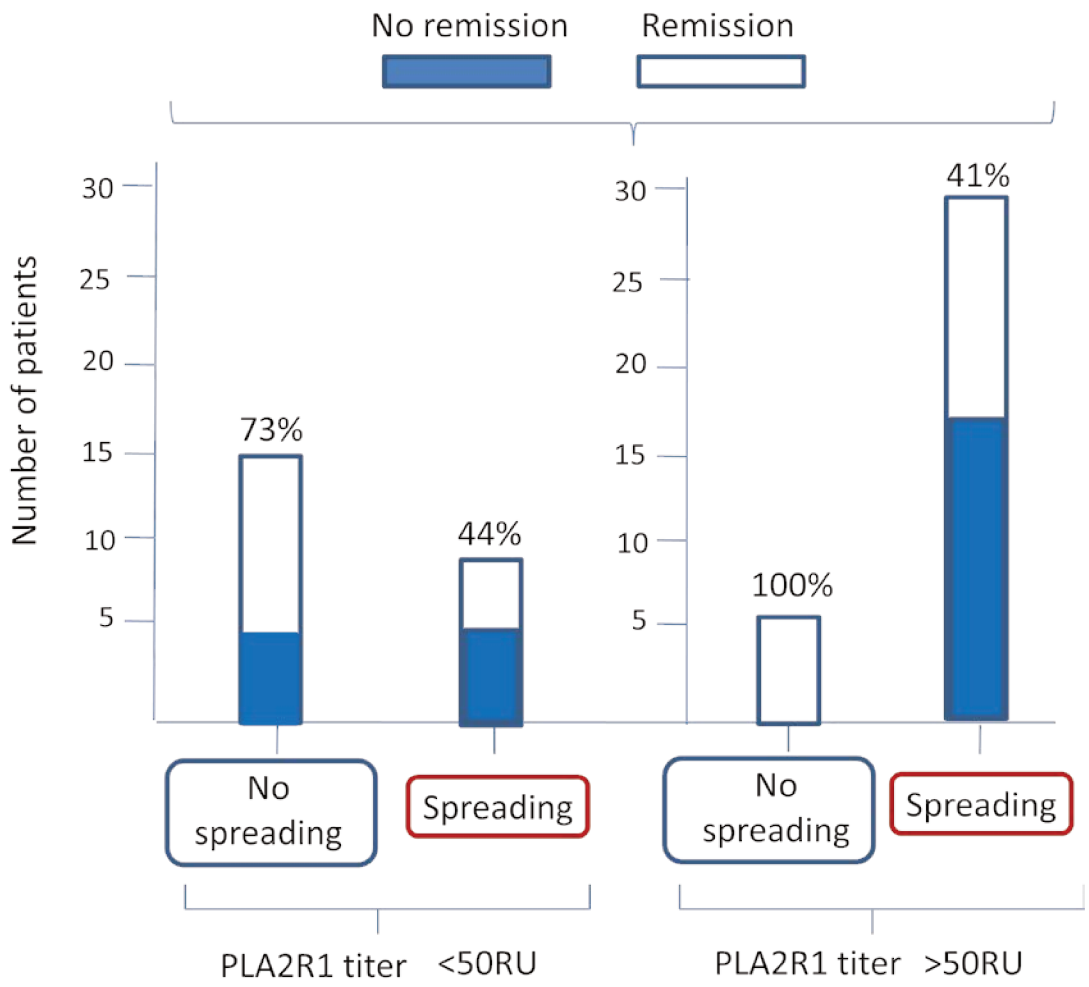

Supplementary Figure 2: Rate of remission at last follow-up according to antibody titer and epitope spreading. The numbers above the bars indicate the % remission in the various combinations.

Supplementary Table 1: Association of epitope group with clinical characteristics of the GEMRITUX cohort (n=58) at baseline.

Characteristics at baseline	Negative n=4	CysR n=16	CysRC1 n=8	CysRC7 n=10	CysRC1C7 n=20	P value
Age	58.5 [43.5 ; 62.0]	57.5 [43.5 ; 62.0]	47.5 [38.5 ; 64.0]	48.5 [41.0 ; 64.0]	59.5 [41.5 ; 63.5]	0.9391
Time from diagnosis to inclusion (months)	8.0 [6.0 ; 17.5]	8.0 [6.5 ; 17.5]	7.0 [6.0 ; 8.0]	8.0 [6.0 ; 11.0]	8.5 [6.0 ; 10.0]	0.8019
Gender						
Male	15 (75.0)	11 (68.75)	6 (75.00)	6 (60.00)	15 (75.00)	0.8118
Female	5 (25.0)	5 (31.25)	2 (25.00)	4 (40.00)	5 (25.00)	
Anti-PLA2R1 antibody (RU/mL)	31.6 [18.0 ; 54.4]	33.7 [18.0 ; 54.4]	292.9 [109.6 ; 1085.0]	469.4 [35.1 ; 710.0]	359.0 [58.2 ; 1066.5]	0.0002
Proteinuria (g/g of Creat)	7.9 [3.5 ; 8.5]	7.3 [3.5 ; 8.4]	9.4 [6.4 ; 12.9]	9.7 [6.8 ; 11.7]	7.0 [5.2 ; 9.6]	0.1639
Albuminemia (g/dL)	2.2 [2.0 ; 2.6]	2.3 [2.1 ; 2.8]	1.9 [1.7 ; 2.3]	2.3 [2.1 ; 2.7]	2.0 [1.7 ; 2.5]	0.2976

Creat, serum creatinine
Data are shown as n (%) or median [IQR].
Patients were divided into 4 epitope groups

SupplementaryTable 2: Association of epitope spreading with clinical characteristics of the GEMRITUX cohort (n=58) at baseline.

Characteristics at baseline	No spreading n=20	Spreading N=38	P value
Age	58.5 [43.5 ; 62.0]	52.0 [41.0 ; 64.0]	0.8386
Time from diagnosis to inclusion (months)	8.0 [6.0 ; 17.5]	8.0 [6.0 ; 9.0]	0.4987
Gender			
Male	15 (75.0)	27 (71.05)	1
Female	5 (25.0)	11 (28.95)	
Anti-PLA2R1 antibody (RU/mL)	31.6 [18.0 ; 54.4]	376.9 [75.8 ; 746.5]	<.0001
Proteinuria (g/g of Creat)	7.9 [3.5 ; 8.5]	8.3 [6.2 ; 10.4]	0.1649
Albuminemia (g/dL)	2.2 [2.0 ; 2.6]	2.1 [1.8 ; 2.5]	0.5252

Creat, serum creatinine
Data are shown as n (%) or median [IQR].
Patients were divided into “no spreading” (CysR only patients) and “spreading” (at least one additional epitope to CysR) groups.

Supplementary Table 3: Comparison of epitope reactivity subtypes at various timepoints between the NIAT only group and the NIAT-Rituximab group

	NIAT			NIAT+RITUX		
	M0	**M3**	**M6**	**M0**	**M3**	**M6**
Negative	0	0	0	0	12	17
CysR	11	7	12	9	3	2
CysRC1	4	6	4	4	3	1
CysRC7	6	3	2	4	3	0
CysRC1C7	8	7	6	12	5	6
Total	29	23	24	29	26	26

SupplementaryTable 4: Clinical and immunological characteristics of patients according to outcome at M6

Characteristics	Remission n=15	No remission n=43	P value
Age	58.0 [43.0 ; 63.0]	51.0 [41.0 ; 63.0]	0.4966
Gender			
Male	11 (73.33)	31 (72.09)	1
Female	4 (26.67)	12 (27.91)	
Proteinuria (g/g of Creat) M0	7.4 [3.6 ; 12.8]	8.2 [5.6 ; 9.8]	0.9859
Albuminemia (g/dL) M0	2.1 [1.7 ; 2.4]	2.2 [1.9 ; 2.6]	0.6645
Anti-PLA2R1 antibody (RU/mL)M0	35.4 [24.2 ; 216.3]	199.5 [35.1 ; 538.5]	0.1435
Anti-CysR(RU/mL)	369.0 [258.0 ; 2710.0]	1575.0 [528.0 ; 3356.0]	0.0796
Anti-CTLD1(RU/mL)	16.0 [0.0 ; 257.0]	424.0 [0.0 ; 3477.0]	0.1748
Anti-CTLD7(RU/mL)	30.0 [0.0 ; 223.0]	272.0 [48.0 ; 706.0]	0.0098
Epitope group M0			0.0809
CysR	9 (60.00)	11 (25.58)	
CysRC1	2 (13.33)	6 (13.95)	
CysRC7	2 (13.33)	8 (18.60)	
CysRC1C7	2 (13.33)	18 (41.86)	
Spreading M0	6 (40)	32 (74.42)	0.0262
Anti-PLA2R1 antibody (RU/mL) M3*	0.0 [0.0 ; 30.5]	55.9 [16.2 ; 137.8]	0.0093
Epitope group M3**			
Negative	6 (46.15)	6 (16.67)	
CysR	5 (38.46)	5 (13.89)	0.0130
CysRC1	0 (0.00)	9 (25.00)	
CysRC7	0 (0.00)	6 (16.67)	
CysRC1C7	2 (15.38)	10 (27.78)	
Spreading M3 **	2/13(13.33)	25/36(58.14)	0.0011
Treatment			
NIAT	6 (40.0)	23(53.5)	0.55
RITUX	9 (60.0)	20(46.5)	

*: 8 missing values, **: 9 missing values.Creat, serum creatinine
Data are shown as n (%) or median [IQR].
Note that lack of remission was associated with higher level ofanti-CTLD7 antibody and higher rate of spreading at baseline whereas PLA2R1-Ab titer did not reach statistical significance.

Supplementary Table 5: Clinical and immunological characteristics of patients according to outcome at last follow-up

Characteristics	Remission n=32	No remission n=26	P value
Age	56.5 [43.5 ; 63.0]	53.5 [39.0 ; 64.0]	0.6857
Gender			
Male	19 (73.08)	23()71.88	1
Female	7 (26.92)	9 (28.13)	
Proteinuria (g/g of Creat) M0	7.9 [4.3 ; 10.1]	8.3 [6.3 ; 9.7]	0.6353
Albuminemia (g/dL) M0	2.1 [1.9 ; 2.6]	2.2 [1.9 ; 2.5]	0.6402
Anti-PLA2R1 antibody (RU/mL) M0	63.1 [26.9 ; 304.6]	363.7 [37.9 ; 710.0]	0.0967
Anti-CysR (RU/mL)	963.5 [276.0 ; 2141.0]	2139.5 [959.0 ; 3356.0]	0.0358
Anti-CTLD1 (RU/mL)	12.5 [0.0 ; 847.0]	1730.5 [12.0 ; 5803.0]	0.0065
Anti-CTLD7 (RU/mL)	81.5 [14.5 ; 259.5]	473.0 [36.0 ; 1115.0]	0.0143
Epitope group M0			0.0196
CysR	16 (50.00)	4 (15.38)	
CysRC1	3 (9.38)	5 (19.23)	
CysRC7	6 (18.75)	4 (15.38)	
CysRC1C7	7 (21.88)	13 (50.00)	
Spreading M0	16(50)	22(84.62)	0.0114
Anti-PLA2R1 antibody (RU/mL) M3*	0.0 [0.0 ; 49.1]	102.5 [41.1 ; 325.9]	0.0006
Epitope group M3**			0.0007
Negative	11 (37.93)	1 (5.00)	
CysR	9 (31.03)	1 (5.00)	
CysRC1	3 (10.34)	6 (30.00)	
CysRC7	3 (10.34)	3 (15.00)	
CysRC1C7	3 (10.34)	9 (45.00)	
Spreading M3**	9/29 (31.03)	18/20(90.0)	< 0.0001
Treatment			0.1964
NIAT	13(40.6)	16(61.5)	
RITUX	19(59.4)	10(38.5)	

*8 missing values; ** 9 missing.Creat, serum creatinine
Data are shown as n (%) or median [IQR].
Note that lack of remission was associated with spreading at baseline and M3, and PLA2R-Ab titer at M3.

5 Discussion and perspectives

Membranous nephropathy and its natural history have a number of specific clinical characteristics and pathophysiological features that I will further discussed below, with emphasis on the key points identified for THSD7A–associated MN, including age and sex at disease onset and the possible link to malignancy, predominance for IgG4 autoantibodies, and a possible mechanism of epitope spreading or immunodominance, potentially linked to disease activity or outcome. Furthermore, in an attempt to better understand the underlying pathophysiological mechanisms of the disease and propose new hypotheses or disease scenarios at play in MN, it is certainly of interest to compare the different MN features with those of several other related autoimmune diseases. I will thus discuss below, in a step–by–step way, the above features of MN, from the etiology to podocyte injury with comparison to other relevant autoimmune diseases (Figure 5.4).

5.1 Clinical features and etiology of THSD7A–associated MN

The field of membranous nephropathy witnessed significant clinical advances after the identification of PLA2R1 and THSD7A as the key autoantigens expressed in the podocytes and involved in most cases of the so–called primary or idiopathic MN.

– Identification of autoantigens

The identification of PLA2R1 as a major autoantigen in 70% of patients followed by that of THSD7A as second autoantigen in 3% of patients with the fact that both antigens are different and mutually exclusive are not unique features of MN. For instance, the presence of multiple autoantigens in myasthenia gravis appears to be similar to what is now known in MN (Berrih-Aknin et al., 2014). In MG, 85% of the patients raise autoantibodies against the main component of the protein complex of the neuromuscular junction that is the acetylcholine receptor (AchR), another group of 5% raise antibodies against the muscle specific kinase (MuSK) and a third group of 2% against the lipoprotein related protein 4

(LRP4). A final group of 5% only recognize AchR when organized as a protein cluster, as it is present in the neuromuscular junction.

– Predominant IgG subclass

Another interesting feature of MN is the IgG4 subclass predominance with small levels of IgG1 and IgG3 autoantibodies, more specifically present in the early stages of the disease (Huang et al., 2013). In contrast, most systemic autoimmune diseases are mediated by circulating "classical" IgG subclasses (IgG1, 2 and 3), or IgM and IgA antibodies produced against one or several autoantigens (Berentsen et al., 2015; Ludwig et al., 2017), while a rather small number of autoimmune diseases are "IgG4–predominant" (Koneczny, 2018). Another interesting autoimmune disease sharing features with MN is Pemphigus Foliaceus, a skin disease involving desmogleins 1 and 3 as autoantigens (Warren et al., 2003) . Similar to MN, the early autoantibody response is mainly IgG1 and the development of the disease is dependent on a subclass switch to IgG4 autoantibodies. Interestingly, in myasthenia gravis, the predominant IgG subclass is IgG4 in MuSK–associated MG but IgG1 and IgG3 in AchR– associated MG and IgG1 in LRP4–associated MG (Berrih-Aknin et al., 2014). In both PLA2R1– and THSD7A–associated MN entities, IgG4 is clearly the predominant IgG subclass, which is in contrast with the secondary cases of MN and alloimmune MN where other IgGs are more present. Whether the remaining cases of primary MN (about 15–27%) for which the autoantigens are not yet identified are also IgG4–predominant or not is an open question.

– Role of gender in MN

In addition to the above factors, a gender effect may exist in patients with THSD7A–associated MN. A typical 2:1 male–female ratio is documented in the general MN population and in PLA2R1–associated MN cohorts (Beck et al., 2014; Cattran et al., 2008; Ronco et al., 2015). Interestingly, in our cohort of THSD7A–associated MN, we found a contrasting 1.3:1 male–female ratio (Chapter 4.1) as previously noticed in the initial study on THSD7A in MN (Tomas et al., 2014) and in a next study (Hoxha et al., 2017).

If we compare MN to other autoimmune diseases, the majority of autoimmune diseases are more prevalent in females while some others occur more frequently in males or do not show

prevalence bias for sex (Chiaroni-Clarke et al., 2016; Lamason et al., 2006). The underlying mechanisms responsible for the sex–biased autoimmune disease is not well understood. The immune response is gender–dependent, and females have an increased antibody production in response to infection while males exhibit more severe inflammation instead. The stronger antibody production in response to infection may also translate into a higher production of autoantibodies, irrespective of the autoimmune disease condition, thereby increasing the risk of development of autoimmune diseases. These different sexually influenced immune responses have been associated to age and the role of sex hormones. In MN, the higher prevalence for males (2:1 male–female ratio) is at odds of the above view, but can be partially explained by the late age onset of the disease and the fact that women have lower levels of proteinuria and lower blood pressure, participating to better outcome (Cattran et al., 2008). Thus, the manifestation of the clinical response in female patients with MN is often attenuated and this may explain the lower prevalence of MN in females.

Furthermore, the gender–based influence "by antigen" and "age onset" in autoimmune diseases is not unique to MN and gender dimorphism is evidenced in myasthenia gravis. Here, like what is now known for MN, the MG population of patients are classified into subgroups, according to the nature of the antigens and corresponding autoantibodies. As already mentioned above, in 85% of MG cases, autoantibodies target AchR, compared to 5% and 2% of patients having autoantibodies targeting MusK or LRP4, respectively. In an additional group of 5%, the autoantibodies recognize only the clustered AchR but not the receptor in its solubilized form. Interestingly, patients targeting the AchR are characterized by a female predominance at the early–onset of MG (at age of 50) (Carr et al., 2010) while patients at late–onset of MG (after the age of 60) are characterized by a male predominance (Alkhawajah et al., 2013). Patients between the age of 50 and 60 have no gender predominance. Moreover, patients with anti–Musk or anti–LRP4 are typically young females (Berrih-Aknin et al., 2014).

– Etiologies and environmental factors

The underlying etiologies and molecular mechanisms behind the autoimmune events triggering the loss of self–tolerance and the production of the corresponding autoantibodies are still largely unknown (Figure 5.4). Although MN can be considered as an organ–specific

disease, the initial site of exposure of the autoantigens to the immune system is also not yet identified, and in fact may not be the podocyte microenvironment. Studies on genetic factors increasing the risk to develop MN is likely the most advanced part, at least for PLA2R1, with polymorphisms identified on both the autoantigen and key molecules of the immune system involved in the autoimmune response, such as the HLA genes.

Conceptually, the autoimmune response to PLA2R1 or THSD7A may occur at distance from the podocytes, i.e. in a cellular microenvironment of any tissue (including thymus), where PLA2R1 or THSD7A may be already present or induced by inflammation or other triggers, and would become autoantigens because they would present to the immune system with a "non–natural" structure due to some conformational changes triggered by one or multiple etiological factors and detected by the immune system as a danger. As reviewed in the introduction, PLA2R1 and THSD7A are expressed in various tissues and cells such as alveolar macrophages in the lung, other immune cells, endothelial cells or thymic epithelial cells, or pre–tumoral epithelial cells where they play a likely role in inflammatory diseases or cancers, and this constitutes a non–exhaustive list of cellular microenvironments and disease conditions where such an autoimmune response may occur (Figure 5.3). In addition, the complex ternary and quaternary structure of both PLA2R1 and THSD7A may increase the risk to adapt a misfolded or aberrant conformation considered as "pathogenic" for the immune system. An alternative scenario would be the so–called mechanism of epitope mimicry, where the immune system originally produces antibodies against a pathogenic micro–organism, which in turn would cross–react with host molecules becoming autoantigens, because of protein similarities between the molecules. Finally, a last scenario would be that the complete maturation of PLA2R1 and THSD7A includes a number of –still unknown– highly specific post–translational modifications (PTMs) required for their –still unknown– biological functions, and that a defect or perturbation of such PTMs would lead to immunogenic and pathogenic conformations driving the autoimmune response and pathogenicity of MN, irrespective (or not) of their implications in any of the above disease conditions, hence appearing as a "purely idiopathic" disease. For instance, dysregulations in specific PTMs and associated enzymes have been involved in the autoimmune response towards the autoantigens involved in Goodpasture's kidney disease (collagen IV) (Vanacore et al., 2011) and rheumatoid arthritis (multiple citrullinated autoantigens) (Darrah et al., 2018). Of note, the enzymes involved in such

PTMs are regulated by inflammation and other disease conditions such as cancer (Yuzhalin, 2019). Interestingly, in this scenario, various types of autoantibodies targeting not only the antigens but also the PTMs enzymes can be detected in a subset of patients many years before disease onset (Derksen et al., 2017; McCall et al., 2018). In sum, the central question about the etiology of MN associated with either PLA2R1 or THSD7A and currently qualified as "primary/idiopathic" MN, is to determine whether there is a unique etiological factor (environmental factor?) associated with a unique molecular mechanism (PTM?) "at play" for each autoantigen, which would lead to the same autoimmune response, or whether the causes of PLA2R1– and THSD7A–associated MN are multiple and differ between patients (age, sex, genetics, etc.), with variable autoimmune responses.

With the above concepts in mind, and despite the fact that the discovery of PLA2R1 and THSD7A in MN was respectively 10 and 5 years ago, our knowledge on the etiology of primary MN is still very partial and puzzling. Besides the increased risk of PLA2R1–associated MN attributed to genetic polymorphisms in PLA2R1 and HLA–D alleles, epidemiological studies have proposed that environmental pollutant particles may be a cause of increased MN in China, where PLA2R1 might become an autoantigen after exposure of lung cells to small particulate matters (<2.5 μm) present in airborne pollutants (Xu et al., 2018; Zhang et al., 2018). Similarly, smoking has been proposed as another risk factor of MN in Japan (Yamaguchi et al., 2014). Based on protein sequence identity between the CysR domain of PLA2R1 and a protein present in the cell wall of several bacteria, a mechanism of molecular mimicry following the exposure to a microorganism has been proposed by Fresquet et al (Fresquet et al., 2015; Zhang et al., 2018).

Furthermore, MN disease is associated with many other diseases including various types of cancer and infections, other autoimmune diseases and syndromes, defining either secondary MN or being one or more underlying causes (or at least providing the cellular context) to develop primary MN, yet the causality between the two diseases remains a major debate. For instance, various types of chronic viral infections (HBV, HCV, HIV) and bacterial infections (tuberculosis, syphilis, Helicobacter, etc.) or allergies are associated with MN (Long et al., 2018) while PLA2R1 may play a role in such conditions (Nolin et al., 2016; Yokota et al., 2000). Similarly, cancer could be a specific cause of MN (Lefaucheur et al., 2006) while both PLA2R1 and THSD7A may play a role at various stages of tumorigenesis (Augert et al., 2009; Augert et al., 2013; Vindrieux et al., 2013).

More specifically, the incidence of THSD7A–associated MN has been linked with malignancy (Beck, 2010; Hoxha et al., 2017; Hoxha et al., 2016; Lin et al., 2018), but this remains controversial as MN is in general associated with cancer and may be more co–incidental than causal. A recent study reported that 20% of the THSD7A–positive MN patients had an associated malignancy within a median time of 3 months from diagnosis of MN suggesting that THSD7A–associated MN patients are at higher risk of having an underlying malignant disease (Hoxha et al., 2017). In our study, we thoroughly analyzed the clinical history of our patients and we could only report 16% of cancer cases of which only 6% had MN in the 2 years period preceding MN diagnosis (Chapter 4.1). However, we had in our study one female patient with a thymoma whose the surgical resection led to remission of MN. Our results contrast with studies suggesting that THSD7A detected in malignant tumor tissue might serve as the trigger of the autoimmune response and reported that tumor treatment leads to depletion of anti–THSD7A antibodies in circulation. (Hoxha et al., 2017; Hoxha et al., 2016; Stahl et al., 2017; Wang et al., 2019). Overall, these findings could provide one etiological mechanism leading to THSD7A–associated MN but this does not exclude other possible mechanisms at play. The same may be true for PLA2R1, since about 9% of PLA2R1–associated MN patients develop malignancies (Timmermans et al., 2013). We thus proposed that cancer and THSD7A–associated MN occurrence may be co–incidental or linked with ageing for most cases. However, for some cases, the development of a cancer may provide the micro–environment for the initiation and progression of an autoimmune response, with the tumor tissue playing a role as a tertiary lymphoid structure (hence the removal the tumor tissue by surgery will have a direct impact on autoantibody levels and clinical remission of MN).

Here also, the possible link between malignancy and MN is not unique as many other autoimmune diseases are associated with cancer in a bilateral manner (Giat et al., 2017). On one hand, the autoimmune disease can increase the risk of malignancies or on the other hand some malignancies can increase the risk of development of autoimmune diseases. For instance, among others, patients with rheumatoid arthritis have increased risk of malignancies (Smitten et al., 2008). The development of the autoimmune reaction may be due to the generation of autoantibodies targeting oncoproteins, proliferation associated antigens, etc. (Abu-Shakra et al., 2001).

5.2 Immunological phase of THSD7A–associated MN

5.2.1 Epitope profile

In autoimmune diseases, the dysregulation of the immune system causes the rise of autoantibodies against endogenous antigens. To enhance the antigen recognition, improve the neutralization function of the autoantibodies and to increase the efficiency of the immune response, a mechanism of epitope spreading occurs (Cornaby et al., 2015; Di Zenzo et al., 2011; Li et al., 2003) (Figure 5.4). This mechanism is characterized by the concerted development of the B– and T–cell response leading to a diversification of the epitopes recognized by the immune system from one initial immunodominant epitope to several secondary epitopes. Such spreading can progress among multiple epitopes on a single antigen (intramolecular spreading), or from one antigenic molecule to others (intermolecular spreading). We aimed to improve the understanding of the pathophysiological mechanism of MN by characterizing the autoantibodies targeting epitopes on THSD7A and their diversification which might rely to a mechanism of epitope spreading.

We tested the reactivity of 38 THSD7A–associated MN patients against a series of 11 deletion constructs of THSD7A by ELISA and we identified up to 10 distinct epitopes regions on THSD7A, differentially recognized by each patient (Chapter 4.2). The highest prevalence of reactivity was found against D1–D2 (74%) followed by D9–D10 (58%) and D13–D14 (47%). Interestingly, the anti–THSD7A titer increases together with the number of recognized epitopes. There was no evidence for any association between epidemiological or clinical characteristics and the number of recognized epitopes. Similar results were found when Seifert et al. analyzed a cohort of 31 THSD7A–associated patients for epitope profiling by western blot (Seifert et al., 2018). Although they provided important insights on the extracellular domain structure of THSD7A and the epitope regions, some limitations ought to be mentioned in their experimental approach. Indeed, we previously showed that although western blot is as sensitive detection technique, it remains only semi–quantitative and does not allow a measurement of epitope–specific titer. Furthermore, the positivity for some epitopes is possibly jeopardized by the transfer conditions of the assay including the denaturing conditions due to SDS and boiling (even in non–reducing conditions). Additionally, the reactivity of patients' sera to the different epitope regions was tested at a

serum dilution of 1:100. Knowing that full anti–THSD7A titer in that cohort ranged from 1:10 to 1:3200, it is likely that the 100 times serum dilution is not optimal for all the different serum samples and the use of more concentrated serum is probably limited by the amount of serum available. Overall, we believe that the use of ELISA for epitope determination in our work holds more potential in comparison to western blot, ending up with a more comprehensive picture of the autoimmune response in patients with THSD7A–associated MN.

5.2.2 Epitopes and immunodominance

We observed in our cohort that the difference in the percentage of recognition (prevalence) of D1–D2 (74%) versus D9–D10 (58%) epitopes was rather small. We also evidenced that for patients with single epitope positivity, the main targeted epitope was either D1–D2 or D9–D10. Based on these observations, we investigated for the first time the hypothesis of having 2 major immunodominant epitopes in THSD7A. Besides studying the prevalence by direct ELISA on each epitope domain, we used competition ELISA assays to address which epitopes might be the most immunodominant, i.e. responsible for the major part of the total immune reactivity when measuring anti–THSD7A titer using full THSD7A as antigen. Our results show that patients with THSD7A–associated MN can be divided into four "immunodominant groups" based on competition assays measuring which epitope drives the strength of the immune response and direct ELISA assays measuring which epitope is the more prevalent. It appears that D9–D10 is the major immunodominant epitope domain driving the autoimmune response for 40% of the patients followed by D1–D2 for 34% of the patients. In 9% of patients, the autoantibodies targeted almost equally D1–D2 and D9–D10. We thus defined 3 groups of patients referred to as "the immunodominant groups", with antibodies targeting either D1–D2 or D9–D10 or both immunodominant epitopes. Interestingly, most of these patients have high titers, associated with disease activity and clinical outcome. In the last group of patients representing only 7%, the autoantibodies could also target D1–D2 or D9–D10, at least for some patients, but none of the two epitopes appeared to be immunodominant compared to other epitopes such as D7–D8, D11–D12, D13–D14. We called this group the "non–immunodominant group". Interestingly, all but one patient had low titers.

Together, this suggests that titer increase is driven by positivity towards an immunodominant epitope, followed by proliferation of the B cell clones raised against this epitope and increased production of the corresponding antibody. Along with the production of additional B cell epitopes, this would define a mechanism of epitope spreading. We did not see any significant difference between patients in the three immunodominant epitope groups. Nonetheless, patients in the non–immunodominant group had significantly lower titer and seem to have a milder disease when compared to patients in the immunodominant groups.

One might ask why it is important to identify the immunodominant epitope region on the autoantigen. As mentioned above, many etiologies could trigger the autoimmune reaction in MN. Our findings led to the hypothesis that two distinct epitopes in THSD7A can be not only the initial targets of the immune system but also the epitopes driving the autoimmune response with increased titers. The presence of two different immunodominant epitopes characterizing two groups of patients suggests two different etiological events of the autoimmune response, may be associated with differences in the genetics of patients driving the autoimmune response against either D1–D2 or D9–D10. For instance, can we observe that a difference in the immunodominance profile between patients with malignancy–associated MN and others? A further validation of these results in larger and well–characterized cohorts of THSD7A–associated MN is needed as we describe for the first time an emerging theory on immunodominant epitopes for THSD7A.

5.2.3 Epitope spreading in THSD7A

The progression of the autoimmune response in PLA2R1–associated MN has been proposed to be associated with a mechanism of epitope spreading (Figure 5.4). In a recent study, our laboratory showed that 33% of the patients recognized only the CysR domain of PLA2R1 with evidence for epitope spreading towards CTLD1 and CTLD7 (Seitz-Polski et al., 2016). We also showed that patients called "spreaders" i.e. with spreading towards CTLD1 and CTLD7 had a poor clinical outcome compared to non–spreader patients (Chapter 4.3).

In the previous study for patients in THSD7A–associated MN, a mechanism of epitope spreading did not come up, at least it was not as evident as for PLA2R1–associated MN

(Seifert et al., 2018). In our study, we found that among 38 patients, 5 patients (13%) had single epitope positivity against D1–D2, D9–D10 or D11–D12, which are the two immunodominant epitopes, and patients had low titer at this point. In most of the remaining patients, their positivity for either of the two immunodominant epitope domains D1–D2 or D9–D10 associated with reactivity towards additional epitope domains and an increase in titer suggested that a mechanism of spreading does occur by both "interdomain spreading" towards secondary epitopes present in almost all other domains of THSD7A and "intradomain epitope spreading" on either of the two immunodominant epitope domains, i.e. D1–D2 or D9–D10, this latter event being likely the main driver of the autoimmune response. Our last small group of patients considered as "non–immunodominant" would be the ones who did not yet had full epitope spreading (i.e. with activation of B cells towards the immunodominant epitope domains) or who were in immunological remission. The fact that the immune reaction seemed spread to multiple epitopes in most of our patients could be explained by an early occurrence of epitope spreading which renders documenting the early pathophysiological events more challenging, as observed previously in autoimmune bullous diseases (Didona et al., 2018).

From a different perspective, the epitope spreading may be demonstrated by looking at reverse spreading from multiple epitopes (ex. CysRCTLD1 in PLA2R1) back to the initial immunodominant epitope (ex. CysR in PLA2R1). This was illustrated in the analysis of the GEMRITUX cohort of PLA2R1–associated MN after treatment with rituximab (Chapter 4.3). In this analysis, we observed that the number of epitopes on PLA2R1 at baseline significantly decreased in patients receiving rituximab treatment after 3 and 6 months. The results showed a reversal of the epitope spreading accompanied by a decrease of anti–PLA2R1 titer after treatment with rituximab (Chapter 4.3).

As for THSD7A patients, we could illustrate a reversal of epitope spreading in the case of the patient MN13 (Figure 5.1). At baseline, the patient had high anti–THSD7A titer and autoantibodies targeting D1–D2, D9–D10, D7–D8 and D19–D21. Upon treatment with rituximab, anti–THSD7A and the epitope antibody titers decreased simultaneously. Following a second rituximab treatment, the anti–D9–D10 titer remained detectable and followed the same evolution trend of the anti–THSD7A titer while the titer for anti–D1–D2 decreased to undetectable levels.

Our observations are further documented by Seifert et al. where they examined the anti–THSD7A antibody levels and the epitope profiles in serial serum samples from16 THSD7A–associated MN patients (Seifert et al., 2018). Interestingly, patients with decreasing anti–THSD7A titer show a reverse spreading towards the immunodominant epitopes (D1–D2 and D9–D10). These preliminary findings suggest that epitope spreading does occur in THSD7A–associated MN patients but this needs to be confirmed in larger in particular prospective cohorts of patients with THSD7A–associated MN.

The identification of the epitope regions and the corresponding anti–THSD7A titer allowed to observe some discrepancies: 1) Patients can have similar epitope profiling yet considerably distinct anti–THSD7A titer, and conversely 2) Patients can have different epitope profiles but comparable anti–THSD7A titers. The first case is exemplified by patients MN1 and MN17 with an epitope profile D1–D2 and D9–D10 yet with anti–THSD7A titer of 13920 RU/mL and 545 RU/mL respectively.

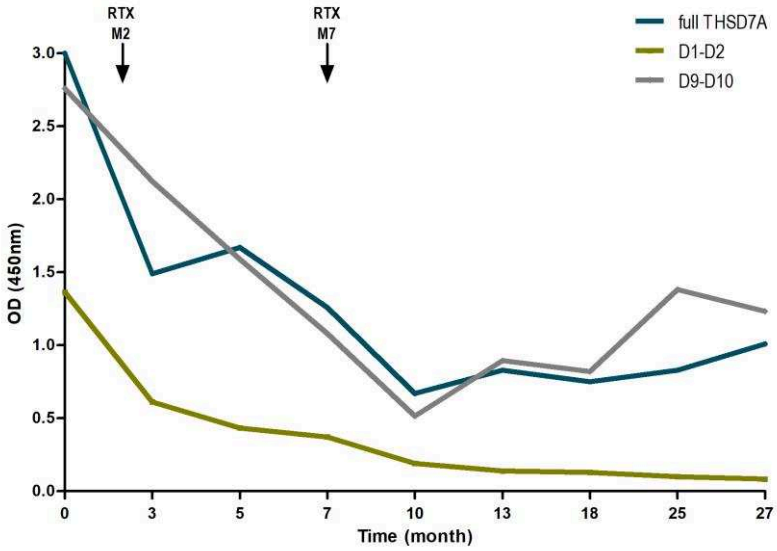

Figure 5.1 – Epitope reversal during follow–up in MN13. Graph illustrating the evolution of the OD_{450nm} of antibodies targeting full THSD7A, D1–D2 and D9–D10. The patient MN13 had nephrotic range proteinuria at baseline and received 2 courses of rituximab at months 2 and 7. At baseline, the patient had high anti–THSD7A titer and was positive for anti–D1–D2, D9–D10 and D7–D8, D19–D21 (not shown). Following the first course of rituximab, anti–D1–D2 decreased and reached undetectable levels after the second course of rituximab in month 7. Anti–D7–D8 and anti–D19–D21 disappeared after the first course of rituximab. D9–D10 decreased after the 2 rituximab treatments and followed the full THSD7A titer changes. Of note, the slight increase in full THSD7A titer between month 18 and 27 was accompanied by an increase of anti–D9–D10 titer.

Here, we suggest that the patients have antibodies targeting not only the “macro–epitopes” (D1–D2 or D9–D10) but also several “micro–epitopes” on each of the two epitope regions. In this case, it is possible that an “intra–domain” epitope spreading occurs and this would explain the increase of full anti–THSD7A titer without the increase in the number of targeted epitopes in some patients.

A similar phenomenon has been documented for myeloperoxidase, a dimer of two subunits of 70 kDa identified as one of the main autoantigens in ANCA disease. The tridimensional structure showed that one subunit of MPO consists of one heavy (59 kDa) and one light (13.5 kDa) chain, making the full protein as a homodimer of two subunits, each consisting of two chains. Interestingly, seven epitope regions have been identified on the surface of the protein among which 6 are localized on the heavy chain of MPO and the remaining epitope is in the pro–peptide region. Furthermore, it is suggested that epitope spreading produces the disease–causing antibodies (Land et al., 2014; Roth et al., 2013). These findings demonstrate the possibly of epitope spreading can occur within a globular protein and cannot necessarily be limited to one epitope per domain. The investigation of the “micro–epitopes” regions on D1–D2 or D9–D10 can be important to further understand the development of the immune response yet is challenging as these antibodies only recognize conformational epitopes.

As for the second case, it is illustrated by the patients MN19 and MN20 having close anti–THSD7A titer (376 RU/mL and 302 RU/mL respectively) but different epitope profiles (1 epitope vs. 5 epitopes). In this context, one might question the pathogenic power of the same total concentration of antibodies but with different antibody composition, i.e. is the pathogenicity the same for "monoclonal" antibodies targeting the same immunodominant region compared to that of "polyclonal" antibodies targeting many immunodominant and non–immunodominant epitopes, when the total concentration of antibodies would be the same. In a passive HN rat model, Allegri et al. studied the formation of electron dense immune deposits by monoclonal versus polyclonal anti–gp330 autoantibodies (Allegri et al., 1986). Polyclonal antibodies induced subepithelial immune deposits while monoclonal antibodies where unable to produce such immune deposits, even when injected at high doses. In other words, these findings suggest that patients with epitope spreading evidenced by multiple reactivities ("polyclonal antibodies") on THSD7A may have a more

severe disease and a poorer prognosis, as compared to those with no spreading reactivity towards multiple epitopes ("monoclonal antibodies").

Studying the epitope spreading and the cascade of the targeted epitopes may be of important clinical value. In human autoimmune diseases, the link between epitope spreading and clinical severity is not always demonstrated. This could be due to the small cohort sizes to evaluate this phenomenon or because the epitope spreading reaction has already largely matured at the time of serum sampling at diagnosis, when the patient has already the clinical signs of the disease, in our case, MN. Therefore, the detailed description of the full mechanism of epitope spreading is difficult to collect from already sick MN patients, and one need to have access to serum samples from patients in the preclinical stages, months or years before the onset of MN disease (Joshi et al., 2018), or develop experimental animal models to bring new knowledge. In an autoimmune encephalomyelitis animal model for multiple sclerosis, reactivity against myelin epitopes mediates the disease relapse (McRae et al., 1995). Moreover, blockage of the co–stimulation of B and T cells by anti–CD154 antibodies disturbed the CD40–CD154 interaction could block the spreading mechanism and impair the clinical expression of the disease (Howard et al., 1999). Also, in a type 1 diabetes mouse model, the progression of the disease is associated with the diversification of the autoimmune response against insulin beyond the dominant initiating epitope Ins B9–23 (Prasad et al., 2012).

5.2.4 In Vivo Experimental Epitope Spreading for THSD7A

We injected human THSD7A in rabbits with the idea that this immunization procedure would mimic the mechanism of autoimmune response and possibly epitope spreading that occurs in humans, even though the THSD7A antigen is not from rabbits and it is thus not an autoimmune response with loss of immune tolerance. At day 0, 2 rabbits received a primary injection of 30 μg of the full extracellular region of recombinant human THSD7A in complete Freund's adjuvant. After 21, 42 and 63 days, the rabbits received boosts of 20 μg of THSD7A in incomplete Freund's adjuvant. We collected serial serum samples during immunization and analyzed their titer and epitope profile for hTHSD7A reactivity as performed with our cohort of patients with THSD7A–associated MN (Figure 5.2–A).

Our preliminary data showed that each rabbit developed a strong but different immune response against hTHSD7A (Figure 5.2). Anti–THSD7A antibodies were detectable as soon as 11 days post–injection in both rabbits and remained in the circulation until day 95 (Figure 5.2–BD). We observed that although the two rabbits responded by targeting different epitopes on THSD7A, the immune response targeted epitopes in both the N– and C– terminal ends of THSD7A. These results are in contrast with those found by Seifert et al. where three rabbits were co–immunized with human and mouse THSD7A. In their study, the rabbits were not injected with recombinant proteins but with 12 mg of plasmid expression vectors coding for full–length human and mouse THSD7A (i.e. membrane–bound), conjugated to gold particles and not injected with complete Freund's adjuvant. Four injections were performed each 3 to 6 weeks, indicating a long immunization procedure with 3 repeated boosts. Rabbit serum was not analyzed over the time of immunization but only at 3 weeks after the last immunization. Interestingly, two rabbits reacted only against the N–terminal end of THSD7A and one rabbit reacted against both the N– and the C–terminal end (Seifert et al., 2018).

The divergence between these two studies could be explained by differences in the nature of the antigens injected and the immunization protocol, which may result in the exposure of different epitope regions to the immune system. Indeed, the three–dimensional structure of THSD7A likely differs when present at the cell surface or as a free antigen in solution. However, in the study by Seifert et al., it is also possible that the membrane–bound THSD7A is cleaved and produced also as a secreted soluble antigen. Furthermore, Seifert et al. co–injected mouse and human THSD7A, which may significantly modify the pattern of the immune response while they were not analyzing the direct immune response to each antigen versus the cross–reactivity of antibodies present in rabbit sera towards each antigen. Finally, the strong immune reaction observed in our study might be caused by the complete Freund's adjuvant having the highest immunostimulatory effect among other adjuvants (Stills, 2005) and which was used by Heymann and colleagues in the active model of MN for megalin (Heymann et al., 1959). Seifert et al apparently did not use any adjuvant in their procedure.

Overall, by investigating the immune response to THSD7A and the epitope profile in rabbits over 95 days, we illustrated the kinetics of the immune reaction against THSD7A and a potential mechanism of epitope spreading.

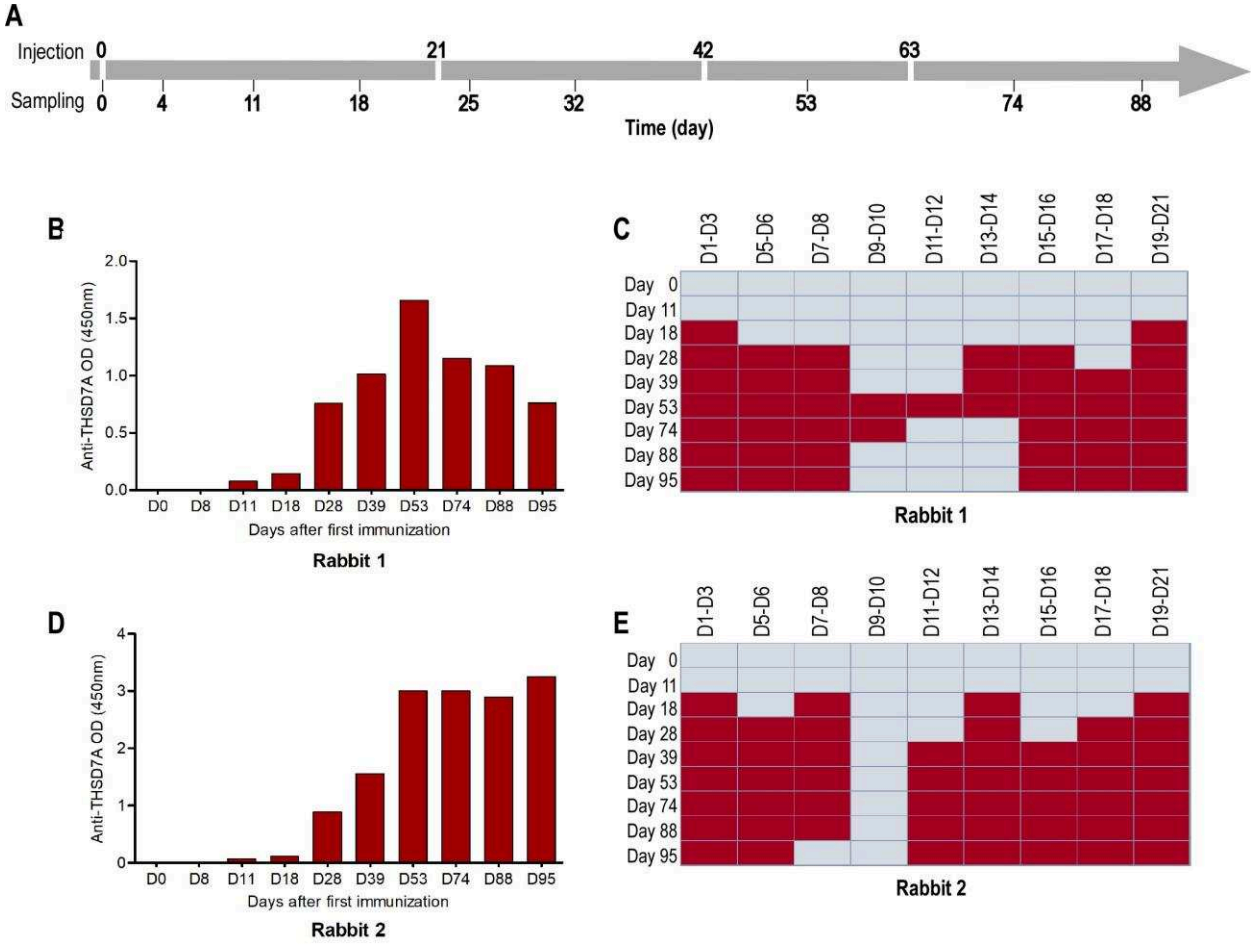

Figure 5.2 – Immune response and THSD7A epitope domains recognized by rabbit sera over the time course of immunization with human THSD7A. The yellow areas indicate positive reactivity to the domain while the blue areas indicate no reactivity for the domains. (A) Timeline of the *in vivo* immunization of 2 rabbits with human soluble recombinant THSD7A. At day zero, 2 rabbits were injected with 30 μg of recombinant human THS7DA in complete Freund's adjuvant. Boosts received at days 21, 42 and 63 consisted of 20 μg of the same recombinant THSD7A in incomplete Freund's adjuvant. Serum sampling were performed at the indicated times below the timeline. (B and D) Bar graph showing the kinetics of rabbit 1 and 2 serum reactivity towards the full THSD7A by ELISA. (C and E) Heatmap illustrating the kinetics of rabbit 1 and 2 serum reactivity towards the different THSD7A constructs. The reactivity was evaluated by ELISA with affinity–captured soluble constructs of THSD7A on immobilized anti–HA or anti–Flag antibodies, as for analysis of patients with THSD7A–associated MN.

We observed that the variation of the anti–THSD7A titer is associated with variation of the epitope profiles in the two rabbits. In rabbit 1, we observed an increase in anti–THSD7A titer correlated with an increase in the number of epitopes recognized on THSD7A between day 11 and day 53. The subsequent decrease in the anti–THSD7A titers after day 53 seems to be in line with the loss of recognition of 3 epitope domains (Figure 5.2–BC). Similar results were obtained in rabbit 2 between day 11 and day 39 but interestingly, the increase in anti–THSD7A titer between day 39 and 53 did not induce further epitope recognition since almost all the epitopes on THSD7A were already targeted (except 1 domain). We would explain these observations by an increased titer due to "intra–domain" spreading as proposed in results obtained in humans (Figure 5.2–DE).

In summary, our current data in this *in vivo* epitope model are still very preliminary at this point and rely on only 2 rabbits. At present, they depict the immune reaction against an exogenous antigen and did not allow the identification of the immunodominant epitope domain(s). In the long run, to investigate the specific contribution of the different epitope domains in the pathogenesis of THSD7A–associated MN and to study the epitope spreading *in vivo* with relevance to the autoimmune reaction, it would be ideal to challenge the immune response by immunizing rabbits with rabbit THSD7A domains (D1–D2 or D9–D10) while inducing a loss of tolerance with specific adjuvants. By doing so, rabbit would develop antibodies targeting the injected rabbit THSD7A which would then bind to endogenous THSD7A on podocytes and lead to podocyte injury.

This approach was used by Shah et al. to evidence a mechanism of intramolecular epitope spreading within megalin and show its role in the pathogenesis of active Heymann nephritis (Shah et al., 2007; Tramontano et al., 2006). In their studies, they immunized rats with either various recombinant forms of rat megalin as antigens and in the last most demonstrative experiments of in vivo spreading, they injected only the relatively small rat L6 fragment present in the first N–terminal LBD of rat megalin. Of note, they likely used the strong immunogenic properties of the "boosted" complete Freund's adjuvant originally used by Heymann and colleagues to break tolerance when injecting rat antigens to rat animals (Heymann et al., 1959). Four weeks after of the initial injection, rat sera reacted uniquely against the L6 fragment. However, 8 weeks post–injection, rat sera reacted against the 4 main LBD domains of megalin. Hence, they could prove that the reactivity against the L6 fragment induced a mechanism of epitope spreading starting by an initial

response against the immunodominant epitope domain (L6) and then spreading on the endogenous protein to secondary LBD epitope domains.

5.3 Pathological effector phase

As an organ–specific disease, the pathological effector phase of MN concerns the reaction of autoantibodies with their cognate antigens including 1) the direct pathogenic effects of anti–PLA2R1 and anti–THSD7A antibodies on podocytes, 2) the mechanisms of immune deposit formation *in situ* on podocytes and the glomerular basement membrane, and 3) complement activation likely inducing podocyte injury, proteinuria and finally leading to end stage renal disease (Figure 5.4).

It is well established that autoantibodies of IgG4 subclass are predominant in idiopathic MN. (Beck et al., 2009; Hofstra et al., 2012; Tomas et al., 2014; Zaghrini et al., 2019). We further confirmed these results in our study with 49 patients with THSD7A–associated MN and found that 88% of patients had IgG4 antibodies compared to 14, 18, and 20% for IgG1, IgG2, and IgG3 (Chapter 4.1). The major question is whether the IgG4 antibodies are pathogenic by themselves or if their apparent pathogenic effect is in fact due to the effect of the small amounts of other IgGs (Tomas et al., 2016) such as IgG1 or IgG3, yet these subclasses are not present in all patients, and are in fact more present in secondary cases of MN. Furthermore, if IgG4 autoantibodies are truly pathogenic, then what is their pathogenic pathway? A first hypothesis may involve a direct effect of IgG4 upon binding to the autoantigen target, by blocking or perturbating its (still unknown for PLA2R1 and THSD7A) physiological function, or by inducing its internalization and degradation. In this context, disruption of the antigen function would impact on the glomerular filtration barrier structure and lead to proteinuria. The second hypothesis would include the activation of the complement pathway by IgG4 autoantibodies knowing that IgG4 normally is unable to bind the complement components.

5.3.1 Pathogenicity of anti–THSD7A

THSD7A is a transmembrane protein proposed to be involved in cell adhesion (Wang et al., 2010). Tomas et al have shown that the intravenous injection of purified anti–THSD7A

autoantibodies (all anti–THSD7A IgG subclasses purified on a THSD7A affinity column) in mice affected the cellular architecture of the THSD7A expressing cells and induced proteinuria without evidence for complement activation (Tomas et al., 2016). This suggests that the function of THSD7A on the podocytes is crucial to maintain the structure of the slit diaphragm and that binding of the autoantibodies to THSD7A in MN disrupts the adhesion of podocyte foot processes on the glomerular basement membrane and leads to their retraction and increased proteinuria.

In other autoimmune diseases such as pemphigus vulgaris and myasthenia gravis, a pathogenic role of IgG4 has been proven by passive transfer studies. In pemphigus vulgaris, Dsg3 plays a crucial role in cell adhesion of keratinocytes within the deep stratified squamous epithelium. The knockout mouse model of Dsg3 showed spontaneous erosion of the skin with lesions similar to those observed in pemphigus vulgaris. The pathogenicity of IgG4 anti–desmoglein antibodies is probably caused by interference with the adhesion function of Dsg3 leading to loss of cell adhesion (Koch et al., 1997). On the other hand, in myasthenia gravis, muscle–specific kinase (MuSK) is a receptor tyrosine kinase required for synaptic differentiation and maintenance. Synapse formation and AchR clustering is controlled by neuronally released agrin that binds to LRP4 causing this latter to bind and activate MuSK. Once tyrosine–phosphorylated, MuSK recruits additional signaling molecules essential for synapse formation. Anti–MuSK IgG4 inhibited the interaction between LRP4 and MuSK and reduced agrin–induced AChR closeting *in vitro* (Koneczny et al., 2013). Furthermore, injection of anti–MuSK–positive patient IgG in mice downregulates MuSK signaling activity and the retention of junctional AChR in the postsynaptic membrane (Ghazanfari et al., 2014).

5.3.2 Shedding of THSD7A

The mechanism of immune deposit formation *in situ* on podocytes and the glomerular basement membrane likely requires shedding or proteolytic cleavage of the antigen from the cell surface of the podocyte. The proteolytic cleavage of the extracellular domain of membrane receptors or protein precursors or extrinsic membrane proteins is a physiological process observed in all cell types, and known as "ectodomain shedding" (Lichtenthaler et al., 2018; Werb et al., 1998). It is controlled by numerous types of proteases called

"sheddases" and allows the release and secretion of many adhesion molecules, receptors, cytokines, hormones or enzymes, and contributes to the cell to cell communication and remodeling of the cellular micro–environment under both physiological and pathophysiological conditions. In Heymann nephritis, binding of epitope–specific antibodies to megalin form immune complexes on the podocyte membrane. This is followed by shedding (through the regulated intramembrane proteolysis (RIP)) and fast immobilization of the complex in the glomerular basement membrane thus preventing clearing of these complexes by endocytosis of the podocyte. Repeated cycles of this mechanism lead to large immune deposit formation (Biemesderfer, 2006; Kerjaschki et al., 1987).

We have obtained preliminary data showing that membrane–bound THSD7A undergoes both constitutive and regulated cleavage or shedding in transfected HEK293 cells, with a truncated soluble fragment released in cell medium and a short transmembrane fragment still embedded to the plasma membrane (Figure 5.3). As soon as membrane–bound THSD7A is expressed in HEK293 cells, it is constitutively shed *in vitro* at least in one site. This cleavage occurs at the juxta membrane region generating a residual membrane fragment of 17 kDa which can be easily detected in a solubilized cell membrane preparation by western blot (Figure 5.3). Interestingly, the extracellular domain of THSD7A is not as readily detectable in crude cell medium but its detection requires more than 100–fold concentration of medium. These preliminary results were in agreement with previous findings from Kuo et al. who documented that HUVECs also release a soluble form of THSD7A implicated in cell migration and angiogenesis (Kuo et al., 2011).

In additional preliminary experiments, we demonstrated that membrane–bound THSD7A transfected in HEK293 cells is cleaved by ADAM10 and/or ADAM17. These enzymes belong to the ADAM family (a disintegrin and metalloproteinase) involved in the shedding of proteins along with other enzymes such as the MMP (Matrix Metalloproteinase) and the aspartic protease family (such as BACE1 the β–secretase responsible for cleavage of β–APP) (Uhlén et al., 2015). We observed that treatment of HEK293 cells expressing membrane–bound THSD7A with GW280264X, an inhibitor of the metalloproteinase ADAM10 and ADAM17 decreases the cleavage of THSD7A as evidenced by a decrease of the small intracellular 17 kDa fragment on western blot and by an apparent diminution of the shed extracellular domain by ELISA (data not shown).

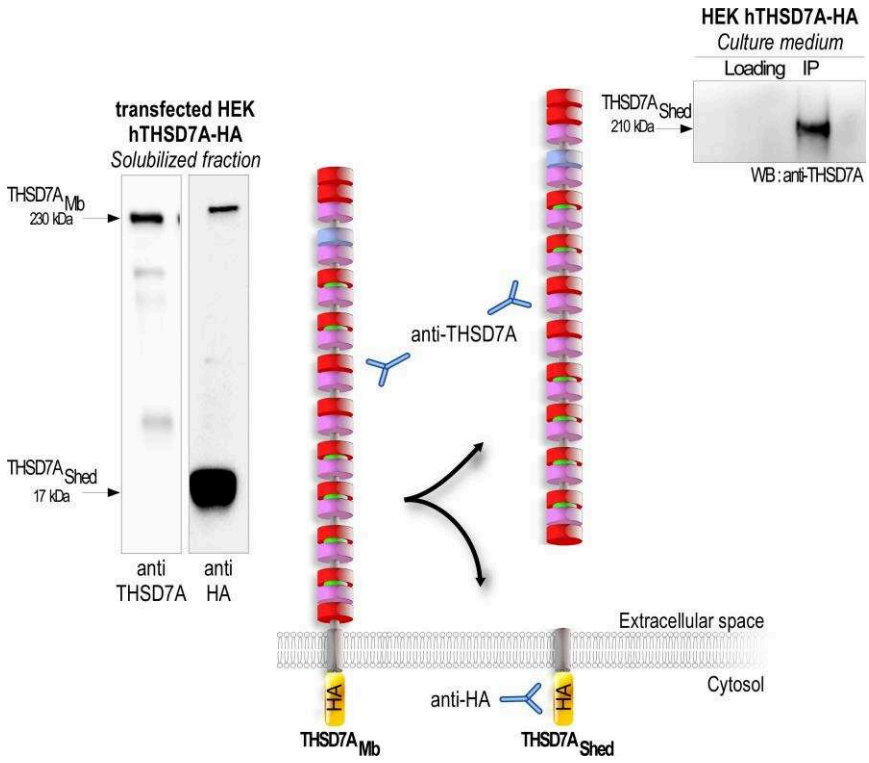

Figure 5.3 – Shedding of THSD7A *in vitro*. Membrane–bound THSD7A is cleaved by a mechanism of shedding in HEK293 cells. (Left panel) The cleavage results in two fragments of THSD7A detected by western blot: the full membrane form ($THSD7A_{Mb}$) of around 250 kDa detected using antibodies targeting the extracellular domain region and the intracellular membrane fragment ($THSD7A_{shed}$) detected at around 17 kDa only detected using antibodies targeting the HA tag inserted at the C–terminal end of the protein. (Right panel) The shedding of THSD7A also releases a soluble extracellular form of THSD7A of around 230 kDa in the culture medium. This form is only detected after affinity–capture and concentration on a Wheat Germ Agglutinin column that binds N–glycosylated proteins such as THSD7A. "Loading" is the crude culture medium and IP is the result of affinity–capture from 4.5 mL of cell medium.

Knowledge gained on the mechanism of THSD7A shedding could be relevant to understand not only the pathogenic effect of anti–THSD7A but also the mechanism leading to immune deposit formation.

The expression of THSD7A at the podocyte level and its localization in the foot processes at the slit diaphragm (Gödel et al., 2015) and its possible role as an adhesion protein suggest a role in maintaining the ultrastructure of the glomerular filtration barrier. Knowing this, one can speculate that the shedding properties of THSD7A might be connected to its function as a cell adhesion molecule and its localization, with shedding

required to detach foot processes and allows membrane dynamics at the level of foot processes. For instance, the cleavage of THSD7A from the podocyte surface might be important for foot processes mobility along the glomerular capillary walls.

Irrespective of its function as an adhesion protein or not, shedding of THSD7A may fuel the glomerular basement membrane with more soluble antigen that will form with circulating autoantibodies the large immune deposits. A similar mechanism of shedding is likely to occur for the other membrane–bound antigens involved in MN, i.e. megalin (Biemesderfer, 2006), NEP (Kuruppu et al., 2014) and PLA2R1 (Higashino et al., 2002), and shedding has also been documented for these proteins.

5.3.3 Complement activation in MN

As reviewed in the introduction, one or more pathways of the complement system is/are activated in the pathogenesis of MN, but it is not clear whether one or more IgG subclasses of anti–PLA2R1 and anti–THSD7A autoantibodies are leading to complement activation (Figure 5.4). Since anti–PLA2R1 and anti–THSD7A autoantibodies are predominantly of the IgG4 subclass, one can ask whether these particular autoantibodies are pathogenic not only by themselves, but also by activating complement, and how. The hypothesis suggesting the activation of the complement by the IgG4 subclass is supported by the detection of C3, C4 and C5b–9 accumulation in the immune deposits and from the urinary excretion of C5b –9 (Salant, 2019). The presence of C4 suggests complement activation through the lectin pathway while the absence of C1q is consistent with the inability of IgG4 antibodies to bind C1q and activate the classical pathway(Kusunoki et al., 1989; Ma et al., 2013; Val-Bernal et al., 2011). It is noteworthy that MBL binds to acetylated glycans including N–acetyl–galactosamine (GalNAc) and N–acetylglucosamine (GlcNAc) and forms a complex with MASPs to bind and activate C4. In rheumatoid arthritis, it has been shown that galactose deficiency in the Fc domain of the IgG4 antibodies exposes GLcNAc residues, allowing lectin binding and activation of the MBL pathway (Malhotra et al., 1995).

Ongoing experiments mostly performed in the laboratory of Dr. Andreas Kistler from Zurich and in collaboration with our laboratory support a new mechanism by which anti–PLA2R1 IgG4 autoantibodies can activate the MBL complement pathway and induce podocyte injury (Haddad, Seeger, Brandt and Zaghrini et al, Manuscript in preparation).

Using human podocytes over–expressing PLA2R1 as an *in vitro* model of MN and a highly purified preparation of anti–PLA2R1 IgG4, it was shown that addition of these antibodies to podocytes induces cytoskeleton podocyte injury, including cleavage of synaptopodin and Neph–1, but only in the presence of complement. Further investigation showed that the IgG4 anti–PLA2R1 antibodies bind to MBL and activate the MBL lectin pathway, as demonstrated by the use of specific complement inhibitors. Strikingly, IgG4 antibodies from MN patients with high titers of anti–PLA2R1 have an altered N–glycosylation pattern, as measured by mass spectrometry analysis. In comparison, IgG4 antibodies from serum of healthy donors appeared normal. These in vitro findings were also supported in vivo on human biopsy of patients with MN showing increased staining for the complement receptors involved in the MBL pathway and decreased staining for synaptopodin and Neph–1.

Keeping in mind that other pathways of the complement system may be activated in MN associated with PLA2R1 and THSD7A when other subclasses of IgGs are more predominant or when patients are deficient for MBL (Bally et al., 2016; Hayashi et al., 2018; Ma et al., 2013; Yang et al., 2016), the above findings may depict a central pathway of MN pathogenesis involving the predominant IgG4 subclass present in most of not all patients with PLA2R1– and THSD7A–associated MN as well as in other "double negative" cases of idiopathic/primary MN and activation of the uncommon MBL pathway by a mechanism linked to galactose deficiency of IgG4 antibodies in MN patients. If confirmed, this will potentially have an important impact on the therapeutic approach for MN patients. Patients receiving immunosuppressive treatment reach indeed clinical and immunological remission but with a delayed period because of the persistence of immune deposits (Beck et al., 2011; Salant, 2019). During this period, there is continuing podocyte injury and glomerular basement alteration thus limiting the restoration of the normal filtration barrier structure. By suppressing activation of the MBL pathway, this persistent injury will be immediately blunted, until the complete elimination of circulating autoantibodies by immunosuppressive therapy.

Most of the above results have been obtained so far for PLA2R1–associated MN but it is most likely that the same mechanism would be at play for patients with THSD7A–associated MN, since anti–THSD7A autoantibodies are also predominantly IgG4. The presence of MBL in the biopsy of patients with THSD7A–associated MN already supports this mechanism.

Overall, we have discussed here many of the key factors identified in THSD7A–associated MN and in other autoimmune diseases leading to the initiation and progression of the autoimmune response. In the scheme below, we propose a scenario of the pathophysiological events that might initiate the autoimmune response and lead to the progression of the disease (Figure 5.4). In the next section, we will be discussing the clinical advances in THSD7A–associated MN and propose a new serology–based classification for MN.

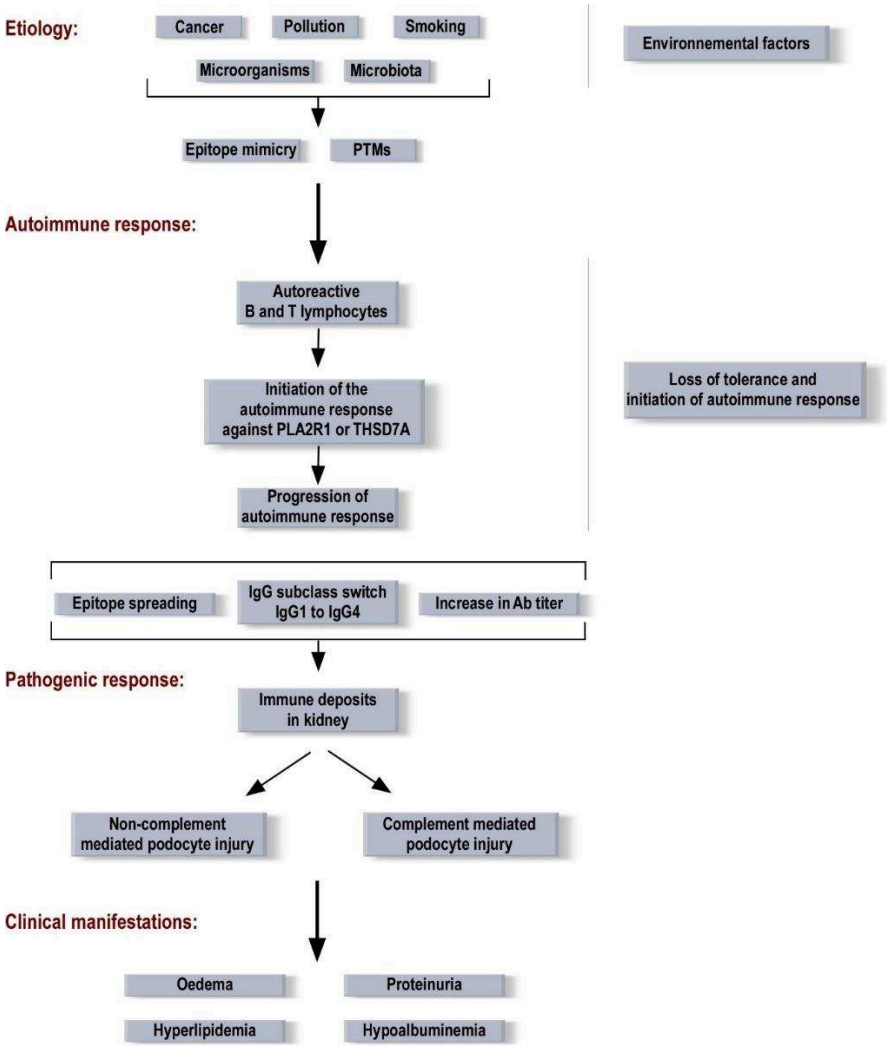

Figure 5.4 – Potential pathophysiological mechanisms of MN. Various environmental factors including cancer, pollution etc. might offer favorable conditions for triggering the autoreactive response of B and T lymphocytes through either epitope mimicry or difference in post–translational modifications (PTMs) of the autoantigens. After the initiation of the autoimmune reaction targeting either PLA2R1, THSD7A or other unknown autoantigens, progression of the autoimmune response is associated increased antibody titer, IgG subclass switch along with an increase of IgG4 autoantibodies and epitope spreading. Podocyte injury is achieved by complement and non–complement dependent mechanisms leading to proteinuria and other clinical manifestations as a consequence of this injury.

5.3.4 Clinical advances for THSD7A–associated MN

During this PhD, we reported the first ELISA that quantitatively measures anti–THSD7A titer in MN patients. We used this assay to screen 1012 biopsy–proven MN patients and identified 28 THSD7A–positive patients, which together with 21 additional patients, led us to establish one of the largest cohorts with 49 THSD7A–associated MN patients. This cohort allowed us to investigate in more details the clinical characteristics of THSD7A–associated patients, who represent only a minor subgroup of patients with MN, with a prevalence of 3%. There was no significant correlation between anti–THSD7A titer and proteinuria levels, yet there was an association with disease activity. This was similar to other studies on PLA2R1–associated MN patients where no or barely significant correlation between anti–PLA2R1 titers and proteinuria were found with larger populations (Hofstra et al., 2011; Hofstra et al., 2012). Overall, these quite unexpected results are explained by the lag time between the immunological activity defined by the circulating antibodies and the clinical disease activity mostly defined by proteinuria. This notion is best exemplified in patients undergoing complete remission after immunosuppressive treatment where antibody titer becomes undetectable several months before reaching levels of proteinuria in the non–nephrotic range (Beck et al., 2010).

Nonetheless, anti–THSD7A titers were high in patients with active disease compared to those in partial or complete remission, either after spontaneous or treatment–induced remission, showing that antibody titer correlates with disease activity. We also demonstrated that low anti–THSD7A titer at baseline predicted a better clinical outcome. Our results are in agreement with what was observed in PLA2R1–associated MN (Bech et al., 2014 ; Hoxha et al., 2014; Kanigicherla et al., 2013).

In summary, the results we obtained in this study demonstrated that anti–THSD7A titer is a relevant biomarker not only for diagnosis purposes but also to monitor disease activity during follow–up and in response to treatment, as well as for prognosis.

5.3.5 THSD7A epitopes as biomarkers of MN

The identification of PLA2R1 and THSD7A epitopes will help to better understand the molecular mechanisms of the autoimmune response but can also be helpful as additional

biomarkers of disease activity. There is no doubt that anti–PLA2R1 and recently anti–THSD7A are pertinent biomarkers of MN. High antibody titers appear to correlate with poor renal outcome in most cases but in some cases, high antibody titer may persist during clinical remission and conversely a decrease in this titer may not be associated with clinical remission (Hoxha et al., 2014; Seitz-Polski et al., 2014). Therefore, it is crucial to identify additional significant biomarkers for prognosis of MN and to stratify patient's response after treatment. Our study on the epitope profile of 58 PLA2R1–associated MN patients from the GEMRITUX cohort showed that the analysis of epitope profiling on PLA2R1 is a useful biomarker for early therapeutic interventions with immunosuppressors and confirmed that epitope spreading at baseline predicts poor outcome.

As for THSD7A–associated MN, we could not evidence a clear mechanism of epitope spreading, i.e. the path by which the immune system diversifies its response starting from an initial "monoclonal serum" targeting a likely immunodominant epitope to a "polyclonal serum" targeting multiple secondary epitopes. Although we observed a significant increase in anti–THSD7A titer in patients' sera targeting multiple epitopes compared to those targeting a single epitope domain, we could not evidence any clinical association to this difference. These findings were similar to the previous study by Seifert et al. (Seifert et al., 2018). Our results were likely underpowered due to the limited size of our cohort, and a larger cohort may be needed to demonstrate the relationships between titer, epitope spreading and disease activity as shown for PLA2R1–associated MN patients (Seitz-Polski et al., 2016).

The importance of epitope profile analysis was similarly demonstrated in other autoimmune diseases such as bulbous pemphigoid characterized by autoantibodies targeting the hemi–desmosome components BP180 and BP230. In a multicenter prospective study, Di Zenzo et al. showed that the levels of antibodies targeting the NC16A fragment of BP180 in addition to the C–terminal epitope region correlated with the disease severity. They also suggest that antibodies targeting the BP180 ectodomain are pathogenic compared to those targeting BP230 that seem to play a secondary role in the pathogenesis of the bulbous pemphigoid (Di Zenzo et al., 2008). Additionally, epitope specific on myeloperoxidase (MPO) in ANCA disease is required as certain epitopes on MPO were found to be specific for an active disease state while other epitopes remained present in remission states or in healthy individuals (Land et al., 2014; Roth et al., 2013).

5.3.6 Additional biomarkers of disease activity in MN

In addition to anti–PLA2R1 and anti–THSD7A as the main biomarkers of disease activity, we aimed to evaluate the potential use of autoantibodies targeting α–ENO (Bruschi et al., 2011), SOD2 and AR (Prunotto et al., 2010) as additional biomarkers and predictors of disease activity in MN.

In a collaborative work with Dr. GianMarco Ghiggeri in Genoa, we assessed the prevalence of autoantibodies targeting not only PLA2R1 and THSD7A, the membrane–bound autoantigens, but also alpha–ENO, SOD2 and AR, the intracellular podocyte autoantigens, in a large cohort of 285 MN patients (Ghiggeri et al, manuscript in preparation). We analyzed serum positivity for all five autoantibodies and we stratified the patients into 4 main subgroups based on their profile: the group A included patients PLA2R1+ and IC+ (positive for either alpha–ENO, SOD2 or AR), the group B for PLA2R1+ and IC–, the group C for DN (double negative) and IC+ and the group D for DN and IC–. In this study, we showed for the first time that a combined antibody positivity against PLA2R1 and the intracellular antigens is associated with poor outcome while the absence of both types of autoantibody is associated with better outcome.

It is noteworthy that unlike anti–PLA2R1 and anti–THSD7A, autoantibodies targeting the intracellular antigens are not exclusive to MN disease and are detected in other autoimmune diseases such as lupus. Also, the absence of alpha–ENO autoantibodies in the immune deposits indicates that they have distinct pathogenic effects (Kimura et al., 2017). Overall, our results showed that although the autoantibodies against podocyte intracellular antigens are not exclusive to MN, their evaluation has an additional diagnostic value.

5.3.7 Towards a serology–based classification of MN disease?

Historical classification of MN — Before the discovery of PLA2R1 and THSD7A and in fact even until now, patients with membranous nephropathy were classified as idiopathic or secondary MN based on careful clinical and pathological investigation. When no associated disease is found, MN is typically considered as idiopathic or primary (MN I), hence the cause of the disease is simply unknown. Primary MN represents about 85% of all MN cases. When an associated disease like cancer, infection or another autoimmune disease is

diagnosed, MN can be considered as secondary MN (MN II) (Couser et al., 1974), yet there is doubt between a true classification as MN I and II, since the other disease may be the cause of the disease (hence secondary MN) or simply co–incidental or even viewed as an aggravating factor but not as the true etiological cause. Secondary MN represents about 15% of all MN cases (Beck et al., 2014). Finally, classification into I and II MN can be oriented by biopsy staining of the immune deposits for IgG subclasses (irrespective of the antigen involved or known), with classification as I MN when the staining for IgG4 is predominant, and II MN when one or more other IgG subclasses are present (Huang et al., 2013; Makker et al., 2011; Ohtani et al., 2004).

Towards a serological classification of MN — When discovered, anti–PLA2R1 and anti–THSD7A autoantibodies have been found in patients with idiopathic MN with a respective prevalence of about 70% and 3–5%, with rare detection of autoantibodies in cases of II MN like lupus (Beck et al., 2009; Tomas et al., 2014). Later on, anti–PLA2R1 and anti–THSD7A autoantibodies were detected in various possible causes of secondary MN such as cancer (Hoxha et al., 2016; Larsen et al., 2013), hepatitis B (Xie et al., 2015) or sarcoidosis (Stehlé et al., 2015), but with a prevalence always lower than 20%. Thus, while detection of anti–PLA2R1 and anti–THSD7A appears as a preferential biomarker of I versus II MN, this is confusing. Another important feature of anti–PLA2R1 and anti–THSD7A is that none of these antibodies have been detected in any other disease conditions (Dähnrich et al., 2013; Zaghrini et al., 2019) like other glomerulonephritis or other autoimmune diseases (in fact as far as this has been checked) indicating that these antibodies are currently highly specific of MN disease, irrespective of known or unknown possible etiologies, i.e. primary versus secondary MN classification. In recent years, clinicians have considered that the serological analysis of anti–PLA2R1 and anti–THSD7A is an essential tool to investigate the type of MN and many introduced the notion of PLA2R1–associated and THSD7A–associated MN, somehow again irrespective of I versus II MN classification (Beck, 2017; De Vriese et al., 2017; Hoxha et al., 2017). Thus, the current trend is to classify MN no longer based on the historical I and II classification, but on specific serological assays detecting anti–PLA2R1 and anti–THSD7A antibodies, and thereby defining MN as PLA2R1–associated and THSD7A–associated. Obviously, patients should be still screened for any other associated diseases and patient's healthcare and treatment will be oriented by both detection of antibodies and other concurrent diseases. The classification of double negative

patients for both antibodies remains difficult and their MN can be considered as I (possibly due to a third unknown autoantigen?) or II (any other cause), and an exhaustive search for associated diseases should be performed "as in the past", before PLA2R1 and THSD7A were found as the key autoantigens.

Finally, because anti–PLA2R1 are highly specific for MN disease, a noninvasive approach based on the identification of circulating anti–PLA2R1 autoantibodies has been recently proposed (Bobart et al., 2019). The same may apply for anti–THSD7A autoantibodies. If the serological analysis is positive for one or the other autoantibodies, then the gold standard kidney biopsy may no longer be required for diagnosis of MN. If the patient is negative, then a biopsy will be required. This new diagnosis algorithm will be less costly and invasive, especially for patients at high risk of complications. This serological approach for diagnosis is in line with a new classification or stratification of patients in subgroups with either PLA2R1– or THSD7A–associated MN versus other cases with other unknown autoantigens or any secondary causes.

5.4 Conclusion

Membranous nephropathy is a rare autoimmune kidney disease but a major cause of nephrotic syndrome, representing about 20% of this latter. The identification of PLA2R1 as the main target autoantigen in 70% of patients with MN induced a paradigm shift in the field of MN. It was only a few years later that THSD7A was identified as the second autoantigen in 10% of the PLA2R1 negative MN patients, i.e. about 3% of all cases of MN. These discoveries provided a new impetus to better understand the pathogenesis of the disease and have been rapidly translated to clinical practice for improved patients' healthcare (Beck, 2017; Glassock, 2012; Ronco et al., 2015; Salant, 2019). However, many basic and clinical research questions remain unresolved. During this thesis, we tackled several of the key questions raised after the identification of THSD7A in MN.

We developed a novel ELISA assay allowing the quantification of circulating anti–THSD7A antibodies in serum and we established the largest cohort of THSD7A–associated MN patients to date (49 patients). This allowed us to thoroughly investigate the clinical characteristics of these patients and demonstrate the role of anti–THSD7A autoantibodies as biomarkers for diagnosis and prognosis of patients with THSD7A–associated MN. We demonstrated that the antibody titer correlates with disease activity and that high titer is associated with poor renal outcome, as shown in PLA2R1–associated MN.

We then identified the various epitope domains in THSD7A. For this, we designed and expressed in HEK293 cells 12 soluble deletion mutants of THSD7A spanning the full extracellular domain. We tested the reactivity of 38 THSD7A–associated MN patients for the different mutants by ELISA and identified up to 10 different reactive domains with different prevalences. Interestingly, we found that D1–D2 and D9–D10 domains were the most reactive domains for 74 and 58% of patients, respectively. We then investigated the immunodominance between these epitopes by competition assays against the full antigen. We presented a new model of epitope spreading mechanism with two immunodominant epitopes and spreading towards additional epitopes. The clinical impact of our finding is currently limited by the small cohort size and should be investigated in larger prospective cohorts of patients with THSD7A–associated MN.

In connection with this, I participated in the analysis of the epitope spreading in PLA2R1–associated MN patients. We could demonstrate here that epitope spreading is an

important prognosis tool and a predictor of poor renal outcome. which should be added to the therapeutic algorithm. Patients with low anti–PLA2R1 titer and a spreader profile should be treated with Rituximab at diagnosis without waiting for months, as suggested by the KDIGO guidelines, while patients with high anti–PLA2R1 titer but no spreading may be watched and only eventually treated with immunosuppressors.

In this work, we thus established new tools and biomarkers for the diagnosis and prognosis of patients with THSD7A– and PLA2R1–associated MN. We hope that these findings will be validated in further studies and will be implemented in clinical practice not only to improve diagnosis but also to better evaluate disease activity, towards more personalized medicine in MN. As for the pathogenic mechanism of antibodies and epitope immunodominance and spreading, it will be needed to validate our preliminary model in larger cohorts of MN patients as it was done in PLA2R1–associated MN. In future studies, it will be important to investigate why certain patients seem to develop a strong autoimmune response on D1–D2 while others develop a response on D9–D10. Whether these differences in epitope immunodominance reflect different etiologies of MN or are due to the genetic background of these patients, or to a different stage of the disease before a switch from one immunodominant epitope domain to another are open and challenging questions.

In the end, antibodies targeting PLA2R1 and THS7DA would provide a mechanism of the autoimmune response for only about 85% of idiopathic MN cases (this value will depend on the studied cohorts), including the rare cases of dual positivity for about 0.3% of MN cases. This still leaves a group of about 15% of idiopathic MN patients with an undefined MN disease, with patients "orphans" for the autoantigen(s) involved in their disease. Are these patients "false–negative" and misclassified with a PLA2R1– or THSD7A–associated MN (Debiec et al., 2011; Guerry et al., 2016; van de Logt et al., 2015), because of cut–off issues in ELISA detection assays or variations in antibody levels at the time of assays? (Liu et al., 2018; Tampoia et al., 2018) Or is their disease due to other autoantibodies, IgG4 or non–IgG4 and targeting other autoantigens, as in myasthenia gravis or other autoimmune diseases? Future studies are clearly needed to identify the remaining so called "third autoantigen" if any, or vice–versa, even more than three (Beck, 2017). One might also question, what are the genetic, immunological and biological factors behind the real molecular trigger of the autoimmune response? Is there a common mechanism initiating or

triggering the immune response against one or another autoantigen and stimulating progression of the disease by intramolecular or intermolecular epitope spreading? What do happen at the podocyte level and in the glomerular basement membrane where immune complexes form and induce podocyte injury and proteinuria, and what is the role of IgG subclasses and complement pathways? Can we identify additional clinical biomarkers for MN and last but not least, can we identify new and more specific treatments, beyond the use of immunosuppressors? These are some of the key questions for the next decade of research in MN.

References

A

Abu-Shakra, M., Buskila, D., Ehrenfeld, M., Conrad, K., &Shoenfeld, Y. (2001). Cancer and autoimmunity: autoimmune and rheumatic features in patients with malignancies. *Ann Rheum Dis, 60*(5), 433-441.

Adams, J. (2001). Thrombospondins: multifunctional regulators of cell interactions. *Annu Rev Cell Dev Biol, 17*, 25-51.

Adams, J. C., &Lawler, J. (2011). The thrombospondins. *Cold Spring Harb Perspect Biol, 3*(10), a009712.

Adams, J. C., &Tucker, R. P. (2000). The thrombospondin type 1 repeat (TSR) superfamily: diverse proteins with related roles in neuronal development. *Dev Dyn, 218*(2), 280-299.

Aissani, B., Zhang, K., &Wiener, H. (2015). Evaluation of GWAS candidate susceptibility loci for uterine leiomyoma in the multi-ethnic NIEHS uterine fibroid study. *Front Genet., 6*, 241.

Akiyama, S., Akiyama, M., Imai, E., Ozaki, T., Matsuo, S., &Maruyama, S. (2014). Prevalence of anti-phospholipase A2 receptor antibodies in Japanese patients with membranous nephropathy. *Clinical and Experimental Nephrology, 19*(4), 653–660.

Aleshin, A. E., Schraufstatter, I. U., Stec, B., Bankston, L. A., Liddington, R. C., &DiScipio, R. G. (2012). Structure of complement C6 suggests a mechanism for initiation and unidirectional, sequential assembly of membrane attack complex (MAC). *J Biol Chem, 287*(13), 10210-10222.

Alkhawajah, N. M., &Oger, J. (2013). Late-onset myasthenia gravis: a review when incidence in older adults keeps increasing. *Muscle Nerve, 48*(5), 705-710.

Allegri, L., Brianti, E., Chatelet, F., Manara, G. C., Ronco, P., &Verroust, P. (1986). Polyvalent antigen-antibody interactions are required for the formation of electron-dense immune deposits in passive Heymann's nephritis. *Am J Pathol, 125*(1), 1-6.

Ancian, P., Lambeau, G., &Lazdunski, M. (1995). Multifunctional activity of the extracellular domain of the M-type (180 kDa) membrane receptor for secretory phospholipases A2. *Biochemistry, 34*, 13146-13151.

Ancian, P., Lambeau, G., Mattei, M. G., &Lazdunski, M. (1995). The human 180-kDa receptor for secretory phospholipases A2. molecular cloning, identication of a secreted soluble form, expression, and chromosomal localization. *J. Biol. Chem, 270*(15), 8963-8970.

Aoki, V., Rivitti, E. A., Diaz, L. A., &Research, C. G. o. F. S. (2015). Update on fogo selvagem, an endemic form of pemphigus foliaceus. *J Dermatol., 42*(1), 18-26.

Arbuckle, M. R., McClain, M. T., Rubertone, M. V., Scofield, R. H., Dennis, G. J., James, J. A., &Harley, J. B. (2003). Development of autoantibodies before the clinical onset of systemic lupus erythematosus. *N Engl J Med., 349*(16), 1526-1533.

Asami, Y., Ishiguro, H., Ueda, A., &Nakajima, H. (2016). First report of membranous nephropathy and systemic lupus erythematosus associated with abatacept in rheumatoid arthritis. *Clin Exp Rheumatol, 34*(6), 1122.

Augert, A., Payré, C., de Launoit, Y., Gil, J., Lambeau, G., &Bernard, D. (2009). The M-type receptor PLA2R regulates senescence through the p53 pathway. *EMBO Rep., 10*(3), 271-277.

Augert, A., Vindrieux, D., Girard, C. A., Le Calvé, B., Gras, B., Ferrand, M., Bouchet, B. P., Puisieux, A., de Launoit, Y., Simonnet, H., Lambeau, G., &Bernard, D. (2013). PLA2R1 kills cancer cells by inducing mitochondrial stress. *Free Radic Biol Med, 65*, 969-977.

B

Baenziger, N., Brodiet, G. N., &Majerust, P. W. (1971). A Thrombin-Sensitive Protein ofHuman Platelet Membranes. *Proceedings of the National Academy of Sciences, 68*(1), 240-243.

Baker, P. J., Ochi, R. F., Schulze, M., Johnson, R. J., Campbell, C., &Couser, W. G. (1989). Depletion of C6 prevents development of proteinuria in experimental membranous nephropathy in rats. *Am J Pathol, 135*(1), 185-194.

Bally, S., Debiec, H., Ponard, D., Dijoud, F., Rendu, J., Fauré, J., Ronco, P., &Dumestre-Perard, C. (2016). Phospholipase A2 Receptor-Related Membranous Nephropathy and Mannan-Binding Lectin Deficiency. *J Am Soc Nephrol., 27*(12), 3539-3544.

Bech, A. P., Hofstra, J. M., Brenchley, P. E., &Wetzels, J. F. M. (2014). Association of Anti-PLA2R Antibodies with Outcomes after Immunosuppressive Therapy in Idiopathic Membranous Nephropathy. *Clin J Am Soc Nephrol., 9*(8), 1386–1392.

Beck, L. H. J. (2010). Membranous nephropathy and malignancy. *Semin Nephrol, 30*(6), 635-644.

Beck, L. H. J. (2017). PLA2R and THSD7A: Disparate Paths to the Same Disease? *J Am Soc Nephrol., 28*(9), 2579-2589.

Beck, L. H. J., Bonegio, R. G., Lambeau, G., Beck, D. M., Powell, D. W., Cummins, T. D., Klein, J. B., &Salant, D. J. (2009). M-type phospholipase A2 receptor as target antigen in idiopathic membranous nephropathy. *N. Engl. J. Med., 361*(1), 11-21.

Beck, L. H. J., Fervenza, F. C., Beck, D. M., Bonegio, R. G., Malik, F. A., Erickson, S. B., Cosio, F. G., Cattran, D. C., &Salant, D. J. (2011). Rituximab-induced depletion of anti-PLA2R autoantibodies predicts response in membranous nephropathy. *J Am Soc Nephrol, 22*(8), 1543-1550.

Beck, L. H. J., &Salant, D. J. (2010). Membranous nephropathy: recent travels and new roads ahead. *Kidney Int, 77*(9), 765-770.

Beck, L. J., &Salant, D. J. (2014). Membranous nephropathy: from models to man. *J Clin Invest., 124*(6), 2307-2314.

Beck, S., Beck, G., Ostendorf, T., Floege, J., Lambeau, G., Nevalainen, T., Radeke, H. H., Gurrieri, S., Haas, U., Thorwart, B., Pfeilschifter, J., &Kaszkin, M. (2006).

Upregulation of group IB secreted phospholipase A(2) and its M-type receptor in rat ANTI-THY-1 glomerulonephritis. *Kidney Int., 70*(7), 1251-1260.

Beck, S., Lambeau, G., Scholz-Pedretti, K., Gelb, M. H., Janssen, M. J., Edwards, S. H., Wilton, D. C., Pfeilschifter, J., &Kaszkin, M. (2003). Potentiation of tumor necrosis factor alpha-induced secreted phospholipase A2 (sPLA2)-IIA expression in mesangial cells by an autocrine loop involving sPLA2 and peroxisome proliferator-activated receptor alpha activation. *J Biol Chem, 278*(32), 29799-29812.

Behnert, A., Fritzler, M. J., Teng, B., Zhang, M., Bollig, F., Haller, H., Skoberne, A., Mahler, M., &Schiffer, M. (2013). An anti-phospholipase A2 receptor quantitative immunoassay and epitope analysis in membranous nephropathy reveals different antigenic domains of the receptor. *PLoS One., 8*(4), e61669.

Bell, E. T. (1946). "Renal diseases". *Renal Diseases*, 141-253.

Berentsen, S., &Sundic, T. (2015). Red blood cell destruction in autoimmune hemolytic anemia: role of complement and potential new targets for therapy. *Biomed Res Int*, 363278.

Bernier, V., Lagacé, M., Bichet, D. G., &Bouvier, M. (2004). Pharmacological chaperones: potential treatment for conformational diseases. *Trends Endocrinol Metab, 15*(5), 222-228.

Berrih-Aknin, S., Frenkian-Cuvelier, M., &Eymard, B. (2014). Diagnostic and clinical classification of autoimmune myasthenia gravis. *J Autoimmun., 48-49*, 143-148.

Biemesderfer, D. (2006). Regulated intramembrane proteolysis of megalin: linking urinary protein and gene regulation in proximal tubule? *Kidney Int, 69*(10), 1717-1721.

Bobart, S. A., De Vriese, A. S., Pawar, A. S., Zand, L., Sethi, S., Giesen, C., Lieske, J. C., &Fervenza, F. C. (2019). Noninvasive diagnosis of primary membranous nephropathy using phospholipase A2 receptor antibodies. *Kidney Int, 85*(2), 429-438.

Bockenhauer, D., Debiec, H., Sebire, N., Barratt, M., Warwicker, P., Ronco, P., &Kleta, R. (2008). Familial membranous nephropathy: an X-linked genetic susceptibility? *Nephron Clin Pract., 108*(1), c10-15.

Borza, D. B. (2016). Alternative Pathway Dysregulation and the Conundrum of Complement Activation by IgG4 Immune Complexes in Membranous Nephropathy. *Front Immunol., 7*, 157.

Bosco, N., Pelliccia, F., &Rocchi, A. (2010). Characterization of FRA7B, a human common fragile site mapped at the 7p chromosome terminal region. *Cancer Genet Cytogenet. 2010 Oct 1;, 202*(1), 47-52.

Brenchley, P. E., Coupes, B., Short, C. D., O'Donoghue, D. J., Ballardie, F. W., &Mallick, N. P. (1992). Urinary C3dg and C5b-9 indicate active immune disease in human membranous nephropathy. *Kidney Int., 41*(4), 933-937.

Bruschi, M., Carnevali, M. L., Murtas, C., Candiano, G., Petretto, A., Prunotto, M., Gatti, R., Argentiero, L., Magistroni, R., Garibotto, G., Scolari, F., Ravani, P., Gesualdo, L., Allegri, L., &Ghiggeri, G. M. (2011). Direct characterization of target podocyte antigens and auto-antibodies in human membranous glomerulonephritis: Alfa-enolase and borderline antigens. *J Proteomics., 74*(10), 2008-2017.

C

Cambier, J. F., &Ronco, P. (2012). Onco-nephrology: glomerular diseases with cancer. *Clin J Am Soc Nephrol, 7*(10), 1701-1712.

Canfield, S. M., &Morrison, S. L. (1991). The binding affinity of human IgG for its high affinity Fc receptor is determined by multiple amino acids in the CH2 domain and is modulated by the hinge region. *J Exp Med, 173*(6), 1483-1491.

Cao, H., Lei, S., Deng, H. W., &Wang, Y. P. (2012). Identification of genes for complex diseases using integrated analysis of multiple types of genomic data. *PLoS One, 7*(9), e42755.

Cao, Y. (2007). Angiogenesis modulates adipogenesis and obesity. *J Clin Invest., 117*, 2362–2368.

Carlson, C. B., Lawler, J., &Mosher, D. F. (2008). Structures of thrombospondins. *Cell Mol Life Sci, 65*(5), 672-686.

Carr, A. S., Cardwell, C. R., McCarron, P. O., &McConville, J. (2010). A systematic review of population based epidemiological studies in Myasthenia Gravis. *BMC Neurol, 10*(46).

Cattran, D. C., Appel, G. B., Hebert, L. A., Hunsicker, L. G., Pohl, M. A., Hoy, W. E., Maxwell, D. R., Kunis, C. L., &Group, N. A. N. S. S. (2001). Cyclosporine in patients with steroid-resistant membranous nephropathy: a randomized trial. *Kidney Int., 59*(4), 1484-1490.

Cattran, D. C., Pei, Y., Greenwood, C. M., Ponticelli, C., Passerini, P., &Honkanen, E. (1997). Validation of a predictive model of idiopathic membranous nephropathy: its clinical and research implications. *Kidney Int., 51*(3), 901-907.

Cattran, D. C., Reich, H. N., Beanlands, H. J., Miller, J. A., Scholey, J. W., Troyanov, S., &Genes, G. a. G. G. (2008). The impact of sex in primary glomerulonephritis. *Nephrol Dial Transplant, 23*(7), 2247-2253.

Cetin, H., &Vincent, A. (2018). Pathogenic Mechanisms and Clinical Correlations in Autoimmune Myasthenic Syndromes. *Semin Neurol, 38*(3), 344-354.

Chen, H., Herndon, M. E., &Lawler, J. (2000). The cell biology of thrombospondin-1. *Matrix Biol, 19*(7), 597-614.

Cheng, G., Liu, J., Gilbert, A., Cao, Y., An, C., Lv, Z., Wang, C., Nie, R., Zhang, J., Liu, Y., Xia, M., Li, S., Cai, H., Li, Y., Li, Y., &Qin, X. (2018). Serum phospholipase A2 receptor antibodies and immunoglobulin G subtypes in adult idiopathic membranous nephropathy: Clinical value assessment. *Clin Chim Acta., 490*, 135-141.

Chiaroni-Clarke, R. C., Munro, J. E., &Ellis, J. A. (2016). Sex bias in paediatric autoimmune disease - Not just about sex hormones? *J Autoimmun, 69*, 12-23.

Churg, J., &Ehrenreich, T. (1973). Membranous nephropathy. *Perspect Nephrol Hypertens, 1*, 443-448.

Coenen, M. J., Hofstra, J. M., Debiec, H., Stanescu, H. C., Medlar, A. J., Stengel, B., Boland-Augé, A., Groothuismink, J. M., Bockenhauer, D., Powis, S. H., Mathieson, P. W., Brenchley, P. E., Kleta, R., Wetzels, J. F., &Ronco, P. (2013). Phospholipase

A2 receptor (PLA2R1) sequence variants in idiopathic membranous nephropathy. *J Am Soc Nephrol., 24*(4), 677-683.

Cornaby, C., Gibbons, L., Mayhew, V., Sloan, C. S., Welling, A., &Poole, B. D. (2015). B cell epitope spreading : mechanisms and contribution to autoimmune diseases. *Immunol Lett, 163*, 56-68.

Couser, W. G., Johnson, R. J., Young, B. A., Yeh, C. G., Toth, C. A., &Rudolph, A. R. (1995). The effects of soluble recombinant complement receptor 1 on complement-mediated experimental glomerulonephritis. *J Am Soc Nephrol., 5*(11), 1888-1894.

Couser, W. G., Steinmuller, D. R., Stilmant, M. M., Salant, D. J., &Lowenstein, L. M. (1978). Experimental glomerulonephritis in the isolated perfused rat kidney. *J Clin Invest., 62*(6), 1275-1287.

Couser, W. G., Wagonfeld, J. B., Spargo, B. H., &Lewis, E. J. (1974). Glomerular deposition of tumor antigen in membranous nephropathy associated with colonic carcinoma. *Am J Med, 57*(6), 962-970.

Craig, W. S., Cheng, S., Mullen, D. G., Blevitt, J., &Pierschbacher, M. D. (1995). Concept and progress in the development of RGD-containing peptide pharmaceuticals. *Biopolymers, 37*(2), 157-175.

Cui, W., Maimaitiyiming, H., Qi, X., Norman, H., &Wang, S. (2013). Thrombospondin 1 mediates renal dysfunction in a mouse model of high-fat diet-induced obesity. *Am J Physiol Renal Physiol, 305*(6), F871-880.

Cui, Z., Xie, L. J., Chen, F. J., Pei, Z. Y., Zhang, L. J., Qu, Z., Huang, J., Gu, Q. H., Zhang, Y. M., Wang, X., Wang, F., Meng, L. Q., Liu, G., Zhou, X. J., Zhu, L., Lv, J. C., Liu, F., Zhang, H., Liao, Y. H., Lai, L. H., Ronco, P., &Zhao, M. H. (2017). MHC Class II Risk Alleles and Amino Acid Residues in Idiopathic Membranous Nephropathy. *J Am Soc Nephrol., 28*(5), 1651-1664.

Cupillard, L., Mulherkar, R., Gomez, N., Kadam, S., Valentin, E., Lazdunski, M., &Lambeau, G. (1999). Both group IB and group IIA secreted phospholipases A2 are natural ligands of the mouse 180-kDa M-type receptor. *J Biol Chem, 274*(11), 7043-7051.

Cybulsky, A. V., Rennke, H. G., Feintzeig, I. D., &D.J., S. (1986). Complement-induced glomerular epithelial cell injury. Role of the membrane attack complex in rat membranous nephropathy. . *J Clin Invest, 77*(4), 1096–1107.

D

Dabade, T. S., Grande, J. P., Norby, S. M., Fervenza, F. C., &Cosio, F. G. (2008). Recurrent idiopathic membranous nephropathy after kidney transplantation: a surveillance biopsy study. *Am J Transplant, 8*(6), 1318-1322.

Dahan, K., Debiec, H., Plaisier, E., Cachanado, M., Rousseau, A., Wakselman, L., Michel, P. A., Mihout, F., Dussol, B., Matignon, M., Mousson, C., Simon, T., Ronco, P., &Group., G. S. (2017). Rituximab for Severe Membranous Nephropathy: A 6-Month Trial with Extended Follow-Up. *J Am Soc Nephrol, 28*(1), 348-358.

Dahan, K., Gillion, V., Johanet, C., Debiec, H., &Ronco, P. (2017). The Role of PLA2R Antibody in Treatment of Membranous Nephropathy. *Kidney Int Rep, 3*(2), 498-501.

Dähnrich, C., Komorowski, L., Probst, C., Seitz-Polski, B., Esnault, V., Wetzels, J. F., Hofstra, J. M., Hoxha, E., Stahl, R. A., Lambeau, G., Stöcker, W., &Schlumberger, W. (2013). Development of a standardized ELISA for the determination of autoantibodies against human M-type phospholipase A2 receptor in primary membranous nephropathy. *Clin Chim Acta., 421*, 213-218.

Darrah, E., &Andrade, F. (2018). Rheumatoid arthritis and citrullination. *Curr Opin Rheumatol, 30*(1), 72-78.

De Vriese, A., Glassock, R., Nath, K., Sethi, S., &Fervenza, F. (2017). A Proposal for a Serology-Based Approach to Membranous Nephropathy. *J Am Soc Nephrol., 28*(2), 421-430.

Debiec, H., Guigonis, V., Mougenot, B., Decobert, F., Haymann, J. P., Bensman, A., Deschenes, G., &Ronco, P. M. (2002). Antenatal membranous glomerulonephritis due to anti-neutral endopeptidase antibodies. *N. Engl. J. Med., 346*(26), 2053-2060.

Debiec, H., Hanoy, M., Francois, A., Guerrot, D., Ferlicot, S., Johanet, C., Aucouturier, P., Godin, M., &Ronco, P. (2012). Recurrent membranous nephropathy in an allograft caused by IgG3κ targeting the PLA2 receptor. *J Am Soc Nephrol., 23*(12), 1949-1954.

Debiec, H., Lefeu, F., Kemper, M. J., Niaudet, P., Deschênes, G., Remuzzi, G., Ulinski, T., &Ronco, P. (2011). Early-childhood membranous nephropathy due to cationic bovine serum albumin. *N Engl J Med., 364*(22), 2101-2110.

Debiec, H., Nauta, J., Coulet, F., van der Burg, M., Guigonis, V., Schurmans, T., de Heer, E., Soubrier, F., Janssen, F., &Ronco, P. (2004). Role of truncating mutations in MME gene in fetomaternal alloimmunisation and antenatal glomerulopathies. *Lancet., 364*(9441), 1252-1259.

Debiec, H., &Ronco, P. (2011). PLA2R autoantibodies and PLA2R glomerular deposits in membranous nephropathy. *N Engl J Med., 364*(7), 689-690.

Debiec, H., &Ronco, P. (2014). Immunopathogenesis of membranous nephropathy : an update. *Semin Immunopathol, 36*(4), 381-397.

Derksen, V. F. A. M., Huizinga, T. W. J., &van der Woude, D. (2017). The role of autoantibodies in the pathophysiology of rheumatoid arthritis. *Semin Immunopathol, 39*(4), 437-446.

Di Zenzo, G., Thoma-Uszynski, S., Calabresi, V., Fontao, L., Hofmann, S. C., Lacour, J. P., Sera, F., Bruckner-Tuderman, L., Zambruno, G., Borradori, L., &Hertl, M. (2011). Demonstration of epitope-spreading phenomena in bullous pemphigoid: results of a prospective multicenter study. *J Invest Dermatol., 131*(11), 2271-2280.

Di Zenzo, G., Thoma-Uszynski, S., Fontao, L., Calabresi, V., Hofmann, S. C., Hellmark, T., Sebbag, N., Pedicelli, C., Sera, F., Lacour, J. P., Wieslander, J., Bruckner-Tuderman, L., Borradori, L., Zambruno, G., &Hertl, M. (2008). Multicenter prospective study of the humoral autoimmune response in bullous pemphigoid. *Clin Immunol, 128*(3), 415-426.

Didona, D., &Giovanni, D. Z. (2018). Humoral Epitope Spreading in Autoimmune Bullous Diseases. *Front Immunol., 9*, 779.

Dixon, F. J., Feldman, J. D., &Vazquez, J. J. (1961). Experimental glomerulonephritis. The pathogenesis of a laboratory model resembling the spectrum of human glomerulonephritis. *J Exp Med., 113*, 899–920.

Doi, T., Mayumi, M., Kanatsu, K., Suehiro, F., &Hamashima, Y. (1984). Distribution of IgG subclasses in membranous nephropathy. *Clin Exp Immunol., 58*(1), 57-62.

Du, Y., Li, J., He, F., Lv, Y., Liu, W., Wu, P., Huang, J., Wei, S., &Gao, H. (2014). The diagnosis accuracy of PLA2R-AB in the diagnosis of idiopathic membranous nephropathy: a meta-analysis. *PLoS One., 9*(8), e104936.

E – F

East, L., &Isacke, C. M. (2002). The mannose receptor family. *Biochim Biophys Acta., 1572*(2-3), 364-386.

Farnoodian, M., Sorenson, C. M., &Sheibani, N. (2018). Negative Regulators of Angiogenesis, Ocular Vascular Homeostasis, and Pathogenesis and Treatment of Exudative AMD. *J Ophthalmic Vis Res, 13*(4), 470-486.

Farquhar, M., Vernier, R., &Good, R. (1957). An electron microscope study of the glomerulus in nephrosis, glomerulonephritis and lupus erythematosus. *J Exp Med, 106*, 649-660.

Feenstra, K., van den Lee, R., Greben, H. A., Arends, A., &Hoedemaeker, P. J. (1975). Experimental glomerulonephritis in the rat induced by antibodies directed against tubular antigens. i. the natural history : a histologic and immunohistologic study at the light microscopic and the ultrastructural level *Laboratory investigation ; a journal of technical methods and pathology, 32*, 235-242.

Fervenza, F. C., Sethi, S., &Specks, U. (2008). Idiopathic membranous nephropathy: diagnosis and treatment. *Clin J Am Soc Nephrol, 3*(3), 905-919.

Floege, J., &Amann, K. (2016). Primary glomerulonephritides. *Lancet., 387*(10032), 2036-2048.

Francis, J. M., Beck, L. H. J., &Salant, D. J. (2016). Membranous Nephropathy: A Journey From Bench to Bedside. *Am J Kidney Dis, 68*(1), 138-147.

Fresquet, M., Jowitt, T. A., Gummadova, J., Collins, R., O'Cualain, R., McKenzie, E. A., Lennon, R., &Brenchley, P. E. (2015). Identifcation of a major epitope recognized by PLA2R autoantibodies in primary membranous nephropathy. *J Am Soc Nephrol, 26*, 302-313.

G

Garcia-Vives, E., Solé, C., Moliné, T., Alvarez-Rios, A. M., Vidal, M., Agraz, I., Ordi-Ros, J., &Cortés-Hernández, J. (2019). Antibodies to M-type phospholipase A2 receptor (PLA2R) in membranous lupus nephritis. *Lupus, 28*(3), 396-405.

Germuth, F. G., Pace, M. G., &Tippett, J. C. (1955). Comparative histologic and immunologic studies in rabbits of induced hypersensitivity of the serum sickness

type. II. The effect of sensitization to homologous and cross-reactive antigens on the rate of antigen elimination and the development of allergic lesions. *J Exp Med., 101*, 135–150.

Ghazanfari, N., Morsch, M., Reddel, S. W., Liang, S. X., &Phillips, W. D. (2014). Muscle-specific kinase (MuSK) autoantibodies suppress the MuSK pathway and ACh receptor retention at the mouse neuromuscular junction. *J Physiol, 592*(13), 2881-2897.

Giat, E., Ehrenfeld, M., &Shoenfeld, Y. (2017). Cancer and autoimmune diseases. *Autoimmun Rev, 16*(10), 1049-1057.

Girard, C. A., Seitz-Polski, B., Dolla, G., Augert, A., Vindrieux, D., Bernard, D., &Lambeau, G. (2014). New physiopathological roles for the PLA2R1 receptor in cancer and membranous nephropathy. *Med Sci (Paris), 30*(5), 519-525.

Glassock, R. J. (1992). Secondary membranous glomerulonephritis. *Nephrol Dial Transplant*, 1, 64-71.

Glassock, R. J. (2009). Human idiopathic membranous nephropathy-a mystery solved? *N Engl J Med., 361*(1), 81-83.

Glassock, R. J. (2010). Idiopathic membranous nephropathy: getting better by itself. *J Am Soc Nephrol., 21*(4), 551-552.

Glassock, R. J. (2010). The pathogenesis of idiopathic membranous nephropathy: a 50-year odyssey. *Am J Kidney Dis, 56*(1), 157-167.

Glassock, R. J. (2012). The pathogenesis of membranous nephropathy: evolution and revolution. *Curr Opin Nephrol Hypertens., 21*(3), 235-242.

Gödel, M., Grahammer, F., &Huber, T. B. (2015). Thrombospondin type-1 domain-containing 7A in idiopathic membranous nephropathy. *N Engl J Med., 372*(11), 1073.

Gora, S., Perret, C., Jemel, I., Nicaud, V., Lambeau, G., Cambien, F., Ninio, E., Blankenberg, S., Tiret, L., &Karabina, S. A. (2009). Molecular and functional characterization of polymorphisms in the secreted phospholipase A2 group X gene: relevance to coronary artery disease. *J. Mol. Med, 87*, 723-733.

Granata, F., Petraroli, A., Boilard, E., Bezzine, S., Bollinger, J., Del Vecchio, L., Gelb, M. H., Lambeau, G., Marone, G., &Triggiani, M. (2005). Activation of cytokine production by secreted phospholipase A2 in human lung macrophages expressing the M-type receptor. *J. Immunol., 174*(1), 464-474.

Gratz, I., &Campbell, D. (2014). Organ-specific and memory treg cells: specificity, development, function, and maintenance. *Front Immunol, 5*, 333.

Guerry, M. J., Vanhille, P., Ronco, P., &Debiec, H. (2016). Serum anti-PLA2R antibodies may be present before clinical manifestations of membranous nephropathy. *Kidney Int, 89*(6), 1399.

Guo, N., Krutzsch, H., Neegre, E., Vogel, T., Blake, D., &Roberts, D. (1992). Heparinand sulfatide-binding peptides from the type I repeats of human thrombospondin promote melanoma cell adhesion. *Proc Natl Acad Sci U S A, 89*, 3040.

Gupta, A., &Quigg, R. J. (2015). Glomerular Diseases Associated With Hepatitis B and C. *Adv Chronic Kidney Dis, 22*(5), 343-351.

Gutiérrez, J. M., &Lomonte, B. (2013). Phospholipases A2: unveiling the secrets of a functionally versatile group of snake venom toxins. *Toxicon, 62*, 27-39.

H

Haddad, G., &Kistler, A. A. (2017). An in vitro model of idiopathic membranous nephropathy reveals PLA2R- and complement-dependent pathways of podocyte injury. *J Am Soc Nephrol, 20*(109A).

Haga, S., Nakaoka, H., Yamaguchi, T., Yamamoto, K., Kim, Y. I., Samoto, H., Ohno, T., Katayama, K., Ishida, H., Park, S. B., Kimura, R., Maki, K., &Inoue, I. (2013). A genome-wide association study of third molar agenesis in Japanese and Korean populations. *J Hum Genet, 58*(12), 799-803.

Hanasaki, K., Yokota, Y., Ishizaki, J., Itoh, T., &Arita, H. (1997). Resistance to endotoxic shock in phospholipase A2 receptor-deficient mice. *J Biol Chem, 272*(52), 32792-32797.

Haraldsson, B., Nyström, J., &Deen, W. M. (2008). Properties of the glomerular barrier and mechanisms of proteinuria. *Physiol Rev., 88*(2), 451-487.

Hayashi, N., Okada, K., Matsui, Y., Fujimoto, K., Adachi, H., Yamaya, H., Matsushita, M., &Yokoyama, H. (2018). Glomerular mannose-binding lectin deposition in intrinsic antigen-related membranous nephropathy. *Nephrol Dial Transplant., 33*(5), 832-840.

Heymann, W., Hackel, D. B., Harwood, S., Wilson, S. G., &Hunter, J. L. (1959). Production of nephrotic syndrome in rats by Freund's adjuvants and rat kidney suspensions. *Proc Soc Exp Biol Med., 100*(4), 660-664.

Higashino, K., Ishizaki, J., Kishino, J., Ohara, O., &Arita, H. (1994). Structural comparison of phospholipase A2-binding regions in phospholipase A2 receptors from various mammals. *Eur. J. Biochem., 225*(1), 375-382.

Higashino, K. K., Yokota, Y., Ono, T., Kamitani, S., Arita, H., &Hanasaki, K. (2002). Identification of a soluble form phospholipase A2 receptor as a circulating endogenous inhibitor for secretory phospholipase A2. *J Biol Chem, 277*, 13583–13588.

Hihara, K., Iyoda, M., Tachibana, S., Iseri, K., Saito, T., Yamamoto, Y., Suzuki, T., Wada, Y., Matsumoto, K., &Shibata, T. (2016). Anti-phospholipase A2 receptor (PLA2R) antibody and glomerular PLA2R expression in Japanese patients with membranous nephropathy. *PLoS One., 11*(6).

Hirayama, K., Ebihara, I., Yamamoto, S., Kai, H., Muro, K., Yamagata, K., Kobayashi, M., &Koyama, A. (2002). Predominance of type-2 immune response in idiopathic membranous nephropathy. Cytoplasmic cytokine analysis. *Nephron, 91*(2), 255-261.

Hofstra, J. M., Beck, L. H. J., Beck, D. M., Wetzels, J. F., &Salant, D. J. (2011). Anti-phospholipase A_2 receptor antibodies correlate with clinical status in idiopathic membranous nephropathy. *Clin J Am Soc Nephrol, 6*(6), 1286-1291.

Hofstra, J. M., Debiec, H., Short, C. D., Pellé, T., Kleta, R., Mathieson, P. W., Ronco, P., Brenchley, P. E., &Wetzels, J. F. (2012). Antiphospholipase A2 receptor antibody titer and subclass in idiopathic membranous nephropathy. *J Am Soc Nephrol., 23*(10), 1735-1743.

Hong, M., Salant, D. J., &Beck, L. H. (2015). Autoantibodies target multiple epitopes in THSD7A in primary membranous nephropathy. *in Oral presentation given at the JASN Kidney Week*.

Hou, Z., Abudureheman, A., Wang, L., Hasim, A., Ainiwaer, J., Zhang, H., Niyaz, M., Upur, H., &Sheyhidin, I. (2017). Expression, prognosis and functional role of Thsd7a in esophageal squamous cell carcinoma of Kazakh patients, Xinjiang. *Oncotarget, 8*(36), 60539-60557.

Howard, L. M., Miga, A. J., Vanderlugt, C. L., Dal Canto, M. C., Laman, J. D., Noelle, R. J., &Miller, S. D. (1999). Mechanisms of immunotherapeutic intervention by anti-CD40L (CD154) antibody in an animal model of multiple sclerosis. *J Clin Invest, 103*(2), 281-290.

Hoxha, E., Beck, L. H. J., Wiech, T., Tomas, N. M., Probst, C., Mindorf, S., Meyer-Schwesinger, C., Zahner, G., Stahl, P. R., Schöpper, R., Panzer, U., Harendza, S., Helmchen, U., Salant, D. J., &Stahl, R. A. (2017). An Indirect Immunofluorescence Method Facilitates Detection of Thrombospondin Type 1 Domain-Containing 7A-Specific Antibodies in Membranous Nephropathy. *J Am Soc Nephrol, 28*(2), 520-531.

Hoxha, E., Harendza, S., Zahner, G., Panzer, U., Steinmetz, O., Fechner, K., Helmchen, U., &Stahl, R. A. (2011). An immunofluorescence test for phospholipase-A_2-receptor antibodies and its clinical usefulness in patients with membranous glomerulonephritis. *Nephrol Dial Transplant., 26*(8), 2526-2532.

Hoxha, E., Kneissler, U., Stege, G., Zahner, G., Thiele, I., Panzer, U., Harendza, S., Helmchen, U. M., &Stahl, R. A. (2012). Enhanced expression of the M-type phospholipase A2 receptor in glomeruli correlates with serum receptor antibodies in primary membranous nephropathy. *Kidney Int., 82*(7), 797–804.

Hoxha, E., Thiele, I., Zahner, G., Panzer, U., Harendza, S., &Stahl, R. A. (2014). Phospholipase A2 receptor autoantibodies and clinical outcome in patients with primary membranous nephropathy. *J Am Soc Nephrol., 25*(6), 1357-1366.

Hoxha, E., von Haxthausen, F., Wiech, T., &Stahl, R. A. K. (2017). Membranous nephropathy-one morphologic pattern with different diseases. *Pflugers Arch., 469*(7-8), 989-996.

Hoxha, E., Wiech, T., Stahl, P. R., Zahner, G., Tomas, N. M., Meyer-Schwesinger, C., Wenzel, U., Janneck, M., Steinmetz, O. M., Panzer, U., Harendza, S., &Stahl, R. A. (2016). A Mechanism for Cancer-Associated Membranous Nephropathy. *N Engl J Med., 374*(20), 1995-1996.

Hu, P., Xuan, Q., Hu, B., Lu, L., &Qin, Y. H. (2013). Anti-neutral endopeptidase, natriuretic peptides disarrangement, and proteinuria onset in membranous nephropathy. *Mol Biol Rep, 40*(4), 2963-2967.

Huang, C. C., Lehman, A., Albawardi, A., Satoskar, A., Brodsky, S., Nadasdy, G., Hebert, L., Rovin, B., &Nadasdy, T. (2013). IgG subclass staining in renal biopsies with

membranous glomerulonephritis indicates subclass switch during disease progression. *Mod Pathol., 26*(6), 799-805.

Hugo, C., &Daniel, C. (2009). Thrombospondin in renal disease. *Nephron Exp Nephrol, 111*(3), 61-66.

I – J

Ishizaki, J., Hanasaki, K., Higashino, K., Kishino, J., Kikuchi, N., Ohara, O., &Arita, H. (1994). Molecular cloning of pancreatic group I phospholipase A2 receptor. *J Biol Chem, 269*(8), 5897-5904.

Iwakura, T., Fujigaki, Y., Katahashi, N., Sato, T., Ishigaki, S., Tsuji, N., Naito, Y., Isobe, S., Ono, M., Sakao, Y., Tsuji, T., Ohashi, N., Kato, A., Miyajima, H., &Yasuda, H. (2016). Membranous Nephropathy with an Enhanced Granular Expression of Thrombospondin Type-1 Domain-containing 7A in a Pregnant Woman. *Intern Med, 55*(18), 2663-2668.

Iwakura, T., Ohashi, N., Kato, A., Baba, S., &Yasuda, H. (2015). Prevalence of enhanced granular expression of thrombospondin type-1 domain-containing 7A in the glomeruli of Japanese patients with idiopathic membranous nephropathy. *PLoSOne, 10*(9), e0138841.

Jarad, G., &Miner, J. H. (2009). Update on the glomerular filtration barrier. *Curr Opin Nephrol Hypertens., 18*(3), 226-232.

Jefferson, J. A., &Couser, W. G. (2003). Therapy of membranous nephropathy associated with malignancy and secondary causes. *Semin Nephrol*, 23(4), 400-405.

Jennette, J. C., &Nachman, P. H. (2017). ANCA Glomerulonephritis and Vasculitis. *Clin J Am Soc Nephrol, 12*(10), 1680–1691.

Johnson, R. J., Hurtado, A., Merszei, J., Rodriguez-Iturbe, B., &Feng, L. (2003). Hypothesis: dysregulation of immunologic balance resulting from hygiene and socioeconomic factors may infl uence the epidemiology and cause of glomerulonephritis worldwide. *Am J Kidney Dis., 42*, 575–581.

Jones, D. B. (1957). Nephrotic Glomerulonephritis. *Am J Pathol., 33*(2), 313–329.

Joshi, M. R., Burbelo, P. D., Waldman, M. A., Gordon, S. M., Thurlow, J. S., &Olson, S. W. (2018). Pre-Diagnostic Evaluation of Anti-Phospholipase A2 Receptor Antibodies in Primary Membranous Nephropathy. *J Am Soc Nephrol 29*, 823.

K

Kanigicherla, D., Gummadova, J., McKenzie, E. A., Roberts, S. A., Harris, S., Nikam, M., Poulton, K., McWilliam, L., Short, C. D., Venning, M., &Brenchley, P. E. (2013). Anti-PLA2R antibodies measured by ELISA predict long-term outcome in a prevalent population of patients with idiopathic membranous nephropathy. *Kidney Int., 83*(5), 940-948.

Kao, L., Lam, V., Waldman, M., Glassock, R. J., &Zhu, Q. (2015). Identification of the immunodominant epitope region in phospholipase A2 receptor-mediating autoantibody binding in idiopathic membranous nephropathy. *J Am Soc Nephrol., 26*(2), 291-301.

Kerjaschki, D., Exner, M., Ullrich, R., Susani, M., Curtiss, L. K., Witztum, J. L., Farquhar, M. G., &Orlando, R. A. (1997). Pathogenic antibodies inhibit the binding of apolipoproteins to megalin/gp330 in passive Heymann nephritis. *J Clin Invest, 100*(9), 2303-2309.

Kerjaschki, D., &Farquhar, M. (1983). Immunocytochemical localization of the Heymann nephritis antigen (gp330) in glomerular epithelial cells of normal Lewis rats. *J Exp Med., 157*, 667-686.

Kerjaschki, D., &Farquhar, M. G. (1982). The pathogenic antigen of Heymann nephritis is a membrane glycoprotein of the renal proximal tubule brush border. *Proc Natl Acad Sci U S A., 79*(18), 5557-5561.

Kerjaschki, D., Miettinen, A., &Farquhar, M. G. (1987). Initial events in the formation of immune deposits in passive Heymann nephritis. gp330-anti-gp330 immune complexes form in epithelial coated pits and rapidly become attached to the glomerular basement membrane. *J Exp Med, 166*(1), 109-128.

Kerjaschki, D., Ullrich, R., Exner, M., Orlando, R. A., &Farquhar, M. G. (1996). Induction of passive Heymann nephritis with antibodies specific for a synthetic peptide derived from the receptor-associated protein. *J Exp Med., 183*(5), 2007-2015.

Kimura, Y., Miura, N., Debiec, H., Morita, H., Yamada, H., Banno, S., Ronco, P., &Imai, H. (2017). Circulating antibodies to α-enolase and phospholipase A2 receptor and composition of glomerular deposits in Japanese patients with primary or secondary membranous nephropathy. *Clin Exp Nephrol., 21*(1), 117-126.

Kini, R. M., &Evans, H. J. (1989). A model to explain the pharmacological effects of snake venom phospholipases A2. *Toxicon, 27*(6), 613-635.

Kistler, A. D., Singh, G., Altintas, M. M., Yu, H., Fernandez, I. C., Gu, C., Wilson, C., Srivastava, S. K., Dietrich, A., Walz, K., Kerjaschki, D., Ruiz, P., Dryer, S., Sever, S., Dinda, A. K., Faul, C., &Reiser, J. (2013). Transient receptor potential channel 6 (TRPC6) protects podocytes during complement-mediated glomerular disease. *J Biol Chem, 288*(51), 36598-36609.

Klenotic, P. A., Page, R. C., Misra, S., &Silverstein, R. L. (2011). Expression, purification and structural characterization of functionally replete thrombospondin-1 type 1 repeats in a bacterial expression system. *Protein Expr Purif, 80*(2), 253-259.

Klouda, P. T., Manos, J., Acheson, E. J., Dyer, P. A., Goldby, F. S., Harris, R., Lawler, W., Mallick, N. P., &Williams, G. (1979). Strong association between idiopathic membranous nephropathy and HLA-DRW3. *Lancet., 2*(8146), 770-771.

Koch, P. J., Mahoney, M. G., Ishikawa, H., Pulkkinen, L., Uitto, J., Shultz, L., Murphy, G. F., Whitaker-Menezes, D., &Stanley, J. R. (1997). Targeted disruption of the pemphigus vulgaris antigen (desmoglein 3) gene in mice causes loss of keratinocyte cell adhesion with a phenotype similar to pemphigus vulgaris. *J Cell Biol., 137*(5), 1091-1102.

Koneczny, I. (2018). A New Classification System for IgG4 Autoantibodies. *Front Immunol., 9*, 97.

Koneczny, I., Cossins, J., Waters, P., Beeson, D., &Vincent, A. (2013). MuSK myasthenia gravis IgG4 disrupts the interaction of LRP4 with MuSK but both IgG4 and IgG1-3 can disperse preformed agrin-independent AChR clusters. *PLoS One, 8*(11), e80695.

Kuo, M. W., Wang, C. H., Wu, H. C., Chang, S. J., &Chuang, Y. J. (2011). Soluble THSD7A is an N-glycoprotein that promotes endothelial cell migration and tube formation in angiogenesis. *PLoSOne, 6*(12), e29000.

Kuo, M. W., Wang, C. H., Wu, H. C., Chang, S. J., &Chuang, Y. J. (2011). Soluble THSD7A is an N-glycoprotein that promotes endothelial cell migration and tube formation in angiogenesis. *PLoS One, 6*(12), e29000.

Kuroki, A., Iyoda, M., Shibata, T., &Sugisaki, T. (2005). Th2 cytokines increase and stimulate B cells to produce IgG4 in idiopathic membranous nephropathy. *Kidney Int, 68*(1), 302-310.

Kuruppu, S., Rajapakse, N. W., Minond, D., &Smith, A. I. (2014). Production of soluble Neprilysin by endothelial cells. *Biochem Biophys Res Commun, 446*(2), 423-427.

Kusunoki, Y., Itami, N., Tochimaru, H., Takekoshi, Y., Nagasawa, S., &Yoshiki, T. (1989). Glomerular deposition of C4 cleavage fragment (C4d) and C4-binding protein in idiopathic membranous glomerulonephritis. *Nephron, 51*(1), 17-19.

L

Lai, W. L., Yeh, T. H., Chen, P. M., Chan, C. K., Chiang, W. C., Chen, Y. M., Wu, K. D., &Tsai, T. J. (2015). Membranous nephropathy: a review on the pathogenesis, diagnosis, and treatment. *J Formos Med Assoc., 114*(2), 102-111.

Lamason, R., Zhao, P., Rawat, R., Davis, A., Hall, J. C., Chae, J. J., Agarwal, R., Cohen, P., Rosen, A., Hoffman, E. P., &Nagaraju, K. (2006). Sexual dimorphism in immune response genes as a function of puberty. *BMC Immunol, 7*, 2.

Lambeau, G., Ancian, P., Barhanin, J., &Lazdunski, M. (1994). Cloning and expression of a membrane receptor for secretory phospholipases A2. *J. Biol. Chem., 269*, 1575-1578.

Lambeau, G., Ancian, P., Nicolas, J. P., Beiboer, S. H., Moinier, D., Verheij, H., &Lazdunski, M. (1995). Structural elements of secretory phospholipases A2 involved in the binding to M-type receptors. *J Biol Chem, 270*(10), 5534-5540.

Lambeau, G., Barhanin, J., Schweitz, H., Qar, J., &Lazdunski, M. (1989). Identication and properties of very high affinity brain membrane-binding sites for a neurotoxic phospholipase from the taipan venom. *J. Biol. Chem., 264*(19), 11503-11510.

Lambeau, G., &Lazdunski, M. (1999). Receptors for a growing family of secreted phospholipases A2. *Trends Pharmacol Sci., 20*(4), 162-170.

Lambeau, G., Schmid-Alliana, A., Lazdunski, M., &Barhanin, J. (1990). Identification and purification of a very high affinity binding protein for toxic phospholipases A2 in skeletal muscle. *J Biol Chem., 265* 9526-9532.

Land, J., Rutgers, A., &Kallenberg, C. G. (2014). Anti-neutrophil cytoplasmic autoantibody pathogenicity revisited: pathogenic versus non-pathogenic anti-neutrophil cytoplasmic autoantibody. *Nephrol Dial Transplant., 29*(4), 739-745.

Larsen, C. P., Cossey, L. N., &Beck, L. H. (2016). THSD7A staining of membranous glomerulopathy in clinical practice reveals cases with dual autoantibody positivity. *Mod Pathol, 29* 421-426.

Larsen, C. P., Messias, N. C., Silva, F. G., Messias, E., &Walker, P. D. (2013). Determination of primary versus secondary membranous glomerulopathy utilizing phospholipase A2 receptor staining in renal biopsies. *Mod Pathol., 26*(5), 709-715.

Larsen, C. P., Trivin-Avillach, C., Coles, P., Collins, A. B., Merchant, M., Ma, H., Wilkey, D. W., Ambruzs, J. M., Messias, N. C., Cossey, L. N., Rosales, I. A., Wooldridge, T., Walker, P. D., Colvin, R. B., Klein, J., Salant, D. J., &Beck, L. H. J. (2018). LDL Receptor-Related Protein 2 (Megalin) as a Target Antigen in Human Kidney Anti-Brush Border Antibody Disease. *J Am Soc Nephrol, 29*(2), 644-653.

Lawler, J. (2002). Thrombospondin-1 as an endogenous inhibitor of angiogenesis and tumor growth. *J Cell Mol Med, 6*(1), 1-12.

Lawler, J., Weinstein, R., &Hynes, R. O. (1988). Cell attachment to thrombospondin: the role of ARG-GLY-ASP, calcium, and integrin receptors. *J Cell Biol, 107*((6 Pt 1)), 2351-2361.

Le, W. B., Shi, J. S., Zhang, T., Liu, L., Qin, H. Z., Liang, S., Zhang, Y. W., Zheng, C. X., Jiang, S., Qin, W. S., Zhang, H. T., &Liu, Z. H. (2017). HLA-DRB1*15:01 and HLA-DRB3*02:02 in PLA2R-Related Membranous Nephropathy. *J Am Soc Nephrol., 28*(5), 1642-1650.

Lee, Y., Yoon, K. A., Joo, J., Lee, D., Bae, K., Han, J. Y., &Lee, J. S. (2013). Prognostic implications of genetic variants in advanced non-small cell lung cancer: a genome-wide association study. *Carcinogenesis, 34*(2), 307-313.

Lefaucheur, C., Stengel, B., Nochy, D., Martel, P., Hill, G. S., Jacquot, C., Rossert, J., &Group, G.-P. S. (2006). Membranous nephropathy and cancer: Epidemiologic evidence and determinants of high-risk cancer association. *Kidney Int., 70*(8), 1510-1507.

Li, N., Aoki, V., Hans-Filho, G., Rivitti, E. A., &Diaz, L. A. (2003). The role of intramolecular epitope spreading in the pathogenesis of endemic pemphigus foliaceus (fogo selvagem). *J Exp Med., 197*(11), 1501-1510.

Lichtenthaler, S. F., Lemberg, M. K., &Fluhrer, R. (2018). Proteolytic ectodomain shedding of membrane proteins in mammals-hardware, concepts, and recent developments. *EMBO J, 37*(15), e99456.

Lin, C. Y., Huang, Z., Wen, W., Wu, A., Wang, C., &Niu, L. (2015). Enhancing Protein Expression in HEK-293 Cells by Lowering Culture Temperature. *PLoS One., 10*(4), e0123562.

Lin, F., Zhang, D., Chang, J., Tang, X., Guan, W., Jiang, G., Zhu, C., &Bian, F. (2018). THSD7A-associated membranous nephropathy in a patient with neurofibromatosis type 1. *Eur J Med Genet, 61*(2), 84-88.

Lionaki, S., Derebail, V. K., Hogan, S. L., Barbour, S., Lee, T., Hladunewich, M., Greenwald, A., Hu, Y., Jennette, C. E., Jennette, J. C., Falk, R. J., Cattran, D. C., Nachman, P. H., &Reich, H. N. (2012). Venous thromboembolism in patients with membranous nephropathy. *Clin J Am Soc Nephrol., 7*(1), 43-51.

Liu, L. Y., Lin, M. H., Lai, Z. Y., Jiang, J. P., Huang, Y. C., Jao, L. E., &Chuang, Y. J. (2016). Motor neuron-derived Thsd7a is essential for zebrafish vascular development via the Notch-dll4 signaling pathway. *J Biomed Sci, 23*(1), 59.

Liu, Y., Li, X., Ma, C., Wang, P., Liu, J., Su, H., Zhuo, H., Kong, X., Xu, D., &Xu, D. (2018). Serum anti-PLA2R antibody as a diagnostic biomarker of idiopathic membranous nephropathy: The optimal cut-off value for Chinese patients. *Clin Chim Acta, 476*, 9-14.

Lleo, A., Invernizzi, P., Gao, B., Podda, M., &Gershwin, M. E. (2010). Definition of human autoimmunity–autoantibodies versus autoimmune disease. *Autoimmun Rev, 9*, A259–266.

Long, J. D., Rutledge, S. M., &Sise, M. E. (2018). Autoimmune Kidney Diseases Associated with Chronic Viral Infections. *Rheum Dis Clin North Am, 44*(4), 675-698.

Lönnbro-Widgren, J., Ebefors, K., Mölne, J., Nyström, J., &Haraldsson, B. (2015). Glomerular IgG subclasses in idiopathic and malignancy-associated membranous nephropathy. *Clin Kidney J, 8*(4), 433-439.

Ludwig, R. J., Vanhoorelbeke, K., Leypoldt, F., Kaya, Z., Bieber, K., McLachlan, S. M., Komorowski, L., Luo, J., Cabral-Marques, O., Hammers, C. M., Lindstrom, J. M., Lamprecht, P., Fischer, A., Riemekasten, G., Tersteeg, C., Sondermann, P., Rapoport, B., Wandinger, K. P., Probst, C., El Beidaq, A., Schmidt, E., Verkman, A., Manz, R. A., &Nimmerjahn, F. (2017). Mechanisms of Autoantibody-Induced Pathology. *Front Immunol, 8*(603).

Luo, R., Wang, Y., Xu, P., Cao, G., Zhao, Y., Shao, X., Li, Y. X., Chang, C., Peng, C., &Wang, Y. L. (2016). Hypoxia-inducible miR-210 contributes to preeclampsia via targeting thrombospondin type I domain containing 7A. *Sci Rep, 6*, 19588.

M

Ma, H., Beck, L. H., &Salant, D. J. (2011). Membranous nephropathy-associated anti-phospholipase A2 receptor IgG4 autoantibodies activate the lectin complement pathway [abstract]. *J Am Soc Nephrol*, 22:62A.

Ma, H., Sandor, D. G., &Beck, L. J. (2013). The role of complement in membranous nephropathy. *Semin Nephrol., 33*(6), 531-542.

Maimaitiyiming, H., Zhou, Q., &Wang, S. (2016). Thrombospondin 1 Deficiency Ameliorates the Development of Adriamycin-Induced Proteinuric Kidney Disease. *PLoS One, 11*(5), e0156144.

Maisonneuve, P., Agodoa, L., Gellert, R., Stewart, J. H., Buccianti, G., Lowenfels, A. B., Wolfe, R. A., Jones, E., Disney, A. P., Briggs, D., McCredie, M., &Boyle, P. (2000). Distribution of primary renal diseases leading to end-stage renal failure in the

United States, Europe, and Australia/New Zealand: results from an international comparative study. *Am J Kidney Dis., 35*(1), 157-165.

Makker, S. P., &Tramontano, A. (2011). Idiopathic membranous nephropathy: an autoimmune disease. *Semin Nephrol, 31*(4), 333-340.

Malhotra, R., Wormald, M. R., Rudd, P. M., Fischer, P. B., Dwek, R. A., &Sim, R. B. (1995). Glycosylation changes of IgG associated with rheumatoid arthritis can activate complement via the mannose-binding protein. *Nat Med., 1*(3), 237-243.

Masli, S., Sheibani, N., Cursiefen, C., &Zieske, J. (2014). Matricellular protein thrombospondins: influence on ocular angiogenesis, wound healing and immuneregulation. *Curr Eye Res, 39*(8), 759-774.

McCall, A. S., Bhave, G., Pedchenko, V., Hess, J., Free, M., Little, D. J., Baker, T. P., 3rd. Pendergraft, W. F., Falk, R. J., Olson, S. W., &Hudson, B. G. (2018). Inhibitory Anti-Peroxidasin Antibodies in Pulmonary-Renal Syndromes. *J Am Soc Nephrol, 29*(11), 2619-2625.

McGrogan, A., Franssen, C. F., &de Vries, C. S. (2011). The incidence of primary glomerulonephritis worldwide: a systematic review of the literature. *Nephrol Dial Transplant, 26*(2), 414-430.

McLachlan, S. M., &Rapoport, B. (2017). Thyroid Autoantibodies Display both "Original Antigenic Sin" and Epitope Spreading. *Front Immunol, 8*, 1845.

McRae, B. L., Vanderlugt, C. L., Dal Canto, M. C., &Miller, S. D. (1995). Functional evidence for epitope spreading in the relapsing pathology of experimental autoimmune encephalomyelitis. *J Exp Med, 182*(1), 75-85.

Mellors, R. C., Ortega, L. G., &Holman, H. R. (1957). Role of gammaglobulins in pathogenesis of renal lesions in systemic lupus erythematosus and chronic membranous glomerulonephritis, with an observation of the lupus erythematosus cell reaction. *J Exp Med, 1065*, 191-202.

Meyer-Schwesinger, C., Dehde, S., Klug, P., Becker, J. U., Mathey, S., Arefi, K., Balabanov, S., Venz, S., Endlich, K. H., Pekna, M., Gessner, J. E., Thaiss, F., &Meyer, T. N. (2011). Nephrotic syndrome and subepithelial deposits in a mouse model of immune-mediated anti-podocyte glomerulonephritis. *J Immunol*, 187(6), 3218-3229.

Meyer-Schwesinger, C., Lambeau, G., &Stahl, R. A. (2015). Thrombospondin type-1 domain-containing 7A in idiopathic membranous nephropathy. *N Engl J Med, 372*(11), 1074-1075.

Moodie, F., Leaker, B., Cambridge, G., Totty, N., &Segal, A. (1993). Alpha-enolase : a novel cytosolic autoantigen in ANCA positive vasculitis*., 43*, 675-681.

Mori, S., Kou, I., Sato, H., Emi, M., Ito, H., Hosoi, T., &Ikegawa, S. (2008). Association of genetic variations of genes encoding thrombospondin, type 1, domain-containing 4 and 7A with low bone mineral density in Japanese women with osteoporosis. *J Hum Genet., 53*(8), 694-697.

Movat, H. Z., &McGregor, D. D. (1959). The fine structure of the glomerulus in membranous glomerulonephritis (lipoid nephrosis) in adults. *Am J Clin Pathol., 32*, 100-127.

Murtas, C., Bruschi, M., Carnevali, M. L., Petretto, A., Corradini, E., Prunotto, M., Candiano, G., degl'Innocenti, M., Ghiggeri, G., &Allegri, L. (2011). In vivo characterization of renal auto-antigens involved in human auto-immune diseases: the case of membranous glomerulonephritis. *Proteomics Clin Appl., 5*(1-2), 90-97.

N

Nakahara, K., Takahashi, H., Okuse, C., Shigefuku, R., Yamada, N., Murao, M., Matsunaga, K., Koike, J., Yotsuyanagi, H., Suzuki, M., Kimura, K., &Itoh, F. (2010). Membranous nephropathy associated with chronic hepatitis B occurring in a short period after acute hepatitis B virus infection. *Intern Med., 49*(5), 383-388.

Nangaku, M., Shankland, S. J., &Couser, W. G. (2005). Cellular response to injury in membranous nephropathy. *J Am Soc Nephrol, 16*(5), 1195-1204.

Nicolas, J. P., Lambeau, G., &Lazdunski, M. (1995). Identification of the binding domain for secretory phospholipases A2 on their M-type 180-kDa membrane receptor. *J Biol Chem, 270*(48), 28869-28873.

Nishida, M., Kato, R., &Hamaoka, K. (2015). Coexisting Membranous Nephropathy and IgA Nephropathy. *Fetal Pediatr Pathol., 34*(6), 351-354.

Nizamuddin, S., Govindaraj, P., Saxena, S., Kashyap, M., Mishra, A., Singh, S., Rotti, H., Raval, R., Nayak, J., Bhat, B. K., Prasanna, B. V., Dhumal, V. R., Bhale, S., Joshi, K. S., Dedge, A. P., Bharadwaj, R., Gangadharan, G. G., Nair, S., Gopinath, P. M., Patwardhan, B., Kondaiah, P., Satyamoorthy, K., Valiathan, M. S., &Thangaraj, K. (2015). A novel gene THSD7A is associated with obesity. *Int J Obes (Lond), 39*(11), 1662-1665.

Nolin, J. D., Ogden, H. L., Lai, Y., Altemeier, W. A., Frevert, C. W., Bollinger, J. G., Naika, G. S., Kicic, A., Stick, S. M., Lambeau, G., Henderson, W. R. J., Gelb, M. H., &Hallstrand, T. S. (2016). Identification of Epithelial Phospholipase A2 Receptor 1 as a Potential Target in Asthma. *Am J Respir Cell Mol Biol, 55*(6), 825-836.

O – P

Ohtani, H., Wakui, H., Komatsuda, A., Okuyama, S., Masai, R., Maki, N., Kigawa, A., Sawada, K., &Imai, H. (2004). Distribution of glomerular IgG subclass deposits in malignancy-associated membranous nephropathy. *Nephrol Dial Transplant, 19*(3), 574-579.

Okuda, R., Kaplan, M. H., Cuppage, F. E., &Heymann, W. (1965). Deposition of autologous gamma globulin in kidneys of rats with nephrotic renal disease of various etiologies. *J Lab Clin Med., 66*, 204–215.

Olsen, J. G., &Kragelund, B. B. (2014). Who climbs the tryptophan ladder? On the structure and function of the WSXWS motif in cytokine receptors and thrombospondin repeats. *Cytokine Growth Factor Rev., 25*(3), :337-341.

P. Judge, R. H., M. J. Landray, C. Baigent (2015). Neprilysin inhibition in chronic kidney disease. *Nephrol Dial Transplant, 30*, 738-743.

Pääkkönen, K., Tossavainen, H., Permi, P., Rakkolainen, H., Rauvala, H., Raulo, E., Kilpeläinen, I., &Güntert, P. (2006). Solution structures of the first and fourth TSR domains of F-spondin. *Proteins, 64*(3), 665-672.

Perico, L., Perico, N., &Benigni, A. (2019). The incessant search for renal biomarkers: is it really justified. *Curr Opin Nephrol Hypertens, 28*(2), 195-202.

Petermann, A. T., Krofft, R., Blonski, M., Hiromura, K., Vaughn, M., Pichler, R., Griffin, S., Wada, T., Pippin, J., Durvasula, R., &Shankland, S. J. (2003). Podocytes that detach in experimental membranous nephropathy are viable. *Kidney Int, 64*(4), 1222-1231.

Pierschbacher, M. D., &Ruoslahti, E. (1984). Cell attachment activity of fibronectin can be duplicated by small synthetic fragments of the molecule. *Nature, 309*(5963), 30-33.

Polanco, N., Gutiérrez, E., Covarsí, A., Ariza, F., Carreño, A., Vigil, A., Baltar, J., Fernández-Fresnedo, G., Martín, C., Pons, S., Lorenzo, D., Bernis, C., ArrizabalagaP. , Fernández-Juárez, G., Barrio, V., Sierra, M., Castellanos, I., Espinosa, M., Rivera, F., Oliet, A., Fernández-Vega, F., Praga, M., &Nefrología., G. d. E. d. l. E. G. d. l. S. E. d. (2010). Spontaneous remission of nephrotic syndrome in idiopathic membranous nephropathy. *J Am Soc Nephrol., 21*(4), 697-704.

Pollak, M. R., Quaggin, S. E., Hoenig, M. P., &Dworkin, L. D. (2014). The glomerulus: the sphere of influence. *Clin J Am Soc Nephrol, 9*(8), 1461-1469.

Ponticelli, C., Altieri, P., Scolari, F., Passerini, P., Roccatello, D., Cesana, B., Melis, P., Valzorio, B., Sasdelli, M., Pasquali, S., Pozzi, C., Piccoli, G., Lupo, A., Segagni, S., Antonucci, F., Dugo, M., Minari, M., Scalia, A., Pedrini, L., Pisano, G., Grassi, C., Farina, M., &Bellazzi, R. (1998). A randomized study comparing methylprednisolone plus chlorambucil versus methylprednisolone plus cyclophosphamide in idiopathic membranous nephropathy. *J Am Soc Nephrol., 9*(3), 444-450.

Ponticelli, C., &Anders, H. J. (2017). Thrombospondin immune regulation and the kidney. *Nephrol Dial Transplant, 32*(7), 1084-1089.

Ponticelli, C., &Glassock, R. J. (2014). Glomerular diseases: membranous nephropathy--a modern view. *Clin J Am Soc Nephrol., 9*(3), 609-616.

Pourcine, F., Dahan, K., Mihout, F., Cachanado, M., Brocheriou, I., Debiec, H., &Ronco, P. (2017). Prognostic value of PLA2R autoimmunity detected by measurement of anti-PLA2R antibodies combined with detection of PLA2R antigen in membranous nephropathy: A single-centre study over 14 years. *PLoS One, 12*(3), e0173201.

Pozdzik, A., Brochériou, I., David, C., Touzani, F., Goujon, J. M., &Wissing, K. M. (2018). Membranous Nephropathy and Anti-Podocytes Antibodies: Implications for the Diagnostic Workup and Disease Management. *Biomed Res Int., 2018*(6281054).

Prabakaran, T., Nielsen, R., Larsen, J. V., Sorensen, S. S., Feldt-Rasmussen, U., Saleem, M. A., Petersen, C. M., Verroust, P. J., &Christensen, E. I. (2011). Receptormediated endocytosis of alpha-galactosidase A in human podocytes in Fabry disease. *PLoS One, 6*(9), e25065.

Prasad, S., Kohm, A. P., McMahon, J. S., Luo, X., &Miller, S. D. (2012). Pathogenesis of NOD diabetes is initiated by reactivity to the insulin B chain 9-23 epitope and involves functional epitope spreading. *J Autoimmun, 39*(4), 347-353.

Pratesi, F., Moscato, S., Sabbatini, A., Chimenti, D., Bombardieri, S., &Migliorini, P. (2000). Autoantibodies specific for alpha-enolase in systemic autoimmune disorders. *J Rheumatol., 27*(1), 109-115.

Prunotto, M., Carnevali, M. L., Candiano, G., Murtas, C., Bruschi, M., Corradini, E., Trivelli, A., Magnasco, A., Petretto, A., Santucci, L., Mattei, S., Gatti, R., Scolari, F., Kador, P., Allegri, L., &Ghiggeri, G. M. (2010). Autoimmunity in membranous nephropathy targets aldose reductase and SOD2. *J Am Soc Nephrol., 21*(3), 507-519.

Puelles, V. G., Hoy, W. E., Hughson, M. D., Diouf, B., Douglas-Denton, R. N., &Bertram, J. F. (2011). Glomerular number and size variability and risk for kidney disease. *Curr Opin Nephrol Hypertens, 20*(1), 7-15.

Q

Qin, H., Zhang, M., Le, W., Ren, Q., Chen, D., Zeng, C., Liu, L., Zuo, K., Xu, F., &Liu, Z. (2016). Combined Assessment of Phospholipase A2 Receptor Autoantibodies and Glomerular Deposits in Membranous Nephropathy. *J Am Soc Nephrol, 27*(10), 3195-3203.

Qin, W., Beck, L. H. J., Zeng, C., Chen, Z., Li, S., Zuo, K., Salant, D. J., &Liu, Z. (2011). Anti-phospholipase A2 receptor antibody in membranous nephropathy. *J Am Soc Nephrol., 22*(6), 1137-1143

Qiu, W., Li, Y., Zhou, J., Zhao, C., Zhang, J., Shan, K., Zhao, D., &Wang, Y. (2011). TSP-1 promotes glomerular mesangial cell proliferation and extracellular matrix secretion in Thy-1 nephritis rats. *J Biomed Res, 25*(6), 402-410.

Qu, Z., Liu, G., Li, J., Wu, L. H., Tan, Y., Zheng, X., Ao, J., &Zhao, M. H. (2012). Absence of glomerular IgG4 deposition in patients with membranous nephropathy may indicate malignancy. *Nephrol Dial Transplant, 27*(5), 1931-1937.

Quintana, L. F., Blasco, M., Seras, M., Pérez, N. S., López-Hoyos, M., Villarroel, P., Rodrigo, E., Viñas, O., Ercilla, G., Diekmann, F., Gómez-Roman, J. J., Fernandez-Fresnedo, G., Oppenheimer, F., Arias, M., &Campistol, J. M. (2015). Antiphospholipase A2 Receptor Antibody Levels Predict the Risk of Posttransplantation Recurrence of Membranous Nephropathy. *Transplantation, 99*(8), 1709-1714.

R

Radhakrishnan, J., &Cattran, D. C. (2012). The KDIGO practice guideline on glomerulonephritis: reading between the (guide)lines--application to the individual patient. *Kidney Int., 82*(8), 840-856.

Reichert, L. J., Koene, R. A., &Wetzels, J. F. (1998). Prognostic factors in idiopathic membranous nephropathy. *Am J Kidney Dis, 31*(1), 1-11.

Remuzzi, G., Chiurchiu, C., Abbate, M., Brusegan, V., Bontempelli, M., &Ruggenenti, P. (2002). Rituximab for idiopathic membranous nephropathy. *Lancet, 360*(9337), 1416–1425.

Resovi, A., Pinessi, D., Chiorino, G., &Taraboletti, G. (2014). Current understanding of the thrombospondin-1 interactome. *Matrix Biol, 37*, 83-91.

Rhoden, S., Fresquet, M., Jowitt, T. A., Gummadova, J. O., Roberts, I., Lennon, R., &Brenchley, P. E. (2017). Similarities between THSD7A and PLA2R Antigens in Autoimmune Membranous Nephropathy (AMN). *J Am Soc Nephrol*.

Rhoden, S. J., Lausecker, F., Fresquet, M., Adamson, A., Jowitt, T. A., Brenchley, P. E., &Lennon, R. (2018). Generating a Mouse Model of Membranous Nephropathy (MN). *J Am Soc Nephrol 29, 823*

Roccatello, D., Sciascia, S., Di Simone, D., Solfietti, L., Naretto, C., Fenoglio, R., Baldovino, S., &Menegatti, E. (2016). New insights into immune mechanisms underlying response to Rituximab in patients with membranous nephropathy: A prospective study and a review of the literature. *Autoimmun Rev, 15*(6), 529-538.

Rodien, P., Madec, A. M., Ruf, J., Rajas, F., Bornet, H., Carayon, P., &Orgiazzi, J. (1996). Antibody-dependent cell-mediated cytotoxicity in autoimmune thyroid disease: relationship to antithyroperoxidase antibodies. *J Clin Endocrinol Metab., 81*(7), 2595-2600.

Ronco, P., &Debiec, H. (2010). Antigen identification in membranous nephropathy moves toward targeted monitoring and new therapy. *J Am Soc Nephrol, 21*(4), 564-569.

Ronco, P., &Debiec, H. (2012). Pathogenesis of membranous nephropathy: recent advances and future challenges. *Nat Rev Nephrol, 8*(4), 203-213.

Ronco, P., &Debiec, H. (2015). Pathophysiological advances in membranous nephropathy: time for a shift in patient's care. *Lancet., 385*(9981), 1983-1992.

Ronco, P., &Debiec, H. (2015). Membranous nephropathy: A fairy tale for immunopathologists, nephrologists and patients. *Mol Immunol*, 68(1), 57-62.

Ronco, P., &Debiec, H. (2017). A podocyte view of membranous nephropathy: from Heymann nephritis to the childhood human disease. *Pflugers Arch., 469*(7-8), 997-1005.

Rosenzwajg, M., Languille, E., Debiec, H., Hygino, J., Dahan, K., Simon, T., Klatzmann, D., &Ronco, P. (2017). B- and T-cell subpopulations in patients with severe idiopathic membranous nephropathy may predict an early response to rituximab. *Kidney Int, 92*(1), 227-237.

Roth, A. J., Ooi, J. D., Hess, J. J., van Timmeren, M. M., Berg, E. A., Poulton, C. E., McGregor, J., Burkart, M., Hogan, S. L., Hu, Y., Winnik, W., Nachman, P. H., Stegeman, C. A., Niles, J., Heeringa, P., Kitching, A. R., Holdsworth, S., Jennette, J. C., Preston, G. A., &Falk, R. J. (2013). Epitope specificity determines pathogenicity and detectability in ANCA-associated vasculitis. *J Clin Invest., 123*(4), 1773-1783.

Rouault, M., Le Calvez, C., Boilard, E., Surrel, F., Singer, A., Ghomashchi, F., Bezzine, S., Scarzello, S., Bollinger, J., Gelb, M. H., &Lambeau, G. (2007). Recombinant production and properties of binding of the full set of mouse secreted phospholipases A2 to the mouse M-type receptor. *Biochemistry, 46*(6), 1647-1662.

Ruggenenti, P., Chiurchiu, C., Brusegan, V., Abbate, M., Perna, A., Filippi, C., &Remuzzi, G. (2003). Rituximab in idiopathic membranous nephropathy: a one-year prospective study. *J Am Soc Nephrol, 14*(7), 1851-1857.

Ruggenenti, P., Cravedi, P., &Remuzzi, G. (2007). Latest treatment strategies for membranous nephropathy. *Expert Opin Pharmacother., 8*(18), 3159-3171.

Ruggenenti, P., Cravedi, P., &Remuzzi, G. (2009). Rituximab for membranous nephropathy and immune disease: less might be enough. *Nat Clin Pract Nephrol, 5*(2), 76-77.

Ruggenenti, P., Debiec, H., Ruggiero, B., ChiancaA. , Pellé, T., Gaspari, F., Suardi, F., Gagliardini, E., Orisio, S., Benigni, A., Ronco, P., &Remuzzi, G. (2015). Antiphospholipase A2 receptor antibody titer predicts post-rituximab outcome of membranous nephropathy. *J Am Soc Nephrol, 26*, 2545–2558.

Ruggenenti, P., &Remuzzi, G. (2013). Idiopathic membranous nephropathy: back to the future? *Lancet, 381*(9868), 706-708.

Ruoslahti, E., &Pierschbacher, M. D. (1987). New perspectives in cell adhesion: RGD and integrins. *Science, 238*(4826), 491-497.

S

Saeed, M., Beggs, M. L., Walker, P. D., &Larsen, C. P. (2014). PLA2R-associated membranous glomerulopathy is modulated by common variants in PLA2R1 and HLA-DQA1 genes. *Genes Immun., 15*(8), 556-561.

Sakaguchi, S., Miyara, M., Costantino, C., &Hafler, D. (2010). FOXP3+ regulatory T cells in the human immune system. *Nat Rev Immunol, 10*(7), 490-500.

Salant, D. J. (2019). Unmet challenges in membranous nephropathy. *Curr Opin Nephrol Hypertens., 28*(1), 70-76.

Salant, D. J., Belok, S., Madaio, M. P., &Couser, W. G. (1980). A new role for complement in experimental membranous nephropathy in rats. *J Clin Invest, 66*(6), 1339-1350.

Salant, D. J., &Cybulsky, A. V. (1988). Experimental glomerulonephritis. *Methods Enzymol, 162*, 421-461.

Salant, D. J., Quigg, R. J., &Cybulsky, A. V. (1989). Heymann nephritis: mechanisms of renal injury. *Kidney Int, 35*(4), 976-984.

Sarma, J. V., &Ward, P. A. (2011). The complement system. *Cell Tissue Res, 343*(1), 227-235.

Schewe, M., Franken, P. F., Sacchetti, A., Schmitt, M., Joosten, R., Böttcher, R., van Royen, M. E., Jeammet, L., Payré, C., Scott, P. M., Webb, N. R., Gelb, M., Cormier, R. T., Lambeau, G., &Fodde, R. (2016). Secreted Phospholipases A2 Are Intestinal Stem Cell Niche Factors with Distinct Roles in Homeostasis, Inflammation, and Cancer. *Cell Stem Cell, 19*(1), 38-51.

Schieppati, A., Mosconi, L., Perna, A., Mecca, G., Bertani, T., Garattini, S., &Remuzzi, G. (1993). Prognosis of untreated patients with idiopathic membranous nephropathy. *N Engl J Med., 329*(2), 85-89.

Schulze, M., Donadio, J. V. J., Pruchno, C. J., Baker, P. J., Johnson, R. J., Stahl, R. A., Watkins, S., Martin, D. C., Wurzner, R., Gotze, O., &Couser, W. G. (1991). Elevated urinary excretion of the C5b-9 complex in membranous nephropathy. *Kidney Int, 40*(3), 533-538.

Scolari, F., Amoroso, A., Savoldi, S., Borelli, I., Valzorio, B., Costantino, E., Bracchi, M., Usberti, M., Prati, E., &Maiorca, R. (1998). Familial membranous nephropathy. *J Nephrol, 11*(1), 35-39.

Scott, R. P., &Quaggin, S. E. (2015). Review series : The cell biology of renal filtration. *J Cell Biol, 209*, 199-210.

Segarra-Medrano, A., Jatem-Escalante, E., Carnicer-Cáceres, C., Agraz-Pamplona, I., Salcedo, M. T., Valtierra, N., Ostos-Roldán, E., Arredondo, K. V., &Jaramillo, J. (2014). Evolution of antibody titre against the M-type phospholipase A2 receptor and clinical response in idiopathic membranous nephropathy patients treated with tacrolimus. *Nefrologia, 34*(4), 491-497.

Segawa, Y., Hisano, S., Matsushita, M., Fujita, T., Hirose, S., Takeshita, M., &Iwasaki, H. (2010). IgG subclasses and complement pathway in segmental and global membranous nephropathy. *Pediatr Nephrol*, 25(6), 1091-1099.

Segerer, S., &Schlöndorff, D. (2008). B cells and tertiary lymphoid organs in renal inflammation. *Kidney Int, 73*(5), 533-537.

Seifert, L., Hoxha, E., Eichhoff, A. M., Zahner, G., Dehde, S., Reinhard, L., Koch-Nolte, F., Stahl, R. A. K., &Tomas, N. M. (2018). The Most N-Terminal Region of THSD7A Is the Predominant Target for Autoimmunity in THSD7AAssociated Membranous Nephropathy. *J Am Soc Nephrol., 29(5)*, 1536-1548.

Seikrit, C., Ronco, P., &Debiec, H. (2018). Factor H Autoantibodies and Membranous Nephropathy. *N Engl J Med., 379*(25), 2479-2481.

Seitz-Polski, B., Dolla, G., Payré, C., Girard, C. A., Polidori, J., Zorzi, K., Birgy-Barelli, E., Jullien, P., Courivaud, C., Krummel, T., Benzaken, S., Bernard, G., Burtey, S., Mariat, C., Esnault, V. L., &Lambeau, G. (2016). Epitope Spreading of Autoantibody Response to PLA2R Associates with Poor Prognosis in Membranous Nephropathy. *J Am Soc Nephrol., 27*(5), 1517-1533.

Seitz-Polski, B., Dolla, G., Payré, C., Tomas, N. M., Lochouarn, M., Jeammet, L., Mariat, C., Krummel, T., Burtey, S., Courivaud, C., Schlumberger, W., Zorzi, K., Benzaken, S., Bernard, G., Esnault, V. L., &Lambeau, G. (2015). Cross-reactivity of anti-PLA2R1 autoantibodies to rabbit and mouse PLA2R1 antigens and development of two novel ELISAs with different diagnostic performances in idiopathic membranous nephropathy. *Biochimie., 118*, 104-115.

Seitz-Polski, B., Payré, C., Ambrosetti, D., Albano, L., Cassuto-Viguier, E., Berguignat, M., Jeribi, A., Thouret, M. C., Bernard, G., Benzaken, S., Lambeau, G., &Esnault, V. L. (2014). Prediction of membranous nephropathy recurrence after transplantation by monitoring of anti-PLA2R1 (M-type phospholipase A2 receptor) autoantibodies: a case series of 15 patients. *Nephrol Dial Transplant., 29*(12), 2334-2342.

Shah, P., Tramontano, A., &Makker, S. P. (2007). Intramolecular epitope spreading in Heymann nephritis. *J Am Soc Nephrol., 18*(12), 3060-3066.

Shoemark, D. K., Ziegler, B., Watanabe, H., Strompen, J., Tucker, R. P., Özbek, S., &Adams, J. C. (2019). Emergence of a Thrombospondin Superfamily at the Origin of Metazoans. *Mol Biol Evol*, msz060.

Sims, J. N., &Lawler, J. (2015). Thrombospondin-1-Based Antiangiogenic Therapy. *J Ocul Pharmacol Ther, 31*(7), 366-370.

Sis, B., Tasanarong, A., Khoshjou, F., Dadras, F., Solez, K., &Halloran, P. F. (2007). Accelerated expression of senescence associated cell cycle inhibitor p16INK4A in kidneys with glomerular disease. *Kidney Int, 71*(3), 218-226.

Skoberne, A., Behnert, A., Teng, B., Fritzler, M. J., Schiffer, M., Pajek, M., Lindic, J., Haller, H., &Schiffer, M. (2014). Serum with phospholipase A2 receptor autoantibodies interferes with podocyte adhesion to collagen. *Eur J Clin Invest, 44*(8), 753-765.

Smitten, A. L., Simon, T. A., Hochberg, M. C., &Suissa, S. (2008). A meta-analysis of the incidence of malignancy in adult patients with rheumatoid arthritis. *Arthritis Res Ther, 10*(2), R45.

SP. Makker, A. T. (2011). Idiopathic membranous nephropathy: an autoimmune disease. *Semin Nephrol., 31*(4), 333-340.

Šribar, J., Oberčkal, J., &Križaj, I. (2014). Understanding the molecular mechanism underlying the presynaptic toxicity of secreted phospholipases A(2): an update. *Toxicon, 89*(9-16).

Stahl, P. R., Hoxha, E., Wiech, T., Schröder, C., Simon, R., &Stahl, R. A. (2017). THSD7A expression in human cancer. *Genes Chromosomes Cancer, 56*(4), 314-327.

Stahl, R., Hoxha, E., &Fechner, K. (2010). PLA2R autoantibodies and recurrent membranous nephropathy after transplantation. *N Engl J Med, 363*(5), 496-498.

Stanescu, H. C., Arcos-Burgos, M., Medlar, A., Bockenhauer, D., Kottgen, A., Dragomirescu, L., Voinescu, C., Patel, N., Pearce, K., Hubank, M., Stephens, H. A., Laundy, V., Padmanabhan, S., Zawadzka, A., Hofstra, J. M., Coenen, M. J., den Heijer, M., Kiemeney, L. A., Bacq-Daian, D., Stengel, B., Powis, S. H., Brenchley, P., Feehally, J., Rees, A. J., Debiec, H., Wetzels, J. F., Ronco, P., Mathieson, P. W., &Kleta, R. (2011). Risk HLA-DQA1 and PLA(2)R1 alleles in idiopathic membranous nephropathy. *N Engl J Med., 364*(7), 616-626.

Stehlé, T., Audard, V., Ronco, P., &Debiec, H. (2015). Phospholipase A2 receptor and sarcoidosis-associated membranous nephropathy. *Nephrol Dial Transplant, 30*(6), 1047-1050.

Stills, H. F. J. (2005). Adjuvants and antibody production: dispelling the myths associated with Freund's complete and other adjuvants. *ILAR J., 46*(3), 280-293.

Stoddard, S. V., Welsh, C. L., Palopoli, M. M., Stoddard, S. D., Aramandla, M. P., Patel, R. M., Ma, H., &Beck, L. H. J. (2018). Structure and function insights garnered from in silico modeling of the thrombospondin type-1 domain-containing 7A antigen. *Proteins*.

Suckau, D., Köhl, J., Karwath, G., Schneider, K., Casaretto, M., Bitter-Suermann, D., &Przybylski, M. (1990). Molecular epitope identification by limited proteolysis of an immobilized antigen-antibody complex and mass spectrometric peptide mapping. *Proc Natl Acad Sci U S A., 87*(24), 9848-9852.

Svobodova, B., Honsova, E., Ronco, P., Tesar, V., &Debiec, H. (2013). Kidney biopsy is a sensitive tool for retrospective diagnosis of PLA2R-related membranous nephropathy. *Nephrol Dial Transplant, 28*(7), 1839-1844.

syndrome, C. s. o. t. a. i. n. (1979). A controlled study of short-term prednisone treatment in adults with membranous nephropathy. *N. Engl. J. Med., 13*, 1301 -1306.

T

Taguchi, S., Koshikawa, Y., Ohyama, S., Miyachi, H., Ozawa, H., &Asada, H. (2019). Thrombospondin type-1 domain-containing 7A-associated membranous nephropathy after resection of rectal cancer: a case report. *BMC Nephrol., 20*(1), 43.

Takahashi, S., Watanabe, K., Watanabe, Y., Fujioka, D., Nakamura, T., Nakamura, K., Obata, J. E., &Kugiyama, K. (2015). C-type lectin-like domain and fibronectin-like type II domain of phospholipase A(2) receptor 1 modulate binding and migratory responses to collagen. *FEBS Lett, 589*, 829-835.

Takekoshi, Y., Tanaka, M., Miyakawa, Y., Yoshizawa, H., Takahashi, K., &Mayumi, M. (1979). Free "small" and IgG-associated "large" hepatitis B e antigen in the serum and glomerular capillary walls of two patients with membranous glomerulonephritis. *N Engl J Med., 300*(15), 814-819.

Tampoia, M., Migliucci, F., Villani, C., Abbracciavento, L., Rossini, M., Fumarulo, R., Gesualdo, L., &Montinaro, V. (2018). Definition of a new cut-off for the anti-phospholipase A2 receptor (PLA2R) autoantibody immunoassay in patients affected by idiopathic membranous nephropathy. *J Nephrol, 31*(6), 899-905.

Tan, K., Duquette, M., Liu, J. H., Dong, Y., Zhang, R., Joachimiak, A., Lawler, J., &Wang, J. H. (2002). Crystal structure of the TSP-1 type 1 repeats: a novel layered fold and its biological implication. *J Cell Biol, 159*(2), 373-382.

Tao, M. H., Smith, R. I., &Morrison, S. L. (1993). Structural features of human immunoglobulin G that determine isotype-specific differences in complement activation. *J Exp Med, 178*(2), 661-667.

Timmermans, S. A., Ayalon, R., van Paassen, P., Beck, L. H. J., van Rie, H., Wirtz, J. J., Verseput, G. H., Frenken, L. A., Salant, D. J., Cohen Tervaert, J. W., &Renal, L. (2013). Anti-phospholipase A2 receptor antibodies and malignancy in membranous nephropathy. *Am J Kidney Dis., 62*(6), 1223-1225.

Timmermans, S. A., Damoiseaux, J. G., Heerings-Rewinkel, P. T., Ayalon, R., Beck, L. H. J., Schlumberger, W., Salant, D. J., van Paassen, P., Tervaert, J. W., &Registry, L. R. (2014). Evaluation of anti-PLA2R1 as measured by a novel ELISA in patients with idiopathic membranous nephropathy: a cohort study. *Am J Clin Pathol, 142*(1), 29-34.

Tomas, N. M., Beck, L. H. J., Meyer-Schwesinger, C., Seitz-Polski, B., Ma, H., Zahner, G., Dolla, G., Hoxha, E., Helmchen, U., Dabert-Gay, A. S., Debayle, D., Merchant, M., Klein, J., Salant, D. J., Stahl, R. A., &Lambeau, G. (2014). Thrombospondin type-1 domain-containing 7A in idiopathic membranous nephropathy. *N Engl J Med, 371*(24), 2277-2287.

Tomas, N. M., Hoxha, E., Reinicke, A. T., Fester, L., Helmchen, U., Gerth, J., Bachmann, F., Budde, K., Koch-Nolte, F., Zahner, G., Rune, G., Lambeau, G., Meyer-Schwesinger, C., &Stahl, R. A. (2016). Autoantibodies against thrombospondin type 1 domain-containing 7A induce membranous nephropathy. *J Clin Invest, 126*(7), 2519-2532.

Tomas, N. M., Meyer-Schwesinger, C., von Spiegel, H., Kotb, A. M., Zahner, G., Hoxha, E., Helmchen, U., Endlich, N., Koch-Nolte, F., &Stahl, R. A. K. (2017). A Heterologous Model of Thrombospondin Type 1 Domain-Containing 7A-Associated Membranous Nephropathy. *J Am Soc Nephrol, 28*(11), 3262-3277.

Tongren, J. E., Drakeley, C. J., McDonald, S. L., Reyburn, H. G., Manjurano, A., Nkya, W. M., Lemnge, M. M., Gowda, C. D., Todd, J. E., Corran, P. H., &Riley, E. M. (2006). Target antigen, age, and duration of antigen exposure independently regulate immunoglobulin G subclass switching in malaria. *Infect Immun., 74*(1), 257-264.

Tramontano, A., Knight, T., Vizzuso, D., &akker, S. P. (2006). Nested N-terminal megalin fragments induce high-titer autoantibody and attenuated Heymann nephritis. *J Am Soc Nephrol, 17*(7), 1979-1985.

Tucker, R. P. (2004). The thrombospondin type 1 repeat superfamily. *Int J Biochem Cell Biol, 36*(6), 969-974.

U – V

Uhlén, M., Fagerberg, L., Hallström, B. M., Lindskog, C., Oksvold, P., Mardinoglu, A., Sivertsson, A., Kampf, C., Sjöstedt, E., Asplund, A., Olsson, I., Edlund, K., Lundberg, E., Navani, S., Szigyarto, C. A., Odeberg, J., Djureinovic, D., Takanen, J. O., Hober, S., Alm, T., Edqvist, P. H., Berling, H., Tegel, H., Mulder, J., Rockberg, J., Nilsson, P., Schwenk, J. M., Hamsten, M., von Feilitzen, K., Forsberg, M., Persson, L., Johansson, F., Zwahlen, M., von Heijne, G., Nielsen, J., &Pontén, F. (2015). Proteomics. Tissue-based map of the human proteome. *Science, 347*(6220), 1260419.

Val-Bernal, J. F., Garijo, M. F., Val, D., Rodrigo, E., &Arias, M. (2011). C4d immunohistochemical staining is a sensitive method to confirm immunoreactant deposition in formalin-fixed paraffin-embedded tissue in membranous glomerulonephritis. *Histol Histopathol, 26*(11), 1391-1397.

Van Damme, B. J., Fleuren, G. J., Bakker, W. W., Vernier, R. L., &Hoedemaeker, P. J. (1978). Experimental glomerulonephritis in the rat induced by antibodies directed against tubular antigens. V. Fixed glomerular antigens in the pathogenesis of heterologous immune complex glomerulonephritis. *Lab Invest, 38*, 502–510.

van de Logt, A. E., Hofstra, J. M., &Wetzels, J. F. (2015). Serum anti-PLA2R antibodies can be initially absent in idiopathic membranous nephropathy: seroconversion after prolonged follow-up. *Kidney Int, 87*(6), 1263-1264.

van den Brand, J. A., van Dijk, P. R., Hofstra, J. M., &Wetzels, J. F. (2014). Long-term outcomes in idiopathic membranous nephropathy using a restrictive treatment strategy. *J Am Soc Nephrol, 25*(1), 150-158.

van der Neut Kolfschoten, M., Schuurman, J., Losen, M., Bleeker, W. K., Martínez-Martínez, P., Vermeulen, E., den Bleker, T. H., Wiegman, L., Vink, T., Aarden, L. A., De Baets, M. H., van de Winkel, J. G., Aalberse, R. C., &Parren, P. W. (2007). Anti-inflammatory activity of human IgG4 antibodies by dynamic Fab arm exchange. *Science, 317*(5844), 1554-1557.

Vanacore, R., Pedchenko, V., Bhave, G., &Hudson, B. G. (2011). Sulphilimine cross-links in Goodpasture's disease. *Clin Exp Immunol, 164*(Suppl 1), 4-6.

Vaughan, R. W., Demaine, A. G., &Welsh, K. I. (1989). A DQA1 allele is strongly associated with idiopathic membranous nephropathy. *Tissue Antigens., 34*(5), 261-269.

Vidarsson, G., Dekkers, G., &Rispens, T. (2014). IgG subclasses and allotypes: from structure to effector functions. *Front Immunol, 5*, 520.

Vindrieux, D., Augert, A., Girard, C., Gitenay, D., Lallet-Daher, H., Wiel, C., Le Calvé, B., Gras, B., Ferrand, M., Verbeke, S., de Launoit, Y., Leroy, X., Puisieux, A., Aubert, S., Perrais, M., Gelb, M., Simonnet, H., Lambeau, G., &Bernard, D. (2013). PLA2R1 mediates tumor suppression by activating JAK2. *Cancer Res, 73*(20), 6334-6345.

Vindrieux, D., Devailly, G., Augert, A., Le Calve, B., Ferrand, M., Pigny, P., Payen, L., Lambeau, G., Perrais, M., Aubert, S., Simonnet, H., Dante, R., &Bernard, D. (2014). Repression of PLA2R1 by c-MYC and HIF-2alpha promotes cancer growth. *Oncotarget 5, 5*(4), 1004-1013.

Vivarelli, M., Emma, F., Pellé, T., Gerken, C., Pedicelli, S., Diomedi-Camassei, F., Klaus, G., Waldegger, S., Ronco, P., &Debiec, H. (2015). Genetic homogeneity but IgG subclass-dependent clinical variability of alloimmune membranous nephropathy with anti-neutral endopeptidase antibodies. *Kidney Int., 87*(3), 602-609.

von Haxthausen, F., Reinhard, L., Pinnschmidt, H. O., M., R., Soave, A., Hoxha, E., &Stahl, R. A. K. (2018). Antigen-Specific IgG Subclasses in Primary and Malignancy-Associated Membranous Nephropathy. *Front Immunol, 9*, 3035.

W

Wakui, H., Imai, H., Komatsuda, A., &Miura, A. B. (1999). Circulating antibodies against alpha-enolase in patients with primary membranous nephropathy (MN). *Clin Exp Immunol., 118*(3), 445-450.

Wang, B., Zuo, K., Wu, Y., Huang, Q., Qin, W., Zeng, C., Li, L., &Liu, Z. (2011). Correlation between B lymphocyte abnormality and disease activity in patients with idiopathic membranous nephropathy. *J Int Med Res, 39*(2), 86-95.

Wang, C. H., Chen, I. H., Kuo, M. W., Su, P. T., Lai, Z. Y., Wang, C. H., Huang, W. C., Hoffman, J., Kuo, C. J., You, M. S., &Chuang, Y. J. (2011). Zebrafish Thsd7a is a neural protein required for angiogenic patterning during development. *Dev Dyn, 240*(6), 1412-1421.

Wang, C. H., Su, P. T., Du, X. Y., Kuo, M. W., Lin, C. Y., Yang, C. C., Chan, H. S., Chang, S. J., Kuo, C., Seo, K., Leung, L. L., &Chuang, Y. J. (2010). Thrombospondin type I domain containing 7A (THSD7A) mediates endothelial cell migration and tube formation. *J Cell Physiol, 222*, 685-694.

Wang, J., Cui, Z., Lu, J., Probst, C., Zhang, Y. M., Wang, X., Qu, Z., Wang, F., Meng, L. Q., Cheng, X. Y., Liu, G., Debiec, H., Ronco, P., &Zhao, M. H. (2017). Circulating Antibodies against Thrombospondin Type-I Domain-Containing 7A in Chinese Patients with Idiopathic Membranous Nephropathy. *Clin J Am Soc Nephrol, 12*(10), 1642-1651.

Wang, L., Wang, F. S., &Gershwin, M. E. (2015). Human autoimmune diseases: a comprehensive update. *J Intern Med., 278*(4), 369-395.

Wang, T., Zhang, Y., Liu, M., Kang, X., Kang, L., &Zhang, H. (2019). THSD7A as a marker for paraneoplastic membranous nephropathy. *Int Urol Nephrol., 51*(2), 371-373.

Wang, Z., Wen, L., Dou, Y., &Zhao, Z. (2018). Human anti-thrombospondin type 1 domain-containing 7A antibodies induce membranous nephropathy through activation of lectin complement pathway. *Biosci Rep, 38*(3).

Warren, S. J., Arteaga, L. A., Rivitti, E. A., Aoki, V., Hans-Filho, G., Qaqish, B. F., Lin, M. S., Giudice, G. J., &Diaz, L. A. (2003). The role of subclass switching in the pathogenesis of endemic pemphigus foliaceus. *J Invest Dermatol., 120*(1), 104-108.

Watanabe, K., Watanabe, K., Watanabe, Y., Fujioka, D., Nakamura, T., Nakamura, K., Obata, J. E., &Kugiyama, K. (2018). Human soluble phospholipase A2 receptor is an inhibitor of the integrin-mediated cell migratory response to collagen-I. *Am J Physiol Cell Physiol., 315*(3), C398-C408.

Werb, Z., &Yan, Y. (1998). A cellular striptease act. *Science, 282*(5392), 1279-1280.

Wetzels, J. F. M. (2018). Antibodies Against M-Type Phospholipase Receptor and Prediction of Outcome in Membranous Nephropathy: We are Not There Yet. *Am J Nephrol, 48*(6), 434-437.

X – Y

Xie, Q., Li, Y., Xue, J., Xiong, Z., Wang, L., Sun, Z., Ren, Y., Zhu, X., &Hao, C. M. (2015). Renal phospholipase A2 receptor in hepatitis B virus-associated membranous nephropathy. *Am J Nephrol., 41*(4-5), 345-353.

Xu, X., Nie, S., Ding, H., &Hou, F. F. (2018). Environmental pollution and kidney diseases. *Nat Rev Nephrol, 14*(5), 313-324.

Xu, X., Wang, G., Chen, N., Lu, T., Nie, S., Xu, G., Zhang, P., Luo, Y., Wang, Y., Wang, X., Schwartz, J., Geng, J., &Hou, F. F. (2016). Long-Term Exposure to Air Pollution and Increased Risk of Membranous Nephropathy in China. *J Am Soc Nephrol., 27*(12), 3739-3746.

Yamaguchi, M., Ando, M., Yamamoto, R., Akiyama, S., Kato, S., Katsuno, T., Kosugi, T., Sato, W., Tsuboi, N., Yasuda, Y., Mizuno, M., Ito, Y., Matsuo, S., &Maruyama, S. (2014). Smoking is a risk factor for the progression of idiopathic membranous nephropathy. *PLoS One, 9*(6), e100835.

Yang, Y., Wang, C., Jin, L., He, F., Li, C., Gao, Q., Chen, G., He, Z., Song, M., ZhouZ. , Shan, F., Qi, K., &Ma, L. (2016). IgG4 anti-phospholipase A2 receptor might activate lectin and alternative complement pathway meanwhile in idiopathic membranous

nephropathy: an inspiration from a cross-sectional study. *Immunol Res, 64*(4), 919-930.

Yokota, Y., Ikeda, M., Higashino, K., Nakano, K., Fujii, N., Arita, H., &Hanasaki, K. (2000). Enhanced tissue expression and elevated circulating level of phospholipase A(2) receptor during murine endotoxic shock. *Arch Biochem Biophys, 379*(1), 7-17.

Yoshida, K., Suzuki, J., Kume, K., Suzuki, S., Isome, M., Kato, K., &Suzuki, H. (1996). Sjögren's syndrome with membranous glomerulonephritis detected by urine screening of schoolchildren. *Acta Paediatr Jpn, 38*(5), 533-536.

Young, G. D., &Murphy-Ullrich, J. E. (2004). The tryptophan-rich motifs of the thrombospondin type 1 repeats bind VLAL motifs in the latent transforming growth factor-beta complex. *J Biol Chem, 279*(46), 47633-47642.

Yu, C., Gershwin, M. E., &Chang, C. (2014). Diagnostic criteria for systemic lupus erythematosus: a critical review. *J Autoimmun., 48-49*, 10-13.

Yuzhalin, A. E. (2019). Citrullination in Cancer. *Cancer Res*.

Z

Zaghrini, C., Seitz-Polski, B., Justino, J., Dolla, G., Payré, C., Jourde-Chiche, N., Van de Logt, A. E., Booth, C., Rigby, E., Lonnbro-Widgren, J., Nystrom, J., Mariat, C., Cui, Z., Wetzels, J. F. M., Ghiggeri, G., Beck, L. H. J., Ronco, P., Debiec, H., &Lambeau, G. (2019). Novel ELISA for thrombospondin type 1 domain-containing 7A autoantibodies in membranous nephropathy. *Kidney Int, 95*(3), 666-679.

Zeisberg, M., Tampe, B., LeBleu, V., Tampe, D., Zeisberg, E. M., &Kalluri, R. (2014). Thrombospondin-1 deficiency causes a shift from fibroproliferative to inflammatory kidney disease and delays onset of renal failure. *Am J Pathol, 184*(10), 2687-2698.

Zhang, J. J., Malekpour, M., Luo, W., Ge, L., Olaru, F., Wang, X. P., Bah, M., Sado, Y., Heidet, L., Kleinau, S., Fogo, A. B., &Borza, D. B. (2012). Murine membranous nephropathy: immunization with α3(IV) collagen fragment induces subepithelial immune complexes and FcγR-independent nephrotic syndrome. *J Immunol*, 188(7), 3268-3277.

Zhang, X. D., Cui, Z., &Zhao, M. H. (2018). The genetic and environmental factors of primary membranous nephropathy: an overview from China. *Kidney Dis (Basel), 4*, 65–73.

Zhou, H., Mori, S., Kou, I., Fuku, N., Naka Mieno, M., Honma, N., Arai, T., Sawabe, M., Tanaka, M., Ikegawa, S., &Ito, H. (2013). Association of the formiminotransferase N-terminal sub-domain containing gene and thrombospondin, type 1, domain-containing 7A gene with the prevalence of vertebral fracture in 2427 consecutive autopsy cases. *J Hum Genet, 58*(2), 109-112.

Zvaritch, E., Lambeau, G., &Lazdunski, M. (1996). Endocytic properties of the M-type 180-kDa receptor for secretory phospholipases A2. *J Biol Chem, 271*(1), 250-257.

Abstract

Membranous nephropathy (MN) is a rare autoimmune kidney disease with an incidence of 1.3/100,000 in Europe yet it is a leading cause of nephrotic syndrome in adults. Histologically, MN is characterized by the accumulation of immune deposits along the glomerular basement membrane leading to podocyte injury. Clinically, the outcome of the disease varies from spontaneous remission to end–stage kidney disease, with high proteinuria. Considerable advances have been made in the understanding of the pathophysiology of MN with the identification of the phospholipase A2 receptor 1 (PLA2R1) as the major autoantigen for about 70% of patients and of thrombospondin–type 1 domain containing 7A (THSD7A) as a second autoantigen for another group of patients of 2–5%. MN treatment is controversial, and clinical biomarkers of the disease are needed to identify patients at risk of severe disease and to guide therapy. Anti–PLA2R1 titers correlate with disease severity and have a predictive value for prognosis. Moreover, three distinct epitope domains of PLA2R1 have been identified and linked by a mechanism of epitope spreading. This mechanism was associated with disease worsening and a poor prognosis. We believe that a similar disease mechanism holds for THSD7A.

In this thesis, we focused on the identification of the molecular properties of THSD7A in the context of MN. THSD7A is different from PLA2R1 and is a member of the thrombospondin repeats superfamily. It is a large type I transmembrane protein (250 kDa) with an extracellular region mainly composed of 21 alternating domains of thrombospondin–type 1 like repeat as in thrombospondin–1 or complement component 6. Little is known about THSD7A. It is implicated in cell migration and angiogenesis but its function in the podocyte is unknown.

The first objective was to develop a clinical assay to identify patients with THSD7A–associated MN. We thus designed the first robust ELISA for sensitive and quantitative detection of anti–THSD7A autoantibodies in serum from MN patients. We established and analyzed the largest cohort of 49 patients with THSD7A–associated MN, with different etiologies and clinical outcome. We observed that the anti–THSD7A titer is a relevant biomarker to monitor disease activity during follow–up and treatment and for prognosis. Second, by site–directed mutagenesis, we identified autoantibodies targeting up to 6 distinct immunogenic domains of THSD7A. We investigated which of these epitope domains

are immunodominant or part of a mechanism of epitope spreading and analyzed their clinical value. Together, this work has led to a better understanding of THSD7A–associated MN disease, and opens new avenues for personalized medicine in MN.

Keywords: Membranous nephropathy, PLA2R1, THSD7A, diagnosis, ELISA, epitope.

Résumé

La glomérulonéphrite extra–membraneuse (GEM) est une maladie auto–immune rénale rare et une des causes principales de syndrome néphrotique chez l'adulte. La GEM est caractérisée par une accumulation de dépôts immuns sur la membrane basale glomérulaire, ce qui entraîne des lésions podocytaires. Le devenir des patients est variable, depuis une rémission spontanée jusqu'à une insuffisance rénale terminale, avec une forte protéinurie. Récemment, le récepteur des phospholipases A2 sécrétées (PLA2R1) a été identifié comme l'autoantigène majeur pour environ 70% des patients et la thrombospondine 7A contenant des domaines de type 1 (THSD7A) comme le second autoantigène pour 2 à 5% des patients.

Le traitement de la GEM est complexe, avec ou sans immunosuppresseurs. Des biomarqueurs spécifiques pourraient permettre d'identifier les patients présentant un risque de maladie grave et d'adapter le traitement. Par exemple, un fort titre d'anticorps anti–PLA2R1 est associé à une maladie grave et suggère un mauvais pronostic de la fonction rénale. De plus, les anticorps anti–PLA2R1 ciblent trois domaines distincts de PLA2R1 et sont liés par un mécanisme d'étalement épitopique. La présence de plusieurs anticorps est associée à une aggravation de la maladie et à un mauvais pronostic. Le même mécanisme pourrait exister pour THSD7A.

L'objectif principal de cette thèse était d'identifier les propriétés moléculaires de THSD7A dans le contexte de la GEM. THSD7A est une protéine transmembranaire de type I de 250 kDa, composée d'une alternance de 21 domaines répétés de type thrombospondine–1 comme ceux présents dans la thrombospondine–1 ou dans le facteur du complément C6. Peu de choses sont connues sur THSD7A. Il pourrait être impliqué dans la migration cellulaire et l'angiogenèse mais sa fonction dans le podocyte est inconnue.

Notre premier objectif était de développer le premier test ELISA permettant une détection sensible et quantitative des anticorps anti–THSD7A dans le sérum des patients. Nous avons pu établir la plus grande cohorte de patients GEM associée à THSD7A (49 patients) et analyser leurs caractéristiques cliniques. Nous avons montré que le titre des anti–THSD7A est un biomarqueur fiable de l'activité de la maladie au cours du suivi et du traitement, ainsi que pour le pronostic. Deuxièmement, par mutagenèse dirigée, nous avons identifié 6 domaines immunogéniques de THSD7A ciblés par les autoanticorps, déterminé quels épitopes sont immunodominants ou associés à un mécanisme d'étalement épitopique,

et analysé leur valeur clinique. En conclusion, mes travaux de thèse ont contribué à une meilleure compréhension de la GEM associée à THSD7A, et ouvrent de nouvelles perspectives vers une médecine personnalisée de la GEM.

Mots–clés: glomérulonéphrite extra–membraneuse, PLA2R1, THSD7A, ELISA, diagnostique, épitope.